In vivo and *in vitro* characterization of *Staphylococcus aureus* and *Bacillus subtilis* polyglycerolphosphate lipoteichoic acid synthases

Mirka Elisabeth Wörmann

Department of Medicine

Imperial College London

June 2011

A thesis submitted for the degree of Doctor of Philosophy

Abstract

Staphylococcus aureus lipoteichoic acid (LTA) consists of a 1,3-linked polyglycerolphosphate chain retained in the bacterial membrane by a glycolipid anchor. The LTA backbone is produced by the lipoteichoic acid synthase LtaS, a membrane protein with five transmembrane helices and a large extracellular enzymatic domain (eLtaS). Proteomic studies revealed that LtaS is efficiently cleaved, and here it was demonstrated that the eLtaS domain is released into the culture supernatant as well as partially retained within the cell wall fraction. However, using an *in vivo* LtaS activity assay, it was shown that only the full-length LtaS enzyme is able to synthesize LTA. Neither expression of a secreted eLtaS variant, created by replacing the N-terminal membrane domain with a conventional signal sequence, nor expression of eLtaS fused to a single or multi-transmembrane domains of other staphylococcal proteins resulted in the production of LTA. These data indicate that the transmembrane domain of LtaS play an essential, yet unknown, role in LtaS enzyme function. In addition, the protease responsible for LtaS cleavage was identified. It was found that a *S. aureus* strain in which the gene encoding for the essential signal peptidase SpsB was cloned under inducible expression control showed an accumulation of the full-length LtaS enzyme in the absence of the inducer. These data suggest that SpsB is involved in LtaS cleavage.

Four LtaS orthologues, YflE, YfnI, YqgS and YvgJ, are present in *Bacillus subtilis*. Using an *in vitro* enzyme assay and purified protein, it was determined that all four *B. subtilis* proteins are Mn^{2+}-dependent metal enzymes that use the lipid phosphatidylglycerol as substrate. It was shown that YflE, YfnI and YqgS are bona-fide LTA synthases capable of producing polyglycerolphosphate chains, while YvgJ appears to function as an LTA primase, as indicated by the accumulation of a glycolipid with the expected chromatographic mobility of GroP-Glc_2-DAG. Taken together, experimental evidence for the enzyme function of all four *B. subtilis* LtaS-type proteins is provided in this work and it was shown that all four enzymes are involved in the LTA synthesis process.

Declaration of Authorship

I certify that this thesis entitled "*In vivo* and *in vitro* characterization of *Staphylococcus aureus* and *Bacillus subtilis* polyglycerolphosphate lipoteichoic acid synthases" is written entirely by myself and that the research to which it refers to is my own. I confirm that all main sources of help have been acknowledged and that any ideas or quotations from the work of others have always clearly been referenced.

Mirka Elisabeth Wörmann

Acknowledgments

First and foremost I would like to thank my supervisor Dr Angelika Gründling for her advice, help and guidance during my PhD. I am very grateful for all the chances and opportunities I was given. This work certainly would not have been same without her, so thanks a lot Angelika. I would also like to take this opportunity to express my gratitude to Imperial College for funding this project.

I am very grateful to past and present members of the Gründling lab as well as the whole of CMMI3 for creating such a pleasant and friendly work environment. Special thanks must go to Bea, Helen, Rebecca, Nathalie, Rachael, Michaella, Kevin, Alex and Tim for all the laughs, coffee breaks and for introducing the word 'thingy' to me. I have made great friends during my PhD for which I will always be grateful.

Finally, I would like to thank my family and friends for their support throughout my PhD.

Table of Contents

Abbreviations

Antibiotics:

AmpR	Ampicillin resistance
CamR	Chloramphenicol resistance
ErmR	Erythromycin resistance
KanR	Kanamycin resistance
SpecR	Spectinomycin resistance
TetR	Tetracycline resistance

aa	amino acid (s)
Atet	anhydrotetracycline
ATP	adenosine triphosphate
BSA	bovine serum albumin
CA-MRSA	community acquired methicillin resistant *S. aureus*
1d	one-dimensional
DAG	diacylglycerol
ddH_2O	double distilled water
DNA	deoxyribonucleic acid
D_2O	deuterium oxide
dNTP	deoxyribonucleotide triphosphate
ECL	enhanced chemi-luminescence
G+C	guanine + cytosine
GFP	green fluorescent protein
Glc_2-DAG	di-glucosyl-diacylglycerol
GroP	glycerolphosphate
h	hour (s)
HA-MRSA	hospital acquired methicillin resistant *S. aureus*
HRP	horseradish peroxidase
IPTG	isopropyl β-D-thiogalactoside
K	kelvin
kb	kilo base pairs
kDa	kilo dalton

LTA	lipoteichoic acid
mA	milliampere
MALDI-TOF	matrix-assisted laser desorption/ionization-time of flight
Mb	mega base pairs
Mhz	mega hertz
min	minute (s)
MRSA	methicillin resistant *S. aureus*
m/z	mass to charge ratio
NADH	nicotinamide-adenine-dinucleotide
NADPH	nicotinamide-adenine-dinucleotide-phosphate
NMR	nuclear magnetic resonance
OD	optical density
PCR	polymerase chain reaction
PG	phosphatidylglycerol
RBS	ribosomal binding site
RT	room temperature
SCC	staphylococcal cassette chromosome
SDS-PAGE	sodium dodecyl sulphate-polyacrylamide gel electrophoresis
sec	second (s)
TLC	thin layer chromatography
TM	transmembrane domain
Tris	tris (hydroxylmethyl) aminomethane
U	unit (s)
UV	ultraviolet
V	volt
VISA	vancomycin intermediate *S. aureus*
VRSA	vancomycin resistant *S. aureus*
v/v	volume per volume
WT	wild type
WTA	wall teichoic acid
w/v	weight per volume
× *g*	times gravity (relative centrifugal force)

List of Figures

List of Tables

Chapter 1
Introduction

1.1 Aims and objectives of this study

Recently, the enzyme responsible for polyglycerolphosphate LTA backbone synthesis, LtaS, was discovered in *S. aureus* and shown to be essential for bacterial growth under standard laboratory conditions (Gründling & Schneewind, 2007a). LtaS assembles in five N-terminal membrane-spanning helixes (5TM) followed by a large C-terminal extracellular enzymatic domain (eLtaS). The LtaS protein is cleaved during bacterial growth and the eLtaS released into the culture supernatant (Gatlin *et al*, 2006; Ziebandt *et al*, 2001). The first aim of this study was to characterize the LtaS enzyme in view of its functional requirements and to identify the protease responsible for LtaS cleavage. To this end, the contribution of the 5TM to LtaS function *in vivo* was investigated. A previously described *in vivo* LtaS activity assay was used to test the functionality of several LtaS variants in which the 5TM domain was replaced with either a conventional signal sequence or single or multi-transmembrane domains of other staphylococcal proteins. Staphylococcal proteins that were used to construct the LtaS hybrid fusion proteins were protein A, SrtA and LtaA and these proteins are discussed in the introduction.

S. aureus secretes a range of proteases, among which are serine, cysteine and metalloproteases. Further information on these proteases is provided in the introduction. These proteases function on the outside of the cell and could therefore be responsible for LtaS processing. To assess their contribution to LtaS processing, LtaS protein cleavage was analyzed in *S. aureus* strains with defined protease deficiencies. Moreover, evidence is provided in the literature that LtaS-type enzymes are substrates for type-I signal peptidases (Antelmann *et al*, 2001; Powers *et al*, 2011). *S. aureus* expresses one functional type-I signal peptidase, SpsB, and its contribution to LtaS cleavage was investigated in this work.

Four LtaS orthologues are present in *B. subtilis*, namely YflE, YfnI, YqgS and YvgJ. A recent study demonstrated that YflE was able to restore growth and LTA production in a *S. aureus ltaS* depleted mutant strain (Gründling & Schneewind, 2007a). Functional complementation of *ltaS* depletion with *B. subtilis* YfnI resulted in LTA synthesis, but the polyglycerolphosphate product displayed an altered mobility on SDS-PAGE compared to wild type LTA. However, YfnI expression failed to restore staphylococcal growth, suggesting that the function of LTA does not only rely

on its polyglycerolphosphate backbone. No enzyme activity was observed for *B. subtilis* YqgS and YvgJ (Gründling & Schneewind, 2007a).

The second aim of this study was to characterize the four *B. subtilis* LtaS-type enzymes *in vitro* and to identify *in vivo* functions for *B. subtilis* YqgS and YvgJ. For the latter aim, LTA production was analysed in *S. aureus* strains expression single *B. subtilis* LtaS-like proteins, and in defined *B. subtilis* strains lacking individual *ltaS*-like genes or combinations of the four genes. In addition, investigations to identify structural differences between LTA polymers synthesized by *S. aureus* LtaS and *B. subtilis* YfnI were undertaken. To this end, LTA was extracted from *S. aureus* mutant strains expressing either wild type LtaS or *B. subtilis* YfnI, and the resultant polyglyerolphosphate products analyzed by NMR and standard biochemical assay.

1.2 *Staphylococcus aureus*

Staphylococcus aureus is an immotile, non-sporulating bacterium that forms microscopically grape like clusters. *S. aureus* belongs to the bacterial family of *Staphylococcaceae* within the phylum of Gram-positive *Firmicutes* and is closely related to *Enterococcus*, *Bacillus* and *Listeria* species. The genus *Staphylococcus* contains about thirty species, thirteen of which are associated with humans (Schleifer & Kroppenstedt, 1990). The Staphylococci can be divided into two groups depending on their ability to produce the enzyme coagulase. Coagulase is a surface protein that stimulates human blood to clump by activating prothrombin, which is part of the coagulation pathway. This reaction can be used to differentiate the coagulase-positive *S. aureus* from other species of staphylococci. Several animal models of infection have demonstrated that coagulase is a virulence determinant of *S. aureus* (Hasegawa & San Clemente, 1978; Jonsson *et al*, 1985; Sawai *et al*, 1997). Unlike other staphylococci, *S. aureus* produces staphyloxanthin, which protects the bacteria against reactive oxygen species and gives the organism its characteristic yellow pigmentation (Liu *et al*, 2005). *S aureus* is halotolerant, tolerating NaCl concentrations as high as 15 % (w/v), and grows at temperatures ranging from 15-45°C. Under high NaCl stress conditions, *S. aureus* shortens its peptidoglycan interpeptide bridges in order to reinforce the cell wall (Vijaranakul *et al*, 1995). The genome of *S. aureus* is approximately 3 Mb in size with a low G+C content and contains strain specific combinations of variable sequence elements such as prophages, pathogenicity islands and staphylococcal cassette chromosomes (SCC) (Baba *et al*, 2008).

Humans are a natural reservoir of *S. aureus,* where the bacterium can occur as both a commensal and a pathogen. The most frequent sites of colonisation are on the skin or in the anterior nares, resulting in approximately 10-20 % of healthy individuals becoming life-long carriers (Peacock *et al*, 2001). *S. aureus* is capable of causing a variety of diseases in humans. The most common types of *S. aureus* infections are those of skin and soft tissues such as boils, impetigo and abscesses. Breaches of the skin or surgical incisions provide a situation where *S. aureus* can enter the bloodstream and cause bacteraemia resulting in a mortality rate of 11 to 43 % (Lowy, 1998). Once in the bloodstream the bacteria can spread to other sites of the human body and infect joints (septic arthritis), bones (osteomyelitis), the lungs (pneumonia) and kidneys (nephritis) (Lowy, 1998). The ability of *S. aureus* to survive

and multiple inside the body is based on the expression of numerous virulence factors, which promote colonisation and survival of the bacteria inside the host.

Treatment of *S. aureus* infections has become extremely difficult over the past few decades due to the appearance of multi-drug resistance strains (Diekema *et al*, 2001). Resistance to penicillin is mediated by the β-lactamase, an enzyme that hydrolyzes the β-lactam ring in penicillin and less than 5 % of *S. aureus* isolates remain sensitive to the drug (Lowy, 1998). Methicillin resistant *S. aureus* (MRSA) strains that are resistant to methicillin and all other β-lactam antibiotics carry the *mecA* gene, which encodes a modified penicillin binding protein, PBP 2a, with low affinity to β-lactam antibiotics (Hartman & Tomasz, 1984). PBP 2a cross-links peptidoglycan strands in the presence of β-lactam antibiotics and thus confers resistance to this major class of antibiotics. The *mecA* gene is carried on a mobile genetic element, SCC*mec*. Five SCC*mec* variants, which significantly vary in size, have been identified in *S. aureus* (Daum *et al*, 2002; Ito *et al*, 2001; Ito *et al*, 2004; Ma *et al*, 2002). In glucose-limited conditions, some of the SCC*mec* elements reduce the fitness of MRSA, which is most likely due to the transcription of other genes located on the SCC*mec* region (Lee *et al*, 2007). Five antibiotics, namely vancomycin, linezolid, quinupristin-dalfopristin, tigecycline and daptomycin, are currently in use to fight MRSA infections (Hancock, 2005; Schmidt-Ioanas *et al*, 2005). However, strains with either intermediate (VISA) or high (VRSA) vancomycin resistance have already been described. The genetic basis for the VRSA phenotype is the presence of the enterococcal *vanA* gene. The *vanA* gene product is a ligase allowing the production of a D-Ala-D-Lac depsipeptide, which replaces the normal D-Ala-D-Ala dipeptide in peptidoglycan (Perichon & Courvalin, 2009). This substitution reduces the affinity of vancomycin for the peptidoglycan precursor and results in high resistance to the drug (Perichon & Courvalin, 2009). VISA strains lack the *vanA* gene and these strains are thought to become resistance to vancomycin by producing excess amounts of peptidoglycan, which results in a thickened cell wall. It has been suggested that the thicker cell wall of VISA-type strains reduces the diffusion rate of the incoming vancomycin molecules to the tip of the division septum, where the concentration of the peptidoglycan precursor is high (Pereira *et al*, 2007). Linezolid and quinupristin-dalfopristin display antibacterial properties against MRSA by inhibiting protein synthesis; however, resistant strains to these antibiotics have already

been described (Hancock, 2005; Schmidt-Ioanas *et al*, 2005). MRSA infections are usually hospital associated (HA-MRSA), but also occur in otherwise healthy individuals (CA-MRSA). The most common isolate of CA-MRSA is USA300, which has been shown to be responsible for 97 % of all CA-MRSA infections (Moran *et al*, 2006). CA-MRSA carry the type IV SCC*mec* region, which only contains the *mecA* gene and thus is small in size. Due to its small size the type IV SCC*mec* element might only have a small impact on the fitness of these strains and this might partially explain the success of CA-MRSA in community settings (Diep & Otto, 2008).

1.3 *Bacillus subtilis*

Bacillus subtilis is a sporulating, rod-shaped, non-pathogenic bacterium. Taxonomally *B. subtilis* belongs to the bacterial family of *Bacillaceae* within the Gram-positive phylum Firmicutes. The main reservoirs of *B. subtilis* are the soil, water sources and in association with plants (Priest, 1989). The genus *Bacillus* contains more than 60 species including pathogenic and non-pathogenic strains (Claus & Fritze, 1989). *B. subtilis* was the first Gram-positive bacterium for which the complete genome sequence became available in 1997. This achievement revealed a low G+C content of the 4.2 Mb chromosome and identified more than 4100 genes encoded within the *B. subtilis* genome (Kunst *et al*, 1997). *B. subtilis* is naturally genetic competent. Under conditions of nutritional starvation *B. subtilis* expresses an efficient DNA uptake system that allows the bacterium to internalize exogenous double stranded DNA (Dubnau, 1991). *B subtilis* and other members of the genus (*B. amyloliquefaciens, B. licheniformes*) are able to produce and secrete high quantities of protein directly into the growth medium and thus are important objects in industrial applications (Harwood, 1992; Jensen *et al*, 2000). Due to the wealth of information available on *B. subtilis* and its close phylogenetic relation to other pathogens, such as *Listeria* and Staphylococci, *B. subtilis* became a model organism for investigating general biological questions.

1.4 The cell wall envelope of Gram-positive bacteria

The cell wall envelope of Gram-positive bacteria is composed of multiple layers of peptidoglycan that cover the entire cell surface and protect the underlying protoplast against mechanical and osmotic lysis (Scheffers & Pinho, 2005 and Fig. 1). Several other components are associated with the Gram-positive cell wall including proteins and teichoic acids. Two types of teichoic acids, wall teichoic acid (WTA) and lipoteichoic acid (LTA), are present in most Gram-positive bacteria (Weidenmaier & Peschel, 2008). WTA is a structure attached to the peptidoglycan layer and LTA is a surface polymer tethered to the bacterial membrane via a glycolipid anchor. Teichoic acids are further described in section 1.5. Some Gram-positive bacteria, including several clinical isolates of *S. aureus*, produce a capsule, which forms a protective layer around the cell (O'Riordan & Lee, 2004). The following sections discuss the capsule and the membrane composition of *S. aureus*. The structure of peptidoglycan and its synthesis are discussed with regard to *S. aureus* and *B. subtilis*.

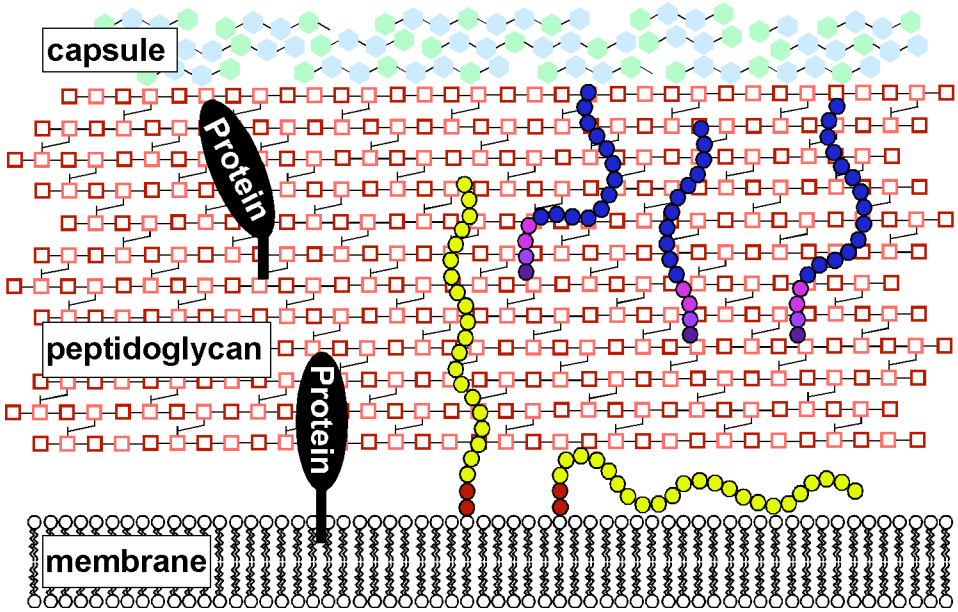

Figure 1: Schematic representation of the Gram-positive cell wall envelope. The cell envelope of Gram-positive bacteria consists of a thick peptidoglycan layer that is decorated with peptidoglycan linked WTA (depicted in blue) and membrane-linked LTA (depicted in yellow) polymers. In addition, cell surface proteins are covalently linked to the peptidoglycan or tethered to the lipid bilayer. Some bacteria strains express a polysaccharide capsule.

1.4.1 The *S. aureus* polysaccharide capsule

The capsule is a cell surface structure that exists outside the bacterial cell wall and is usually composed of polysaccharides. The capsule is common feature of *S. aureus* and produced by approximately 90 % of all *S. aureus* isolates (Sompolinsky *et al*, 1985). To date 11 capsule serotypes have been described for *S. aureus* of which serotype 5 and 8 are the most abundant ones (Arbeit *et al*, 1984; Sompolinsky *et al*, 1985). Type 5 and 8 polysaccharides are structurally similar and both contain N-acetylfucosamine and N-acetylmannosaminuronic acid (Fournier *et al*, 1987; Fournier *et al*, 1984; Moreau *et al*, 1990). However, the two polysaccharides differ in their sugar linkages and O-acetylation sites of the mannosaminuronic acid residues. The mechanism by which the capsule is anchored to the *S. aureus* cell wall has not been elucidated yet (O'Riordan & Lee, 2004). The genes involved in capsule synthesis of serotype 5 and 8 (*cap*5 and *cap*8) are organized in a cluster on the chromosome (Sau *et al*, 1997). The *cap*5 and *cap*8 clusters are allelic and comprise 16 genes, which are transcribed in one orientation (Sau *et al*, 1997). Expression of *cap*5 and *cap*8 is positively regulated by Agr and SarA, but the effect of SarA on *cap*5 and *cap*8 expression is minor compared to that of Agr (Dassy *et al*, 1993; Luong *et al*, 2002; van Wamel *et al*, 2002). In addition, expression of *cap*5 is downregulated by CO_2, indicating that CO_2 serves as an environmental signal for type 5 polysaccharide capsule expression (Herbert *et al*, 1997). Bacterial capsules are thought to enhance virulence by preventing bacteria opsonisation and thus killing by phagocytes (Peterson *et al*, 1978; Thakker *et al*, 1998). It has been suggested that complement fragments and antibodies bind to the cell wall beneath the capsular layer, where they are inaccessible for recognition by phagocytic cells (Wilkinson & Holmes, 1979; Wilkinson *et al*, 1979).

1.4.2 *S. aureus* and *B. subtilis* peptidoglycan

Peptidoglycan is a bacterial macromolecule and a major component of the cell wall envelope. The Gram-positive cell wall is comprised of multiple peptidoglycan layers that cover the entire cell surface and provide physical integrity to the cell (Scheffers & Pinho, 2005). The main structural features of peptidoglycan are repeating units of the disaccharide N-acetyl glucosamine (GlcNAc) and N-acetylmuramic acid (MurNAc) that are cross-linked via short peptide bridges. These

peptide bridges are attached to the D-lactyl moiety of MurNAc and cross-linked to peptides of adjacent glycan strands thereby generating a three-dimensional molecular network. In *S. aureus* the peptide consist of L-alanine (L-Ala), D-glutamic acid (D-Glu), L-lysine (L-Lys) and D-alanine (D-Ala) of which the L-Lys is further modified with five glycine residues. The glycine pentapeptides are covalently linked to the D-Ala residues of neighbouring wall peptides (Navarre & Schneewind, 1999). The presence of pentaglycine peptides in *S. aureus* peptidoglycan renders this organism susceptible to cleavage by lysostaphin, a product naturally produced by *Staphylococcus simulans* (Schindler & Schuhardt, 1964). The degree of cross-linking is approximately 90 % for *S. aureus* and 40 to 44 % for *B. subtilis* depending on the strain and growth conditions (Atrih *et al*, 1999; Gally & Archibald, 1993; Strominger *et al*, 1967). It has been suggested that the long and flexible pentaglycine peptide in *S. aureus* peptidoglycan connects peptide moieties from different peptidoglycan layers, thus allowing a high degree of cross-linking (Gally & Archibald, 1993; Lapidot & Irving, 1979). Moreover, the pentaglycine peptide serves as an attachment site for the covalent anchoring of surface proteins to the cell wall envelope of *S. aureus* (section 1.4.2.1).

B. subtilis peptidoglycan contains *meso*-diaminopimelic acid (*m*-A_2pm) in place of L-Lys and the glycan strands are directly interlinked via a covalent bond between the *m*-A_2pm moiety of one chain and the D-Ala residue of another chain (Scheffers & Pinho, 2005). In *B. subtilis*, peptidoglycan strands have an average length of 96 disaccharide units (Hayhurst *et al*, 2008; Ward, 1973). In contrast, *S. aureus* synthesizes much shorter peptidoglycan strands with an average of 6 disaccharides (Boneca *et al*, 2000). In addition, approximately 60 % of the MurNAc residues in *S. aureus* peptidoglycan are O-acetylated at position C6-hydroxyl (Bera *et al*, 2005; Ghuysen & Strominger, 1963). This modification of peptidoglycan is mediated by the O-acetyltransferase OatA and renders *S. aureus* resistant to lysozyme (Bera *et al*, 2005).

Peptidoglycan synthesis can be divided into three stages that occur in distinct sub-cellular compartments. The first stage takes place in the cytoplasm and leads to the formation of UDP-MurNAc. The synthesis of UDP-MurNAc is a two-step process. First, the enolpyruvate moiety from phosphoenolpyruvate is transferred to position 3 of GlcNAc to yield UDP-GlcNAc enolpyruvate. In a second reaction the

enolpyruvate group is reduced to lactoyl to yield UDP-MurNAc. Five amino-acids (L-Ala, D-Glu, L-Lys (*S. aureus*) or *m*-A_2pm (*B. subtilis*) and the D-Ala-D-Ala dipeptide) are consecutively attached to UDP-MurNAc to generate the peptidoglycan precursor UDP-MurNAc-pentapeptide (Park's nucleotide). The second stage of peptidoglycan synthesis occurs at the bacterial membrane and requires the activity of two enzymes, MraY and MurG. MraY is a membrane bound enzyme that catalyzes the attachment of the MurNAc-pentapeptide to the undecaprenylphosphate carrier molecule resulting in the production of lipid I. MurG is a glycosyltransferase which then transfers GlcNAc to the C4-hydroxyl MurNAc in lipid I to generate the disaccharide lipid II (Navarre & Schneewind, 1999; Scheffers & Pinho, 2005; van Heijenoort, 2001). In *S. aureus* lipid II is further modified by the peptidyl transferases FemABX, which attach five glycine residues to the ε-amino group of L-Lys (Ehlert *et al*, 1997; Schneider *et al*, 2004). Finally, lipid II is translocated across the bacterial membrane by FtsW, an essential division protein with 10 predicted transmembrane helices (Mohammadi *et al*, 2011). The third stage of peptidoglycan synthesis occurs on the cell surface and involves the incorporation of the peptidoglycan precursor molecule, lipid II, into the nascent peptidoglycan. This is achieved through the activity of penicillin binding proteins (PBPs). PBPs are bifunctional enzymes that catalyze the polymerization of glycan strands (transglycosylation) and promote the formation of cross-links between cell wall peptides (transpeptidation). The transpeptidation reaction involves the proteolytic cleavage of the D-Ala-D-Ala bond in the peptidoglycan precursor and the concomitant formation of an enzyme-substrate intermediate. The cleavage event and the release of the terminal D-Ala provide the energy that is required for the subsequent transpeptidation reaction. In the next step a peptide bridge is formed between the penultimate D-Ala of a donor peptide and an amino group of an acceptor cell wall peptide (Scheffers & Pinho, 2005). Peptidoglycan is a unique and essential structure in bacteria and thus enzymes involved in its synthesis represent effective targets for antimicrobial agents (e.g. β-lactam antibiotics).

In *S. aureus* peptidoglycan synthesis occurs exclusively at the division site (Pinho & Errington, 2003). In contrast, *B. subtilis* inserts newly synthesized peptidoglycan not only at the future division site, but also in helical patterns along the lateral wall thus allowing cell elongation before division (Daniel & Errington, 2003).

It has been suggested that the actin-like MreB proteins direct peptidoglycan synthesis of the sidewall and therefore play important roles in determining the cell wall architecture and hence the cell shape of *B. subtilis* (Carballido-Lopez & Errington, 2003; Jones *et al*, 2001).

1.4.2.1 Anchoring of *S. aureus* surface proteins to the cell wall

S. aureus expresses about 20 surface proteins that are covalently anchored to the cell wall envelope by a mechanism called 'sorting'. Cell wall sorting requires the activity of sortase enzymes that attach the proteins to the peptidoglycan (Mazmanian *et al*, 2001). Proteins for sortase mediated cell wall anchoring contain an N-terminal signal peptide, which allows the sec-dependent secretion of the protein, and a C-terminal cell wall sorting signal (Fischetti *et al*, 1990). The cell wall sorting signal consists of an LPXTG motif followed by a hydrophobic region and a positively charged tail (Fischetti *et al*, 1990; Mazmanian *et al*, 2001). It has been suggested that the charged tail serves as a retention signal to retain the polypeptide chain in the bacterial membrane during the cell wall sorting process (Schneewind *et al*, 1993). SrtA of *S. aureus* cleaves the LPXTG motif between the threonine and the glycine residue and subsequently forms an amide bond between the threonine and pentaglycine cross-bridge in the cell wall (Mazmanian *et al*, 1999). The protein portion C-terminal of the LPXTG motif is released and degraded. Experimental evidence suggests that SrtA uses the peptidoglycan precursor lipid II as an acceptor molecule; however, it is also possible that the enzyme recognizes additional, non-cross linked sites in the mature peptidoglycan structure (Ruzin *et al*, 2002; Ton-That *et al*, 1998). *S. aureus* expresses two sortase enzymes, SrtA and SrtB (Pallen *et al*, 2001). Both proteins are membrane anchored via a single N-terminal hydrophobic domain. SrtA anchors proteins bearing an LPXTG motif and SrtB cleaves the iron-regulated surface protein IsdC within an NPQTN sequence motif and attaches the protein to the cell wall envelope (Mazmanian *et al*, 1999; Mazmanian *et al*, 2002). An *S. aureus srtA* mutant strain displayed reduced virulence in animal infection models of septic arthritis and endocarditis (Jonsson *et al*, 2003; Weiss *et al*, 2004). In contrast, an *S. aureus* strain lacking *srtB* only showed a slight defect in establishing murine arthritis (Jonsson *et al*, 2003).

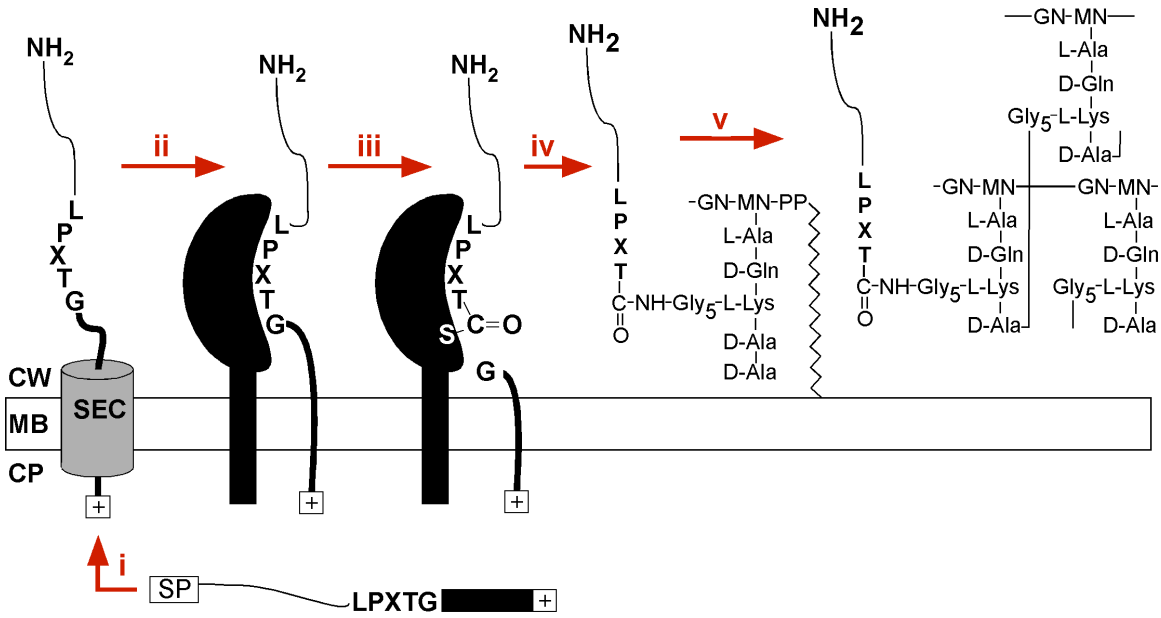

Figure 2: Anchoring of surface proteins in *S. aureus*. (i) Export. Precursor proteins bearing an N-terminal signal peptide (SP) are initiated into the secretory (sec) translocation machinery and the SP is degraded. (ii) Retention. The C-terminal sorting signal retains polypeptides within the sec pathway. (iii) Cleavage. The sortase A enzyme cleaves between the threonine and glycine of an LPXTG motif with the concomitant formation of an enzyme-substrate intermediate. (iv) Linkage. Formation of an amide bond between the carboxyl-group of threonine and the amino-group of the pentaglycine moiety in lipid II. (v) Cell wall incorporation. The lipid linked surface protein is integrated into the peptidoglycan by transglycosylation. Finally the penultimate D-Ala of the pentapeptide subunit with attached surface protein is cross-linked to another cell wall peptide. CW=cell wall, MB=membrane, CP=cytoplasm. Adapted from Mazmanian *et al*, 2001.

1.4.2.2 Immunoglobulin binding proteins of *S. aureus*

S. aureus expresses two immunoglobulin binding surface proteins, protein A (Spa) and Sbi. Spa is a 42 kDa cell wall anchored protein that is present in over 95 % of *S. aureus* strains (Forsgren & Nordstrom, 1974). The protein is comprised of 4 or 5 immunoglobulin-binding repeats followed by a polymorphic variable sequence and a C-terminal cell wall anchoring domain (Moks *et al*, 1986; Uhlen *et al*, 1984). Spa is synthesized as a preprotein and its signal peptide contains an YSIRK/GS sequence motif, which has been shown to address proteins to the future division site (DeDent *et al*, 2008). Spa binds with high affinity to the Fc region of IgG and to the Fab portion of V_H3 class immunoglobulins (Inganas, 1981; Inganas & Johansson, 1981). Binding of the IgG Fc region to Spa results in bacteria coating with IgG molecules in the incorrect orientation not recognized by the neutrophil Fc receptors. As a consequence the bacteria escape phagocytosis by neutrophils (Gemmell *et al*, 1991; Peterson *et al*, 1977). Furthermore, Spa binds to the von Willebrand factor (vWF), a multimeric glycoprotein with the potential to immobilise platelets at the site of endothelial

damage resulting in the formation of a blood clot (Hartleib *et al*, 2000; O'Seaghdha *et al*, 2006). The interaction between Spa and vWF is thought to contribute to the ability of *S. aureus* to adhere to damaged blood vessels (O'Seaghdha *et al*, 2006). In addition, Spa binds and activates the tumour-necrosis factor-α receptor 1 on epithelial cells, which has been shown to induce inflammation during *S. aureus* pneumonia (Gomez *et al*, 2004; Gomez *et al*, 2006).

A second *S. aureus* immunoglobulin binding protein was identified by phage display and denoted Sbi (Jacobsson & Frykberg, 1995; Zhang *et al*, 1998). The 50 kDa Sbi protein is present in many *S. aureus* strains and consists of four globular domains (I-IV) (Burman *et al*, 2008; Zhang *et al*, 1998). Domain I and II are functional immunoglobulin-binding motifs that interact with the IgG Fc fragment, but unlike Spa, not with the IgG Fab sequence (Atkins *et al*, 2008). Sbi domain IV has been shown to bind to β_2-glycoprotein I, a protein with implications in blood coagulation (Zhang *et al*, 1999). Moreover, domains III and IV together and domain IV on its own bind the complement components C3 and factor H (Burman *et al*, 2008; Haupt *et al*, 2008). It has been suggested that Sbi is associated with the bacterial surface, most likely via electrostatic interactions, as the Sbi protein does not contain a C-terminal cell wall sorting signal (Zhang *et al*, 1998). However, in a more recent study it was suggested that Sbi is in fact secreted into the growth medium (Burman *et al*, 2008).

1.4.3 The *S. aureus* cell membrane

The cell membrane of *S. aureus* is a phospholipid bilayer with integrated membrane proteins. The major membrane lipids in *S. aureus* are: diglucosyl diacylglycerol (Glc_2-DAG), phosphatidylglycerol (PG), diacylglycerol (DAG) and lysyl-phosphatidylglycerol (Lys-PG), which represent 8 %, 50 %, 24 % and 10 % of the total lipid content (Koch *et al*, 1984). LTA is only present in the outer leaflet of the bacterial membrane where its concentration is approximately 12 % (Fischer, 1994; Koch *et al*, 1984). Lys-PG is synthesized by MprF, a membrane enzyme, which transfers the lysyl group from lysyl-tRNA to PG resulting in the production of Lys-PG (Nesbitt & Lennarz, 1968; Staubitz *et al*, 2004). The amino group of Lys-PG is believed to impart a positive charge onto the cell membrane resulting in the repulsion of antimicrobial peptides (Peschel & Collins, 2001).

PG is synthesized from phosphatidic acid and glycerolphosphate and serves as a central molecule in *S. aureus* lipid metabolism and as a substrate for LTA synthesis. Based on pulse-chase experiments it was estimated that the pool of PG turns over 3 times in one bacterial doubling (Koch *et al*, 1984). The glycerolphosphate moiety of PG is utilized for LTA synthesis and the resulting DAG is either recycled to PG via phosphatidic acid or used for the synthesis of the glycolipid Glc_2-DAG (Koch *et al*, 1984). An essential enzyme in the recycling pathway is the diacylglycerol kinase DgkB, which phosphorylates DAG to produce phosphatidic acid. The gene encoding for DgkB has been identified in *B. subtilis*, but to date not in *S. aureus* (Jerga *et al*, 2007).

During post-logarithmic growth and under high salt conditions, *S. aureus* accumulates cardiolipin (CL) with the concomitant loss of PG (Kanemasa *et al*, 1972; Short & White, 1971). CL is synthesized from the conversion of two PG molecules to one molecule of CL and one molecule of glycerol (Short & White, 1972). A high CL content may affect membrane fluidity/permeability and help *S. aureus* to cope with stress conditions. Furthermore, CL does not serve as a donor for LTA synthesis (Koch *et al*, 1984). LTA synthesis is a high energy consuming process and therefore the conversion of PG to CL might help *S. aureus* to reduce energy costs under non-dividing or stress conditions.

1.5 WTA and LTA in Gram-positive bacteria

Teichoic acids are polyanionic surface structures that are present in a wide range of Gram-positive bacteria. Two types of teichoic acids can be distinguished: wall teichoic acid (WTA), which is covalently linked to the peptidoglycan and lipoteichoic acid (LTA), which is tethered to the membrane by a lipid anchor. WTA polymers are commonly made up of glycerol- or ribitolphosphate subunits, but tetroses, hexoses or complex sugar combinations have also been reported. LTA is usually less diverse and often consists of a glycerolphosphate chain retained by a glycolipid anchor in the bacterial membrane (Fischer, 1988; Fischer *et al*, 1990; Weidenmaier & Peschel, 2008). Both types of TA can be decorated with additional sugars and amino acids. Most Gram-positive bacteria contain at least one WTA and one LTA type polymer; however, the synthesis of WTA and LTA proceeds through separate pathways even when the actual subunits of the two polymers are the same

(Fischer, 1988). *S. aureus* primarily makes polyribitolphosphate WTA (Baddiley *et al*, 1961), while *B. subtilis* synthesizes two different WTAs, a major and a minor polymer. The major WTA in *B. subtilis* consists of polyglycerolphosphate or polyribitolphosphate subunits depending on the strain (Burger & Glaser, 1964; Karamata *et al*, 1987). The minor polymer comprised of glucose-N-acetyl-galactosamine-phosphate repeating units (Duckworth *et al*, 1972; Shibaev *et al*, 1973). Under phosphate limiting conditions *B. subtilis* produces teichuronic acid, which is devoid of phosphate groups (Ellwood & Tempest, 1972). Both *S. aureus* and *B. subtilis* synthesize LTA of the polyglycerolphosphate type (section 1.5.1).

While the exact function of the TAs is not clear, they are believed to play important roles in bacterial physiology. TAs bind Mg^{2+} ions and thus provide a storage mechanism for ions close to the membrane which might be required for enzyme activity (Heptinstall *et al*, 1970; Lambert *et al*, 1977). Furthermore, TAs are often decorated with positively charged D-alanine residues, which protect bacteria against cationic antimicrobial peptides (Peschel & Collins, 2001). TAs also bind to autolysin enzymes and this interaction might be important for proper targeting of the autolysins to the cell wall envelope (Fischer *et al*, 1981; Suginaka *et al*, 1979). Other proposed functions for TAs include biofilm formation, adhesion, cell division and providing a receptor for bacteriophages (Chatterjee *et al*, 1969; Gross *et al*, 2001; Fedtke *et al*, 2007; Gründling & Schneewind, 2007a). Furthermore, LTA has been shown to interact with the InlB protein of *Listeria monocytogenes* and with the aggregation substance protein of *Enterococcus faecalis* (Jonquieres *et al*, 1999; Waters *et al*, 2004). This interaction might provide a mechanism for the non-covalent attachment of proteins to the cell wall envelope of Gram-positive bacteria. A number of studies have demonstrated that LTA plays a crucial role in activating the immune system via Toll-like receptor 2 (Hermann *et al*, 2002; Morath *et al*, 2001; Morath *et al*, 2002). However, these findings have been challenged by the discovery that most of the commonly used LTA preparations were contaminated with lipoproteins (Hashimoto *et al*, 2006). Thus the proinflammatory potency of LTA remains to be clarified.

WTA was initially thought to be essential for bacterial growth (Bhavsar *et al*, 2004). However, later it was discovered that the mutation was lethal due to the accumulation of a toxic intermediate and that WTA deficient mutants can be obtained

by deleting the *tagO* gene encoding for the first enzyme in the WTA pathway (D'Elia *et al*, 2006). LTA deficient mutants have only recently become available through the discovery of the key enzyme in LTA synthesis, LtaS (Gründling & Schneewind, 2007a). The analysis of WTA or LTA deficient strains demonstrated that these polymers have distinct roles in the cell. For example the absence of WTA in *B. subtilis* leads to cell rounding (D'Elia *et al*, 2006), while the absence of LTA leads to the formation of long filaments that spiral along their long axes (Schirner *et al*, 2009). *S. aureus* cells lacking WTA show slight morphological alterations and are less virulent (Weidenmaier *et al*, 2004; Weidenmaier *et al*, 2005), while the absence of LTA causes severe morphological defects and bacteria are only viable under certain growth conditions (Gründling & Schneewind, 2007a; Oku *et al*, 2009). However, a combined absence of WTA and LTA is lethal for both *S. aureus* and *B. subtilis* (Oku *et al*, 2009; Schirner *et al*, 2009), making enzymes involved in their synthesis promising new drug targets (Falconer & Brown, 2009).

1.5.1 Structure and synthesis of polyglycerolphosphate LTA in *S. aureus* and *B. subtilis*

S. aureus and *B. subtilis* synthesize polyglycerolphosphate LTA consisting of an unbranched 1,3-linked polyglycerolphosphate chain (approximately 23 repeating units) tethered to the bacterial membrane by a glucosyl (β1-6) glucosyl (β1-3) diacylglycerol (Glc_2-DAG) glycolipid (Duckworth *et al*, 1975; Fischer, 1988; Fischer, 1994 and Fig. 3). The hydroxyl groups at the C2 position of the glycerolphosphate subunits are esterified to a varying degree with D-alanine residues and glycosyl modifications are also present in many *Bacillus* sp. (Fischer, 1988; Fischer, 1994; Fischer & Rosel, 1980; Iwasaki *et al*, 1986; Iwasaki *et al*, 1989).

Polyglycerolphosphate LTA is the most widespread LTA type among Gram-positive bacteria and is present in several important human pathogens such as *Bacillus anthracis*, *E. faecalis*, Group A and B Streptococci and *L. monocytogenes*.

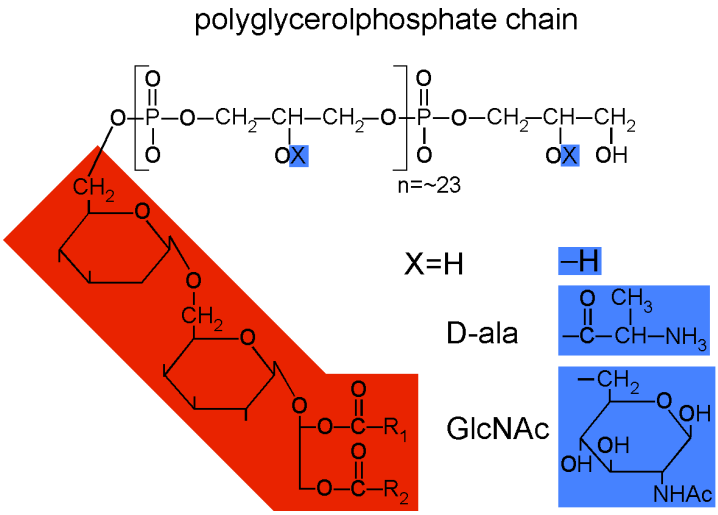

Figure 3: Chemical structure of polyglycerolphosphate LTA. *S. aureus* and *B. subtilis* both synthesize polyglycerolphosphate type LTA, which is tethered to the bacterial membrane by a diglucosyl-diacylglycerol (Glc_2-DAG) glycolipid (red box). The hydroxyl groups at the C2 position of the glycerolphosphate subunits are modified with D-alanine residues in both organisms. *B. subtilis* additionally incorporates N-acetylglucosamine into the LTA polymer. R_1, R_2 = fatty acids. Adapted from Reichmann & Gründling, 2011.

In *S. aureus* and *B. subtilis* LTA synthesis starts in the cytoplasm with the production of the glycolipid anchor Glc_2-DAG (Fig. 4). Three enzymes, PgcA, GtaB and YpfP (UgtB in *B. subtilis*) are required for Glc_2-DAG synthesis. PgcA is α-phosphoglucomutase, which catalysis the conversion of glucose-6-phosphate to glucose-1-phosphate (Gründling & Schneewind, 2007b; Lazarevic *et al*, 2005; Lu & Kleckner, 1994). Glucose-1-phosphate is then activated by the UTP:α-glucose-1-phosphate uridyltransferase GtaB leading to the formation of UDP-Glc (Gründling & Schneewind, 2007b; Pooley *et al*, 1987). The processive glycosyltransferase YpfP transfers two activated glucose moieties from UDP-Glc to DAG resulting in the production of the glycolipid Glc_2-DAG (Jorasch *et al*, 1998; Kiriukhin *et al*, 2001). In the absence of *pgcA*, *gtaB* or *ypfP*, glycolipid synthesis is abrogated, but LTA is still produced. It is assumed that in these mutants the polyglycerolphosphate LTA backbone is directly linked to DAG (Kiriukhin *et al*, 2001).

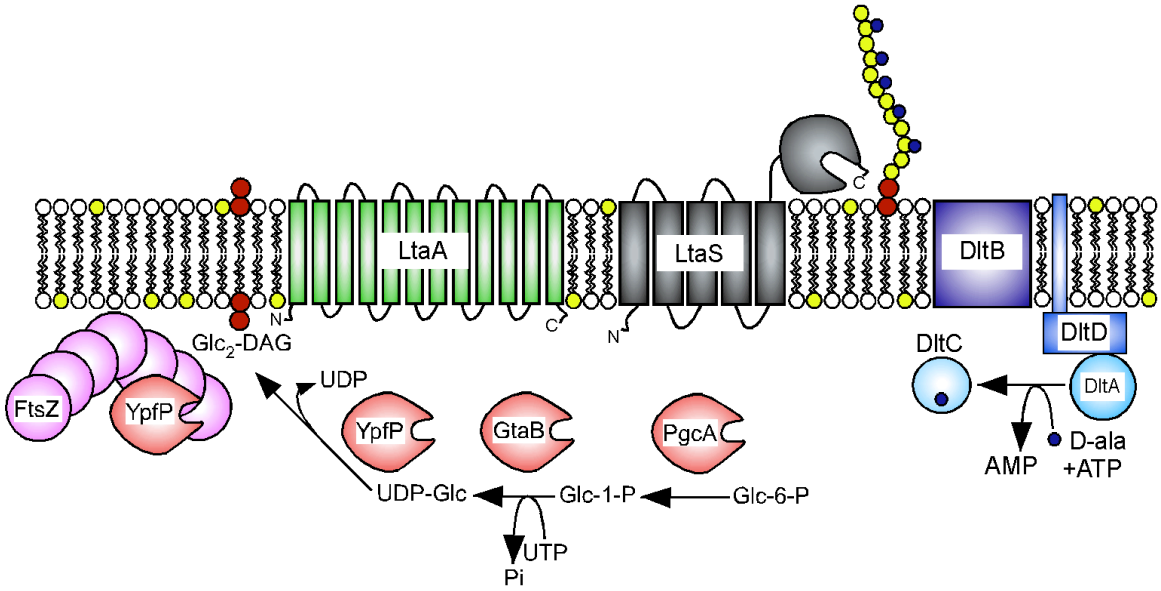

Figure 4: Schematic representation of the LTA synthesis pathway. The cytoplasmic proteins PgcA, GtaB and YpfP (UgtP in *B. subtilis*) are involved in the synthesis of the glycolipid anchor Glc_2-DAG. LtaA is a membrane protein and predicted permease, which is thought to translocate the lipid anchor from the inner to the outer leaflet of the bacterial membrane. On the outside of the membrane, the lipoteichoic acid synthase LtaS attaches glycerolphosphate subunits to the glycolipid resulting in the formation of a linear polyglycerolphosphate chain. D-alanine esters are incorporated into the mature LTA polymer and proteins involved in this process are DltA-DltD.

Inactivation of *ypfP* in *S. aureus* SA113, but not RN4220, resulted in an 87 % reduction of cell-associated and released LTA, indicating that the strain background significantly contributes to the LTA phenotype (Fedtke *et al*, 2007). In addition, the autolytic activity of the SA113 *ypfP* mutant was strongly reduced and its ability to form biofilm on plastic devises completely abrogated (Fedtke *et al*, 2007). Using green fluorescent protein fusions it was demonstrated that YpfP localizes to the cell division site in *B. subtilis* (Weart *et al*, 2007). The same study provided *in vitro* evidence that YpfP inhibits FtsZ polymerization in a concentration dependent manner (Weart *et al*, 2007).

Following the synthesis of the glycolipid anchor in the cytoplasm, Glc_2-DAG is transported to the outer leaflet of the bacterial membrane, where it is used for LTA synthesis. In *S. aureus* the LtaA protein is assumed to be involved in this process. LtaA is a member of a major facilitator super-family clan whose structural gene is located in an operon with *ypfP*. Inactivation of *ltaA* resulted in a large fraction of polyglycerolphosphate chains linked to DAG despite the presence of wild type Glc_2-DAG levels (Gründling & Schneewind, 2007b). The LtaA protein appears to be unique to staphylococci and thus it is not known how the glycolipid traverses the

membrane in other Gram-positive bacteria, such as *B. subtilis*. Once the glycolipid is exposed to the outside, the *S. aureus* LtaS enzyme polymerizes the glycerolphosphate LTA backbone chain (Gründling & Schneewind, 2007a). Experimental evidence suggests that the glycerolphosphate subunits are derived from the membrane lipid phosphatidylglycerol and that the subunits are added to the distal end of the growing LTA chain (Koch *et al*, 1984). Four LtaS orthologues are present in *B. subtilis*, YflE (also named $LtaS_{BS}$), YfnI, YqgS and YvgJ and these enzymes are further discussed in section 1.5.1.2. Finally, D-alanine ester substitutions are incorporated into the mature LTA molecule and the proteins involved in this process are encoded by the *dltABCD* operon (Neuhaus & Baddiley, 2003). In contrast, the process and function of the LTA modification with glycosyl moieties in *B. subtilis* is largely unknown.

1.5.1.1 LtaS, the lipoteichoic acid synthase of *S. aureus*

The *ltaS* gene coding for the lipoteichoic acid synthase in *S. aureus* was discovered in a genetic screen (Gründling & Schneewind, 2007a). LtaS presumably cleaves the membrane lipid PG and utilizes the glycerolphosphate moiety to polymerize the LTA backbone chain. Experimental evidence for these proposed reactions catalysed by LtaS came from the observation that depletion of *ltaS* in *S. aureus* resulted in the complete absence of polyglycerolphosphate LTA, while expression of LtaS in a Gram-negative host, which naturally lacks LTA, lead to the production of glycerolphosphate polymers (Gründling & Schneewind, 2007a). A *S. aureus* mutant strain deleted for the single *ltaS* gene is temperature sensitive and grows at 30°C, but not at 37°C, in media containing at least 1 % (w/v) NaCl (Oku *et al*, 2009). Temperatures at or above 37°C are only tolerated by the *S. aureus ltaS* mutant strain if the media is supplemented with high salt (7.5 % (w/v)) or high sucrose (40 % (w/v)) concentrations, which presumably provide osmoprotection (Oku *et al*, 2009). However, even under the permissive growth conditions the *S. aureus ltaS* mutant strain displayed aberrant placement of division septa, decreased autolysis and reduced levels of peptidoglycan hydrolases, highlighting the importance of LTA for normal cell morphology and physiology (Oku *et al*, 2009).

LtaS and its homologues in other Gram-positive bacteria are predicted membrane proteins composed of five N-terminal transmembrane helices followed by a linker region and a C-terminal extracellular enzymatic domain (eLtaS) (Fig. 5).

Proteomic studies on secreted proteins in *S. aureus* identified the eLtaS domain in the culture supernatant indicating that the LtaS protein is processed during bacterial growth (Gatlin *et al*, 2006; Ziebandt *et al*, 2001). Moreover, N-terminal protein sequencing suggested that the protein is cleaved C-terminal of the fifth transmembrane helix following the linker region after residues ^{215}Ala-Leu-Ala^{217} (Ziebandt *et al*, 2001). Interestingly, treatment of *Staphylococcus epidermidis* with the type I signal peptidase specific inhibitor arylomycin strongly reduced LtaS cleavage, suggesting an involvement of signal peptidase in LtaS processing (Powers *et al*, 2011).

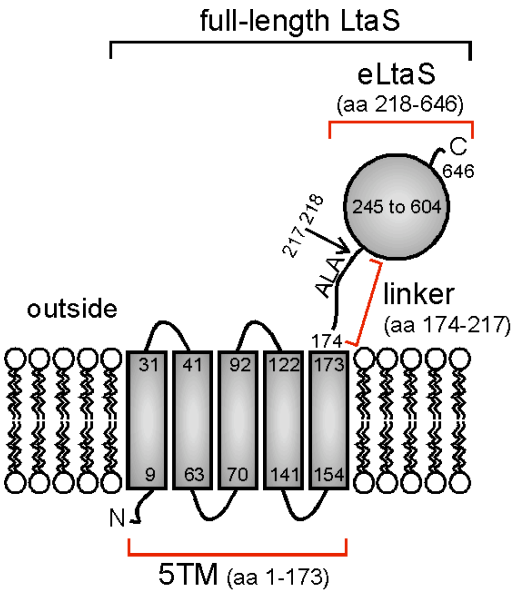

Figure 5: Predicted topology of LtaS. LtaS presumably contains five N-terminal transmembrane helices, which are linked to the extracellular enzymatic domain (eLtaS) via a linker region. The protein is cleaved C-terminal of the five transmembrane domain after residues ^{215}Ala-Leu-Ala^{217} and preceding the eLtaS domain. aa = amino acid.

The crystal structure of the *S. aureus* eLtaS domain alone and in complex with soluble glycerolphosphate has been solved and revealed a threonine as the active site residue (Lu *et al*, 2009). Substitution of this threonine residue with alanine rendered the LtaS protein inactive and unable to synthesize LTA (Lu *et al*, 2009). Moreover, the obtained crystal structure identified a Mn^{2+} ion in the active site center (Lu *et al*, 2009). In agreement with these findings, a recently established *in vitro* assay for LtaS-type enzymes demonstrated that the LtaS protein requires Mn^{2+} for activity (Karatsa-Dodgson *et al*, 2010). The same study provided evidence that the eLtaS domain alone is sufficient to cleave the head group of fluorescently labeled PG producing DAG and

presumably glycerolphosphate, thus providing further evidence that PG is the physiological substrate for LtaS and LTA synthesis (Karatsa-Dodgson *et al*, 2010).

1.5.1.2 LtaS homologues in *B. subtilis*

B. subtilis contains four LtaS orthologues, namely YflE (also named $LtaS_{BS}$), YfnI, YqgS and YvgJ with more than 40 % identity to *S. aureus* LtaS. All four proteins have the same predicted membrane topology and domain structure as *S. aureus* LtaS. Furthermore, in proteomic studies processed forms of YflE and YfnI were detected in the culture supernatant (Hirose *et al*, 2000; Tjalsma *et al*, 2004) showing that at least some of the *B. subtilis* proteins are cleaved and the enzymatic domains released into the supernatant similar to what was observed for *S. aureus* LtaS (Gatlin *et al*, 2006; Lu *et al*, 2009; Ziebandt *et al*, 2001). In both cases the cleavage site was identified C-terminal of the fifth transmembrane domain following an Ala-X-Ala sequence motif (Hirose *et al*, 2000). Moreover, a *B. subtilis* mutant strain deleted for the two signal peptidases *sipT* and *sipV* displayed reduced amounts of cleaved YfnI protein in the culture supernatant, indicating that YfnI is a substrate for SipT and SipV (Antelmann *et al*, 2001).

By expressing each of the four *B. subtilis* orthologues in an *S. aureus ltaS* depletion strain it was revealed that YflE and YfnI encode for LTA synthases, capable of producing polyglycerolphosphate polymers (Gründling & Schneewind, 2007a). However, YfnI-produced polymers could not restore the growth defect of a *S. aureus ltaS* depleted strain and displayed an altered mobility on SDS-PAGE gels, indicative of structural alterations (Gründling & Schneewind, 2007a). No enzyme activity was observed for YqgS or YvgJ. The crystal structure of the YflE enzymatic domain has been solved and revealed the presence of a Mg^{2+} ion in the active center (Schirner *et al*, 2009). These findings are somehow in contrast to the previously reported Mn^{2+} ion observed in the *S. aureus* LtaS active site center (Lu *et al*, 2009). A study on the four LtaS-type enzymes in *B. subtilis* revealed that mutants lacking YflE grew slower in PAB medium compared to the wild type strain and showed a defect in divalent cation homeostasis, an increase in cell chain length, placement of aberrant septa and enhanced cell bending and lysis (Schirner *et al*, 2009). By expressing YflE and YqgS as GFP-fusion proteins it was observed that both proteins localize preferentially to the division site or sporulation septum. Interestingly, a *B. subtilis* mutant strain defective

in *yflE* and *yqgS* expression was unable to form spores (Schirner *et al*, 2009). In contrast to *S. aureus*, a *B. subtilis* mutant with disruptions in all four genes could be readily constructed and was viable. However, this mutant showed severe morphological defects and bacteria formed long filaments that spiralled along their long axes (Schirner *et al*, 2009).

1.5.2 LTA synthesis in other Gram-positive bacteria

Besides *S. aureus* and *B. subtilis*, LTA synthesis has been well studied in *Listeria monocytogenes*. *L. monocytogenes* produces glycerolphosphate type LTA, but the polymer is anchored to the membrane via galactosyl (α1-2) glucosyl (α1-3) DAG (GalGlc-DAG) instead of Glc_2-DAG (Uchikawa *et al*, 1986). Two distinct glycosyltransferases, LafA (LTA anchor formation protein A) and LafB (LTA anchor formation protein B), are required for the synthesis of GalGlc-DAG. LafA is a glucosyltransferase that produces monoglucosyldiacylglycerol (Glc-DAG) and LafB is a galactocyltransferase necessary for adding a galactose moiety to Glc-DAG resulting in the formation of GalGlc-DAG (Webb *et al*, 2009). The genes encoding for *lafA* and *lafB* are organized in an operon together with a third gene *lafC*. Inactivation of *lafC* resulted in the synthesis of an LTA polymer with retarded mobility on SDS-PAGE similar to what was observed for the *S. aureus ltaA* mutant (Gründling & Schneewind, 2007b; Webb *et al*, 2009). However, LafC does not show any homology to the LtaA protein and thus the observed LTA alterations in the *L. monocytogenes lafC* mutant strain do not necessary result from an inefficient transfer of the glycolipid to the outer leaflet of the bacterial membrane. Two LtaS-type enzymes, $LtaP_{LM}$ and $LtaS_{LM}$, are involved in polyglycerolphosphate LTA synthesis in *L. monocytogenes*. $LtaP_{LM}$ transfers the initial glycerolphosphate subunit onto the GalGlc-DAG lipid anchor and $LtaS_{LM}$ polymerizes the LTA backbone chain (Webb *et al*, 2009). In the absence of $LtaP_{LM}$, $LtaS_{LM}$ still synthesizes polyglycerolphosphate, while deletion of $ltaS_{LM}$ in *L. monocytogenes* abrogates polyglycerolphosphate synthesis and leads to severe growth and cell division defects (Webb *et al*, 2009).

Recently, the presence of polyglycerolphosphate type LTA was reported in various species belonging to the phylum Actinomycetes (Rahman *et al*, 2009a; Rahman *et al*, 2009c). However, Actinomycetes appear to lack LtaS homologues and

thus it was suggested that LTA synthesis occurs through an alternative pathway in these bacteria (Rahman *et al*, 2009c).

1.6 Extracellular proteases

S. aureus secretes a range of proteases that have important implications in virulence, tissue destruction, modification of the host immune system and alteration of surface proteins. These extracellular proteases can be divided into three classes based on their catalytic reaction mechanisms: metalloproteases, serine proteases and cysteine proteases. The genes coding for the proteases are organized in three distinct operons, which are: the staphylococcal serine protease (*ssp*) operon, the serine protease like (*spl)* operon, the staphylococcal cysteine protease (*scp*) operon. In addition, *S. aureus* secrets the metalloprotease aureolysin and two related serine proteases $HtrA_1$ and $HtrA_2$ and the corresponding genes for the latter proteases are transcribed on their own (Fig. 6).

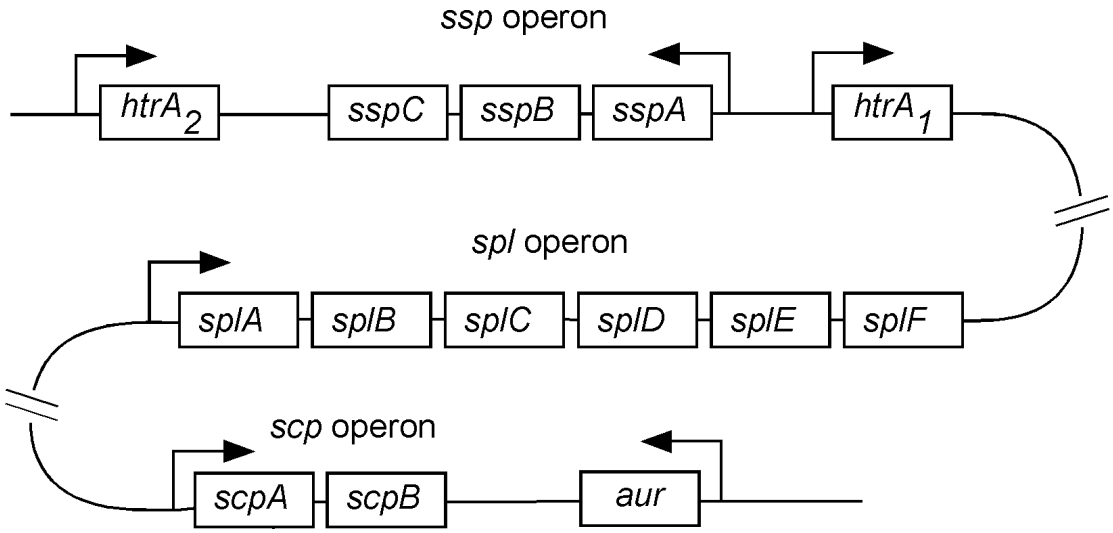

Figure 6: Schematic representation of the chromosomal organization of genes encoding secreted proteases in *S. aureus*. Depicted are the *aur*, $htrA_1$, $htrA_2$ genes and the *ssp* (staphylococcal serine protease), *spl* (serine protease like) and *scp* (staphylococcal cysteine protease) operons. Arrows indicate transcriptional start sites.

1.6.1 Metalloproteases

S. aureus aureolysin is a calcium dependent metalloprotease harbouring a zinc ion in the catalytic centre (Banbula *et al*, 1998). Aureolysin is secreted as a proenzyme and activated upon proteolytic cleavage (Chan & Foster, 1998). Autocatalysis was initially excluded as the activation mechanism, based on the observation that a point mutation in the catalytic centre of aureolysin rendered the protease inactive but did not effect protein processing (Shaw *et al*, 2004). However, in a more recent work the same point mutation did not promote the production of mature aureolysin and only the proenzyme could be detected by western blot (Nickerson *et al*, 2008). The same study demonstrated that the aureolysin propeptide is cleaved by the mature aureolysin protease and suggested a role of the propeptide in proper folding and stabilizing of the protease (Nickerson *et al*, 2008). The *aur* gene occurs in two allelic forms and is highly conserved among *S. aureus* strains, suggesting that the protease may have important housekeeping functions in the processing of surface proteins (Sabat *et al*, 2000). Aureolysin activates the glutamyl endopeptidase SspA (V8) via proteolytic processing and mature SspA in turn cleaves the cysteine protease SspB from its precursor form (Drapeau, 1978; Rice *et al*, 2001). Aureolysin also cleaves *S. aureus* clumping factor B and the human antimicrobial peptide LL-37 (McAleese *et al*, 2001; Sieprawska-Lupa *et al*, 2004). Further studies have demonstrated that aureolysin converts human plasminogen into angiostatin and mini-plasminogen, degrades the plasminogen activator inhibitor-1 and hydrolyses α-antiplasmin (Beaufort *et al*, 2008). Thus aureolysin may play a role in promoting bacterial spread and invasion by activating the fibrinolytic system (Beaufort *et al*, 2008). In addition, aureolysin and SspA have been shown to inhibit protein-dependent biofilm formation in *S. aureus* (Marti *et al,* 2009). Despite the fact that aureolysin modulates virulence factors, an *aur* defective *S. aureus* mutant was not attenuated in an animal model of infection (Calander *et al*, 2004). However, of the three major *S. aureus* extracellular proteases (aureolysin, SspA and SspB), only aureolysin had an impact in survival of *S. aureus* inside macrophages (Kubica *et al*, 2008).

1.6.2 Serine proteases

S. aureus SspA is a serine protease that is synthesized as a proenzyme and is activated by proteolytic cleavage. The protease aureolysin has been shown to promote SspA processing and subsequent activation of the protease (Drapeau, 1978; Nickerson *et al*, 2007). However, in the absence of aureolysin, SspA can also undergo activation by autocatalysis at low levels (Nickerson *et al*, 2007; Shaw *et al*, 2004). The *sspA* gene is organized in an operon with two other genes, which encode for the cysteine protease SspB and the SspB specific inhibitor SspC. Expression of SspA occurs maximum at post-exponentional phase being initiated by Agr (accessory gene regulator) and repressed by SarA (staphylococcal accessory regulator) (Shaw *et al*, 2004). SspA has a narrow substrate specificity cleaving predominantly after glutamic acid and to a lesser extent after aspartic acid (Drapeau *et al*, 1972; Houmard & Drapeau, 1972). SspA cleaves and thus releases the cell wall bound fibronectin binding proteins and protein A, which may facilitate detachment and support bacterial spreading during infection (Karlsson *et al*, 2001; McGavin *et al*, 1997). Furthermore, the SspA protease has been shown to cleave the heavy chains of human immunoglobulins (Prokesova *et al*, 1992). A transposon insertion in *sspA* led to attenuation in multiple animal models, but this was most likely due to downstream effects as a non-polar mutation in *sspA* did not result in attenuated virulence in a tissue abscess model of infection (Coulter *et al*, 1998; Rice *et al*, 2001).

S. aureus secretes two related HtrA (high temperature resistance) serine proteases, $HtrA_1$ and $HtrA_2$. HtrA proteases are highly conserved in bacteria, yeasts, plants, and humans and are associated with stress resistance and survival. The protease was first described in *E. coli* and shown to degrade damaged proteins during thermal stress, but also contain chaperone activity at low temperatures (Krojer *et al*, 2002; Strauch *et al*, 1989). Interestingly, only *S. aureus* $HtrA_1$ was able to fully rescue the thermo-resistance phenotype to a *Lactococcus lactis htrA*-defective mutant (Rigoulay *et al*, 2004). It has been suggested that HtrA proteins have different roles in *S. aureus* depending on the background strain (Rigoulay *et al*, 2005). This was based on the observation that both HtrA proteins were essential for thermal stress survival in the COL strain, but not in RN6390 (Rigoulay *et al*, 2005). A $htrA_1/htrA_2$ RN6390 double mutant displayed defects in the expression of several factors comprising the *agr* regulon and showed diminished virulence in a rat model of endocarditis. In

contrast, only $HtrA_1$ played a minor role in the expression of surface proteins in the background strain COL, but an *htrA*$_1$/*htrA*$_2$ COL mutant strain was not attenuated in virulence (Rigoulay *et al*, 2005).

1.6.3 Cysteine proteases and staphostatins

S. aureus secretes two cysteine proteases, staphopain A (ScpA) and staphopain B (SspB). Both proteases are members of the papain family and are organized in their respective operons *scpAB* and *sspABC* (Dubin, 2003). In both operons the staphopain genes are followed by genes coding for the staphostatins ScpB and SspC, which act as specific inhibitors for their respective staphopains (Massimi *et al*, 2002; Rzychon *et al*, 2003). Furthermore it has been demonstrated that staphostatins and staphopains form non-covalent 1:1 complexes (Rzychon *et al*, 2003). Inactivation of *sspC* in *S. aureus* resulted in a growth defect and reduced protein secretion most likely due to proteolytic inactivation of cytoplasmic proteins by SspB in the absence of SspC (Shaw *et al*, 2005). ScpA and SspB are synthezised as proenzymes and activated by proteolytic cleavage. The latter protease is processed and thus activated by the serine protease SspA (Massimi *et al*, 2002). In contrast, the processing and activation mechanism for ScpA has not been defined yet. ScpA has broad substrate specificity and has been shown to degrade elastin (Bjoorklind & Jornvall, 1974; Potempa *et al*, 1988). In addition, ScpA inactivates the human α1-proteinase inhibitor, although less efficiently compared to the serine protease SspA, which is also able to cleave the inhibitor (Potempa *et al*, 1986). It has been suggested that both proteases function in a cooperative manner to strengthen the effect (Potempa *et al*, 1986). SspB has important implications in virulence as inactivation of *sspB* resulted in significant attenuation of virulence in a mouse abscess model (Shaw *et al*, 2004).

1.6.4 Serine protease-like operon

S. aureus expresses six serine protease-like proteins, which are encoded by the *splA-F* genes and these genes are organized in an operon. Expression of the *spl* operon occurs maximally at post-exponentional phase being positively regulated by Agr (Reed *et al*, 2001). The Spl proteins share significant amino acid sequence identity with each other and with the serine protease SspA. These proteins harbour signal peptides, but lack profragments suggesting that their enzymatic activities do not

depend on activation by proteolytic cleavage (Reed *et al*, 2001). In addition, all Spl proteins contain the conserved amino acids, which make up the classical triad of trypsin like proteases. Proteolytic activities of SplB and SplC were demonstrated and both proteins were shown to degrade casein (Reed *et al*, 2001). SplB has narrow substrate specificity and only cleaves efficiently after the sequence Try-Glu-Leu-Gln (Dubin *et al*, 2008). However, no staphylococcal protein could be identified that contains this sequence, indicating that SplB might function specifically on mammalian proteins (Dubin *et al*, 2008). The structure of SplB has been solved and suggested an unusual activation mechanism in which the protease only forms a functional catalytic machinery upon docking of a substrate with the correct cleavage sequence (Dubin *et al*, 2008). A mutant strain carrying a deletion of the *spl* operon was not attenuated in a rat systemic infection model, suggesting that the Spl proteins do not play a profound role in *S. aureus* virulence (Reed *et al*, 2001).

1.7 Signal peptides and signal peptidases

The majority of proteins that are destined for cell export contain an N-terminal signal peptide. Signal peptides are first recognized in the cytoplasm by soluble factors, which guide the polypeptides to the membrane where they interact with the translocation machinery (van Roosmalen *et al*, 2004). Several translocation machineries have been identified in bacteria of which the general secretion (sec) complex appears to be utilized by the majority of secreted proteins (Rusch & Kendall, 2007). In general, the protein transport across the membrane is an energy dependent process and driven by the hydrolysis of nucleoside triphosphates (Chen & Tai, 1987). After or during the protein transport the signal peptide is cleaved off by signal peptidases and the mature protein is released from the translocase (van Roosmalen *et al*, 2004). The signal peptide is subsequently degraded by signal peptide peptidase (Hussain *et al*, 1982). Notably, membrane proteins that contain signal-like peptides are thought to diffuse laterally from the translocase. Signal peptides of Gram-positive bacteria are on average 32 amino acids long and contain three distinct regions, the N-, H- and C- domain (Nielsen *et al*, 1997b; von Heijne, 1990 and Fig. 7). The N-domain contains positively charged residues and is thought to interact with the translocase and with the negatively charged lipid bilayer (Akita *et al*, 1990; Batenburg *et al*, 1988). Following the N-domain is the H-domain, which consists of a stretch of hydrophobic

residues that are thought to form an α–helical conformation in the membrane (Briggs *et al*, 1986). In the middle of the H-domain, helix breaking residues such as glycine or proline are often present and these residues are thought to allow the loopwise insertion of the signal peptide into the membrane (Inouye & Halegoua, 1980; Inouye *et al*, 1977). The C-domain, following the H-domain, contains the recognition site for the signal peptidase, which removes the signal peptide and subsequently releases the mature protein from the translocase (von Heijne, 1990). Signal peptidases can be divided in two groups, type I and type II. Type I signal peptidases remove signal peptides from secreted preproteins whereas type II signal peptidases are involved in the processing of lipid modified preproteins. The two types of signal peptidases are further discussed below.

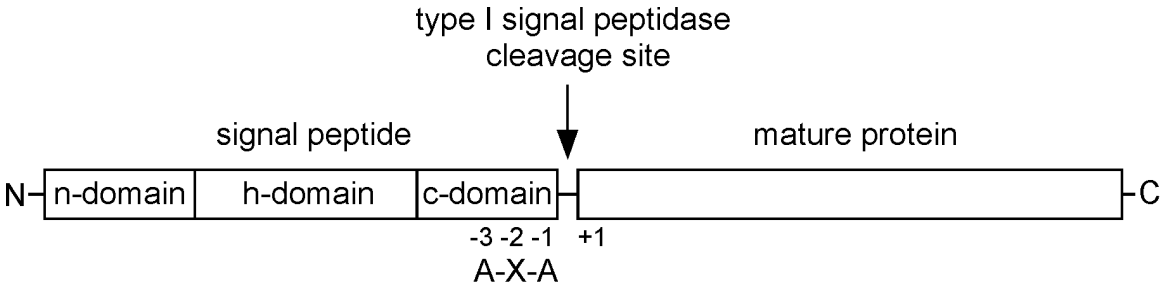

Figure 7: Schematic representation of a secretory preprotein. The signal peptide consists of a positively charged n-domain, a hydrophobic, helical h-domain and a c-domain, which contains the cleavage site. Type I signal peptidases preferentially cleave after an A-X-A motif. Numbers indicate amino-acid positions relative to the cleavage site. Adapted from Buzder-Lantos *et al*, 2009.

1.7.1 Type I signal peptidases

Type I signal peptidases are membrane anchored serine proteases that remove signal peptides from secretory preproteins. These enzymes are highly conserved in bacteria and essential for cell viability. Type I signal peptidases differ from the classical serine proteases in that they use a serine/lysine catalytic dyad for catalysis (Black, 1993). The cleavage sites for type I signal peptidases contain the consensus sequence Ala-X-Ala at position -3 to -1 relative to the cleavage site of which the alanine at position -1 appears to be especially important (Nielsen *et al*, 1997a). Proline seems to be excluded from the +1 position and a proline residue at this position was shown to convert signal peptidase substrates to competitive inhibitors (Barkocy-Gallagher & Bassford, 1992; Bruton *et al*, 2003). Typically, cleavage sites are placed 3-7 residues after the hydrophobic h-domain of a N-terminal signal peptide (Jain *et al*,

1994). This spacing is critical for processing as the signal peptidase active sites are located in close proximity to the bacterial membrane (Jain *et al*, 1994). In general, cleavage by type I signal peptidase is restricted to the first hydrophobic core of a secreted protein; however, signal peptidase processing within a polytopic membrane protein has also been reported (Beltzer *et al*, 1989).

S. aureus expresses two type I signal peptidases, SpsA and SpsB. The genes encoding for the two signal peptidases are organized in an operon together with a third gene, which encodes for a membrane protein with unknown function. SpsA is conserved in all sequenced staphylococcal genomes (Sibbald *et al*, 2006). However, the enzyme is lacking two of the essential residues for catalysis. Thus it is assumed that SpsA is enzymatically inactive. In agreement with this, SpsB, but not SpsA, displayed proteolytic activity in a peptidase *in vitro* enzyme assay (Kavanaugh *et al*, 2007). SpsB is assumed to be the only active signal peptidase present in *S. aureus* and the corresponding gene was shown to be essential in this organism (Cregg *et al*, 1996). The SpsB protein has been expressed in *E. coli* and it was shown that the purified protein cleaves *E. coli* preproteins *in vivo* (Cregg *et al*, 1996). Furthermore, SpsB was shown to remove the N-terminal leader peptide of AgrD, indicating a role of signal peptidase in quorum sensing (Kavanaugh *et al*, 2007). A truncated SpsB version lacking the N-terminal transmembrane domain retained *in vitro* activity; however, the enzymatic activity of the shortened SpsB protein was reduced compared to the wild type enzyme, underscoring the importance of the membrane segment for optimal activity (Rao *et al*, 2009).

In contrast to *S. aureus* which has a single functional type I signal peptidase (SpsB), *B. subtilis* contains five chromosomal encoded type I signal peptidases (SipS, SipT, SipV, SipU, SipW). Some *B. subtilis* strains harbour two additional type I signal peptidases (SipP) and the corresponding genes are encoded on plasmids (Meijer *et al*, 1995). SipT, SipS and SipP are classified as major signal peptidases as *B. subtilis* requires at least one of these proteases for viability (Tjalsma *et al*, 1998; Tjalsma *et al*, 1999b). In contrast, SipU, SipV and SipW play minor roles in prepeptide processing. SipS, SipT, SipV and SipU have overlapping substrate specificity and expression of SipS and SipT is upregulated in the post exponentional growth phase (Tjalsma *et al*, 1997). All *B. subtilis* type I signal peptidases contain a single N-terminal transmembrane domain, with the exception of SipW, which appears to have both, an

N-terminal and a C-terminal membrane anchor. SipW shows a high degree of sequence similarity to eukaryotic type I signal peptidases and contains a histidine residue in place of the catalytic lysine base, a typical feature for eukaryotic type I signal peptidase (Tjalsma *et al*, 1998).

1.7.2 Type II signal peptidases

Type II signal peptidase (Lsp-lipoprotein signal peptidase) are membrane anchored enzymes that remove signal peptides from lipid modified preproteins. Proteins that are anchored to the membrane after translocation contain a conserved lipobox at the C-terminus of their signal peptides (von Heijne, 1989). This lipobox possesses a unique cysteine residue, which is lipid modified by the diacylglyceryl transferase (Lgt-lipoprotein diacylglycerol transferase) (Sankaran & Wu, 1994). Thus, after translocation and subsequent lipid modification the corresponding proteins remain attached to the membrane by their N-terminal lipid modified cysteine residue. Finally, the signal peptide is processed by the type II signal peptidase at the conserved cleavage site within the lipobox and upstream of the conserved cysteine residue (Hutchings *et al*, 2009).

Type II signal peptidases are highly conserved and found in Gram-negative and Gram-positive bacteria, but appear to be absent in eukaryotes (Paetzel *et al*, 2002). Most bacteria, including *S. aureus* and *B. subtilis*, contain a single Lsp and Lgt protein. Type II signal peptidases have a conserved topology and are predicted to span the membrane four times (Paetzel *et al*, 2002). These enzymes are thought to belong to a novel class of proteases that utilize an aspartic acid catalytic dyad for catalysis (Tjalsma *et al*, 1999c). An *lgt* defective *S. aureus* strain was unable to process lipoproteins, indicating that signal peptides can not be removed by type II signal peptidase prior to diacylglycerol acylation (Bubeck Wardenburg *et al*, 2006). Lipoprotein processing by type II signal peptidase is essential for viability in *E. coli*, but not in *B. subtilis* or *S. aureus* (Bubeck Wardenburg *et al*, 2006; Tjalsma *et al*, 1999a; Yamagata *et al*, 1982). Furthermore, a *Mycobacterium tuberculosis* strain inactivated for *lsp* displayed reduced virulence in an animal model of infection (Sander *et al*, 2004). A signature-tagged mutagenesis screen in *S. aureus* identified *lsp* as a potential factor required for virulence in this organism (Mei *et al*, 1997).

However, the calculated LD_{50} value of the *S. aureus lsp* mutant was similar compared to that of the WT strain in a murine model of bacteraemia (Mei *et al*, 1997).

Chapter 2

Materials and Methods

2.1 Bacterial strains, growth conditions and storage

Bacterial strains used in this study are listed in Table 1. *Escherichia coli* strains were grown at 37°C with shaking in Luria Bertani broth (LB) or at 37°C on LB agar. *Staphylococcus aureus* strains were grown at 37°C with shaking in Tryptic Soy Broth (TSB) or at 37°C on Tryptic Soy Agar (TSA). *Bacillus subtilis* strains were grown at 30°C with shaking in Difco Antibiotic Medium 3 (PAB) or at 30°C on LB agar. When appropriate the medium was supplemented with antibiotics, 0.5-1 mM isopropyl β-D-thiogalactoside (IPTG) or 300 ng/ml anhydrotetracycline (Atet) (unless otherwise stated) as indicated in Table 1 or in the text. Antibiotics were used at the following concentrations: for *E. coli* cultures: Ampicillin (Amp), 100 μg/ml; Kanamycin (Kan), 30 μg/ml; Tetracycline (Tet), 10 μg/ml; for *S. aureus* cultures: Erythromycin (Erm), 10 μg/ml; Chloramphenicol (Cam), 7.5 to 10 μg/ml; Kanamycin, 90 μg/ml and IPTG at 1 mM; for *B. subtilis* cultures: Erythromycin, 5 μg/ml; Chloramphenicol, 10 μg/ml; Kanamycin, 10 μg/ml; Spectinomycin (Spec), 100 or 200 μg/ml.

For long-term storage of bacterial strains, 500 μl of an overnight culture was mixed with 500 μl freezer medium (10 % (w/v) BSA, 10 % (w/v) monosodium glutamate) and stored at -80°C.

2.2 Recombinant DNA techniques

2.2.1 Purification of plasmid DNA from *E. coli*

Plasmid DNA was isolated from *E. coli* cells using either miniprep (5 ml overnight culture, Macherey-Nagel plasmid DNA purification kit) or midiprep (200 ml overnight culture, QIAGEN plasmid midi kit) purification systems. The purified plasmids were dissolved in 150 μl ddH_2O (midiprep) or 40 μl 5 mM Tris pH 8 (miniprep) and stored at -20ºC.

2.2.2 Isolation of chromosomal DNA from *S. aureus*

To isolate chromosomal DNA from *S. aureus*, 1.5 ml of an overnight culture was centrifuged for 3 min at 16,000 × *g*. The pellet was suspended in 50 μl TSM buffer (50 mM Tris pH 7.5, 0.5 M sucrose, 10 mM $MgCl_2$) and lysostaphin (AMBI

Products LLC) at a final concentration of 100 μg/ml was added to the cell suspension. The mix was incubated for 1 h at 37ºC and the subsequent preparation steps were completed with the Wizard Genome Purification Kit (Promega, Madison USA) according to the manufacturer's instructions. The isolated chromosomal DNA was rehydrated in 25 μl ddH_2O for 1 h at room-temperature (RT) and stored at -20ºC.

2.2.3 Estimation of DNA concentration

The presence and quality of isolated DNA was either estimated by agarose gel analysis or, when a more accurate measurement was required, determined spectrophotometrically by measuring the absorbance at 260 nm using a NanoDrop Spectrophotometer ND-1000 (Labtech).

2.2.4 Separation of DNA by agarose gel electrophoresis

DNA was visualized by gel electrophoresis using 1 % (w/v) agarose gels. For preparing the gel, electrophoresis grade agarose was dissolved in 1 × Tris-Boric Acid-EDTA buffer (TBE; 89 mM Tris base, 89 mM boric acid, 2 mM EDTA) or 1 × Tris-Acetic Acid-EDTA buffer (TAE; 40 mM Tris base, 40 mM acetic acid, 1 mM EDTA) and SYBR Safe solution (Invitrogen) was added to the molten agarose according to manufacture's guidelines. The gel was immersed in 1 × TBE or 1 x TAE, and the electrophoresis was carried out in a Bio-rad mini agarose gel cell at 100 V. Before loading the gel, DNA samples were mixed with 6 × DNA loading dye (0.25 % (w/v) bromophenol blue, 30 % (w/v) glycerol) and a 1 kb DNA ladder (Invitrogen) was run alongside the samples to size the separated DNA fragments. The DNA bound SYBR safe dye was visualized by exposing the gel to ultraviolet light using a BioDoc-It (Anachem) and the resultant image printed out on a video graphic printer (Sony).

2.2.5 Restriction digestion of DNA

To screen for plasmids containing correct inserts, restriction digestions of the purified plasmids were carried out in a total volume of 20 μl, which included 2 μl buffer (10 ×), 0.1-1 μg DNA and 1 U enzyme. For cloning purposes the reaction was scaled up to 100 μl and 10 μg BSA was added to the mix. All restriction enzymes were purchased from New England Biolabs and digestions were incubated for 3 h

(except digestions using *Bgl*II and *Sal*I which were incubated overnight) in a 37ºC water bath. Depending on the enzyme, reaction specific buffers were used as directed by the manufacturer's guidelines. Double digestions using two restriction enzymes simultaneously were preformed for restriction analysis provided that both enzymes are active in the same buffer. For cloning purposes, digested DNA was purified using the QIAGEN PCR clean-up gel extraction kit and eluted in 40 µl 5 mM Tris pH 8.

2.2.5.1 Vector preparation

Plasmid vectors used for cloning purposes were isolated from *E. coli* cells using the midiprep DNA purification system described in section 2.2.1. Purified plasmid DNA (7.5 µg) was digested with appropriate restriction enzymes and subsequently utilized for ligation reactions.

2.2.6 Polymerase chain reaction (PCR)

PCR was conducted to amplify DNA fragments *in vitro*. Primers used in this study were purchased from Sigma-Aldrich and are listed in Table 2. Specific oligonucleotide primers were designed to introduce appropriate restriction sites to both the 5' and 3' ends. This subsequently allowed the cloning of the PCR-fragment into the target vector. In general, PCR reactions were carried out in a total volume of 50 µl, which included 5 µl Taq buffer (10 ×) or 10 µl Herculase buffer (5 ×), 1 µl forward and reverse primer (10 µM of each), 2 µl dNTPs (40 mM), 10-100 ng template DNA and 1 µl Herculase (Agilent) or 0.5 µl Taq (NEB). The PCR programme comprised of an initial denaturation step at 95ºC for 2 min followed by 5 cycles in which DNA was denatured at 95ºC for 45 sec, annealed at 45ºC for 45 sec, and extended at 72ºC for 1 min/kb. For the next 25 cycles, the annealing temperature was raised to 53ºC. A final extension step of 7 min was carried out before the temperature was dropped and subsequently held at 10ºC. PCR products were purified using the QIAGEN PCR clean-up or gel extraction kit and DNA was eluted in a final volume of 40 µl 5 mM Tris pH 8.

2.2.7 Ligation of DNA fragments

Ligations of cut PCR fragments and cut plasmid vectors were performed using the T4 DNA ligase from New England Biolabs. Typically, reactions were set up in a total volume of 20 µl containing 2 µl ligase-buffer (10 ×), 2 µl vector-DNA, 12 µl Insert-DNA and 1 µl T4-DNA-Ligase. Ligation reactions were incubated at 17ºC overnight and the next day the enzyme was heat inactivated for 20 min at 60ºC in a heat block.

2.2.8 Transformation of *E. coli* cells

2.2.8.1 Preparation of rubidium chloride competent XL1 Blue cells

E. coli XL1 Blue cells were made chemically competent by culturing cells overnight in 10 ml LB medium supplemented with tetracycline. The following day, the culture was diluted 1:100 in 500 ml PSI broth (5 g/l bacto yeast extract, 20 g/l bacto tryptone, pH 7.6, 20 mM $MgSO_4$) and grown at 37ºC with agitation to an optical density (OD_{600}) of 0.6. Cells were then incubated on ice for 15 min and subsequently harvested by centrifugation at 6,000 × *g* for 10 min. The supernatant was discarded and the cell pellet suspended in 10 ml of ice-cold TfbI (30 mM CH_3COOK, 100 mM RbCl, 10 mM $CaCl_2$, 50 mM $MnCl_2$, 15 % (v/v) glycerol, pH 5.8). After adding an additional 190 ml ice-cold TfbI, cells were incubated on ice for a further 15 min and collected by centrifugation as described above. The final pellet was suspended in 15 ml ice-cold TfbII (10 mM MOPS, 75 mM $CaCl_2$, 10 mM RnCl, 15 % (v/v) glycerol, pH 6.5) and 500 µl aliquots were snap frozen in a dry ice/ethanol bath and stored at -80ºC.

2.2.8.2 Transformation of rubidium chloride competent XL1 Blue cells

For transformation of XL1 Blue cells, 100 µl rubidium chloride competent XL1 Blue cells were thawed on ice. Subsequently, 20 µl ligation product was added to the cells and the cells were incubated on ice for 30 min. After heat-shocking at 42ºC for 45 sec, cells were placed on ice for a further 5 min, then immediately transferred to 900 µl SOC medium (5 g/l bacto yeast extract, 20 g/l bacto tryptone, 3.6 g/l glucose, 2.5 mM KCl, pH 7.0) and incubated for 1 h at 37ºC for recovery. An aliquot (100 µl)

of this cell suspension was plated on LB agar containing appropriate antibiotics. The remaining culture was pelleted by centrifugation at 11,000 × *g* for 3 min. The supernatant was discarded and the cells were suspended in a small volume of LB medium and plated on LB agar containing appropriate antibiotics. Plates were incubated at 37ºC overnight.

2.2.8.3 Preparation of electrocompetent CLG190 cells

To make *E. coli* CLG190 cells competent, the cells were grown overnight in 10 ml LB supplemented with tetracycline. The following day, the culture was diluted 1:100 in 100 ml LB and grown at 37ºC with agitation to an OD_{600} of 0.6. After a 15 min incubation period on ice, the cells were harvested by centrifugation at 9,700 × *g* for 10 min. The supernatant was discarded and the pellet suspended in 5 ml of ice-cold sterile ddH_2O. An additional 100 ml ice-cold sterile ddH_2O was added to the cells before repeating the centrifugation step. The final pellet was dissolved in 1.2 ml sterile 10 % (v/v) glycerol and 300 µl aliquots were snap frozen in a dry ice/ethanol bath and stored at -80ºC.

2.2.8.4 Electroporation of CLG190 cells

For electroporation of CLG190 cells, 100 µl electrocompetent cells were thawed on ice. Meanwhile, 10 µl ligation product was dialyzed against ddH_2O for 45 min on a nitrocellulose filter (Millipore) before being added to the cells. The mix was transferred to a 1 mm electroporation cuvette (Equibio) and electroporated using a Biolabs Gene Pulser with the following settings: 200 Ω (Resistance), 1.8 kV (Volts), 25 µFD (Capacitance). Immediately after electroporation, the cell suspension was transferred to 900 µl SOC medium and incubated for 1 h at 37ºC for recovery. An aliquot (100 µl) of this cell suspension and the remaining cells were plated on LB agar containing appropriate antibiotics as described in section 2.2.8.2. Plates were incubated at 37ºC overnight.

2.2.9 Transformation of *S. aureus* cells

2.2.9.1 Preparation of electrocompetent *S. aureus* cells

To make *S. aureus* cells competent, an overnight culture was grown in 4 ml TSB at 37ºC with agitation in the presence of appropriate antibiotics and supplements. The following day the bacterial culture was diluted 1:100 in 150 ml TSB containing appropriate antibiotics and supplements and grown for 3 h to an OD_{600} of approximately 2. The subsequent steps were as described in 2.2.8.1 except that cold sterile 0.5 M sucrose was used as wash solution, and the washing step was repeated 3 times. The final pellet was suspended in 1 ml cold sterile 0.5 M sucrose and 120 µl aliquots were snap frozen in a dry ice/ethanol bath and stored at -80ºC.

2.2.9.2 Electroporation of *S. aureus* cells

Aliquots (100 µl) of frozen electrocompetent *S. aureus* cells were thawed on ice. The plasmid preparation and electroporation process were carried out as described in section 2.2.8.4 except with the following modifications. Electroporation settings were: 100 Ω, 2.5 kV, 25 µFD. Cultures were recovered in 900 µl brain heart infusion (BHI) 0.5 M sucrose medium supplemented with IPTG when appropriate and incubated for 1 h at 37ºC for recovery. Two volumes (75 µl and 150 µl) were plated on TSA containing appropriate antibiotics and supplements, and plates incubated at 37ºC overnight.

2.2.10 Phage transduction

Chromosomal deletions marked with antibiotic-resistance cassettes were transferred between *S. aureus* strains by transduction using phage 85. The first step in the transduction process involved the preparation of a phage plate lysate as follows. The strain containing the marker to be transduced was grown overnight in 2 ml LB/TSB (2:1) at 37ºC with agitation in the presence of appropriate antibiotics and 5 mM $CaCl_2$. The following day, the culture was diluted 1:50 in 5 ml LB/TSB (2:1) supplemented with appropriate antibiotics and 5 mM $CaCl_2$ and grown at 37ºC with agitation for 3 h. One hundred µl of undiluted phage stock, and 100 µl of 10^{-1}, 10^{-2}, 10^{-3} and 10^{-4} phage stock dilutions in TMG (10 mM Tris pH 7.5, 10 mM $MgSO_4$, 0.1 % (w/v) gelatin) were used to infect 500 µl of this bacterial cell suspension. The mixture

was incubated at RT for 30 min to allow for one cycle of replication. Next, 5 ml of molten top agar (0.8 % (w/v) NaCl, 0.8 % (w/v) Bacto-agar) was added to the infected culture and the mixture was spread on TSA containing appropriate antibiotics. Plates were incubated at 37ºC overnight. The following day, plates that displayed confluent lysis were overlayed with 4 ml TMG and incubated at RT for 30 min. The liquid containing the desired phage particles was transferred from the plates to a falcon tube and centrifuged for 20 min at 3,220 × *g*. The supernatant was removed and filtered though a 0.2 μm filter. Phage plate lysates were stored at 4ºC.

A 25 ml culture of the recipient strain was grown overnight in LB/TSB (2:1) supplemented with appropriate antibiotics and 5 mM $CaCl_2$. The following day, the culture was harvested by centrifugation at 3,220 × *g* for 10 min. The supernatant was discarded and the pellet was suspended in 5 ml LB/TSB (2:1) containing 5 mM $CaCl_2$. An aliquot (250 μl) of this concentrated culture was mixed with 200 μl phage lysate and the suspension was incubated at 37ºC with shaking for 20 min. Cells were placed on ice and 24 μl ice-cold 1M sodium citrate was added to the mixture. Cultures were subsequently washed twice, each time by pelleting the cells for 3 min at 11,000 × *g*, discarding the supernatant and resuspending the pellet in 1 ml ice-cold 40 mM sodium citrate. The final pellet was suspended in 300 μl 40 mM sodium citrate and two volumes (100 μl and 200 μl) were plated on TSA containing appropriate antibiotics and 40 mM sodium citrate. Colonies obtained were restreaked once on TSA supplemented with 40 mM sodium citrate and appropriate antibiotics, then twice more on TSA containing appropriate antibiotics but no sodium citrate.

2.3 Cell fractionation

S. aureus overnight cultures were diluted 1:100 and grown at 37°C for 3 ½ h. One ml aliquots of these mid-log cultures were removed and centrifuged at 7,000 × *g* for 15 min. The supernatant was transferred to a fresh tube and proteins therein precipitated with trichloroacetic acid (TCA; referred to as supernatant fraction). The remaining bacterial pellet was suspended in 1 ml lysostaphin digestion buffer (30 % (w/v) raffinose, 50 mM Tris-HCl pH 7.5, 20 mM $MgCl_2$) and incubated for 1 h at 37°C in the presence of 200 μg/ml lysostaphin (AMBI Products LLC). Resultant protoplasts were collected by centrifugation at 6,000 × *g* for 20 min, the supernatant

removed and centrifuged at 100,000 × *g* at 4°C for 1 h. Proteins in the supernatant fraction were subsequently precipitated with TCA (referred to as cell wall fraction). Protoplasts were suspended in 1 ml membrane buffer (100 mM Tris-HCl pH 7.5, 10 mM $MgCl_2$, 60 mM KCl), lysed by five cycles of freeze-thawing, and proteins TCA precipitated (referred to as membrane/cytoplasmic fraction). In order to precipitate proteins in the different sample fractions, 10 % (w/v) TCA final concentration was added to the samples. Samples were vortexed briefly, incubated on ice for 1 h and then centrifuged at 17,000 × *g* for 10 min. The supernatant was aspirated and the TCA precipitated protein pellet was washed twice with ice-cold acetone, each time by suspending the pellet in 1 ml ice-cold acetone, incubating the sample on ice for 10 min and centrifugating at 17,000 × *g* for 10 min. After the final centrifugation step, the pellet was air dried and suspended in 2 × sample buffer normalized for OD_{600} of bacterial cultures; that is samples from 1 ml culture with an OD_{600} of 3 were suspended in 45 µl 2 × sample buffer. Samples were boiled for 5 min, centrifuged at 17,000 × *g* for 5 min, and 15 µl aliquots were subsequently separated on a 10 % (w/v) SDS-PAGE and analyzed by western blot. LtaS and control proteins were detected by western blot using rabbit polyclonal primary antibodies at a 1:20,000 dilution and the HRP-linked donkey anti-rabbit IgG antibody (GE Healthcare) at a 1:10,000 dilution.

2.4 *S. aureus* growth curves

For growth curves, *S. aureus* strains were grown overnight at 37ºC in 4 ml TSB medium containing 1 mM IPTG and appropriate antibiotics. The following day, bacteria from 1 ml culture were washed 3 times with 1 ml TSB by centrifugation and re-suspension. Next, 5 ml TSB containing 300 ng/ml Atet and appropriate antibiotics were inoculated with 50 µl washed bacterial suspensions (1:100 dilution) and cultures incubated at 37ºC with shaking. At time 0 and then every 2 h, culture aliquots were removed and OD_{600} values determined. At 4 h all cultures and at 8 h indicated cultures were diluted 1:100 into 5 ml fresh TSB containing 300 ng/ml Atet and appropriate antibiotics to maintain bacteria in the logarithmic growth phase. Growth curves using the inducible *spsB S. aureus* strain ANG2009 were performed with the following slight modifications. Overnight cultures of strain ANG2009 were washed as described above and then diluted 1:100 into 7 ml TSB medium with and without IPTG and appropriate antibiotics. Cultures were grown at 37°C with shaking and bacterial

growth was monitored by determining OD_{600} readings every two hours. At the 4 h time point the culture was washed as described above and back-diluted, and at the 8 h time point bacteria were back-diluted again 1:100 into fresh media to keep bacteria in the logarithmic growth phase.

2.5 LTA and protein detection by western blot

For the detection of *S. aureus* cell associated LTA and proteins by western blot, 1 ml culture samples were withdrawn from bacterial cultures at the 4 or 8 h time point as indicated in the results sections. Samples were mixed with 0.5 ml of 0.1 mm glass beads and subsequently lysed by vortexing upside down for 45 min at 4°C. Glass beads were sedimented by centrifugation for 1 min at 200 × *g* and 0.5 ml of culture supernatant was transferred to a fresh tube. Bacterial debris and LTA were collected by centrifugation at 17,000 × *g* for 15 min and suspended in sample buffer normalized for OD_{600} of bacterial cultures; that is, samples from a culture with on OD_{600} of 1 were suspended in 15 µl 2 × sample buffer. Samples were boiled for 20 min, centrifuged at 17,000 × *g* for 5 min and 10 µl aliquots were separated on a 10 or 15 % (w/v) SDS-PAGE gel and analyzed by western blot. For protein detection in the culture supernatant, 1 ml culture aliquots were centrifuged at 17,000 × *g* for 5 min and 900 µl of the supernatant was transferred to a fresh tube, and proteins were TCA precipitated as described in section 2.3. The protein pellet was air dried and suspended in 2 × sample buffer normalized for OD_{600} readings as described above. Samples were boiled for 5 min, centrifuged at 17,000 × *g* for 5 min and 10 µl aliquots were separated on a 10 % (w/v) SDS-PAGE gel and analyzed by western blot. For LtaS detection in *E. coli*, 1 ml of an overnight culture was harvested by centrifugation at 17,000 × *g* for 10 min. The supernatant was discarded and the cell pellet suspended in 2 × sample buffer normalized for OD_{600} that is, samples from a culture with on OD_{600} of 1 were suspended in 45 µl 2 × sample buffer. Samples were boiled for 30 min, centrifuged at 17,000 × *g* for 5 min and 7.5 µl aliquots were separated on a 10 % (w/v) SDS-PAGE and analyzed by western blot. For LTA detection, the polyglycerolphosphate-specific LTA antibody (Clone 55 from Hycult biotechnology) and HRP-conjugated anti-mouse IgG (Cell Signaling Technologies, USA) were used at 1:5,000 and 1:10,000 dilutions, respectively. For LtaS protein detection the polyclonal eLtaS specific

antibody (Lu *et al*, 2009) and the HRP-conjugated anti-rabbit antibody (Cell Signaling Technologies, USA) were used at 1:20,000 and 1:10,000 dilutions, respectively. His-tagged proteins were detected with the HRP-conjugated anti-His antibody (Sigma) used at a 1:10,000 dilution.

2.6 *B. subtilis* LTA detection by western blot

For LTA detection in *B. subtilis*, wild type and mutant strains were grown for 20 to 22 h at 30°C in 5 ml PAB medium with shaking. Samples for LTA analysis were prepared from whole cells as follows: bacteria from 3 to 4 ml culture were collected by centrifugation for 30 min at 17,000 × *g*. Bacterial pellets were suspended in 2 × protein sample buffer normalized for OD_{600} readings; that is 100 µl 2 × sample buffer was used per ml culture of OD_{600} = 3. Samples were boiled for 45 min, centrifuged for 5 min at 17,000 × *g* and 10 µl analyzed on a 15 % (w/v) SDS-PAGE gel. The humanized monoclonal LTA antibody (Biosynexus Incorporated; Gaithersburg, MD) and the HRP-conjugated polyclonal rabbit anti-human IgA, IgG, IgM, Kappa, Lambda antibody (DakoCytomation) were used at 1:10,000 dilutions for LTA detection. Membrane blocking and antibody incubations were performed in TBST buffer containing 3 % (w/v) BSA.

2.7 Standard techniques for protein analysis

2.7.1 Protein quantification

The quantity of protein samples was determined with the BCA kit from Pierce. The assay was completed as directed by manufacture's guidelines.

2.7.2 Sodium Dodecyl Sulphate Poly-Acrylamide Gel Electrophoresis (SDS-PAGE)

SDS-PAGE was performed in order to separate proteins according to their molecular weights as well as to analyze LTA. Ten or 15 % (w/v) Tris/glycine SDS-PAGE gels were prepared as described by Sambrook *et al* (1989) and, if not stated otherwise, these gels were used for protein and LTA analysis. The electrophoresis was carried out in 1 × SDS running buffer (14.4 g/l glycine, 3 g/l Tris-base, 1 g/l SDS)

using Hoefer´s Mini Protein Electrophoresis system. Samples were electrophoresed for 45 min at 200 V and a protein ladder (Bench Mark™Prestained, Invitogen) was run alongside the samples to size the proteins. Fifteen % (w/v) trycine SDS-PAGE gels were prepared as described by Schagger & von Jagow (1987) and these gels were used in a Bio-rad Mini-PROTEAN tetra cell according to manufacturer's guidelines. After separation, proteins were either visualized by coomassie staining (section 2.7.3) or samples were transferred to a polyvinylidene difluoride (PVDF) membrane and proteins or LTA detected by western blotting (section 2.7.4).

2.7.3 Protein staining with Coomassie brilliant blue

In order to visualize proteins after separation on SDS-PAGE, gels were immersed in a Coomassie brilliant blue staining solution (2.5 g/l Coomassie brilliant blue R250, 45 % (v/v) methanol, 10 % (v/v) acetic acid) and incubated at RT for 1 h with moderate shaking. Gels were then repeatedly washed with a destaining solution (45 % (v/v) methanol, 10 % (v/v) acetic acid) and subsequently imaged to record the result.

2.7.4 Western blotting

For protein and LTA detection by western blot, samples were transferred from SDS-PAGE gels to a PVDF membrane (Millipore) using Hoefer's electrophoretic transfer cell system. The electrotransfer was conducted for 1 h in transfer buffer (3 g/l Tris-Base, 14.5 g/l glycine, 20 % (v/v) methanol) at 1000 mA and RT. The membrane was subsequently blocked for 1 h with 20 ml of 5 % (w/v) milk in Tris buffered saline containing 0.1 % (v/v) Tween pH 7.4 (TBST). When necessary 10 µg/ml human IgG (Sigma) was added to the blocking solution as well as during antibody incubation in order to prevent antibody binding to *S. aureus* protein A and Sbi. The incubation with the primary antibody was carried out at 4°C overnight in 20 ml of 5 % (w/v) milk in 1 × TBST. The next day, unbound antibody was removed by washing the membrane three times, each time for 10 min with 20 ml 1 × TBST. If required membranes were incubated with a secondary antibody in 20 ml of 5 % (w/v) milk in 1 × TBST for 3 h and afterwards washed as described above. Subsequently, membranes were incubated with ECL (100 mM Tris pH 8.5, 2.5 mM Luminol, 2.5 mM P-Coumaric acid) and 0.009 % (v/v) hydrogen peroxide and the chemiluminescent signal was captured using

Hyperfilm ECL (GE Healthcare). Films were developed using an automated developer (AGFA-Healthcare N.V.).

2.8 Purification of His-tagged LtaS fragments from *S. aureus* culture supernatant

S. aureus strains ANG587 (p*itet-ltaS-his*) and ANG1370 (p*itet-ltaS*$_{S218P}$*-his*) were used for the expression and purification of His-tagged proteins from the respective culture supernatants. To this end, strains ANG587 and ANG1370 were grown overnight at 37°C in 30-50 ml TSB medium containing 1 mM IPTG and appropriate antibiotics. The following day, cultures were washed three times with 30-50 ml TSB by repeated centrifugation and suspension. Subsequently, 2 to 4 L TSB medium containing 300 ng/ml Atet and appropriate antibiotics were inoculated 1:100 with washed bacterial suspensions and cultures were grown at 37°C overnight. Next day, bacteria were removed by centrifugation for 15 min at 13,600 × *g* and the culture supernatants filtered through 0.2 µm nylon membranes (Whatman). His-tagged proteins were purified from these filtered culture supernatants by gravity flow chromatography. Supernatants were applied to equilibrated Ni-NTA columns (1.5 ml column volume, 3 ml resin) (QIAGEN) and extensively washed with buffer A (50 mM Tris pH 7.5, 150 mM NaCl, 5 % (v/v) glycerol), followed by two additional wash steps with buffer A containing 10 and 50 mM imidazole. Proteins were eluted in 4 × 1 ml fractions with buffer A containing 500 mM imidazole. Fractions containing purified protein were pooled and protease inhibitors (Roche) were added to the suspension. Next, proteins were concentrated using Amicon Centricons (10 kDa cutoff) and 20 µl aliquots were separated on 10 % (w/v) SDS-PAGE gels and the proteins visualized by staining with Coomassie brilliant blue. The main protein band was excised from the gel and analyzed by standard tryptic digest and mass spectrometry at the Taplin Biological Mass Spectrometry Facility at the Harvard Medical School.

2.9 *In vitro* enzyme assay for LtaS-type enzymes

2.9.1 Protein purification from *E. coli* cells

E. coli strains ANG1474 (Rosetta pProEX-eYflE), ANG1475 (Rosetta pProEX-eYfnI), ANG1476 (Rosetta pProEX-eYvgJ), ANG1477 (Rosetta pProEX-eYqgS) were used for the expression and purification of eYflE, eYfnI, eYvgJ and eYqgS. To this end, respective strains were grown overnight at 37°C in 50 ml LB supplemented with appropriate antibiotics. The following day, bacterial cultures were diluted 1:50 in 2 L LB medium containing appropriate antibiotics and grown at 37°C with shaking. Once the cultures reached an OD_{600} of 0.4, protein expression was induced for 3-4 h by the addition of 0.5 mM IPTG. Bacteria were collected by centrifugation at 6,000 × *g* for 10 min. Subsequently, bacteria pellets were suspended in 20 ml buffer A (see section 2.8) and cells were lysed by 2 cycles of French pressing at 1,100 psi. Lysates were cleared by centrifugation at 26,000 × *g* for 30 min and His-tagged proteins were purified by gravity flow chromatography as described in section 2.8. Fractions containing the purified proteins were pooled and further purified by size exclusion chromatography using a 16/60 Superdex 200 column (GE Healthcare) and a 50 mM Tris pH 7.4, 200 mM NaCl, 5 % (v/v) glycerol buffer system. Purified protein containing fractions were pooled and concentrated using Amicon centricons with a 10 kDa cut off. The protein concentration was measured and the purity of the protein was estimated by separating 10 µg purified protein on 10 % (w/v) SDS-PAGE gels and Coomassie staining.

2.9.2 Standard enzyme assay for LtaS-type enzymes

The enzymatic activity of purified LtaS-type proteins was measured by following the hydrolysis of NBD-labeled phosphatidylglycerol (NBD-PG) using a method described previously (Karatsa-Dodgson *et al*, 2010). First, the commercially available NBD-PG lipid (Avanti; order number 810163) was purified on TLC plates. To this end, 100 µg NBD-PG was spotted onto pre-run Å60 silica gel plates (Macherey-Nagel) and run for 15 min in a chloroform: methanol: H_2O (65:25:4) solvent system. The major fluorescent band was excised from the TLC plate by scraping the silica gel of the respective area into a falcon tube. Lipids were

subsequently extracted for 15 min at RT with 8 ml of a 1:1 methanol-chloroform mixture and occasional vortexing. Samples were centrifuged at 7,000 × *g* for 10 min and the supernatant was transferred to a fresh tube. The silica gel was extracted a second time as described above and the supernatant was combined with the first extraction. Next, 7.2 ml ddH_20 was added to the mixture, the samples were vortexed vigorously and subsequently centrifuged at 7,000 × *g* for 10 min for phase separation. The bottom phase containing the purified lipid was transferred to a glass vial. Lipids were dried under a stream of nitrogen and stored at -20°C until further use.

For setting up the standard enzyme assay, 1.8 ml of 10 mM sodium succinate buffer, pH 6.0, ionic strength (μ) = 50 mM (adjusted with NaCl) was added to 25 μg of TLC-purified NBD-PG lipid. Lipids were brought into suspension by sonication for 45 sec at 11 amplitude microns using a Soniprep Sanyo sonicator. Next, $MnCl_2$ or other divalent cations were added from a 1 M stock solution to give a final concentration of 10 mM, the samples were vortexed, and 303 μl (~ 4.166 ng lipid) aliquots transferred into test tubes. Reactions were initiated by the addition of 1.52 μM purified protein and assay mixtures were then incubated for 3 h in a 37ºC water bath. Next, reactions were halted and lipids extracted by the addition of $CHCl_3$/MeOH to give a final ratio of assay volume:$CHCl_3$:MeOH of 0.9:1:1. Tubes were vortexed vigorously, centrifuged for 5 min at 17,000 × *g* and fractions of the bottom chloroform phase transferred to a new tube and dried under a stream of nitrogen. Dried lipids were then suspended in 10 μl chloroform, spotted onto pre-run Å60 silica gel plates and separated using a chloroform: methanol: H_2O (65:25:4) solvent system. Plates were dried and subsequently imaged using a Fujifilm FLA-5000 imager equipped with a 473 nm excitation laser and a FITC emission filter. Where indicated, fluorescent signals of lipid reaction products were quantified using the AIDA software (Raytest Isotopenmessgeräte GmbH). The phospholipase PC-PLC (PLC) from *B. cereus* (Sigma EC 3.1.4.3) was used as a positive control and assays with this enzyme were set up as follows: TLC-purified NBD-PG lipid (25 μg) was brought into solution by sonication in 1.8 ml of BPS, pH 7.4. Next, 10 mM $CaCl_2$ final concentration was added to the lipid suspension. Aliquots of 303 μl (~ 4.166 ng lipid) were transferred to a test tube and reactions were initiated by the addition of 2.5 U of PLC. Reactions were incubated at RT on a rotor for 3 h and lipids subsequently extracted as described above.

To gain insight into enzyme kinetics, a time course experiment was performed by removing and analyzing samples at the indicated time points. Reaction products were quantified using a fluorescence plate reader and the AIDA software and percent hydrolysis of input lipid calculated based on the signal obtained for the PLC control reaction, which proceeds to near completion. Reactions were set up with triplicate samples and average values and standard deviations were plotted. Experiments were performed three times and a representative result is shown. Maximal enzyme reaction rates were determined from the slope of the linear fit through the first three data points and average values with standard deviations from the three independent experiments calculated. To determine the enzyme specificity, the fluorescently labeled lipids 16:0-6:0 NBD-PC (Avanti 810130), 16:0-6:0 NBD-PE (Avanti 810153) and 16:0-6:0 NBD-PS (Avanti 810192) were purified on TLC plates and enzyme reactions set up as described above.

2.10 *S. aureus* lipid extraction and glycolipid analysis by TLC

For *S. aureus* lipid extraction and glycolipid analysis, *S. aureus* strains were grown overnight at 37ºC in 10 ml TSB supplemented with 1 mM IPTG and appropriate antibiotics. The next day, cells were collected by centrifugation for 10 min at 1,300 × *g* and bacterial pellets washed 3 times with 10 ml TSB. After the final centrifugation step, washed cultures were suspended in 10 ml TSB and diluted 1:100 into 200 to 800 ml fresh TSB medium supplemented with 300 ng/ml Atet and appropriate antibiotics. Cultures were incubated at 37ºC with shaking for 5 h and then placed on ice for 30 min. Next, bacteria were collected by centrifugation for 10 min at 8,000 × *g*, washed once with 5 ml of ice-cold 0.1 M sodium citrate buffer pH 4.7 and suspended in 3 ml of the same buffer. Bacteria were lysed and lipids extracted using a modified Bligh-Dyer method as described previously (Gründling & Schneewind, 2007b; Kates, 1972). To this end, cultures were dispensed into three 2 ml Fast Prep tubes containing 0.5 ml of 0.1 mm glass beads and cells were lysed by shearing three times for 45 sec in a Fast-Prep machine (Thermo Servant) at setting 6. Bacteria were chilled on ice between each run for 5 min. Glass beads were settled by centrifugation at 200 × *g* for 1 min. The supernatant was transferred to a fresh tube and cell debris

collected by centrifugation at 4,050 × *g* for 30 min. The pellet was washed once with 15 ml of 0.1 M sodium citrate pH 4.7 and the final pellet was dissolved in 1 ml of the same buffer. For lipid extraction, methanol and chloroform were added to give a final ratio of MeOH:$CHCl_3$:buffer of 2:1:0.8. Lipids were subsequently extracted for 2 h at RT with frequent vortexing. Next, samples were centrifuged at 2,600 × *g* for 20 min, the supernatant transferred to a fresh tube and the lipids were extracted a second time as described above. The two extracts were subsequently combined and methanol and buffer was added to obtain a final ratio of MeOH:$CHCl_3$:buffer of 1:1:0.9. Samples were vortexed vigorously and then centrifuged at 2600 × *g* for 20 min. The bottom chloroform phase containing the lipids was transferred to a fresh tube. Lipids were dried under a stream of nitrogen and suspended in chloroform to a final concentration of 50 mg/ml. Ten µl (500 µg lipids) were spotted onto pre-run Å60 silica gel plates (Macherey-Nagel) and the lipids separated using a chloroform : methanol : H_2O (65:25:4) solvent system. Glycolipids were visualized by spraying plates with 0.5 % to 1.5 % (w/v) α-naphthol in 50 % (v/v) methanol and then with 95 % (v/v) H_2SO_4 (Gründling & Schneewind, 2007b; Kates, 1972). Plates were subsequently heated to 100°C until glycolipid bands became visible.

2.10.1 Lipid analysis by MALDI mass spectrometry

MALDI mass spectrometry analysis was essentially performed as described previously (Webb *et al*, 2009), and the lipids extracted and prepared as follows: total membrane lipids were isolated from *S. aureus* strains and 5 × 0.5 mg lipids (2.5 mg total) were spotted and separated on a TLC plate using the same solvent system as described in section 2.10. Areas containing glycolipids were determined by developing one lane of the TLC run in parallel with α-naphthol/H_2SO_4. Appropriate silica gel areas were scraped off and lipids extracted as described previously (Gründling & Schneewind, 2007b). Dried lipids were suspended in 10 µl of 0.5 M 2,5-dihydroxybenzoic acid (DHB) MALDI matrix dissolved in 1:1 methanol : chloroform and 1 µl was spotted directly onto MALDI plates or diluted 1:10 using 0.5 M DHB matrix and 1 µl spotted. Spotted MALDI plates were analysed using a a MALDI micro MX™ machine (Waters, UK) and spectra recorded in the reflector positive ion mode. As an additional calibration standard, 25-50 pmoles of bradykinin

peptide standard (Sigma) with an absolute mass of 757,3997 ($M+H^+$) was spotted in α-cyano-4-hydroxycinnamic acid (CHCA) matrix, which was suspended at 10 mg/ml in 70 % (v/v) acetonitrile 0.1 % (v/v) trifluoroacetic acid (TFA). Samples were analyzed at the Proteomics Facility at Imperial College London.

2.11 LTA purification and structural analysis

2.11.1 LTA purification

LTA was purified from *S. aureus* and *B. subtilis* cells using a previously described 1-butanol extraction method (Gründling & Schneewind, 2007a; Morath *et al*, 2001). Briefly, *S. aureus* strains were grown overnight at 37ºC with shaking in 150 ml TSB supplemented with 1mM IPTG and appropriate antibiotics. The following day, cultures were centrifuged for 10 min at 1,300 × *g* and washed 3 times with 150 ml TSB. Washed cultures were diluted 1:100 into 6 L (strain ANG514) or 12 L (strain ANG515) fresh TSB containing 300 ng/ml Atet and appropriate antibiotics and incubated at 37ºC with shaking for 4 to 5 h. *B. subtilis* strains were grown overnight at 30ºC in 8 L (strain ANG1691 and ANG1697) or 12 L (ANG1696) PAB medium. LTA extraction and purification by hydrophobic interaction chromatography was performed as described previously (Gründling & Schneewind, 2007a). To this end, bacterial cultures were placed on ice for 1 h and then harvested by centrifugation at 6,100 × *g* for 10 min. The supernatant was discarded and the bacterial pellet washed once with 80-160 ml of 0.1 M sodium citrate pH 4.7. The final pellet was suspended in 40 ml of the same buffer and the cell suspension was mixed with 40 ml of 0.1 mm glass beads. Bacteria were disrupted by shearing the cells five times for 2 min at 4ºC in a bead beater (Biospec). Between each run, bacteria were placed on ice for 5 min to chill. Glass beads were settled by centrifugation at 200 × *g* for 1 min and the supernatant was transferred to a fresh tube. Subsequently, glass beads were washed with 40 ml of 0.1 M sodium citrate pH 4.7, sedimented as described above, and the supernatant was combined with the previous one. Bacterial debris were collected by centrifugation at 13,300 × *g* for 40 min and washed once with 45 ml of 0.1 M sodium citrate pH 4.7. For extracting LTA, the final pellet was suspended in 40 ml of 0.1 M sodium citrate pH 4.7, mixed with an equal volume of 1-buthanol and stirred for 30

min at RT. The sample was centrifuged at 13,300 × *g* for 40 min and the liquid transferred to a fresh tube before repeating the centrifugation step. The aqueous (lower) phase containing the LTA was retrieved and the extraction process was repeated once as described above. The final extract was dialyzed against two changes of 4 L of 20 mM sodium citrate pH 4.7 using a Spectra/Por 6 dialysis membrane (1,000-Da cutoff; Spectrum Laboratories, Inc.). Next, the sample was adjusted to give a final concentration of 15 % (v/v) 1-propanol in 0.1 M sodium citrate pH 4.7 and subsequently applied to a 24 × 1.6 cm octylsepharose column equilibrated with 15 % (v/v) 1-propanol in 0.1 M sodium citrate pH 4.7. The column was washed with 100 ml of 15 % (v/v) 1-propanol in 0.1 M sodium citrate pH 4.7 and LTA eluted with a linear 15-65 % (v/v) 1-propanol gradient in 0.05 M sodium citrate pH 4.7. LTA containing fractions were identified by western blot, pooled and dialyzed in the cold 7-11 times against 4 L ddH_2O and subsequently lyophilized.

2.11.2 LTA structure analysis by NMR and biochemical assays

For NMR analysis, 1 mg purified LTA was suspended in 500 µl D_2O of 99.96 % purity (Sigma) and lyophilized. This procedure was repeated once, and the lyophilized LTA sample was then suspended in 500 µl D_2O of 99.99 % purity (Sigma) and the 1d ^1H NMR spectra recorded at 600 MHz (^1H) and 300 K on a Bruker AvanceIII spectrometer equipped with a TCI cryoprobe. To ensure accurate integrals of species with potentially differing ^1H T_1 values, spectra were recorded with a total recycle time of 6 s and a ^1H flip angle of *ca*. 60°. The length of the glycerolphosphate chain as well as the percentage of D-alanine substitution was calculated from the ^1H NMR integrals of the appropriate LTA specific peaks. The LTA length calculation was based on a C15 : C18 fatty acid composition (59 non-exchangeable protons from CH_2/CH_3 groups), which is the most abundant lipid anchor present in *S. aureus* LTA (Fischer, 1994). Glucose, phosphate and D-alanine contents of LTA samples were determined using standard biochemical assays, which were performed as previously described (Grassl & Supp, 1995; Kunst *et al*, 1984; Schnitger *et al*, 1959). Assays to determine the glucose content of purified LTA samples were performed as follows: reactions containing 2 M HCl and 0.2 or 0.4 mg purified LTA were set up in a final volume of 60 µl. Standard reactions containing 0 to 5 mM glucose final concentration were prepared in the same manner in 60 µl 2M HCl. Samples were incubated at 95ºC

for 2 ½ h and subsequently neutralized by the addition of 60 µl 2 M NaOH. Next, 50 µl of neutralized sample was transferred to a fresh tube and 1 ml solution 1 (4 mM $MgSO_4$, 110 mM NaH_2PO_4, 3.2 mM HCl, 1.9 mM ATP, 1.6 mM NADP-Na_2, pH 6.5 adjusted with 2 M NaOH) was added. The mixture was transferred into a low UV cuvette (Fischer) and the absorbance was determined at 339 nm. Subsequently, 10 µl enzyme mix (1 U hexokinase (Sigma), 1.8 U glucose-6-phosphate dehydrogenase (Sigma), 100 mM $MgSO_4$) was added and the reaction was incubated for 20 min at RT before measuring the absorbance a second time. The increase in the absorbance reflects the formation of NADPH, which is proportional to the glucose concentration in the sample.

For determining the D-alanine concentration of the purified LTA samples, assays were set up as follows: reactions were prepared in a final volume of 80 µl containing 0.2 M NaOH and 0.2 or 0.1 mg purified LTA. Standard reactions with D-alanine concentrations ranging from 0 to 5 mM final concentration were included in the assay. Samples were incubated for 1 h at 37ºC and subsequently neutralized by the addition of 4 µl 2 M NaOH. Next, 50 µl neutralized sample was transferred to a low UV cuvette and 917 µl reaction buffer (0.1 M Tris pH 8.5, 0.27 mM NADH, 9.2 U lactate dehydrogenase (Fischer), 8.5 U catalase (Sigma)) was added. The absorbance was measured spectrophotometrically at 339 nm. Next, 66.6 µl of 37.5 U/ml D-amino-acid oxidase (Sigma) was added, samples were incubated at RT for 20 min, and the absorbance was determined. The drop in NADH, measured by the absorbance at 339 nm, is proportional to the D-alanine concentration in the samples.

The phosphate concentration in the purified LTA samples was determined as follows: the assay was performed in a final volume of 280 µl containing 2 M HCl and 40 or 80 µg purified LTA. Standard solutions ranging from 0 to 2.5 mM phosphate final concentration were included in the assay. Samples were incubated at 98ºC for 3 h in a heat block before cooling. Subsequently, 400 µl of an acid solution (13.9 % (v/v) H_2SO_4, 2.6 % (v/v) $HClO_4$) was added and samples incubated at 150ºC for further 3 h. Next, samples were cooled to RT and mixed with 2 ml reduction solution (19.1 mM $(NH_4)_2MoO_4$, 0.25 M CH_3COONa, 56.8 mM $C_6H_8O_6$). The preparation was incubated at 37ºC for 2 h before measuring the absorbance at 578 nm. The regression line obtained from the standard solutions was used to determine the phosphate concentration in the LTA samples. LTA chain length and chain modification were

determined by calculating the ratio of the phosphate : ½ glucose concentration (2 glucose molecules per LTA anchor) and the ratio of phosphate : D-alanine concentration, respectively.

2.12 Strain and plasmid construction

Primers used in this study are listed in Table 2. Plasmid p*itet-sec-eltaS* was constructed for the expression of a secreted eLtaS version. This plasmid was obtained by amplifying the protein A signal peptide sequence from *S. aureus* RN4220 chromosomal DNA with primers 401/404 and the *eltaS* sequence from plasmid pCL55-*ltaS* using primers 405/319. The resulting products were fused by SOE (Splice Overlap Extension) PCR (Horton *et al*, 1989) using primers 401/319. The final PCR product was digested with *Avr*II/*Bgl*II and ligated with plasmid p*itet*, which had been digested with the same enzymes. Plasmid p*itet-sec-eltaS* was initially obtained in *E. coli* XL1 Blue (strain ANG590) and subsequently integrated into the lipase gene *geh* of *S. aureus* ANG499, yielding strain ANG595 (p*itet-sec-eltaS*).

Plasmids p*itet-*TM_{srtA}*-eltaS* and p*itet-*$5TM_{ltaA}$*-eltaS* were constructed for the expression of LtaS variants with altered staphylococcal membrane domains. The TM_{srtA} sequence was amplified from *S. aureus* RN4220 chromosomal DNA using primers 427/432 and the *eltaS* coding sequence from plasmid pCL55-*ltaS* using primers 433/319. The $5TM_{ltaA}$ sequence was amplified from plasmid pCL55-*ypfP/ltaA* using primers 260/438 and the linker + *eltaS* sequence from plasmid pCL55-*ltaS* using primers 439/319. Appropriate PCR fragments were fused by SOE PCR with primers 427/319 (*TM_{srtA}-eltaS*) or 260/319 (*$5TM_{ltaA}$-eltaS*). The final PCR products were cloned as *Avr*II/*Bgl*II fragments into plasmid p*itet* as described above and recovered in *E. coli* XL1 Blue (strains ANG1211 and ANG1214). The plasmids were subsequently electroporated into *S. aureus* ANG499, yielding strains ANG1217 (p*itet-*TM_{srtA}*-eltaS*) and ANG1220 (p*itet-*$5TM_{ltaA}$*-eltaS*).

Plasmids p*itet-1TM-eltaS* and p*itet-3TM-eltaS* were constructed for the expression of LtaS variants with shortened membrane domains. Gene fragments coding for the first or the first three TM helices of *ltaS* were amplified using primer 318 in combination with primer 434 or 436 and the linker + *eltaS* sequence was amplified using primer 319 in combination with primer 435 or 437, respectively. pCL55-*ltaS* was used as template DNA for all PCR reactions. Respective PCR

products were fused by SOE PCR using primers 318/319 and the final PCR fragments were restriction digested with *Avr*II/*Bgl*II and ligated with plasmid p*itet*. The resulting plasmids were recovered in *E. coli* XL1 Blue, giving strains ANG1212 and ANG1213 and subsequently introduced into *S. aureus* ANG499, yielding strains ANG1218 (p*itet-1TM-eltaS*) and ANG1219 (p*itet-3TM-eltaS*).

Plasmids pCN34*itet-sec-eltaS,* pCN34*itet-TM*$_{srtA}$*-eltaS,* pCN34*itet-1TM-eltaS,* pCN34*itet-3TM-eltaS,* and pCN34*itet-5TM*$_{ltaA}$*-eltaS* were constructed for expression of the corresponding fusion proteins from a multi-copy plasmid vector. Respective gene-fusions and the p*itet* promoter region were amplified from plasmids p*itet-sec-eltaS,* p*itet-TM*$_{srtA}$*-eltaS,* p*itet-1TM-eltaS*, p*itet-3TM-eltaS* and p*itet-5TM*$_{ltaA}$*-eltaS* using primer pair 159/877. The resulting PCR products and vector pCN34 were restriction digested with *Kpn*I/*Pst*I and ligated together. Plasmids were initially obtained in *E. coli* strain XL1 Blue (strains ANG2158-2162) and subsequently introduced into *S. aureus* ANG499, yielding strains ANG2165 (pCN34*itet-sec-eltaS)*, ANG2166 (pCN34*itet-TM*$_{srtA}$*-eltaS)*, ANG2167 (pCN34*itet-1TM-eltaS),* ANG2168 (pCN34*itet-3TM-eltaS)*, ANG2169 (pCN34*itet-5TM*$_{ltaA}$*-eltaS*).

Plasmids pCN34-*5TM,* pCN34-*ltaS and* pCN34*itet-ltaS*$_{T300A}$ were constructed to investigate the functionality of a split enzyme. For the construction of plasmids pCN34-*ltaS* and pCN34-*5TM*, the full-length *ltaS* gene or the 5TM region were amplified including the *ltaS* promoter region from plasmid pCL55-*ltaS* using primer pairs 86/87 or 86/424, respectively. The PCR products and the pCN34 vector were digested with *BamH*I/*Sal*I and ligated. For construction of plasmid pCN34*itet-ltaS*$_{T300A}$, *ltaS*$_{T300A}$ and the p*itet* promoter region were amplified from plasmid p*itet-ltaS*-T300A using primers 159/800. The PCR product and pCN34 vector were restriction digested with *Kpn*I/*Sal*I and ligated. Plasmids were recovered in *E. coli* XL1 Blue resulting in strains ANG1221, ANG1222 and ANG1689. These three plasmids and the empty pCN34 vector were then electroporated into *S. aureus* ANG595, yielding strains ANG1226 (pCN34), ANG1227 (pCN34-*5TM*), ANG1228 (pCN34-*ltaS*) and ANG1690 (pCN34*itet-ltaS*$_{T300A}$), respectively.

Plasmids p*itet-ltaS*$_{S218P}$ and p*itet-ltaS*$_{E174}$ were constructed for the expression of LtaS variants with either a serine to proline substitution at amino acid position 218 or with a glutamate to proline substitution at amino acid position 174. The mutations were initially introduced by QuikChange mutagenesis (Stratagene) in vector pOK-*ltaS*

using primers 487/488 or 711/712 and the resulting plasmids pOK-*ltaS*$_{S218P}$ and pOK-*ltaS*$_{E174P}$ were recovered in *E. coli* XL1 Blue (strains ANG1242 and ANG2182). The mutant *ltaS* alleles were then amplified using primers 318/319 and cloned as *Avr*II/*Bgl*II fragments into vector p*itet*. The plasmids p*itet-ltaS*$_{S218P}$ and p*itet-ltaS*$_{E174P}$ were recovered in *E. coli* XL1 Blue (strains ANG1244 and ANG2183) and subsequently electroporated into *S. aureus* strain ANG499, yielding strains ANG1246 (p*itet-ltaS*$_{S218P}$) and ANG2184 (p*itet-ltaS*$_{E174P}$).

Plasmids p*itet-ltaS-his and* p*itet-ltaS*$_{S218P}$*-his* were constructed for the expression of WT LtaS and the LtaS$_{S218P}$ variant fused to a C-terminal His-tag and used for protein purification from supernatants of *S. aureus* cultures. Respective genes were amplified from plasmids pCL55-*ltaS* and p*itet-ltaS*$_{S218P}$ using primers 318/420. The PCR products and the p*itet* plasmid were restriction digested with *Avr*II/*Bgl*II and ligated. Plasmids were obtained in *E. coli* XL1 Blue (strains ANG584 and ANG1368) and subsequently electroporated into *S. aureus* ANG499, yielding strains ANG587 (p*itet-ltaS-his*) and ANG1370 (p*itet-ltaS*$_{S218P}$*-his*).

Plasmids p*itet-yfnI*$_{TMlink}$*-eltaS,* p*itet-ltaS*$_{Tmlink}$*-eyfnI-his,* p*itet-yqgS*$_{Tmlink}$*-eltaS,* p*itet-ltaS*$_{Tmlink}$*-eyqgS-his,* p*itet-ltaS*$_{TM\text{-}link}$*eyfnI-his,* p*itet-yfnI*$_{TM\text{-}link}$*eltaS,* p*itet-ltaS*$_{TM\text{-}link}$*eyflE-his,* p*itet-yflE*$_{TM\text{-}link}$*eltaS,* p*itet-yflE*$_{TM\text{-}link}$*eyfnI-his,* p*itet-yflE*$_{Tmlink}$*-eyfnI-his* were constructed to study the function of hybrid fusions between *S. aureus*/*B. subtilis* LtaS-type enzymes. Plasmids p*itet-yfnI*$_{TMlink}$*-eltaS* and p*itet-yfnI*$_{TM\text{-}link}$*eltaS* were constructed by amplifying the *yfnI*$_{TM}$ and the *yfnI*$_{TM}$ + linker sequence from plasmid pCL55-*yfnI* using primer 322 in combination with primer 495 or 525. The *eltaS* and the linker + *eltaS* sequence were amplified from plasmid pCL55-*ltaS* using primer 319 in combination with primers 494 or 524. Appropriate PCR fragments were fused by SOE PCR with primers 322/319. The final PCR products were digested with *Avr*II/*Bgl*II and ligated with plasmid p*itet*, which has been digested with the same enzymes. Plasmids were recovered in *E. coli* XL1 Blue (strains ANG1330 and ANG1335) and subsequently electroporated into *S. aureus* ANG499, yielding strains ANG1340 (p*itet-yfnI*$_{TMlink}$*-eltaS*) and ANG1345 (p*itet-yfnI*$_{TM\text{-}link}$*eltaS*). For the construction of plasmids p*itet-ltaS*$_{Tmlink}$*-eyfnI-his* and p*itet-ltaS*$_{TM\text{-}link}$*eyfnI-his* the *ltaS*$_{TM}$ and the *ltaS*$_{TM}$ + linker sequence were amplified from plasmid pCL55-*ltaS* using primer 318 in combination with primers 497 or 523. The *eyfnI* and the linker + *eyfnI* sequence were amplified from plasmid pCL55-*yfnI* using primer 504 in combination

with primer 496 or 522 and C-terminal His-tags were introduced with the downstream primers. Respective PCR fragments were fused by SOE PCR using primers 318/504. The final PCR products were cloned as *Avr*II/*Bgl*II fragments into plasmid p*itet* as described above and recovered in *E. coli* XL1 Blue (strains ANG1331 and ANG1334) The plasmids were subsequently electroporated into *S. aureus* ANG499, yielding strains ANG1341 (p*itet-ltaS*$_{Tmlink}$*-eyfnI-his*) and ANG1344 (p*itet-ltaS*$_{TM\text{-}link}$*eyfnI-his)*. Plasmids p*itet-yflE*$_{TM\text{-}link}$*eyfnI-his* and p*itet-yflE*$_{Tmlink}$*-eyfnI-his* were created by amplifying the *yflE*$_{TM}$ and the *yflE*$_{TM}$ + linker sequence from plasmid pCL55-*yflE* using primer 326 in combination with primers 615/617. The *eyfnI* and the linker + *eyfnI* sequence were amplified from plasmid pCL55-*yfnI* using primer 504 in combination with primer 614 or 616 and C-terminal His-tags were introduced with the downstream primers. Appropriate PCR fragments were fused by SOE PCR using primers 318/504. The final PCR products were cloned as *Avr*II/*Bgl*II fragments into plasmid p*itet* as described above. Plasmids were initially obtained in *E. coli* XL1 Blue (strains ANG1338 and ANG1339) and subsequently electroporated into *S. aureus* strain ANG499, yielding strains ANG1348 (p*itet-yflE*$_{TM\text{-}link}$*eyfnI-his*) and ANG1349 (p*itet-yflE*$_{Tmlink}$*-eyfnI-his*). Plasmids p*itet-ltaS*$_{TM\text{-}link}$*eyflE-his* and p*itet-ltaS*$_{Tmlink}$*-eyqgS-his* were constructed by amplifying the *ltaS*$_{TM}$ and the *ltaS*$_{TM}$ + linker sequence from plasmid pCL55-*ltaS* using primer 318 in combination with primers 528/501. The *eyqgS* sequence was amplified from plasmid pCL55-*yqgS* with primer pair 500/503 and the linker + *eyflE* sequence was amplified from plasmid pCL55-*yflE* with primer pair 529/502. C-terminal His-tags were introduced with the downstream primers. Respective PCR fragments were fused by SOE PCR using primers 318/503 (*ltaS*$_{Tmlink}$*-eyqgS-his*) and 318/502 (*ltaS*$_{TM\text{-}link}$*eyflE-his*). The final PCR products were cloned as *Avr*II/*Bgl*II fragments into plasmid p*itet* as described above. Plasmids were recovered in *E. coli* XL1 Blue (strain ANG1333) and CLG190 (strain ANG1336) and subsequently introduced into *S. aureus* strain ANG499, yielding strains ANG1343 (p*itet-ltaS*$_{Tmlink}$*-eyqgS-his*) and ANG1346 (p*itet-ltaS*$_{TM\text{-}link}$*eyflE-his*). For the construction of plasmids p*itet-yqgS*$_{Tmlink}$*-eltaS* and p*itet-yflE*$_{TM\text{-}link}$*eltaS* the *yqgS*$_{TM}$ + linker sequence was amplified from plasmid pCL55-*yqgS* using primers 330/499 and the *yflE*$_{TM}$ sequence was amplified from plasmid pCL55-*yflE* using primers 326/526. The *eltaS* and the linker + *eltaS* sequence were amplified from plasmid pCL55-*ltaS* using primer 319 in combination with primers 498/527. Appropriate PCR fragments

were fused by SOE-PCR using primer pairs 330/319 (*yqgS*$_{Tmlink}$-*eltaS*) and 326/319 (*yflE*$_{TM\text{-}link}$*eltaS*). The final PCR products were cloned as *Avr*II/*Bgl*II fragments into plasmid p*itet* as described above. Plasmids were recovered in *E. coli* XL1 Blue (strains ANG1332 and ANG1337) and subsequently electroporated into *S. aureus* strain ANG499, yielding strains ANG1342 (p*itet-yqgS*$_{Tmlink}$-*eltaS*) and ANG1347 (p*itet-yflE*$_{TM\text{-}link}$*eltaS*). *S. aureus* strain ANG1350 and ANG1351 were constructed as follows. The *yfnI*$_{TM}$ and the *yfnI*$_{TM}$ + linker sequence were amplified from plasmid pCL55-*yfnI* using primer 322 in combination with primers 619/621. The *eyflE* and the linker + *eyflE* sequence were amplified from plasmid pCL55-*yflE* using primer 502 in combination with primers 618/620 and C-terminal His-tags were introduced with the downstream primers. Appropriate PCR fragments were fused by SOE PCR using primers 322/502. The final PCR products were cloned as *Avr*II/*Bgl*II fragments into plasmid p*itet* as described above. Plasmids were directly electroporated into *S. aureus* ANG499, yielding strains ANG1350 (p*itet-yfnI*$_{TM\text{-}link}$*eyflE-his*) and ANG1351 (p*itet-yfnI*$_{Tmlink}$-*eyflE-his)*. Plasmids pCL55-*yfnI* and pCL55-*yflE*, which were used as DNA templates in PCR reactions described above were constructed as follows: *yfnI* and *yflE* genes were amplified from *B. subtilis* 168 chromosomal DNA using primer pair 320/321 and 324/325. Resulting PCR products were restriction digested with *Bam*HI and *Kpn*I and ligated with plasmid pCL55, which had been digested with the same enzymes. Plasmids were subsequently transformed into *E. coli* strain XL1 Blue giving strain ANG504 (pCL55-yfnI) or CLG190 giving strain ANG505 (pCL55-*yflE*).

A *S. aureus* strain with IPTG inducible *spsB* expression was constructed to study the effect on LtaS cleavage upon SpsB depletion. For this strain construction the plasmid pCN34*itet*$_H$, which contains an Atet inducible promoter system, was used. This plasmid was constructed by amplifying the Atet promoter / repressor region from plasmid pALC2073 using primers 909/948 in the first and primers 908/948 in a second PCR reaction to extend the multiple cloning site. The PCR product and vector pCN34 were digested *Nar*I/*Xma*I and ligated. The resulting plasmid pCN34*itet*$_H$ was recovered in *E. coli* XL1 Blue yielding ANG1631. Next, the *spsB* gene was amplified from *S. aureus* RN4220 chromosomal DNA using primers 1007/1008. The PCR product and the plasmid pCN34*itet*$_H$ were digested *Kpn*I/*Sal*I and ligated. The resulting plasmid pCN34*itet*$_H$-*spsB* was initially recovered in *E. coli* XL1 Blue (strain ANG1811) and subsequently introduced into *S. aureus* SEJ1, yielding strain

ANG1816 (pCN34*itet*$_H$-*spsB*). Plasmid pTS1-Δ*spsB::erm* was constructed for the deletion of the *spsB* gene. One kb fragments up- and downstream of *spsB* were amplified from RN4220 genomic DNA with primers 1010/1011 and 1013/1015 and the *erm* cassette was amplified from plasmid pMutin-HA using primers 1012/1014. The three purified PCR products were fused by SOE PCR using primers 1010/1015 and the final PCR product and vector pTS1 were digested *Kpn*I/*Eco*RI and ligated. The plasmid pTS1-Δ*spsB::erm* was recovered in *E. coli* XL1 Blue (strain ANG1815) and subsequently introduced into *S. aureus* ANG1816 (SEJ1 pCN34*itet*$_H$-*spsB*) and stably maintained at 30°C in the presence of chloramphenicol (Cam) and Kanamycin (Kan). Shifting the temperature to 43°C resulted in a single cross over event and integration of the pTS1-Δ*spsB::erm* plasmid into the chromosome. After confirming the chromosomal integration by PCR, the culture was shifted back to 30°C and growth in the absence of Cam but presence of 50 ng/ml Atet (to induce SpsB expression from the covering plasmid pCN34*itet*$_H$-*spsB*) allowed for the second crossover event and deletion/replacement of the chromosomal *spsB* gene with an *erm* marker. Erm resistance of the resulting *S. aureus* strain ANG1820 (SEJ1 *spsB::erm* pCN34*itet*$_H$-*spsB*) was confirmed on selective antibiotic plates and the replacement of the *spsB* gene with the *erm* marker was verified by PCR. The basal expression of SpsB from the covering plasmid pCN34*itet*$_H$-*spsB,* even in the absence of Atet, was too high to use this strain for any further analysis. To this end, *S. aureus* strain ANG2009 with tightly controlled *spsB* expression was constructed, by transducing the chromosomal *spsB::erm* deletion from strain ANG1820 into *S. aureus* strain ANG2008 that contained a copy of the *spsB* gene under IPTG inducible s*pac* promoter control at a different chromosomal location. For this strain construction, an internal *Bam*HI site in *spsB* needed to be inactivated for cloning purposes. This was done by introducing a T to C nucleotide substitution at position 114 within the *spsB* coding sequence by QuikChange mutagenesis in plasmid pCN34*itet*$_H$-*spsB* using primers 1203/1204. This mutation does not alter the protein sequence. Plasmid pCN34*itet*$_H$-*spsB*-T114C was recovered in *E. coli* XL1 Blue yielding strain ANG1963. Next, the mutated *spsB* allele was amplified using primers 896/1183 and the resulting product and vector pMutin-HA were digested *Hind*III/*Kpn*I and ligated. The plasmid pMutinHA-*spsB*-T114C was recovered in *E. coli* XL1 Blue giving strain ANG1964. Subsequently, the mutated *spsB* allele including the IPTG inducible *spac*

promoter and *lacI* repressor region were excised by restriction digesting plasmid pMutinHA-*spsB*-T114C with *Bam*HI and the appropriate DNA fragment was gel purified and ligated with the *Bam*HI cut *S. aureus* single site integration vector pCL55. The plasmid pCL55*spac-spsB*-T114C was obtained in *E. coli* XL1 Blue (strain ANG2007) and subsequently electroporated into *S. aureus* SEJ1, yielding strain ANG2008 (SEJ1 P_{spac}-*spsB*). The *spsB*::*erm* region from strain ANG1820 described above was then transduced using phage Φ85 into strain ANG2008, yielding strain ANG2009 (SEJ1 *spsB*::*erm* P_{spac}-*spsB*) with tightly controlled IPTG inducible *spsB* expression.

Plasmids pCN34*itet-ltaS*, pCN34*itet-yfnI*, pCN34*itet-yflE*, pCN34*itet-yvgJ* and pCN34*itet-yqgS* were constructed to study the functions of the corresponding proteins in an *S. aureus ltaS* depletion strain. For the construction of plasmids pCN34*itet-ltaS* and pCN34*itet-yfnI,* respective genes and the p*itet* promoter region were amplified from plasmids p*itet-ltaS* and p*itet-yfnI* using primer pairs 159/800 and 159/821, respectively. The resulting PCR products were restriction digested with *Kpn*I/*Sal*I (*ltaS*) or *Kpn*I (*yfnI*) and cloned into pCN34 that has been digested with *Kpn*I/*Sal*I (*ltaS* cloning) or *Kpn*I/*Sma*I (*yfnI* cloning). For pCN34*itet-yflE*, pCN34*itet-yvgJ* and pCN34*itet-yqgS* plasmid construction, the respective genes and the p*itet* promoter were amplified from plasmids p*itet-yflE*, p*itet-yvgJ* and p*itet*-RB*ltaS-yqgS* using primer pair 159/877. The resulting PCR products were restriction digested with *Kpn*I and *Pst*I and ligated with pCN34, which has been digested with the same enzymes. Plasmids were subsequently transformed into *E. coli* XL1 Blue resulting in strains ANG1512, ANG1514, ANG1660, ANG1656 and ANG1652. These plasmids and the empty pCN34 control vector were then electroporated into the *ltaS*-inducible *S. aureus* strain ANG499, yielding strains ANG1130 (pCN34), ANG1571 (pCN34*itet-ltaS*), ANG1573 (pCN34*itet-yfnI*), ANG1662 (pCN34*itet-yflE*), ANG1658 (pCN34*itet-yvgJ*) and ANG1654 (pCN34*itet-yqgS*). Plasmid p*itet*-RB*ltaS-yqgS,* which was used to amplify *yqgS* for the construction of pCN34*itet-yqgS*, contains the *yqgS* gene proceeded by the *S. aureus ltaS* ribosome binding site (RBS) under tetracycline inducible promoter control. This plasmid was obtained by amplifying the *ltaS* promoter and ribosomal binding site from plasmid pCL55-*ltaS* using primer pair 086/775 and the *yqgS* coding sequence from plasmid pCL55-*yqgS* using primer pair 796/331. The resulting PCR products were fused by SOE PCR using primer pair

826/331. The final PCR product was digested with *Avr*II/*Bgl*II and *yqgS* with the *ltaS* RBS was placed under tetracycline inducible promoter control by ligating the digested PCR product with the *Avr*II/*Bgl*II digested plasmid p*itet*. The resulting plasmid p*itet*-RB*ltaS-yqgS* was transformed into *E. coli* strain XL1 Blue, yielding strain ANG1615.

Plasmids pCN34*itet-ltaS-his*, pCN34*itet-yfnI-his*, pCN34*itet-yflE-his*, pCN34*itet-yvgJ-his* and pCN34*itet-yqgS-his* were constructed for protein detection purposes in *S. aureus*. For the construction of plasmids pCN34*itet-ltaS-his* and pCN34*itet-yfnI-his,* respective genes and the p*itet* promoter region were amplified from plasmids p*itet-ltaS-his* and p*itet-yfnI-his* using primer pairs 159/800 and 159/821, respectively. The resulting PCR products were restriction digested with *Kpn*I/*Sal*I (*ltaS*) or *Kpn*I (*yfnI*) and cloned into pCN34 that has been digested with *Kpn*I/*Sal*I (*ltaS* cloning) or *Kpn*I/*Sma*I (*yfnI* cloning). Plasmids were initially recovered in *E. coli* XL1 Blue (strains ANG1513 and ANG1515) and subsequently electroporated into *S. aureus* strain ANG499, yielding strains ANG1572 (pCN34*itet-ltaS-his*) and ANG1574 (pCN34*itet-yfnI-his*). Plasmids pCN34*itet-yflE-his*, pCN34*itet-yvgJ-his* and pCN34*itet-yqgS-his* were constructed by amplifying respective genes and the p*itet* promoter region from plasmids p*itet-yflE*, p*itet-yvgJ* and p*itet*-RB*ltaS-yqgS* using primer 159 in combination with primer 912/879/895. The C-terminal His-tags were introduced with the downstream primers. The PCR products and the pCN34 vector were restriction digested with *Kpn*I/*Pst*I and ligated. Plasmids were initially obtained in *E. coli* XL1 Blue (strains ANG1661, ANG1657 and ANG1653) and subsequently introduced into *S. aureus* strain ANG499, yielding strains ANG1663 (pCN34*itet-yflE-his*), ANG1659 (pCN34*itet-yvgJ-his*) and ANG1655 (pCN34*itet-yqgS-his*). Plasmid p*itet-yfnI-his,* which was used to amplify *yfnI* for the construction of pCN34*itet-yfnI-his*, was constructed as follows: the *yfnI* gene was amplified from p*itet-yfnI* using primer 504/322 and the C-terminal His-tag was introduced with the downstream primer. The resultant PCR product was restriction digested with *Avr*II/*Bgl*II and ligated with p*itet*, which has been digested with the same enzymes. The plasmid was initially obtained in *E. coli* strain XL1 Blue (strain ANG1280) and subsequently electroporated into *S. aureus* strain ANG499, yielding strains ANG1282 (p*itet-yfnI-his*).

Plasmids pCN34$_{PltaS}$-*sipT,* pCN34$_{PltaS}$-*sipV,* pCN34$_{PltaS}$-*sipT/S* and pCN34$_{PltaS}$-*sipV/S* were constructed to investigate YfnI processing in the presence of *B. subtilis*

signal peptidases. For the construction of plasmids pCN34$_{PltaS}$-*sipT* and pCN34$_{PltaS}$-*sipV* the native *ltaS* promoter region was amplified from plasmid pCL55-*ltaS* using primer 086 in combination with primers 623/627 and the *sipT* and *sipV* genes were amplified from *B. subtilis* 168 chromosomal DNA using primers 622/624 and 626/628. Appropriate PCR fragments were fused by SOE PCR with primers 086/624 ($_{PltaS}$-*sipT*) or 086/628 ($_{PltaS}$-*sipV*). The final PCR products were restriction digested with *Bam*HI/*Sal*I and ligated with plasmid pCN34, which has been digested with the same enzymes. Plasmids were transformed into *E. coli* XL1 Blue, giving strains ANG1355 and ANG1357. These plasmids and the empty pCN34 vector control were introduced into *S. aureus* ANG1282, yielding strains ANG1708 (pCN34), ANG1359 (pCN34 $_{PltaS}$-*sipT*) and ANG1361 (pCN34 $_{PltaS}$-*sipV*). Plasmids pCN34$_{PltaS}$-*sipT/S* and pCN34$_{PltaS}$-*sipV/S* were constructed by amplifying the *sipT* or *sipV* gene and the native *ltaS* promoter region from plasmids pCN34 $_{PltaS}$-*sipT* and pCN34 $_{PltaS}$-*sipV* using primer 086 in combination with primers 743/745. The *sipS* gene was amplified from *B. subtilis* 168 chromosomal DNA using primers 742/714 and 744/714. Respective PCR fragments were fused by SOE PCR using primers 087/714. The final PCR products were cloned into *Bam*HI/*Sal*I sides of plasmid pCN34 as described above and recovered in *E. coli* XL1 Blue (strain ANG1526) and CLG190 (ANG1522). The plasmids were subsequently electroporated into *S. aureus* ANG1282, yielding strains ANG1524 (pCN34$_{PltaS}$-*sipT/S*) and ANG1528 (pCN34$_{PltaS}$-*sipV/S*).

Plasmids pCN34$_{PltaS}$-*sipT-his,* pCN34$_{PltaS}$-*sipV-his,* pCN34$_{PltaS}$-*sipT/S-his* and pCN34$_{PltaS}$-*sipV/S-his* were constructed for detection of the corresponding proteins in *S. aureus*. For the construction of plasmids pCN34$_{PltaS}$-*sipT-his* and pCN34$_{PltaS}$-*sipV-his* the respective genes were amplified from *B. subtilis* 168 chromosomal DNA using primers 622/625 and 626/629 and C-terminal His-tags were introduced with the downstream primers. The *ltaS* promoter region was amplified from plasmid pCL55-*ltaS* using primer 086 in combination with primers 623/627. Appropriate PCR fragments were fused by SOE PCR with primers 086/625 ($_{PltaS}$-*sipT-his*) or 086/629 ($_{PltaS}$-*sipV-his*). The final PCR products were restriction digested with *Bam*HI/*Sal*I and ligated with plasmid pCN34, which has been digested with the same enzymes. Plasmids were initially recovered in *E. coli* XL1 Blue (strain ANG1356 and ANG1358) and subsequently electroporated into strain ANG1282, yielding strain ANG1360 ($_{PltaS}$-*sipT-his*) and ANG1362 ($_{PltaS}$-*sipV-his*). Plasmids pCN34$_{PltaS}$-*sipT/S-his*

and pCN34$_{PltaS}$-*sipV*/*S-his* were constructed by amplifying the *sipT* or *sipV* gene and the native *ltaS* promoter region from plasmids pCN34 $_{PltaS}$-*sipT* and pCN34 $_{PltaS}$-*sipV* using primer 086 in combination with primers 743/745. The *sipS* gene was amplified from *B. subtilis* 168 chromosomal DNA using primers 742/715 and 744/715 and the C-terminal His-tags were introduced with the downstream primers. Respective PCR fragments were fused by SOE PCR using primers 087/715. The final PCR products were cloned into *Bam*HI/*Sal*I sides of plasmid pCN34 as described above and recovered in *E. coli* XL1 Blue (strain ANG1527) and CLG190 (ANG1523). The plasmids were subsequently electroporated into *S. aureus* ANG1282, yielding strains ANG1525 (pCN34$_{PltaS}$-*sipT*/*S-his*) and ANG1529 (pCN34$_{PltaS}$-*sipV*/*S-his*). *S. aureus* strain ANG1598 served as a control strain and this strain was obtained by introducing the empty pCN34 vector control plasmid into *S. aureus* strain ANG587, yielding strain ANG1598 (pCN34). Sequences of all inserts were verified by fluorescence automated sequencing at the MRC Clinical Science Center Sequencing Facility at Imperial College London. Note that the following plasmids and strains were constructed by Dr. A. Gründling: pCL55-*yfnI*, pCL55-*yflE*, p*itet-ltaS-his*, pCN34*itet*$_H$, pCN34*itet-ltaS*, pCN34*itet-ltaS-his*, pCN34*itet-yfnI*, pCN34*itet-yfnI-his* and *S. aureus* strain ANG587 (*pitet-ltaS-his*).

Tables

Table 1: Bacterial strains used in this study

Strain	Relevant features	Reference
	***Escherichia coli* strains**	
XL1 Blue	Cloning strain, TetR – ANG127	Stratagene
CLG190	Cloning strain, which reduces plasmid copy number, TetR – ANG1141	Dana Boyd (Gründling *et al*, 2003)
ANG126	pTS1 in DH5α; vector with temperature sensitive replication in *S. aureus*; AmpR	(O'Connell *et al*, 1993)
ANG201	pCN34 in *E. coli*; *E. coli* / *S. aureus* shuttle vector; KanR and AmpR	(Charpentier *et al*, 2004)
ANG243	pCL55 in XL1 Blue; *S. aureus* single-site integration vector; AmpR	(Lee *et al*, 1991)
ANG284	p*itet* in XL1 Blue; pCL55 containing Atet-inducible promoter; AmpR	(Gründling & Schneewind, 2007b)
ANG374	pCL55-*ypfP*/*ltaA* in XL1 Blue: AmpR	(Gründling & Schneewind, 2007b)
ANG474	pMutin-HA in *E. coli*; AmpR	Bacillus Genetic Stock Center
ANG482	pOK in XL1 Blue; KanR	(Gründling & Schneewind, 2007a)
ANG483	pOK-*ltaS* in XL1 Blue; KanR	(Gründling & Schneewind, 2007a)
ANG503	pCL55-*ltaS* in XL1 Blue; AmpR	(Wörmann *et al*, 2011)
ANG504	pCL55-*yfnI* in XL1 Blue; AmpR	Lab strain
ANG505	pCL55-*yflE* in CLG190; AmpR	Lab strain
ANG506	pCL55-*yqgS* in XL1 Blue; AmpR	(Wörmann *et al*, 2011)
ANG508	p*itet-ltaS* in XL1 Blue; *ltaS* under Atet inducible promoter; AmpR	(Gründling & Schneewind, 2007a)
ANG509	p*itet-yfnI* in XL1 Blue; *yfnI* under Atet inducible promoter; AmpR	(Gründling & Schneewind, 2007a)
ANG510	p*itet-yflE* in XL1 Blue; *yflE* under Atet inducible promoter; AmpR	(Gründling & Schneewind, 2007b)
ANG512	p*itet-yvgJ* in XL1 Blue; *yvgJ* under Atet inducible promoter; AmpR	(Gründling & Schneewind, 2007b)
ANG584	p*itet-ltaS-his* in XL1 Blue; *ltaS* with C-terminal His-tag under Atet inducible promoter control; AmpR	Lab strain
ANG590	p*itet-sec-eltaS* in XL1 Blue; protein A signal peptide fused to *eltaS* domain under Atet inducible promoter control; AmpR	This study
ANG1112	p*itet-ltaS*-T300A in XL1 Blue; *ltaS*-T300A allele under Atet inducible promoter control; AmpR	(Lu *et al*, 2009)
ANG1211	p*itet-*TM_{srtA}*-eltaS* in XL1 Blue; sortase TM fused to *eltaS* domain under Atet inducible promoter control; AmpR	This study
ANG1212	p*itet-1TM-eltaS* in XL1 Blue; first TM of *ltaS* fused to linker + e*ltaS* domain under Atet inducible promoter control; AmpR	This study
ANG1213	p*itet-3TM-eltaS* in XL1 Blue; first 3TM of *ltaS* fused to linker + e*ltaS* domain under Atet inducible promoter control; AmpR	This study
ANG1214	p*itet-5TM*$_{ltaA}$*-eltaS* in XL1 Blue; first 5TM of *ltaA* fused to linker + e*ltaS* domain under Atet inducible promoter control; AmpR	This study
ANG1221	pCN34-*5TM* in XL1 Blue; 5TM of *ltaS* under native promoter control; KanR, AmpR	This study
ANG1222	pCN34-*ltaS* in XL1 Blue; *ltaS* under native promoter control; KanR, AmpR	This study
ANG1242	pOK-*ltaS*$_{S218P}$ in XL1 Blue; *ltaS*-S218P allele under native promoter control; KanR	This study
ANG1244	p*itet-ltaS*$_{S218P}$ in XL1 Blue; *ltaS*-S218P allele under Atet inducible promoter control; AmpR	This study
ANG1280	p*itet-yfnI-his* in XL1 Blue; *yfnI* with C-terminal His-tag under Atet inducible promoter control; AmpR	This study
ANG1330	p*itet-yfnI*$_{TMlink}$*-eltaS* in XL1 Blue; 5TM and linker of *yfnI* fused to *eltaS* domain under Atet inducible promoter control; AmpR	This study
ANG1331	p*itet-ltaS*$_{Tmlink}$*-eyfnI-his* in XL1 Blue; 5TM and linker of *ltaS* fused to *eyfnI* domain with C-terminal His-tag under Atet inducible promoter control; AmpR	This study
ANG1332	p*itet-yqgS*$_{Tmlink}$*-eltaS* in XL1 Blue; 5TM and linker of *yqgS* fused to *eltaS* domain under Atet inducible promoter control; AmpR	This study
ANG1333	p*itet-ltaS*$_{Tmlink}$*-eyqgS-his* in XL1 Blue; 5TM and linker of *ltaS* fused to *eyqgS* domain with C-terminal His-tag under Atet inducible promoter control; AmpR	This study
ANG1334	p*itet-ltaS*$_{TM^-link}$*eyfnI-his* in XL1 Blue; 5TM of *ltaS* fused to linker + *eyfnI* domain with C-terminal His-tag under Atet inducible promoter control; AmpR	This study
ANG1335	p*itet-yfnI*$_{TM^-link}$*eltaS* in XL1 Blue; 5TM of *yfnI* fused to linker + *eltaS* domain under Atet inducible promoter control; AmpR	This study
ANG1336	p*itet-ltaS*$_{TM^-link}$*eyflE-his* in CLG190; 5TM of *ltaS* fused to linker + *eyflE* domain with C-terminal His-tag under Atet inducible promoter control; AmpR	This study
ANG1337	p*itet-yflE*$_{TM^-link}$*eltaS* in XL1 Blue; 5TM of *yflE* fused to linker + *eltaS* domain under Atet inducible promoter control; AmpR	This study

ANG1338	p*itet-yflE*$_{TM^{-}link}$*eyfnI-his* in XL1 Blue; 5TM of *yflE* fused to linker + *eyfnI* domain with C-terminal His-tag under Atet inducible promoter control; AmpR	This study
ANG1339	p*itet-yflE*$_{Tmlink}$*-eyfnI-his* in XL1 Blue; 5TM and linker of *yflE* fused to *eyfnI* domain with C-terminal His-tag under Atet inducible promoter control; AmpR	This study
ANG1355	pCN34$_{PltaS}$-*sipT* in XL1 Blue; *sipT* under *ltaS* promoter control; KanR, AmpR	This study
ANG1356	pCN34$_{PltaS}$-*sipT-his* in XL1 Blue; *sipT* with C-terminal His-tag under *ltaS* promoter control; KanR, AmpR	This study
ANG1357	pCN34$_{PltaS}$-*sipV* in XL1 Blue; *sipV* under *ltaS* promoter control; KanR, AmpR	This study
ANG1358	pCN34$_{PltaS}$-*sipV-his* in XL1 Blue; *sipV* with C-terminal His-tag under *ltaS* promoter control; KanR, AmpR	This study
ANG1368	p*itet-ltaS*$_{S218P}$*-his* in XL1 Blue; *ltaS*-S218P allele with C-terminal His-tag under Atet inducible promoter control; AmpR	This study
ANG1474	pProEX-eYflE in Rosetta strain; strain use for overexpression of eYflE protein with N-terminal His tag; AmpR	(Wörmann *et al*, 2011)
ANG1475	pProEX-eYfnI in Rosetta strain; strain use for overexpression of eYfnI protein with N-terminal His tag; AmpR	(Wörmann *et al*, 2011)
ANG1476	pProEX-eYvgJ in Rosetta strain; strain use for overexpression of eYvgJ protein with N-terminal His tag; AmpR	(Wörmann *et al*, 2011)
ANG1477	pProEX-eYqgS in Rosetta strain; strain use for overexpression of eYqgS protein with N-terminal His tag; AmpR	(Wörmann *et al*, 2011)
ANG1512	pCN34*itet-ltaS* in XL1 Blue; *ltaS* under Atet inducible promoter; KanR, AmpR	(Wörmann *et al*, 2011)
ANG1513	pCN34*itet-ltaS-his* in XL1 Blue; *ltaS* with C-terminal His-tag under Atet inducible promoter; KanR, AmpR	Lab strain
ANG1514	pCN34*itet-yfnI* in XL1 Blue; *yfnI* under tetracycline inducible promoter; KanR, AmpR	(Wörmann *et al*, 2011)
ANG1515	pCN34*itet-yfnI-his* in XL1 Blue; *yfnI* with C-terminal His-tag under Atet inducible promoter; KanR, AmpR	Lab strain
ANG1522	pCN34$_{PltaS}$-*sipT/S* in CLG190; *sipT* and *sipS* under *ltaS* promoter control; KanR, AmpR	This study
ANG1523	pCN34$_{PltaS}$-*sipT/S-his* in CLG190; *sipT* and *sipS* with C-terminal His-tag under *ltaS* promoter control; KanR, AmpR	This study
ANG1526	pCN34$_{PltaS}$-*siV/S* in XL1 Blue; *sipV* and *sipS* under *ltaS* promoter control; KanR, AmpR	This study
ANG1527	pCN34$_{PltaS}$-*sipV/S-his* in XL1 Blue; *sipV* and *sipS* with C-terminal His-tag under *ltaS* promoter control; KanR, AmpR	This study
ANG1577	pALC2073 in XL1 Blue; AmpR – ANG1577	(Bateman *et al*, 2001)
ANG1615	p*itet*-Rb*ltaS-yqgS* in XL1 Blue; *yqgS* with *ltaS* ribosomal binding site under tetracycline inducible promoter; AmpR	This study (Wörmann *et al*, 2011)
ANG1631	pCN34*itet*$_{H}$ in XL1 Blue; pCN34 containing Atet inducible promoter from pALC2073; KanR, AmpR	Lab strain
ANG1652	pCN34*itet-yqgS* in XL1 Blue; *yqgS* under tetracycline inducible promoter; KanR, AmpR	This study (Wörmann *et al*, 2011)
ANG1653	pCN34*itet-yqgS-his* in XL1 Blue; *yqgS* with C-terminal His-tag under Atet inducible promoter; KanR, AmpR	This study
ANG1656	pCN34*itet-yvgJ* in XL1 Blue; *yvgJ* under tetracycline inducible promoter; KanR, AmpR	This study (Wörmann *et al*, 2011)
ANG1657	pCN34*itet-yvgJ-his* in XL1 Blue; *yvgJ* with C-terminal His-tag under Atet inducible promoter; KanR, AmpR	This study
ANG1660	pCN34*itet-yflE* in XL1 Blue; *yflE (ltaS*$_{BS}$*)* under tetracycline inducible promoter; KanR, AmpR	This study (Wörmann *et al*, 2011)
ANG1661	pCN34*itet-yflE-his* in XL1 Blue; *yflE* with C-terminal His-tag under Atet inducible promoter; KanR, AmpR	This study
ANG1689	pCN34*itet-ltaS*$_{T300A}$ in XL1 Blue; *ltaS*-T300A allele under Atet inducible promoter control; KanR, AmpR	This study
ANG1811	pCN34*itet*$_{H}$*-spsB* in XL1 Blue; *spsB* under Atet inducible promoter; KanR, AmpR	This study
ANG1815	pTS1-Δ*spsB::erm* in XL1 Blue; AmpR	This study
ANG1963	pCN34*itet*$_{H}$*-spsB*-T114C in XL1 Blue; *spsB* with point mutation T114C under Atet inducible promoter control; KanR, AmpR	This study
ANG1964	pMutinHA-*spsB*-T114C in XL1 Blue; *spsB* with point mutation T114C under IPTG inducible promoter control; AmpR	This study
ANG2007	pCL55*spac-spsB*-T114C in XL1 Blue; *spsB* with point mutation T114C under IPTG inducible promoter control; KanR, AmpR	This study
ANG2158	pCN34*itet-sec-eltaS* in XL1 Blue; protein A signal peptide fused to *eltaS* domain under Atet inducible promoter control; KanR, AmpR	This study
ANG2159	pCN34*itet-TM*$_{srtA}$*-eltaS* in XL1 Blue; sortase TM fused to *eltaS* domain under Atet inducible promoter control; KanR, AmpR	This study
ANG2160	pCN34*itet-1TM-eltaS* in XL1 Blue; first TM of *ltaS* fused to linker + e*ltaS* domain under Atet inducible promoter control; KanR, AmpR	This study
ANG2161	pCN34*itet-3TM-eltaS* in XL1 Blue; first 3TM of *ltaS* fused to linker + e*ltaS* domain under Atet inducible promoter control; KanR, AmpR	This study
ANG2162	pCN34*itet-5TM*$_{ltaA}$*-eltaS* in XL1 Blue; first 5TM of *ltaA* fused to linker + *eltaS* domain under Atet inducible promoter control; KanR, AmpR	This study
ANG2182	pOK-*ltaS*$_{E174P}$ in XL1 Blue; *ltaS*-E174P allele under native promoter control; KanR	This study

ANG2183	p*itet-ltaS*$_{E174P}$ in XL1 Blue; *ltaS*-E174P allele under Atet inducible promoter control; AmpR	This study
	***Staphylococcus aureus* strains**	
RN4220	Transformable laboratory strain – ANG113	(Kreiswirth *et al*, 1983)
SEJ1	RN4220Δ*spa* – ANG314	(Gründling & Schneewind, 2007a; Gründling & Schneewind, 2007b)
COL	methicillin resistance clinical strain – ANG527	(Sabath *et al*, 1972)
ANG499	RN4220-*iltaS*; strain with IPTG-inducible *ltaS* expression; ErmR, IPTG	(Gründling & Schneewind, 2007a)
ANG513	p*itet* integrated in strain ANG499; ErmR, CamR, IPTG	(Gründling & Schneewind, 2007a)
ANG514	p*itet-ltaS* integrated in strain ANG499; ErmR, CamR, IPTG	(Gründling & Schneewind, 2007a)
ANG515	p*itet-yfnI* integrated in strain ANG499; ErmR, CamR, IPTG	(Gründling & Schneewind, 2007a)
ANG587	p*itet-ltaS-his* integrated in strain ANG499; ErmR, CamR, IPTG	Lab strain
ANG595	p*itet-sec-eltaS* integrated in strain ANG499; ErmR, CamR, IPTG	This study
ANG1130	ANG499 with pCN34; ErmR, KanR, IPTG	This study (Wörmann *et al*, 2011)
ANG1217	p*itet-TM*$_{srtA}$*-eltaS* integrated in strain ANG499; ErmR, CamR, IPTG	This study
ANG1218	p*itet-1TM-eltaS* integrated in strain ANG499; ErmR, CamR, IPTG	This study
ANG1219	p*itet-3TM-eltaS* integrated in strain ANG499; ErmR, CamR, IPTG	This study
ANG1220	p*itet-5TM*$_{ltaA}$*-eltaS* integrated in strain ANG499; ErmR, CamR, IPTG	This study
ANG1226	ANG595 with pCN34; ErmR, CamR, Kan, IPTG	This study
ANG1227	ANG595 with pCN34-*5TM;* ErmR, CamR, Kan, IPTG	This study
ANG1228	ANG595 with pCN34-*ltaS;* ErmR, CamR, Kan, IPTG	This study
ANG1246	p*itet-ltaS*$_{S218P}$ integrated in strain ANG499; ErmR, CamR, IPTG	This study
ANG1282	p*itet-yfnI-his* integrated in strain ANG499; ErmR, CamR, IPTG	This study
ANG1340	p*itet-yfnI*$_{Tmlink}$*-eltaS* integrated in strain ANG499; ErmR, CamR, IPTG	This study
ANG1341	p*itet-ltaS*$_{Tmlink}$*-eyfnI-his* integrated in strain ANG499; ErmR, CamR, IPTG	This study
ANG1342	p*itet-yqgS*$_{Tmlink}$*-eltaS* integrated in strain ANG499; ErmR, CamR, IPTG	This study
ANG1343	p*itet-ltaS*$_{Tmlink}$*-eyqgS-his* integrated in strain ANG499; ErmR, CamR, IPTG	This study
ANG1344	p*itet-ltaS*$_{TM^-link}$*eyfnI-his* integrated in strain ANG499; ErmR, CamR, IPTG	This study
ANG1345	p*itet-yfnI*$_{TM^-link}$*eltaS* integrated in strain ANG499; ErmR, CamR, IPTG	This study
ANG1346	p*itet-ltaS*$_{TM^-link}$*eyflE-his* integrated in strain ANG499; ErmR, CamR, IPTG	This study
ANG1347	p*itet-yflE*$_{TM^-link}$*eltaS* integrated in strain ANG499; ErmR, CamR, IPTG	This study
ANG1348	p*itet-yflE*$_{TM^-link}$*eyfnI-his* integrated in strain ANG499; ErmR, CamR, IPTG	This study
ANG1349	p*itet-yflE*$_{Tmlink}$*-eyfnI-his* integrated in strain ANG499; ErmR, CamR, IPTG	This study
ANG1350	p*itet-yfnI*$_{TM^-link}$*eyflE-his* integrated in strain ANG499; ErmR, CamR, IPTG	This study
ANG1351	p*itet-yfnI*$_{Tmlink}$*-eyflE-his* integrated in strain ANG499; ErmR, CamR, IPTG	This study
ANG1359	ANG1282 with pCN34$_{PltaS}$-*sipT*; ErmR, CamR, Kan, IPTG	This study
ANG1360	ANG1282 with pCN34$_{PltaS}$-*sipT-his*; ErmR, CamR, Kan, IPTG	This study
ANG1361	ANG1282 with pCN34$_{PltaS}$-*sipV*; ErmR, CamR, Kan, IPTG	This study
ANG1362	ANG1282 with pCN34$_{PltaS}$-*sipV-his*; ErmR, CamR, Kan, IPTG	This study
ANG1370	p*itet-ltaS*$_{S218P}$*-his* integrated in strain ANG499; ErmR, CamR, IPTG	This study
ANG1524	ANG1282 with pCN34$_{PltaS}$-*sipT/S*; ErmR, CamR, Kan, IPTG	This study
ANG1525	ANG1282 with pCN34$_{PltaS}$-*sipT/S-his*; ErmR, CamR, Kan, IPTG	This study
ANG1528	ANG1282 with pCN34$_{PltaS}$-*sipV/S*; ErmR, CamR, Kan, IPTG	This study
ANG1529	ANG1282 with pCN34$_{PltaS}$-*sipV/S-his*; ErmR, CamR, Kan, IPTG	This study
ANG1571	ANG499 with pCN34*itet-ltaS*; ErmR, KanR, IPTG	This study (Wörmann *et al*, 2011)
ANG1572	ANG499 with pCN34*itet-ltaS-his*; ErmR, KanR, IPTG	This study
ANG1573	ANG499 with pCN34*itet-yfnI*; ErmR, KanR, IPTG	This study (Wörmann *et al*, 2011)
ANG1574	ANG499 with pCN34*itet-yfnI-his*; ErmR, KanR, IPTG	This study
ANG1598	ANG587 with pCN34 ErmR, CamR, Kan, IPTG	This study
ANG1654	ANG499 with pCN34*itet-yqgS*; ErmR, KanR, IPTG	This study (Wörmann *et al*, 2011)
ANG1655	ANG499 with pCN34*itet-yqgS-his*; ErmR, KanR, IPTG	This study
ANG1658	ANG499 with pCN34*itet-yvgJ*; ErmR, KanR, IPTG	This study (Wörmann *et al*, 2011)
ANG1659	ANG499 with pCN34*itet-yvgJ-his*; ErmR, KanR, IPTG	This study
ANG1662	ANG499 with pCN34*itet-yflE*; ErmR, KanR, IPTG	This study (Wörmann *et al*, 2011)
ANG1663	ANG499 with pCN34*itet-yflE-his*; ErmR, KanR, IPTG	This study
ANG1690	ANG595 with pCN34*itet-ltaS*$_{T300A}$; ErmR, KanR, IPTG	This study
ANG1708	ANG1282 with pCN34 ErmR, CamR, Kan, IPTG	This study
ANG1755	SEJ1Δ*sbi*Δ*spa*	Lab strain
ANG1786	4S5- SEJ1Δ*ltaS*Δ*spa;*LTA negative suppressor strain that can grow without LTA	Lab strain
ANG1816	SEJ1 with pCN34*itet-spsB*; KanR	This study
ANG1820	SEJ1 *spsB::erm* with pCN34*itet-spsB*; ErmR, KanR	This study
ANG2008	SEJ1 P$_{spac}$-*spsB*; pCL55*spac-spsB*-T114C integrated in strain SEJ1; CamR	This study

ANG2009	SEJ1 *spsB::erm* P_{spac}-*spsB*; *spsB::erm* transduced from strain ANG1820 into strain ANG2008; ErmR, CamR, IPTG	This study
ANG2165	ANG499 with pCN34*itet-sec-eltaS*; ErmR, KanR, IPTG	This study
ANG2166	ANG499 with pCN34*itet-*TM_{srtA}*-eltaS*; ErmR, KanR, IPTG	This study
ANG2167	ANG499 with pCN34*itet-1TM-eltaS*; ErmR, KanR, IPTG	This study
ANG2168	ANG499 with pCN34*itet-3TM-eltaS*; ErmR, KanR, IPTG	This study
ANG2169	ANG499 with pCN34*itet-*$5TM_{ltaA}$*-eltaS*; ErmR, KanR, IPTG	This study
ANG2184	p*itet-*$ltaS_{E174P}$ integrated in strain ANG499; ErmR, CamR, IPTG	This study
RN6390	RN6390; virulent laboratory strain derived from NCTC 8325- ANG2153	(Peng *et al*, 1988)
RN6390$htrA_1$,$htrA_2$	RN6390 $htrA_1$, $htrA_2$; CamR, SpecR - ANG1649	(Rigoulay *et al*, 2005)
AH1263	LAC*; Erm sensitive CA-MRSA LAC strain - ANG1575	(Boles *et al*, 2010)
AH1919	LAC* Δ*aur,* Δ*sspAB*, Δ*scpA*, *spl::erm* (LAC* protease KO) – ANG2038	obtained from Dr. A. Horswill
	***Bacillus subtilis* strains**	
B.subtilis	*Bacillus subtilis* 168 – Transformable lab strain, trpC2 – ANG1691	(Burkholder, 1947)
ANG1692	*Bacillus subtilis* 168 *yfnI::Cam* (Δ*yfnI*)	(Wörmann *et al*, 2011)
ANG1693	*Bacillus subtilis* 168 *yflE::Kan* (Δ*yflE*)	(Wörmann *et al*, 2011)
ANG1694	*Bacillus subtilis* 168 *yqgS::Spec* (Δ*yqgS*)	(Wörmann *et al*, 2011)
ANG1695	*Bacillus subtilis* 168 *yvgJ::Erm* (Δ*yvgJ*)	(Wörmann *et al*, 2011)
ANG1696	*Bacillus subtilis* 168 *yflE::Kan, yqgS::Spec, yvgJ::Erm* (*yfnI only*)	(Wörmann *et al*, 2011)
ANG1697	*Bacillus subtilis* 168 *yfnI::Cam, yqgS::Spec, yvgJ::Erm* (*yflE only*)	(Wörmann *et al*, 2011)
ANG1698	*Bacillus subtilis* 168 *yfnI::Cam, yflE::Kan, yvgJ::Erm* (*yqgS only*)	(Wörmann *et al*, 2011)
ANG1699	*Bacillus subtilis* 168 *yfnI::Cam, yflE::Kan, yqgS::Spec* (*yvgJ only*)	(Wörmann *et al*, 2011)
ANG1701	*Bacillus subtilis* 168 *yfnI::Cam, yflE::Kan, yqgS::Spec, yvgJ::Erm* (4xΔ)	(Wörmann *et al*, 2011)
ANG1702	*Bacillus subtilis* 168 *yflE::Kan, yfnI::Cam (*express-*yvgJ/yqgS)*	(Wörmann *et al*, 2011)
ANG1703	*Bacillus subtilis* 168 *yflE::Kan, yqgS::Spec (*express-*yvgJ/yfnI)*	(Wörmann *et al*, 2011)
ANG1704	*Bacillus subtilis* 168 *yfnI::Cam, yqgS::Spec (*express-*yvgJ/yflE)*	(Wörmann *et al*, 2011)
L5703	*Bacillus subtilis with ribitol-Pi wall teichoic acid (ribitol-Pi WTA)*	(Karamata *et al*, 1987)

Antibiotics were used at the following concentrations: for *E. coli* cultures: Ampicillin (AmpR) 100 μg/ml; Kanamycin (KanR) 30 μg/ml; Tetracycline (TetR) 10 μg/ml; for *S. aureus* cultures: Erythromycin (ErmR) 10 μg/ml; Chloramphenicol (CamR) 7.5 to 10 μg/ml, Kanamycin 90 μg/ml and IPTG at 1 mM; for *B. subtilis* cultures: Erythromycin 5 μg/ml; Chloramphenicol 10 μg/ml, Kanamycin 10 μg/ml; Spectinomycin (Spec) 100 or 200 μg/ml.

Table 2: Primers used in this study

Number	Name	Sequence
ANG086	5'-BamHI +P SAV0719	CGGGATCCGGAATAGAATATAGAATGCAATTAGAAATG
ANG087	3-SalI SAV0719	ACGCGTCGACCCGAGTTCGTGTTTAAATATTATTTTTTAG
ANG159	5-KpnI-tet	GGGGTACCTTGGTTACCGTGAAGTTACCATCACGG
ANG260	5-AvrII-SAV1016	CCGCCTAGGCATCACAACCACAAGAGATTTATGGAAAGGTTCC
ANG318	5-AvrII-SAV719-22bp	CCGCCTAGGctaaataacgggggaaagaatcATGAGTTC
ANG319	3-BglII-SAV719	GAAGATCTCCGAGTTCGTGTTTAAATATTATTTTTTAG
ANG320	5-BamHI-YfnI with P	CGGGATCCGGTGATCGCGCTAAACATTGATGCATACAATAAC
ANG321	3-KpnI-YfnI	GGGGTACCGCAATGCGCCCGCTCAAGGCTCTTTTTCATCTTA
ANG322	5-AvrII-YfnI-33bp	CCGCCTAGGGAACTTAAAGTGTTTAAGAAAGTAGAGGTTGCC
ANG324	5-BamHI-YflE-with P	CGGGATCCCCATTTTATTCCTTTATTTCTAGAAAGATACC
ANG325	3-KpnI-YflE	GGGGTACCAAAGCGGAGAGGGCAACCTCTCCGCTTTTTCTTA
ANG326	5-AvrII-YflE-32bp	CCGCCTAGGGCTCGAACTGGATCGGAAAAAAGGAGTGTAACA
ANG330	5-AvrII-YqgS- 34bp	CCGCCTAGGCTGATTTTTTTGAGCGTGCTGCATAGGAGGTTG
ANG331	3-BglII-YqgS	GAAGATCTCCGCTCACTTCGATGCGGGAGACATTGTGATTA
ANG401	5-AvrII protA SS	CCGCCTAGG GTTATATTATGATGACTTTACAAATACATACAG
ANG404	ProtA SS-719 front-no ala	CTTTTGTTAAGTCATCTTCAGA AGCATTTGCAGCAGGTGTTACG
ANG405	ProtA-719-no ala	CGTAACACCTGCTGCAAATGCT TCTGAAGATGACTTAACAAAAG
ANG420	3-BgIII-His6-719	GAAGATCTttaGTGATGGTGATGGTGATGaccTTTTTTAGAGTTTGCTTTAGGTCCTG
ANG424	3-SalI_Stop_TM_719	ACGCGTCGACttaTGCTAACGCTTTTTGTTGATTATTTTCG
ANG427	5-AvrII_SrtA_TM	CCGCCTAGGtataaaaggagccttaacgtATGAAAAAATGG
ANG432	Front-SrtA_35AA	GTCATCTTCAGActgCTTATTGTCTTTACTCGCCTGTTCTTTTAC
ANG433	Back-SrtA_35AA	GACAATAAGCAGtctGAAGATGACTTAACAAAAGTATTAAATTATAC
ANG434	Front-LtaS_1TM	GTCTGTCAGTTTCaacATAATAAGAAAAATACGTCTTCAAGG
ANG435	Back-LtaS_1TM	CTTATTATGTTgaaACTGACAGACCAGAATTATTAACACG
ANG436	Front-LtaS_3TM	GTCTGTCAGTTTCtctAAAGTACACAACATTGGCATATAATAG
ANG437	Back-LtaS_3TM	GTGTACTTTAGAgaaACTGACAGACCAGAATTATTAACACG
ANG438	Front-LtaA_5TM	GTCTGTCAGTTTCcacTTTGATAAGTAGATTCATAAAAACCATAC
ANG439	Back-LtaA_5TM	CTTATCAAAGTGgaaACTGACAGACCAGAATTATTAACACG
ANG487	F-719-cleave ALAP	CTATCGAAAATAATCAACAAAAAgcgctagcacctGAAGATGACTTAACAAAAG
ANG488	R-719-cleave ALAP	CTTTTGTTAAGTCATCTTCaggtgctagcgcTTTTTGTTGATTATTTTCGATAG
ANG494	F-YfnITM+extr.LtaS	CAAAGAgcctatgcaTCTGAAGATGACTTAACAAAAGTATTAAATTATAC
ANG495	R-YfnITM+extr.LtaS	GTCATCTTCAGAtgcataggcTCTTTGCGTCTCTGTTTGAGC
ANG496	F-LtaSTM+extr.YfnI	AAAgcgctagcaAGCAGCGATGATTTAACAAGTGTCGAGAATTAC
ANG497	R-LtaSTM+extr.YfnI	AATCATCGCTGCTtgctagcgcTTTTTGTTGATTATTTTCGATAG
ANG498	F-YqgSTM+extr.LtaS	GAGAgcgttggcaTCTGAAGATGACTTAACAAAAGTATTAAATTATAC
ANG499	R-YqgSTM+extr.LtaS	GTCATCTTCAGAtgccaacgcTCTCTGTGCGGATTGCTTTGACTG
ANG500	F-LtaSTM+extr.YqgS	AAAgcgctagcaGACAGCAACAGCCTGACGGAGATTGAAAACTAC
ANG501	R-LtaSTM+extr.YqgS	GCTGTTGCTGTCtgctagcgcTTTTTGTTGATTATTTTCGATAG
ANG502	3-BglII-His6-YflE	GAAGATCTttaGTGATGGTGATGGTGATGaccTTTATCTTCGTTATCCTTTGACGTTTC
ANG503	3-BglII-His6-YqgS	GAAGATCTttaGTGATGGTGATGGTGATGaccTGATGCCTGATCAAGCATTTGTTTTTC
ANG504	3-BglII-His6-YfnI	GAAGATCTttaGTGATGGTGATGGTGATGaccTTTGATTTCTTTCTCCTTGCCGTAATG
ANG522	F LtaS TM extr YfnI	cttagcttttgctGAAAAAGACCGTCCGCAACTG
ANG523	R LtaS TM extr YfnI	gacggtctttttcAGCAAAAGCTAAGTTTAAGAAG
ANG524	F YfnI TM extr LtaS	ctgcactatgcgGAAACTGACAGACCAGAATTATTAAC
ANG525	R YfnI TM extr LtaS	ctgtcagtttcCGCATAGTGCAGGTTGATGAAAAAC
ANG526	R YflE TM extr LtaS	ctgtcagtttcCGCAACTGCCAGGTTGATCAAG
ANG527	F YflE TM extr LtaS	ctggcagttgcgGAAACTGACAGACCAGAATTATTAAC
ANG528	R LtaS TM extr YflE	cggtctgattcAGCAAAAGCTAAGTTTAAGAAG
ANG529	F LtaS TM extr YflE	cttagcttttgctGAATCAGACCGTCCTGAATTGC
ANG614	F-YflEtm-linkereYfnI	ctggcagttgcgGAAAAAGACCGTCCGCAACTGC
ANG615	R-YflEtm-linkereYfnI	gacggtctttttcCGCAACTGCCAGGTTGATCAAG
ANG616	F-YflEtmlinker-eYfnI	cgcgcgcttgccAGCAGCGATGATTTAACAAGTG
ANG617	R-YflEtmlinker-eYfnI	atcatcgctgctGGCAAGCGCGCGCTGGCTGTTGGAC
ANG618	F-YfnItm-linkerYflE	ctgcactatgcgGAATCAGACCGTCCTGAATTGCTG
ANG619	R-YfnItm-linkerYflE	cggtctgattcCGCATAGTGCAGGTTGATGAAAAAC
ANG620	F-YfnItmlinker-YflE	gagcctatgcaGATTCCAGCGACGTAACGGAAG
ANG621	R-YfnItmlinker-YflE	gtcgctggaatcTGCATAGGCTCTTTGCGTCTCTG
ANG622	F-PltaS-SipT	ggggaaagaatcTTGACCGAGGAAAAAAATACGAATAC
ANG623	R-PltaS-SipT	ttcctcggtcaaGATTCTTTCCCCCGTTATTTAGATA
ANG625	3-SalI-SipT-His6	ACGCGTCGACTTAGTGATGGTGATGGTGATGaccTTTTGTTTGACGCATTTCGTTAAAC
ANG626	F-PltaS-SipV	ggggaaagaatcATGAAAAAACGGTTTTGGTTTCTTG
ANG624	3-SalI-SipT	ACGCGTCGACTTATTTTGTTTGACGCATTTCGTTAAAC
ANG627	R-PltaS-SipV	cgttttttcatGATTCTTTCCCCCGTTATTTAG
ANG628	3-SalI-SipV	ACGCGTCGACTTATTCGGCATCAGAAATCACACCGAC
ANG629	3-SalI-SipV-His6	ACGCGTCGACTTAGTGATGGTGATGGTGATGaccTTCGGCATCAGAAATCACACCGAC
ANG711	F LtaS P in 174	CTTCTTAAACTTAGCTTTTGCTcctACTGACAGACCAGAATTATTAAC
ANG712	R LtaS P in174	GTTAATAATTCTGGTCTGTCAGTaggAGCAAAAGCTAAGTTTAAGAAG
ANG714	R SipS SalI	ACGCGTCGACctaATTTGTTTTGCGCATTTCGTTAAAC
ANG715	R SipS-His SalI	ACGCGTCGACctaGTGATGGTGATGGTGATGaccATTTGTTTTGCGCATTTCGTTAAAC
ANG742	F-SipT/SipS	CAAACAAAATAAtgaagaccgttgtttattggagg

ANG743	R-SipT/SipS	caacggtcttcaTTATTTTGTTTGACGCATTTCGTTAAAC
ANG744	F-SipV/SipS	GATGCCGAATAAtgaagaccgttgtttattggagg
ANG745	R-SipV/SipS	caacggtcttcaTTATTCGGCATCAGAAATCACACCGAC
ANG775	R-YqgS-PLtaS	CGTTTTTCGCATgattctttcccccgttatttagataataaatc
ANG796	N-F-PltaS-YqgS	ggggaaagaatcATGCGAAAAACGTTTTTTTCGAAGATTTC
ANG800	3-SalI-pCL55	ACGCGTCGACCACGTTTCCATTTATCTGTATACGGATC
ANG821	3-P-pCL55	P-CACGTTTCCATTTATCTGTATACGGATC
ANG826	5'AvrII-PltaS-yqgS	CCGCCTAGGctaaataacgggggaaagaatcATG
ANG877	3-PstI-pCL55	CGGCTGCAGCACGTTTCCATTTATCTGTATACGGATC
ANG879	3'PstI-YvgJ-His6	CGGCTGCAGtcaGTGATGGTGATGGTGATGaccTTCGGAAAACCTGAGCAGGTCACC
ANG895	3'PstI-YqgS-His6	CGGCTGCAGttaGTGATGGTGATGGTGATGaccTGATGCCTGATCAAGCATTTGTTTTTC
ANG896	5-HindIII-SpsB	CCCAAGCTTcttaaaaagaggtgtcaaaaTTG
ANG908	XmaI – pRMC2 primer	TCCCCCGGGcgGAATTCGAGCTCAGATCTGTTAACGGTACCatc
ANG909	pALC2073 primer PCR1	GCTCAGATCTGTTAACGGTACCatcaagcttattttaattatac
ANG912	3-PstI-His6-YflE	CGGCTGCAGttaGTGATGGTGATGGTGATGaccTTTATCTTCGTTATCCTTTGACGTTTC
ANG948	3-NarI - tetR far	CCTTGGCGCCTTAAGACCCACTTTCACATTTAAGTTG
ANG1007	5-KpnI-SpsB	GGGGTACCaatcttaaaaagaggtgtcaaaaTTG
ANG1008	3-SalI-SpsB	ACGCGTCGACcaaacgatgttgtatttgtttc
ANG1010	5KpnI 1kb spsB F	GGGGTACCctatattttaattaacattcaagc
ANG1011	R-spsB-ErmAM	gaaaaaggaagagtTATTTCTTTTTTCAAttttgac
ANG1012	F-spsB-ErmAM	GAAAAAAGAAATAactcttccttttcaatattattg
ANG1013	F-ErmAM-spsB	ggaggaaataaAATTTCAATCCTGAAAATAC
ANG1014	R-ErmAM-spsB	caggattgaaattTTATTTCCTCCCGTTAAATAATAG
ANG1015	3EcoRI 1kb spsB R	CGGAATTCgctttaaatcttgattattg
ANG1183	3-KpnI-SpsB	GGGGTACCcaaacgatgttgtatttgtttc
ANG1203	5-QC-spsB-T114C	caattaaaggtgaatcaatggaCccaactttgaaagatggcgag
ANG1204	3-QC-spsB-T114C	ctcgccatctttcaaagttggGtccattgattcacctttaattg

Relevant restriction sites in primer sequences are underlined.

Chapter 3

Production and proteolytic cleavage of *S. aureus* LtaS

3.1 Objective of chapter 3

The *S. aureus* LtaS enzyme consists of two domains, an N-terminal membrane domain and a C-terminal extracellular enzymatic domain (eLtaS). Proteomic studies identified the eLtaS fragment in the culture supernatant suggesting that LtaS is processed during bacterial growth (Gatlin *et al*, 2006; Ziebandt *et al*, 2001). In this chapter the extent to which LtaS is processed was determined, and the subcellular location of the protein analysed. *S. aureus* secretes a range of proteases and their contribution to LtaS cleavage was investigated in defined mutant strains. Furthermore, two cleavage sites have been proposed for LtaS. Mass spectrometry analysis of secreted *S. aureus* proteins suggested that the LtaS protein is cleaved after residues ^{215}Ala-Leu-Ala^{217} (Ziebandt *et al*, 2001). However, a more recent study hypothesized that LtaS is in fact processed following residues ^{171}Ala-Phe-Ala^{173}, based on analysis using the SignalP 3.0 prediction program (Bendtsen *et al*, 2004; Powers *et al*, 2011). In this chapter the LtaS cleavage site was identified independently, and attempts to construct an uncleavable LtaS variant are discussed.

3.2 Analysis of the sub-cellular location of LtaS

The *S. aureus* LtaS enzyme is synthesized as a membrane protein consisting of five N-terminal transmembrane helices followed by a 44 amino acid (aa) linker region and a C-terminal extracellular enzymatic domain (eLtaS) (Fig. 8A). The latter domain comprises aa 245-604 and is currently annotated as a sulfatase domain. Proteomic studies on secreted proteins in *S. aureus* revealed that the LtaS enzyme is partially processed, releasing a 50 kDa C-terminal fragment into the culture supernatant (Gatlin *et al*, 2006; Ziebandt *et al*, 2001). N-terminal sequencing identified the cleavage site C-terminal of the fifth transmembrane helix after residues ^{215}Ala-Leu-Ala^{217} and preceding the enzymatic domain (Ziebandt *et al*, 2001). To determine what percentage of the enzyme remains unprocessed and what remains cell wall associated, a cell wall fractionation experiment was performed and LtaS and fractionation-control proteins were detected by immuno-blotting (Fig. 8B and C). Proteins used as fractionation-controls were the ribosomal L6 protein, located in the cytoplasm, the membrane protein SrtA which anchors surface proteins containing an LPXTG sequence motif to the cell wall envelope, the cell wall anchored protein SdrD, which is covalently linked to the peptidoglycan and involved in cell adhesion, and alpha-hemolysin (Hla), a secreted bacterial toxin that causes lysis of target cells.

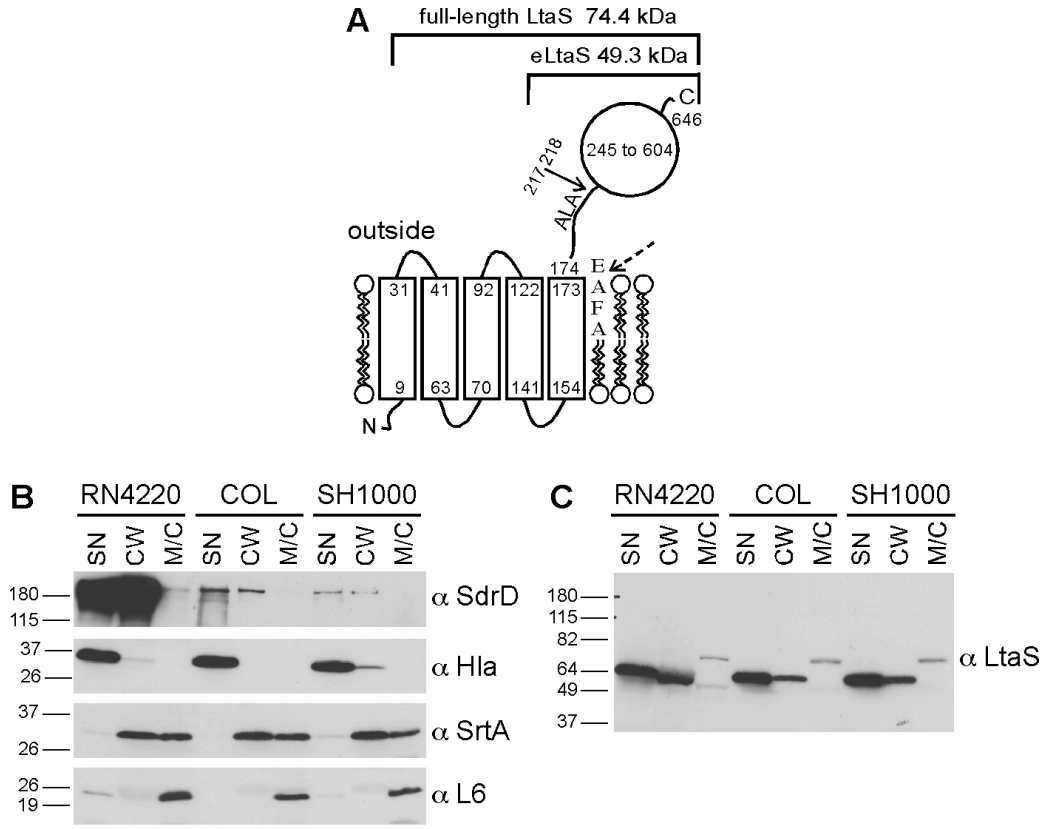

Figure 8: LtaS is efficiently processed in *S. aureus* and localizes to the supernatant and cell wall fraction. (A) Schematic representation of *S. aureus* LtaS. The 74.4 kDa full-length LtaS enzyme assembles in five N-terminal transmembrane spanning helices followed by a 44 amino acid linker region and the extracelluar enzymatic domain (eLtaS). The protein is cleaved following the linker region between amino acids 217 and 218, following an Ala-Leu-Ala motif, and the 49.3 kDa eLtaS domain is released from the bacterial membrane. The solid arrow indictes the LtaS cleavage site identified by proteomic studies and the dashed arrow markes the cleavage site predicted by the computer program SignalP 3.0 (Powers *et al*, 2011). **(B and C) Subcellular location of control proteins (B) and LtaS (C) in *S. aureus* strains RN4220, COL and SH1000.** Mid-log cultures of *S. aureus* strains RN4220, COL and SH1000 were fractionated into supernatant (SN), cell wall (CW) and combined membrane and cytoplasmic (M/C) fractions. LtaS and control proteins SdrD (cell wall anchored), Hla (secreted), SrtA (membrane) and L6 (cytoplasmic) were detected by western blot using polyclonal rabbit antibodies as indicated on the right of the panel. Note that the polyclonal antibody used for LtaS detection was raised against the extracellular eLtaS domain. Sizes of protein standards in kDa are shown on the left.

In all *S. aureus* strains tested (RN4220, COL, SH1000), the 49.3 kDa eLtaS fragment could be detected in both supernatant and cell wall fraction (Fig. 8C). No signal corresponding to the full-length protein was visible in the combined membrane and cytoplasmic (M/C) fractions. These data indicate that despite the fact that LtaS is synthesized as a membrane protein, the enzyme is efficiently processed and the eLtaS domain released into the culture supernatant, as well as being partially retained within the cell wall envelope. A weak 70 kDa signal appeared in all M/C fractions following incubation with the anti-LtaS antibody. This signal most likely resulted from

unspecific antibody binding, as LtaS expression studies in *E. coli* suggest a slightly slower mobility for the full-length protein on SDS-PAGE gels (Fig. 9). It is important to note that the polyclonal eLtaS specific antibody was produced in Chicago before this study was initiated and that therefore the preimmune serum was not available to further analyze the specificity of the antibody.

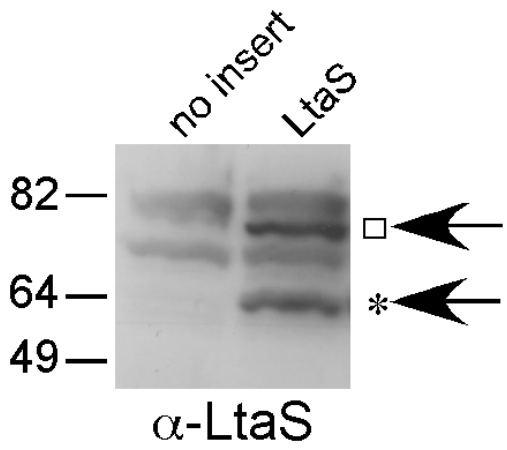

Figure 9: Western blot of LtaS protein detection in *E. coli*. Strains ANG482 (pOK) and ANG483 (pOK-*ltaS*) were grown overnight and whole cell samples were prepared as described in the Materials and Methods chapter (section 2.5). Samples were analysed by western blot using an LtaS-specific antibody. A square (□) indicates full-length LtaS protein and a star (*) denotes the cleaved eLtaS protein fragment. Sizes of protein standards in kDa are shown on the left.

3.3 LtaS expression from different promoters in *S. aureus*

As the LtaS protein could be detected in wild type (WT) *S. aureus*, it was decided to test whether the protein could be detected in *S. aureus* mutant strains with inducible LtaS expression. Two strains, ANG499 and ANG514, were analyzed in this context. *S. aureus* strain ANG499 harbors the native chromosomal *ltaS* gene under IPTG inducible *spac* promoter control (Fig. 10). Upon IPTG depletion, strain ANG499 is unable to synthesize LTA and ceases to grow approximately 4 h after IPTG removal. *S. aureus* strain ANG514 is derived from the integration of the p*itet* plasmid containing the *ltaS* gene under anhydrotetracycline (Atet) inducible promoter control into the chromosome of strain ANG499 (Fig. 10). Thus, strain ANG514 contains two copies of the *ltaS* gene, which are controlled by different promoters. Therefore, in the absence of IPTG and presence of Atet, *ltaS* expression from the native chromosomal location cloned under *spac* promoter control is shut down, while expression of the second *ltaS* copy, controlled by the p*itet* promoter, is induced.

Under these conditions bacterial growth and LTA synthesis solely depends on the functionality of the construct cloned under p*itet* promoter control. This expression system provides a tool to study the functionality of different constructs in terms of *ltaS* complementation and was used throughout this work.

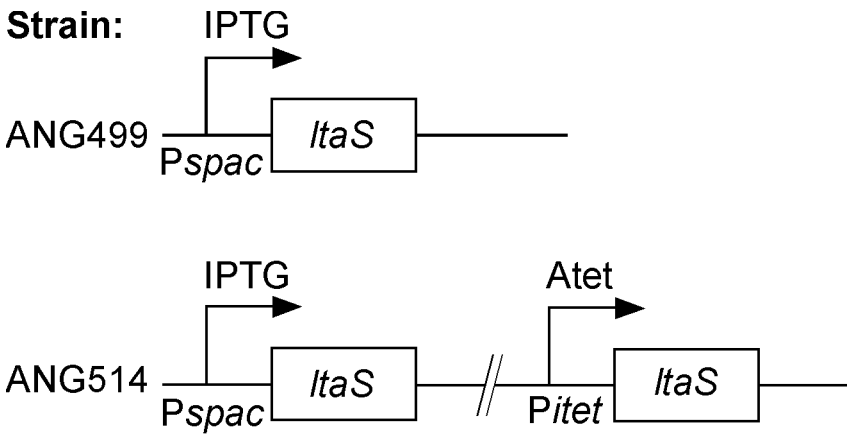

Figure 10: Chromosomal organization of *S. aureus* strains ANG499 and ANG514. Strain ANG499 harbors the chromocomal *ltaS* gene under IPTG inducible *spac* promoter control. Strain ANG514 contains two *ltaS* genes, where one copy is controlled by the *spac* promoter and the other one by the Atet inducible p*itet* promoter.

To investigate LtaS expression levels in the different *S. aureus* mutant strains, strains ANG499, ANG514 and WT *S. aureus* RN4220 (positive control) were grown in the presence and absence of appropriate inducers (Fig. 11A). The growth curve depicted in figure 11A shows a predicted OD that resulted from diluting the bacteria into fresh media at the 4 h time point and at the 8 h time point if necessary. This was done to keep the bacteria in the exponential growth phase. OD readings were subsequently multiplied with the dilution factor introduced at the specified time points. This particular way of plotting a growth curve was used throughout this work. Samples were removed from cultures described above at mid-log phase and analyzed for LTA and LtaS detection by western blot (Fig. 11B and C).

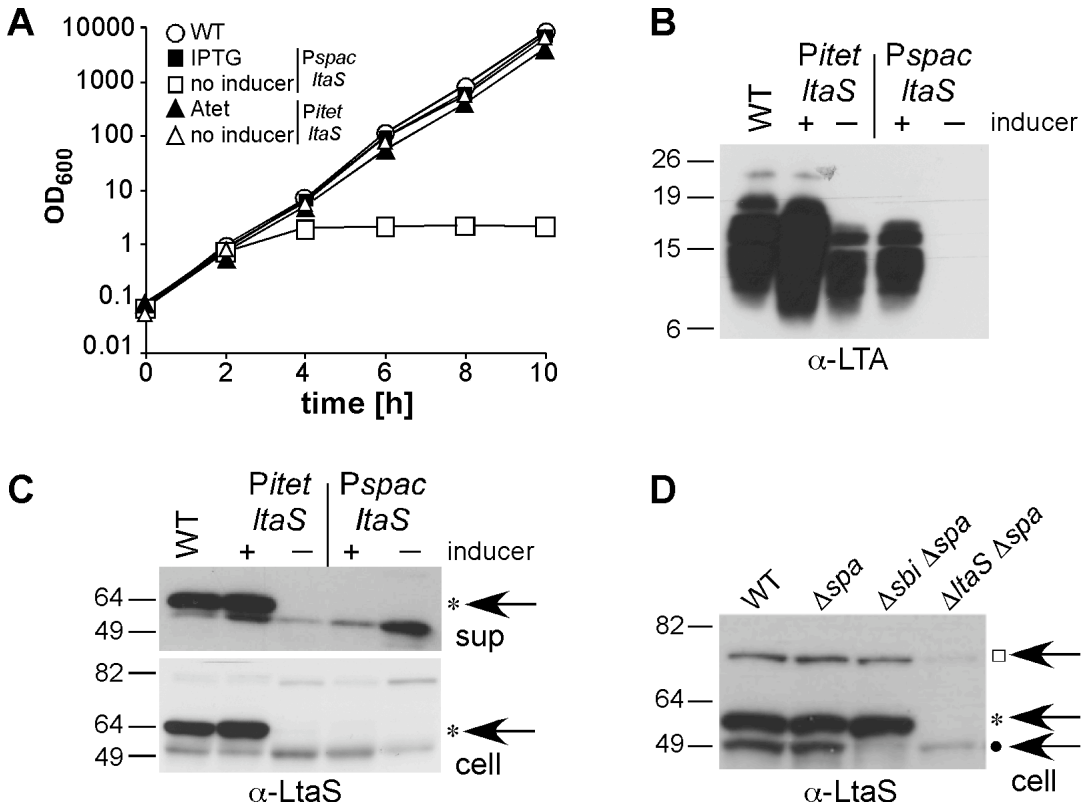

Figure 11: Comparison of LTA and LtaS production from native, IPTG-inducible and Atet-inducible promoters. (A) Bacterial growth curves. Washed overnight cultures of RN4220 (WT), the IPTG inducible *ltaS* expression strain ANG499 (P*spac-ltaS*), and the Atet inducible *ltaS* expression strain ANG514 (P*itet-ltaS*) were diluted 1:100 into fresh media and grown with or without the appropriate inducer. Bacterial growth was monitored by determining OD_{600} readings at the indicated time points. **(B) LTA and (C) LtaS detection by western blot in *S. aureus* mutant strains with inducible *ltaS* expression**. At the 4 h time point, 1 ml culture aliquots were removed from the *S. aureus* strains decribed above. Cell associated LTA was analyzed by western blot using an LTA-specific antibody (B), and supernatant (sup) and whole cell samples (cell) using an LtaS-specific antibody (C). **(D) Western blot of LtaS detection in defined *S. aureus* mutant strains**. Strains RN4220 (WT), SEJ1 (Δ*spa*), SEJ1 (Δ*sbi*Δ*spa*)-ANG1755 and 4S5 (Δ*ltaS*Δ*spa*)-ANG1786 were grown to mid-log phase and cell fractions prepared and analyzed by western blot using an LtaS-specific antibody. Full-length and eLtaS specific bands are indicated on the right of the panel with a square (□) and a star (*) , respectively. Two unspecific bands are present in the Δ*ltaS*Δ*spa* lane. The faint top band is of the same mobility as the full-length LtaS, and the bottom band is the Sbi protein annotated with a filled circle (●). Sizes of protein standards in kDa are shown on the left. Note that the Western blot 11D was obtained from N.T. Reichmann.

Following Atet induction, the cleaved LtaS protein could be detected in the supernatant and cell wall fraction of strain ANG514 (P*itet-ltaS*) (Fig. 11C). Comparable protein amounts were found in samples prepared from the WT *S. aureus* RN4220 control strain, indicating that Atet induced *ltaS* expression in ANG514 restores WT protein levels. In contrast, no protein band corresponding to the cleaved eLtaS product could be detected when expressed from the weak *spac* promoter in strain ANG499, even in the presence of IPTG. However, a second band with a slightly faster mobility as compared to the eLtaS fragment was visible in the supernatant and

cell wall fraction of all strains tested (Fig. 11C). Morover, the induced and uninduced cell wall fraction samples of strains ANG499 and ANG514 displayed an additional protein band that migrated just below 82 kDa (Fig. 11C). Protein A and Sbi are two *S. aureus* proteins known to bind to antibodies. To establish unambiguously, which of the bands recognized by the antibody are LtaS-specific, western blot analysis was performed on cell fraction samples isolated from WT RN4220, the isogenic protein A mutant strain SEJ1 (RN4220Δ*spa*) and the *sbi*/*spa* mutant strains (RN4220 Δ*sbi*Δ*spa*) (Fig. 11D). In addition, the protein A negative *S. aureus* strain 4S5 containing a complete *ltaS* deletion was used in the same experiment. The construction of this strain and the reason why this strain can grow in the absence of LTA are described in Corrigan *et al*. (manuscript under review). Two unspecific bands were detected in the *ltaS* deletion strain despite the fact that human IgG was used during all antibody incubations to block unspecific antibody binding (Fig. 11D). The faster migrating unspecific band corresponds most likely to Sbi, since this band was absent in the sample prepared from the *sbi* mutant strain (Fig. 11D; labeled with a filled circle). A second very faint unspecific band, which had the same mobility as the full-length LtaS protein, was also observed in this *ltaS* deletion strain (Fig. 11D; labeled with a square). However, the intensity of this top (full-length LtaS) band was drastically increased in the LtaS-expressing WT, *spa* and *sbi*/*spa* mutant strains. Therfore the protein bands observed in the supernatant and cell wall fraction of strain ANG499 grown in the presence of IPTG are not LtaS related and hence the protein could not be detected in this strain. However, these "undetectable" LtaS protein amounts were sufficient for LTA production and growth complementation (Fig. 11A and B). On the other hand, the p*itet* promoter appeared to be leaky, and bacterial growth and LTA synthesis of strain ANG514 was observed in medium lacking the inducer (Fig. 11A and B).

3.4 LtaS processing is independent of Aur, Ssp, Scp, Spl and HtrA proteases

From the experiments performed in section 3.2 it was clear that a large fraction of the *S. aureus* LtaS protein is cleaved during bacterial growth (Fig. 8C). *S. aureus* secretes a range of proteases, and to assess their contribution to LtaS processing, LtaS protein cleavage was analyzed in *S. aureus* strains with defined deficiencies in known

extracellular proteases. To this end, a previously described *S. aureus* strain deleted for the two surface serine proteases $HtrA_1$ and $HtrA_2$ (RN6390*htr*A_1*htr*A_2) (Rigoulay *et al*, 2005), and the isogenic WT RN6390 control strain were grown to mid-log phase. Supernatant and whole cell protein fractions were prepared and the LtaS protein detected by western blot. As seen in Fig. 12, LtaS processing was not impaired in the protease mutant strains, and similar amounts of cleaved protein were detected in the culture supernatant of WT and the *htrA* double mutant strain.

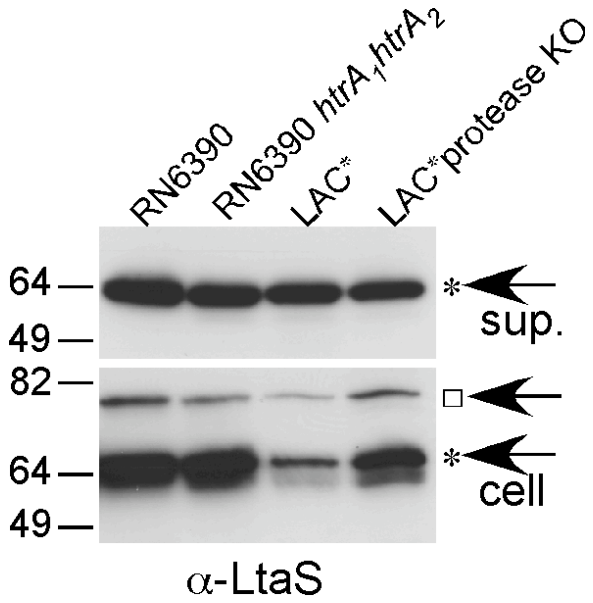

Figure 12: LtaS protein processing in defined *S. aureus* protease mutant strains. LtaS protein detection by western blot. *S. aureus* strains RN6390, the isogenic RN6390*htrA*$_1$*htrA*$_2$ mutant strain, LAC* and the isogenic LAC*Δ*aur* Δ*sspAB* Δ*scpA spl::erm* mutant strain (LAC* protease KO) were grown to mid-log phase and supernatant (sup) and whole cell fractions (cell) prepared as described in the Materials and Methods chapter (section 2.5). The LtaS protein was detected by western blot using an LtaS-specific antibody and sizes of protein standards separated alongside are given in kDa on the left of the panel. A square (□) indicates full-length LtaS protein and a star (*) denotes the cleaved eLtaS protein fragment. The western blot using whole cell samples was exposed 6 times longer than the blot with supernatant fraction samples.

Other known extracellular *S. aureus* proteases are SspA (a serine protease), SplA-F (serine protease like proteins), SspB and ScpA (cysteine proteases) and Aur (a metalloprotease). All the corresponding genes were inactivated in the *S. aureus* strain LAC* to create strain AH1919 (LAC* protease KO; this strain was obtained from Dr. Alexander Horswill). Again, no difference in the amount of secreted LtaS protein was observed in the LAC* protease KO strain as compared to the parental LAC* control strain (Fig. 12). This indicates that none of the currently known extracellular *S. aureus* proteases plays a major role in LtaS processing.

3.5 *S. aureus* signal peptidase SpsB is required for efficient LtaS processing

Recently, it was found that treatment of *S. epidermidis* cultures with the signal peptidase specific inhibitor arylomycin causes a reduction in the amount of cleaved LtaS protein in the culture supernatant (Powers *et al*, 2011). In addition, it has been reported that processing of the *B. subtilis* LtaS orthologue YfnI is diminished in the combined absence of the two signal peptidases SipT and SipV (Antelmann *et al*, 2001). *S. aureus* contains one active type I signal peptidase, which is encoded by *spsB* and thought to be essential for cell viability (Cregg *et al*, 1996). To test whether SpsB is required for LtaS processing in *S. aureus*, the RN4220-derived strain ANG2009 with IPTG inducible *spsB* expression was constructed (Fig. 13A). In this strain the native *spsB* gene is replaced with an Erm cassette, while a functional *spsB* copy is expressed from the IPTG-inducible *spac* promoter at a different chromosomal location. Strain ANG2009 grew in the presence of IPTG; however 4 h after removal of the inducer, the growth rate declined and a growth arrest was seen approximately 10 h after removal of IPTG, indicating successful depletion of the signal peptidase (Fig. 13B). To examine the impact of SpsB depletion on LtaS processing, strain ANG2009 was grown for 8 h with or without IPTG. Supernatant and whole cell protein fractions were prepared from these cultures and analyzed by western blot. In the absence of the inducer, significantly reduced levels of cleaved LtaS protein were observed in the supernatant, and a concomitant accumulation of the full-length LtaS protein was detected in the whole cell fraction (Fig. 13C). Taken together, these data indicate that *S. aureus* signal peptidase SpsB is required for efficient LtaS processing.

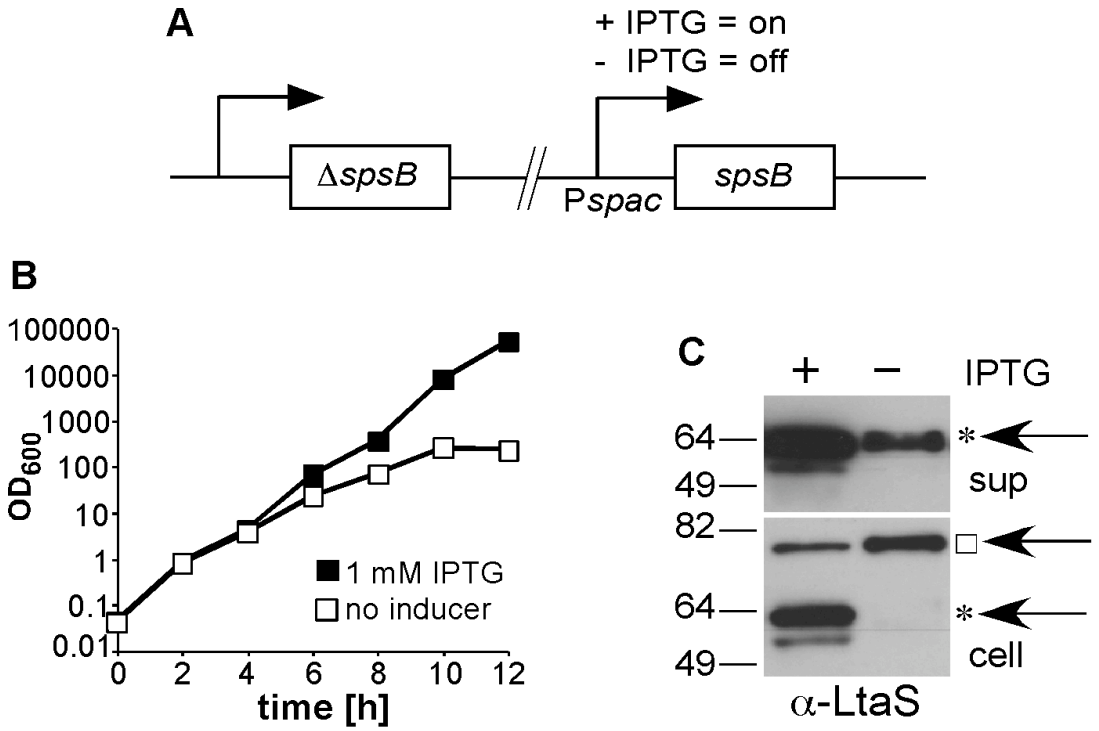

Figure 13: *S. aureus* signal peptidase SpsB is required for efficient LtaS processing. (A) Schematic representation of *S. aureus* strain ANG2009 with IPTG inducible *spsB* expression. Strain ANG2009 carries a copy of the *spsB* gene under IPTG-inducible *spac* promoter control, whilst the native *spsB* gene is replaced with an Erm cassette. **(B) Bacterial growth curves.** Washed overnight cultures of *S. aureus* strain ANG2009 with inducible *spsB* expression were back-diluted into medium with or without IPTG, and bacterial growth monitored by determining OD_{600} readings at the indicated time points. Four h after the initial dilution, cells were washed and back-diluted in fresh medium with or without IPTG, and at the 8 h time point cultures were diluted a second time to maintain them in the logarithmic growth phase. **(C) LtaS detection by western blot.** At the 8 h time point, supernatant (sup) and whole cell (cell) protein samples were prepared, and the LtaS protein detected by western blot using the eLtaS-specific antibody. Sizes of protein standards separated alongside are given in kDa on the left of the panel. A square (□) indicates full-length LtaS protein and a star (*) denotes the cleaved eLtaS protein fragment.

3.6 The main processing site in *S. aureus* LtaS is after Ala^{217} and a variant with reduced processing retains activity

Mass spectrometry analysis of secreted *S. aureus* proteins suggested that the LtaS protein is cleaved following the 5TM domain in the linker region after residues ^{215}Ala-Leu-Ala^{217} (Ziebandt *et al*, 2001). In a recent study, it was suggested that the *S. epidermidis* LtaS protein is cleaved after residues ^{171}Ala-Phe-Ala^{173}, based on analysis using the SignalP 3.0 prediction program (Bendtsen *et al*, 2004; Powers *et al*, 2011). These residues are also present in the *S. aureus* protein (Fig. 8A). To clarify the site of LtaS processing, and to investigate whether cleavage is required for enzyme function, the *S. aureus* LtaS enzyme was expressed as a C-terminal His-tag fusion protein from the p*itet* vector in the RN4220-derived *S. aureus* strain ANG499. The processed LtaS protein products were purified from culture supernatant by nickel affinity chromatography, and large amounts of Coomassie stained purified protein were obtained (Fig. 14A). The purified protein was subsequently subjected to a standard tryptic digest and mass spectrometry analysis at the Taplin Biological Mass Spectrometry Facility at the Harvard Medical School.

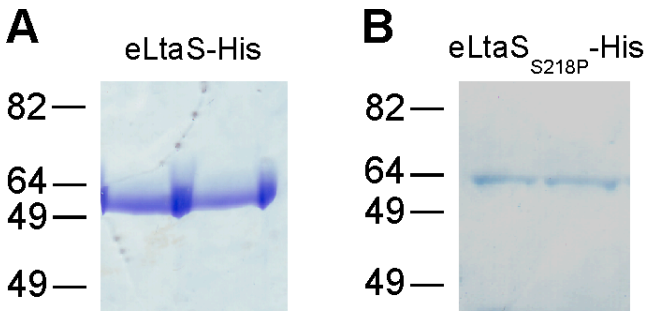

Figure 14: Coomassie stained gel of LtaS protein purified from *S. aureus* culture supernatant. *S. aureus* strains expressing (A) WT LtaS (ANG587) or (B) the LtaS$_{S218P}$ variant (ANG1370) as C-terminal His-tag fusion proteins were grown overnight in the presence of Atet after removal of IPTG. The following day, proteins were purified from culture supernatants as described in the Materials and Methods chapter (section 2.8) and 20 µl aliquots separated on a 10 % (w/v) SDS-PAGE and stained with Coomassie brilliant blue. Sizes of protein standards separated alongside are given in kDa on the left of the panel.

A tryptic peptide starting at alanine 215 was detected; however, the first strong signal for the most N-terminal fragment was obtained for a non-tryptic peptide starting at serine 218, suggesting that the main cleavage site in *S. aureus* LtaS is between amino acids Ala^{217} and Ser^{218} (Fig. 15D). For signal peptidase substrates, it has been established that a proline residue in the +1 position relative to the cleavage site prevents processing and converts signal peptidase substrates to competitive inhibitors (Barkocy-Gallagher & Bassford, 1992; Bruton *et al*, 2003). In analogy, it was reasoned that it might be possible to prevent LtaS processing by replacing Ser^{218} (+1 position) with a proline residue, and that this would allow for the determination of whether LtaS processing is required for function. An $LtaS_{S218P}$ variant was constructed and expressed from an Atet inducible promoter in *S. aureus* strain ANG499, which contains the native chromosomal *ltaS* gene under IPTG inducible expression control (Fig. 15A). Upon IPTG depletion, strain ANG499 is unable to synthesize LTA and ceases to grow unless a functional *ltaS* allele is expressed, in this case elsewhere on the chromosome, from the Atet inducible promoter (Fig. 15A). When this strain is grown in the presence of Atet, but absence of IPTG, it can be used to determine both the processing behavior of the $LtaS_{S218P}$ variant and its functionality based on its ability to complement growth and LTA production. *S. aureus* ANG499 harboring the empty p*itet* plasmid or expressing WT LtaS were included as negative and positive controls, respectively. Compared to WT LtaS, only very small amounts of a processed $LtaS_{S218P}$ form were detected in the supernatant fraction, and a concomitant accumulation of full-length protein in the whole cell fraction was observed (Fig. 15B). The cleaved $LtaS_{S218P}$ form showed a slightly slower mobility on SDS-PAGE gels (Fig. 15B), suggesting that this variant is processed at an alternative site closer to the 5TM domain. Of note, the additional band below the cleaved eLtaS fragment does not appear to be LtaS-specific, as it was also present in the negative (no insert) control strain (Fig. 15B). To investigate this further, the $LtaS_{S218P}$ variant was expressed as a C-terminal His-tag fusion protein, and cleaved protein products were purified from culture supernatants (Fig. 14B) and subjected to tryptic digest and mass spectrometry analysis as described above for WT LtaS. The most N-terminal fragment detected was a non-tryptic peptide starting at residue Lys^{192}, suggesting that the $LtaS_{S218P}$ variant is processed between residues Val^{191} and Lys^{192} (Fig. 15D). There was no indication that the *S. aureus* LtaS protein is processed at the SignalP 3.0 predicted site following

residues ^{171}Ala-Phe-Ala^{173}. Furthermore, mutating the glutamic acid residue at position 174 to a proline (which would be the +1 position for this cleavage site) did not reduce the amount of cleaved LtaS protein compared to WT LtaS (Fig. 15B). It is worth noting that two bands were observed for the processed $LtaS_{E174P}$ variant in the cell wall fraction, suggesting that the mutated protein is cleaved at multiple sites. However, the mutation also abrogated enzyme function, and the protein was no longer capable of promoting LTA synthesis (Fig. 15B). It is possible that by abolishing LtaS function other cleavage sites, which are normally hidden, become accessible to the protease. In summary, these findings indicate that LtaS processing naturally occurs between amino acids Ala^{217} and Ser^{218}. Mutating the conserved LtaS cleavage site blocks protein processing at the natural site and results in inefficient processing at the alternative site (between amino acids Val^{191} and Lys^{192}). Expression of the $LtaS_{S218P}$ variant with drastically reduced cleavage restored both bacterial growth and LTA production to the LtaS depletion strain ANG499 (Fig. 15B and C), indicating that efficient processing is not essential for LtaS function under standard laboratory growth conditions.

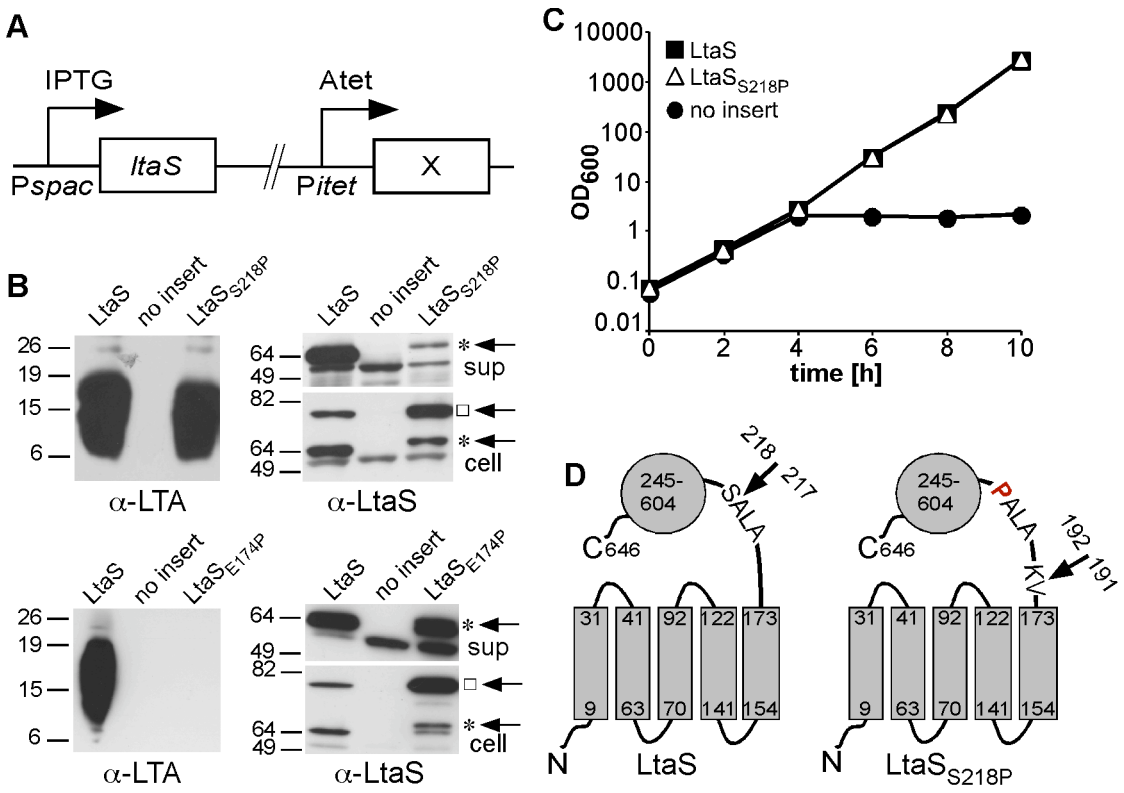

Figure 15: LtaS$_{S218P}$ variant with mutated cleavage site shows reduced processing but retains activity. (A) Schematic representation of complementation assay. *S. aureus* strain(s) used for complementation studies contain the chromosomal copy of *ltaS* gene under IPTG inducible *spac* promoter control, and the LtaS variant under investigation (X) is expressed at ectopic chromosomal location from the Atet inducible promoter. **(B) Detection of LTA and LtaS by western blot**. *S. aureus* strains expressing WT LtaS, the LtaS$_{S218P}$ and the LtaS$_{E174P}$ variants were grown in the presence of Atet, after removal of IPTG, for 4 h. As a negative control, an *S. aureus* strain containing the empty p*itet* vector (no insert) was included in the study. Subsequently, 1 ml culture aliquots were removed and samples prepared and analyzed by western blot. A mouse monoclonal anti-LTA antibody was used for the detection of LTA in the cell-associated fraction, and the eLtaS-specific antibody was used for the detection of LtaS in the supernatant (sup) and the whole cell (cell) fraction. Sizes of protein standards separated alongside are given in kDa on the left of the panel. A square (□) indicates full-length LtaS protein and a star (∗) denotes the cleaved eLtaS protein fragment. *S. aureus* strains ANG513, ANG514, ANG1246 and ANG2184 were used for this experiment. **(C) Bacterial growth curves.** The above strains, excluding the LtaS$_{E174P}$ variant, were induced after removal of IPTG by the addition of Atet, and growth of all cultures was monitored by determining OD$_{600}$ readings at the indicated time points. Cultures were back-diluted 1:100 in fresh medium at the 4 h time point, to maintain cultures in the logarithmic growth phase. **(D) Schematic representation of WT LtaS and the LtaS$_{S218P}$ variant.** Numbers refer to amino acid positions and arrows indicate the main cleavage sites as identified by mass spectrometry analysis. The proline substitution in the LtaS$_{S218P}$ mutant is shown as bold red letter.

Chapter 4

Requirements for LtaS function *in vivo*

4.1 Objective of chapter 4

The *S. aureus* LtaS protein contains five N-terminal transmembrane helices, which are highly conserved among LtaS-type enzymes. In this chapter the contribution of the LtaS membrane domain to enzyme function was investigated. To this end the N-terminal LtaS membrane domain was replaced with single and multiple transmembrane helices of other staphylococcal proteins, and the functionality of the hybrid proteins was tested in an LtaS *in vivo* enzyme assay.

A previous study has demonstrated that the *B. subtilis* LtaS orthologues *yflE* and *yfnI* encode for LTA synthases (Gründling & Schneewind, 2007a). However, expression of YfnI in an *ltaS* depleted *S. aureus* mutant strain resulted in the production of glycerolphosphate polymers with retarded mobility on SDS-PAGE, and no growth complementation was observed (Gründling & Schneewind, 2007a). In this chapter investigations as to which domain of YfnI (membrane versus enzymatic domain) contains the information for the synthesis of a structurally altered LTA polymer were undertaken. For this, hybrid fusions between functional (*S. aureus* LtaS and *B. subtilis* YflE) and the non-functional (*B. subtilis* YfnI) protein were constructed and analysed for *in vivo* function.

4.2 The 5TM domain of LtaS is required for *in vivo* function

Recently, it was shown that the recombinant eLtaS domain retains enzymatic activity in an *in vitro* assay system, and is capable of hydrolyzing fluorescently labeled PG lipid to DAG (Karatsa-Dodgson *et al*, 2010). To investigate if the eLtaS domain is sufficient for LTA production, and to determine the contribution and specificity of the 5TM domain for *in vivo* function, a series of fusion proteins with different membrane domains were constructed (Fig. 16). A secreted eLtaS variant (Sec-eLtaS) was designed by replacing the 5TM domain and linker region with the conventional signal sequence of Protein A. A single TM helix, derived from the *S. aureus* sortase A protein, was fused to eLtaS (TM_{SrtA}-eLtaS) in an attempt to anchor the eLtaS domain to the membrane. Multiple TM helices, derived from the *S. aureus* LtaA membrane protein, were fused to the linker region and eLtaS domain ($5TM_{LtaA}$-eLtaS), while two constructs with shortened LtaS-derived membrane domains were made in which the last four (1TM-eLtaS) or the last two (3TM-eLtaS) TM helices of LtaS were removed.

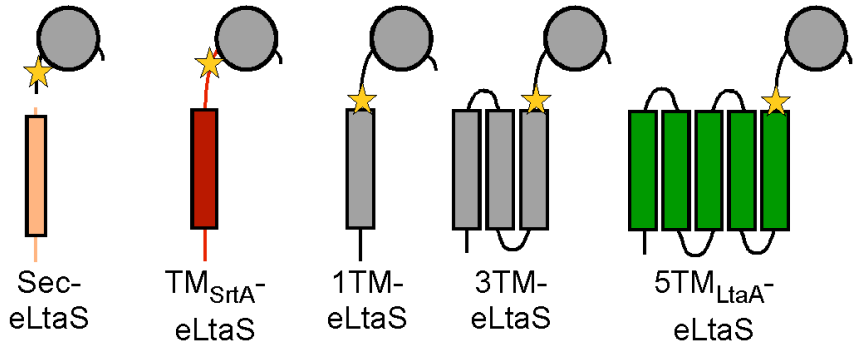

Figure 16: Schematic representation of the different fusion proteins used for complementation analysis. The protein A signal peptide was fused to eLtaS to produce a secreted eLtaS variant (Sec-eLtaS). The eLtaS domain was fused to the single sortase A TM helix (TM_{SrtA}-eLtaS) and to the first 5 TM helices of LtaA ($5TM_{LtaA}$-eLtaS). Shortened LtaS versions with 1 or 3 TM helices were also constructed (1TM-eLtaS and 3TM-eLtaS). Protein portions shown in grey are derived from the *S. aureus* LtaS protein, coloured fragments are derived from other *S. aureus* proteins and fusion sites are indicated by yellow stars. Details on the construction of these fusion proteins can be found in the Materials and Methods chapter (section 2.12).

To test the functionality of these five fusion proteins, they were expressed, as described in section 3.6 for the $LtaS_{S218P}$ variant, in *S. aureus* strain ANG499, which is unable to synthesize LTA and ceases to grow upon IPTG depletion unless a functional LtaS protein is expressed from the Atet inducible promoter (Fig. 15A). In contrast to WT LtaS, expression of the five fusion proteins did neither restore bacterial growth

nor LTA production, and as observed for the negative control strain containing the empty p*itet* vector, growth of all strains ceased after 4 h, and no LTA specific signal was detected on western blots (Fig. 17A - C). Note that only the cell accociated LTA of the *S. aureus* mutant strains expressing the different fusion proteins was analysed. It is possible that no LTA could be detected in these strains because the polymer was released into the supernatant during the cell lysis process. However, this is very unlikely as the technique used to lyze the cells (see Materials and Methods chapter, section 2.5) should not separate the membrane fraction fom the cell debris. In aggrement with this, cell accociated LTA could be detected in the WT LtaS expressing control strain (Fig. 17C).

Expression of all fusion proteins was confirmed by western blot using the eLtaS-specific antibody (Fig. 17D), albeit protein levels differed greatly. It seems unlikely that insufficient protein quantities are the reason for the lack of complementation, as non-detectable amounts of WT LtaS expressed from the weak *spac* promoter are sufficient to promote growth and LTA synthesis (Fig. 11A and B). Taken together, these experiments demonstrate that the 5TM domain of LtaS is essential for enzyme function and polyglycerolphosphate backbone chain production *in vivo*.

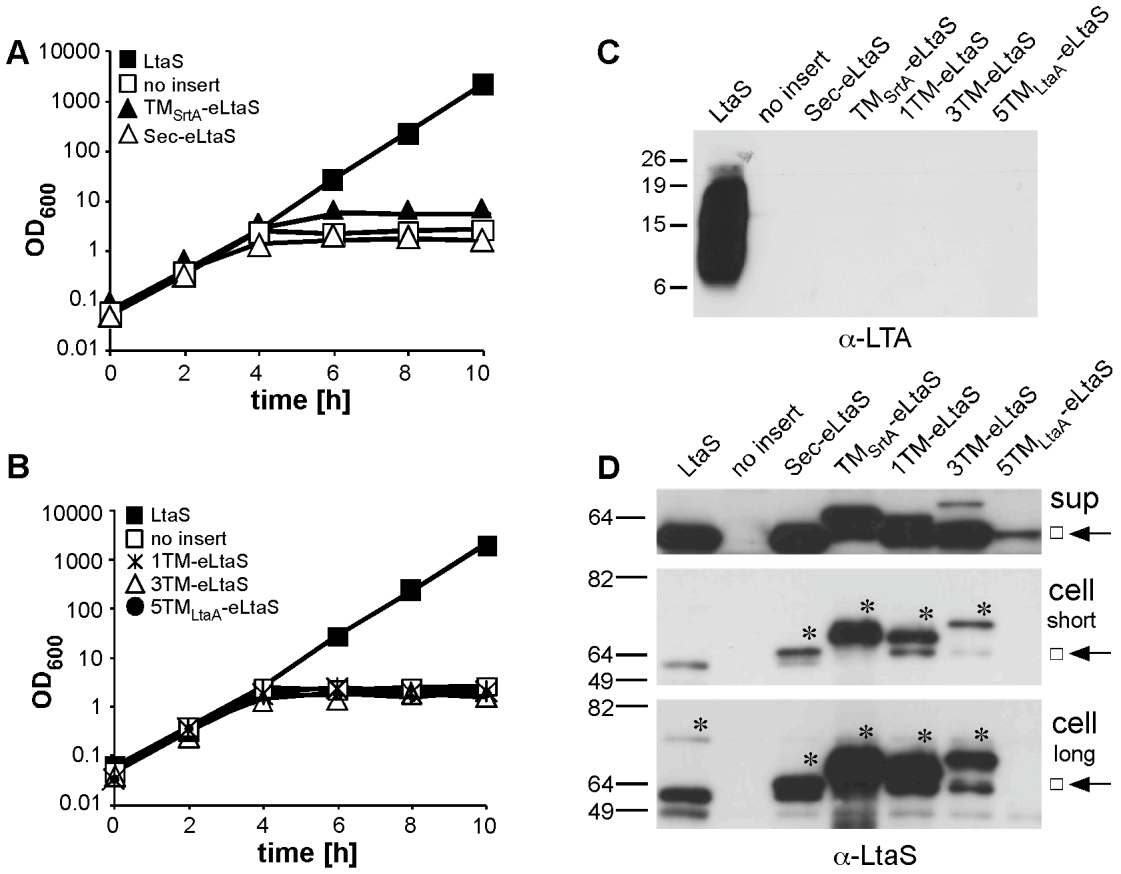

Figure 17: Complementation of growth and LTA production upon expression of different fusion proteins. (A and B) Bacterial growth curves. The fusion proteins indicated in the legend and depicted in Fig. 16 were expressed in *S. aureus* ANG499 by the addition of Atet after removal of IPTG. A strain expressing WT LtaS served as a positive control, while a strain containing the empty p*itet* vector (no insert) acted as a negative control. Bacterial growth was monitored by determining OD_{600} readings at the indicated time points. All cultures were back-diluted 1:100 at the 4 h time point, and the culture with the WT LtaS expressing control strain was back-diluted a second time at the 8 h time point, to maintain the cultures in the logarithmic growth phase. **(C) LTA and (D) LtaS protein detection by western blot.** At the 4 h time point 1 ml aliquots were removed from *S. aureus* cultures described above, the LTA in the cell-associated fraction detected using an LTA specific antibody, and the LtaS protein in the supernatant (sup) and the whole cell (cell) using an eLtaS-specific antibody. Proteins expressed are indicated above each lane, and a square (□) denotes the cleaved eLtaS protein fragment and the assumed full-length LtaS fusion proteins are indicated in each lane separately with a star (∗). Sizes of protein standards separated alongside are given in kDa on the left of the panel. Note that two different exposure times are shown for the cell fraction sample in order to visualize the full-length wild type LtaS protein. *S. aureus* strains ANG513, ANG514, ANG595, ANG1217, ANG1218 ANG1219 and ANG1220 were used for this experiment.

4.3 The 5TM domain of LtaS is needed for the LTA primase reaction

It is assumed that *S. aureus* LtaS not only polymerizes the LTA backbone chain, but also catalyzes the transfer of the initial glycerolphosphate (GroP) subunit onto the glycolipid anchor, resulting in the synthesis of the GroP-Glc_2-DAG intermediate. This intermediate would not have been detected by the western blot analysis described in section 4.2. To test if the eLtaS domain, or any of the other fusion proteins with altered TM domains, retain the ability to synthesize the GroP-glycolipid intermediate, glycolipids produced in *S. aureus* strains expressing the different fusion proteins were analyzed. From studies described in section 7.3, it is known that expression of the *B. subtilis* LTA primase YvgJ, from the Atet inducible promoter and a multi-copy plasmid, leads to the clear accumulation of the GroP-Glc_2-DAG glycolipid intermediate. Therefore, all five fusion proteins were expressed from the same plasmid system in *S. aureus* ANG499. Of note, expression of the fusion proteins from this multi-copy plasmid did neither restore bacterial growth nor LTA production in the *S. aureus* LtaS depletion strain (Fig. 18A-C).

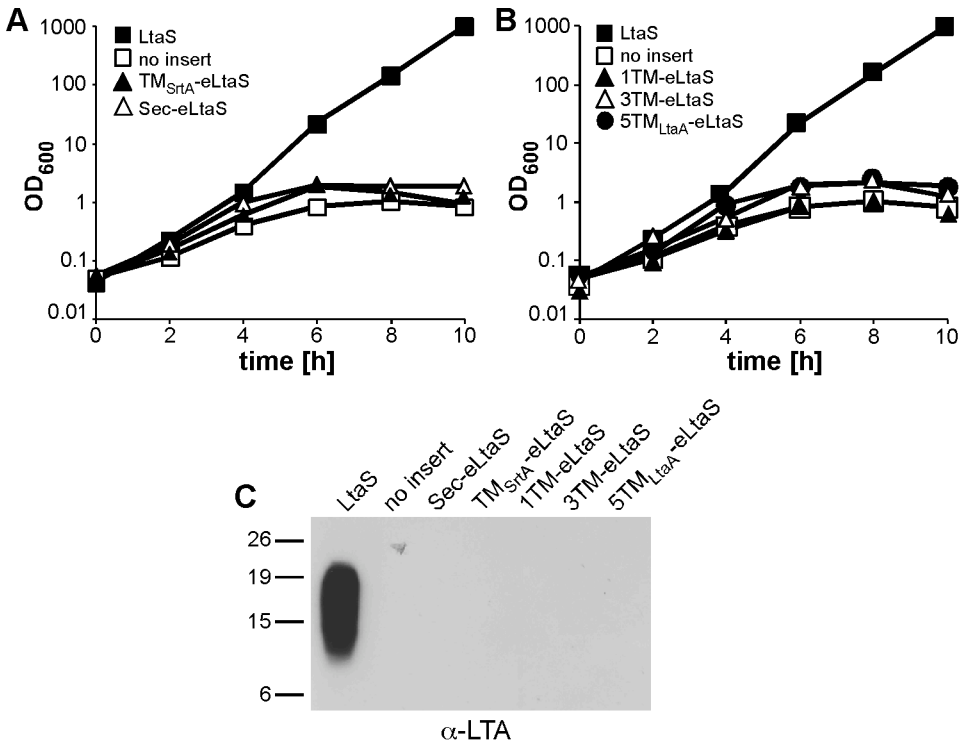

Figure 18: Growth and LTA complementation upon expression of fusion proteins from a high copy plasmid. (A and B) Bacterial growth curves. The fusion proteins depicted in Fig. 16 were expressed from the high-copy plasmid pCN34 in *S. aureus* ANG499 by the addition of Atet after removal of IPTG. A WT LtaS expressing *S. aureus* mutant strain was used as a positive control and a strain containing the empty pCN34 vector (no insert) acted as a negative control. Bacterial growth was followed by OD_{600} measurements at the indicated time points. All cultures were back-diluted 1:100 at the 4 h time point, and the culture with the WT LtaS expressing control strain was back-diluted a second time at the 8 h time point, to maintain the cultures in the logarithmic growth phase. **(C) LTA detection by western blot.** At the 4 h time point, 1 ml aliquots were removed from *S. aureus* cultures and LTA samples prepared and analyzed by western blot as described in the Materials and Methods chapter (section 2.5). Cell-associated LTA was detected by using an LTA specific antibody. Proteins expressed are indicated above each lane and sizes of protein standards separated alongside are given in kDa on the left of the panel. *S. aureus* strains ANG1130, ANG1571, and ANG2165 to ANG2169 were used for this experiment.

Total lipids were extracted from mid-log cultures of *S. aureus* strains either expressing the fusion proteins, *B. subtilis* YvgJ, *S. aureus* WT LtaS, or containing the empty pCN34 vector. Next, the lipids obtained were separated by TLC, and glycolipids visualized by staining with α-naphthol and sulphuric acid (Fig. 19). A glycolipid band corresponding to Glc_2-DAG was detected in all samples. In addition a clear accumulation of the lower migrating glycolipid GroP-Glc_2-DAG was observed in the samples isolated from the YvgJ expressing strain (Fig. 19). However, no signal above that obtained from the strain harboring the empty vector (no insert) control was seen upon expression of all five LtaS fusion proteins (Fig. 19). These data suggest that the eLtaS domain alone is not sufficient to initiate LTA synthesis. Therefore, the 5TM domain is, *in vivo,* critical for both the LTA priming and the polymerization reactions.

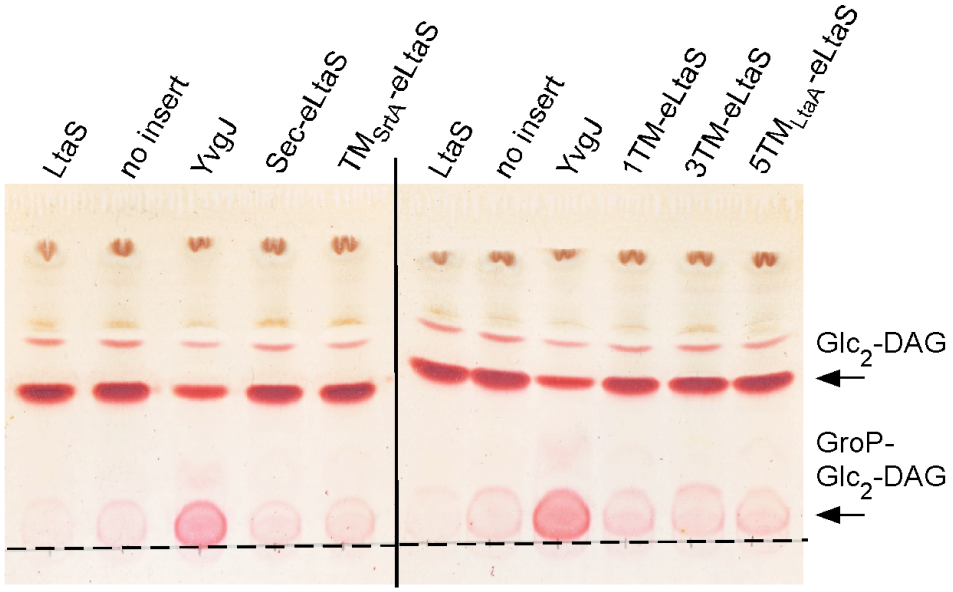

Figure 19: TLC analysis of glycolipids produced by *S. aureus* strains expressing different LtaS fusion proteins. LtaS fusion proteins indicated above each lane were expressed from a multi-copy plasmid by the addition of Atet, after removal of IPTG, in the *S. aureus* LtaS depletion strain ANG499. A strain expressing *S. aureus* LtaS, *B. subtilis* YvgJ or a strain containing the empty plasmid pCN34 (no insert) were used as controls. Cultures were grown to mid-log phase and lipids extracted and separated by TLC as described in the Materials and Methods chapter (section 2.10). Glycolipids were visualized by staining with α-naphthol/sulphuric acid. The origin is marked with a dashed line and the positions of the glycolipids Glc_2-DAG (top band) and GroP-Glc_2-DAG (bottom band) are indicated with an arrow on the right of the panel. *S. aureus* strains ANG1130, ANG1571, ANG1658, and ANG2165 to ANG2169 were used for this experiment.

4.4 The 5TM and eLtaS cannot be expressed separately without loss of function

LtaS is efficiently processed during bacterial growth, and the experiments described in sections 4.2 and 4.3 have shown that the 5TM domain is essential for *in vivo* function. To investigate if the LtaS enzyme retains any activity once split into the 5TM and eLtaS domains, an *S. aureus* strain was constructed in which these two domains were expressed as separate proteins. *S. aureus* strain ANG595 carries the native *ltaS* gene under IPTG inducible promoter control, while the Sec-eLtaS protein is expressed from the Atet inducible promoter (Fig. 20A). A plasmid containing the 5TM domain under native LtaS promoter control was introduced into this strain, allowing for the expression of the 5TM domain and the secreted eLtaS domain as two separate fragments, in the absence of IPTG and presence of Atet (Fig. 20A). The empty plasmid pCN34 and a plasmid for expression of the full-length LtaS protein were also introduced into strain ANG595, and these strains served as controls. No growth complementation or LTA production was observed upon expression of the two domains as separate fragments in contrast to the expression of the full-length protein (Fig. 20B and C). Western blot analysis of supernatant and whole cell fractions confirmed the expression and secretion of the eLtaS domain in all strains tested (Fig. 20D). However, expression of the 5TM domain fragment could not be verified by western blot, neither when expressed as C- nor as N-terminal His-tag fusion proteins. To overcome this problem, the $LtaS_{T300A}$ variant in which the active site threonine is mutated to an alanine residue, was expressed in place of the 5TM domain. The $LtaS_{T300A}$ variant is inactive but stably expressed (Lu *et al*, 2009) and once cleaved the 5TM domain will at least be present temporarily in the membrane. To this end, plasmid pCN34*itet-ltaS*$_{T300A}$ was introduced into *S. aureus* ANG595 (Fig. 20A) and addition of Atet to this strain resulted in the expression of both the $LtaS_{T300A}$ variant and the secreted eLtaS domain (Fig. 20D). However, their co-expression also failed to promote bacterial growth or LTA production (Fig. 20B and C). These results suggest that the 5TM and eLtaS domains cannot be assembled post-synthesis to form a functional enzyme, and consequently the LtaS processing step seems to irreversibly inactivate the enzyme.

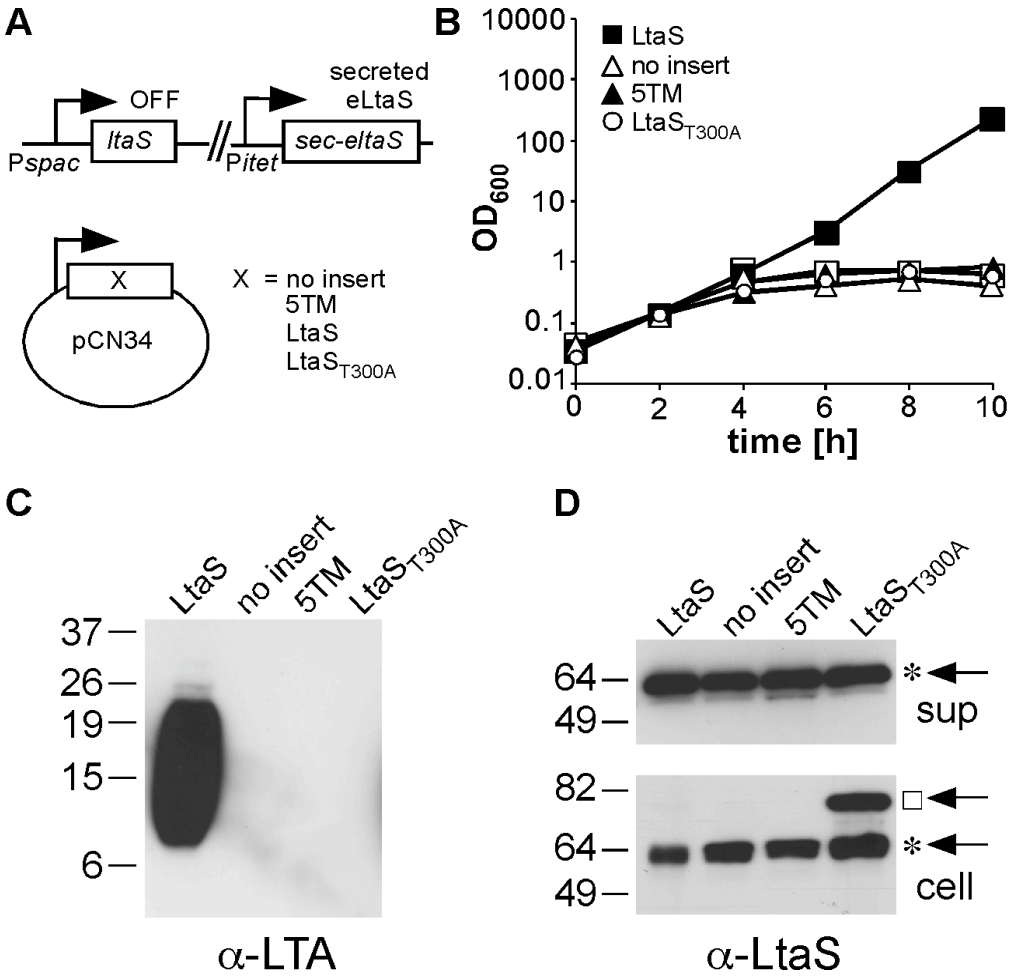

Figure 20: LtaS functions as a full-length but not as a 5TM - eLtaS split enzyme. (A) Schematic representation of *S. aureus* strain used for the separate expression of the 5TM domain and the eLtaS domain. The secreted eLtaS variant (Sec-eLtaS) was expressed from a chromosomal integration vector by the addition of Atet, and the 5TM domain of LtaS (5TM), an inactive full-length LtaS variant ($LtaS_{T300A}$) or WT LtaS (LtaS; positive control) were expressed from a multi-copy plasmid. A strain containing the empty plasmid vector pCN34 (no insert) was used as negative control. **(B) Bacterial growth curves.** The growth of *S. aureus* strains described in (A) was monitored by determining OD_{600} readings at the indicated time points. Cultures were back-diluted 1:100 into fresh medium at the 4 h time point and the culture with the WT LtaS expressing control strain was back-diluted a second time at the 8 h time point, to maintain cultures in the logarithmic growth phase. **(C) LTA and (D) LtaS detection by western blot.** Samples were prepared and analyzed by western blot as described in the Materials and Methods chapter (section 2.5). Sizes of protein standards separated alongside are given in kDa on the left of the panel. A square (□) indicates full-length LtaS protein and a star (∗) denotes the cleaved eLtaS protein fragment. The anti-LtaS western blot with cell samples was exposed twice as long as the western blot with supernatant samples. *S. aureus* strains ANG1226, ANG1227, ANG1228 and ANG1690 were used for this experiment.

4.5 Functional analysis of hybrid fusions between *S. aureus* LtaS and *B. subtilis* orthologues YflE, YfnI and YqgS

BLAST database searches of microbial genomes identified one or more LtaS orthologues in Gram-positive bacteria that synthesize polyglycerolphosphate LTA. For instance, whereas *S. aureus* has one *ltaS* gene, its close relative *B. subtilis* encodes four LtaS orthologues (YflE, YfnI, YqgS and YvgJ) with more than 40 % identity to *S. aureus* LtaS. All four proteins have the same predicted membrane topology and domain structure as *S. aureus* LtaS. In addition, all four proteins contain an Ala-X-Ala sequence motif at the end of the conserved linker region, which is reminiscent of and has been predicted to be a signal peptidase cleavage site (Antelmann *et al*, 2001). Furthermore, in proteomic studies, processed forms of YflE and YfnI were detected in the culture supernatant (Hirose *et al*, 2000; Tjalsma *et al*, 2004), showing that at least some of the *B. subtilis* proteins are cleaved, and the enzymatic domains released into the culture supernatant similar to what was observed for *S. aureus* LtaS (Gatlin *et al*, 2006; Lu *et al*, 2009; Ziebandt *et al*, 2001). By expressing each of the four *B. subtilis* orthologues in an *S. aureus ltaS* depletion strain, it was revealed that YflE and YfnI encode for LTA synthases, capable of producing polyglycerolphosphate polymers (Gründling & Schneewind, 2007a). However, YfnI-produced polymers could not restore the growth defect of a *S. aureus ltaS* depleted strain and had an altered mobility on SDS-PAGE gels, indicative of structural alterations (Gründling & Schneewind, 2007a). No enzyme activity was observed for YqgS or YvgJ.

To investigate which part of the YfnI protein (membrane versus enzymatic domain) is responsible for the synthesis of structurally altered polyglycerolphosphate and for the inability of YfnI to complement staphylococcal growth, hybrid fusions between functional LtaS-type proteins (*S. aureus* LtaS and *B. subtilis* YflE) and the non-functional (in terms of growth complementation) *B. subtilis* YfnI protein were constructed and analyzed for *in vivo* activity. We also designed and tested two fusions between *S. aureus* LtaS and the non-functional *B. subtilis* YqgS enzyme. YqgS was termed non-functional because of its inability to complement growth and LTA production in an *S. aureus ltaS* depleted strain when expressed from a single copy integration vector (Gründling & Schneewind, 2007a). Furthermore, two fusions between functional LtaS-type proteins (*S. aureus* LtaS and *B. subtilis* YflE) were included in the study and served as positive controls. A schematic representation of

the hybrid fusions constructed is shown in Fig. 21. Fusion proteins containing enzymatic domains of the *B. subtilis* LtaS-type enzymes were constructed as C-terminal His-tag proteins for detection purposes, whilst fusions harbouring the *S. aureus* eLtaS domain were detected using an LtaS specific antibody. It was speculated that the conserved linker region within LtaS-type enzymes might interact with the 5TM or with the enzymatic domain in a protein specific manner. It was therefore decided to construct multiple hybrid fusions in which the linker region was either derived from the 5TM or from the enzymatic domain of the fusion protein.

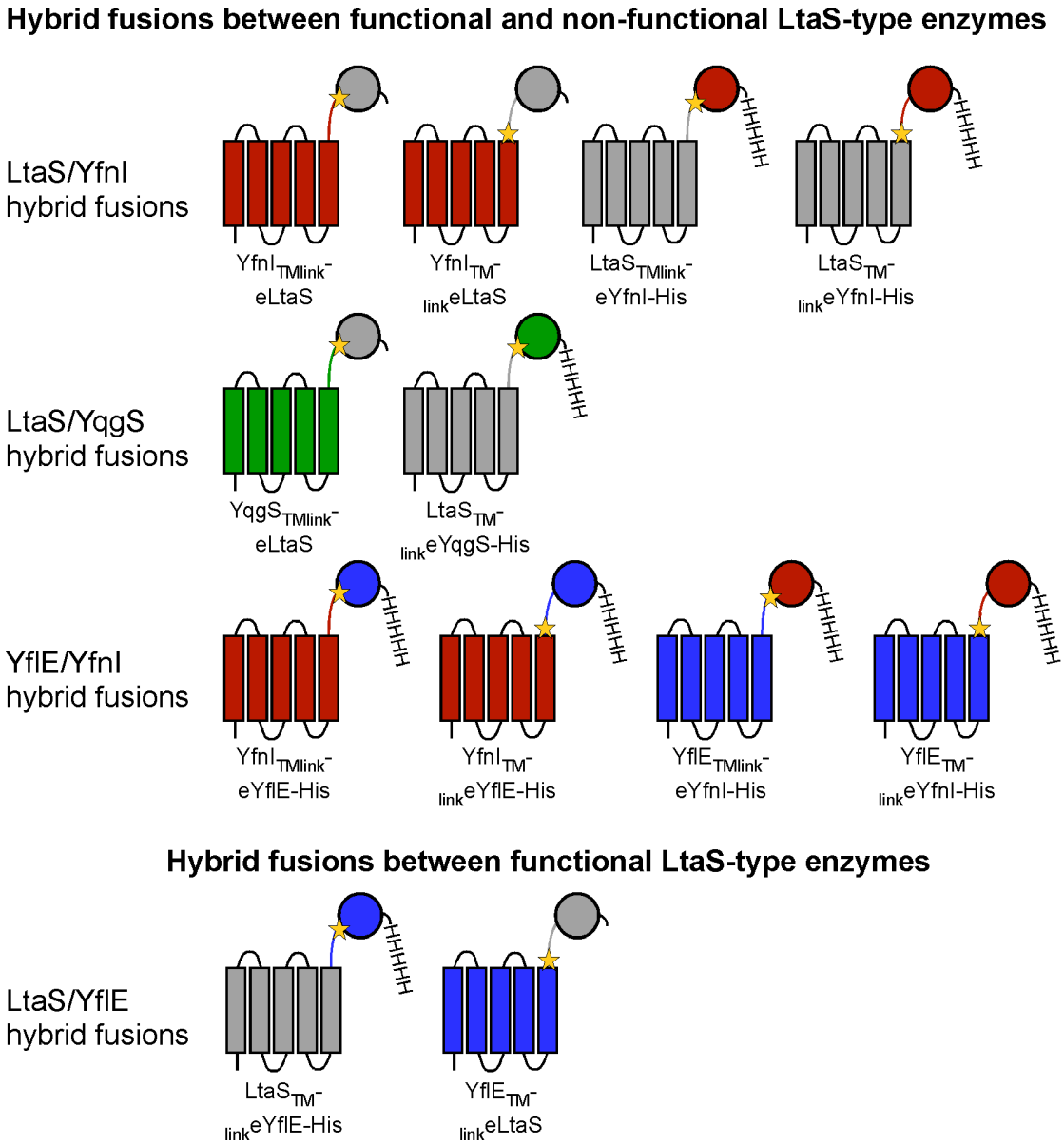

Figure 21: Schematic representation of the different fusions between functional (*S. aureus* LtaS and *B. subtilis* YflE) and non-functional (*B. subtilis* YfnI and YqgS) LtaS-type enzymes used for complementation studies. Protein portions shown in grey are derived from the *S. aureus* LtaS protein, coloured fragments are derived from the *B. subtilis* YfnI (red), YqgS (green) and YflE (blue) proteins and fusion sites are indicated by yellow stars. Hybrid fusions, which contain the enzymatic domains of YflE, YfnI or YqgS, were designed as C-terminal His-tag fusions for protein detection purposes. Details on the construction of these fusion proteins can be found in the Materials and Methods chapter (section 2.12).

To test the functionality of the different hybrid fusion proteins, the same complementation assay as described for the $LtaS_{S218P}$ variant in section 3.6 was used. For this assay, the hybrid fusions were expressed from the Atet inducible p*itet* promoter in *S. aureus* strain ANG499. Functional complementation of *ltaS* depletion was analyzed by adding Atet to the culture medium after removal of IPTG. *S. aureus* control strains ANG499 harbouring the empty p*itet* plasmid (negative control) or p*itet*

with WT *ltaS* (positive control) were included in the experiment. Atet induced expression of WT LtaS restored both bacterial growth and LTA synthesis in a *ltaS* depleted *S. aureus* mutant strain (Fig. 22 and 23A). Similarly, the $YflE_{TM\text{-}link}$eYfnI-His fusion partially restored staphylococcal growth, although no LTA signal could be detected by western blot using Tris/glycine gels (Fig. 22C and 23A). It is plausible that the $YflE_{TM\text{-}link}$eYfnI-His polymer might be very short and thus has a faster mobility on SDS-PAGE compared to WT LTA, and was therefore lost during the separation process. Indeed, it was possible to detect a $YflE_{TM\text{-}link}$eYfnI-His dependent signal for a polyglycerolphosphate polymer by western blot using Trycine gels, which provide a higher resolution for low molecular weight proteins than Tris/glycine gels (Fig. 23B). However, none of the other eleven hybrid proteins, including domain swaps between functional LTA synthases (*S. aureus* LtaS and *B. subtilis* YflE), were able to complement growth and/or LTA production (Fig 22 and 23A). With the exception of the $YqgS_{TMlink}$-eLtaS construct, expression of all other hybrid fusions was confirmed by western blot using the eLtaS-specific antibody or a His-tag specific antibody (Fig. 23C). It is possible that the inability to detect the $YqgS_{TMlink}$-eLtaS fusion results from a general instability of the protein. Alternatively, the *B. subtilis* YqgS ribosomal binding site might not be recognized efficiently by the staphylococcal translation machinery and therefore translation levels of the hybrid fusion protein might be low. Processed forms of some of the hybrid fusions could be detected in culture supernatants. In general, constructs containing the eYfnI domain were not processed in *S. aureus,* whereas fusions containing the eLtaS, eYqgS or eYflE domain were cleaved. In summary, while these data demonstrate that one of the *B. subtilis* / *S. aureus* LtaS hybrid proteins, namely $YflE_{TM\text{-}link}$eYfnI-His, retains some *in vivo* enzyme activity, these data also suggest a specific interaction between the 5TM and the enzymatic domain of LtaS-type enzymes, which is essential for enzyme function. This proposed interaction appears to be protein specific, based on the observation that hybrid fusions between functional LtaS-type enzymes resulted in non-functional proteins. The fact that the $YflE_{TM\text{-}link}$eYfnI-His hybrid fusion could partially restore staphylococcal growth and LTA synthesis indicates that the interaction between the two domains is, to some extent, repaired in this construct. However, the construct only shows *in vivo* activity if the linker region is derived from the YfnI enzyme, as a hybrid fusion containing the same domains but the YflE linker

region ($YflE_{TMlink}$-eYfnI-His), proved to be non-functional. These findings indicate that the enzymatic domain of LtaS-type enzymes interacts with both the 5TM and the linker region in a protein specific manner and that both interactions are required for enzyme function.

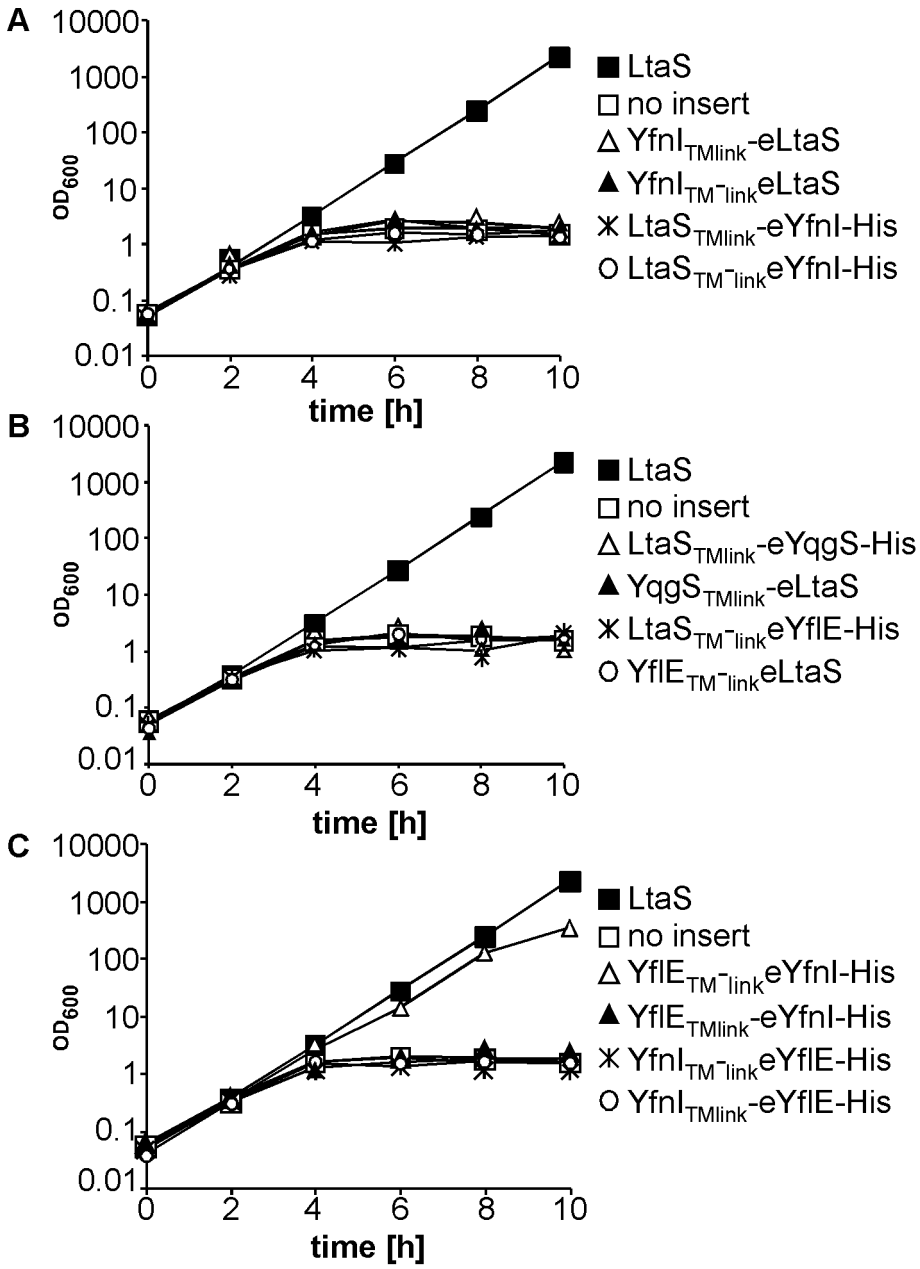

Figure 22: (A-C) Bacterial growth curves of *S. aureus* mutants expressing hybrid fusions between *S. aureus*/ *B. subtilis* LtaS-type enzymes. The hybrid fusion proteins depicted in Fig. 21 were expressed in *S. aureus* ANG499 by the addition of Atet, after removal of IPTG. A strain expressing WT LtaS served as positive and a strain containing the empty p*itet* vector (no insert) as a negative control. Bacterial growth was monitored by OD_{600} measurements of staphylococcal cultures. At the 4 h time point all cultures and at the 8 h time point WT LtaS expressing cultures were back-diluted 1:100 in fresh medium, to maintain bacteria in the logarithmic growth phase. *S. aureus* strains ANG514, ANG513 and ANG1340-1351 were used for this experiment.

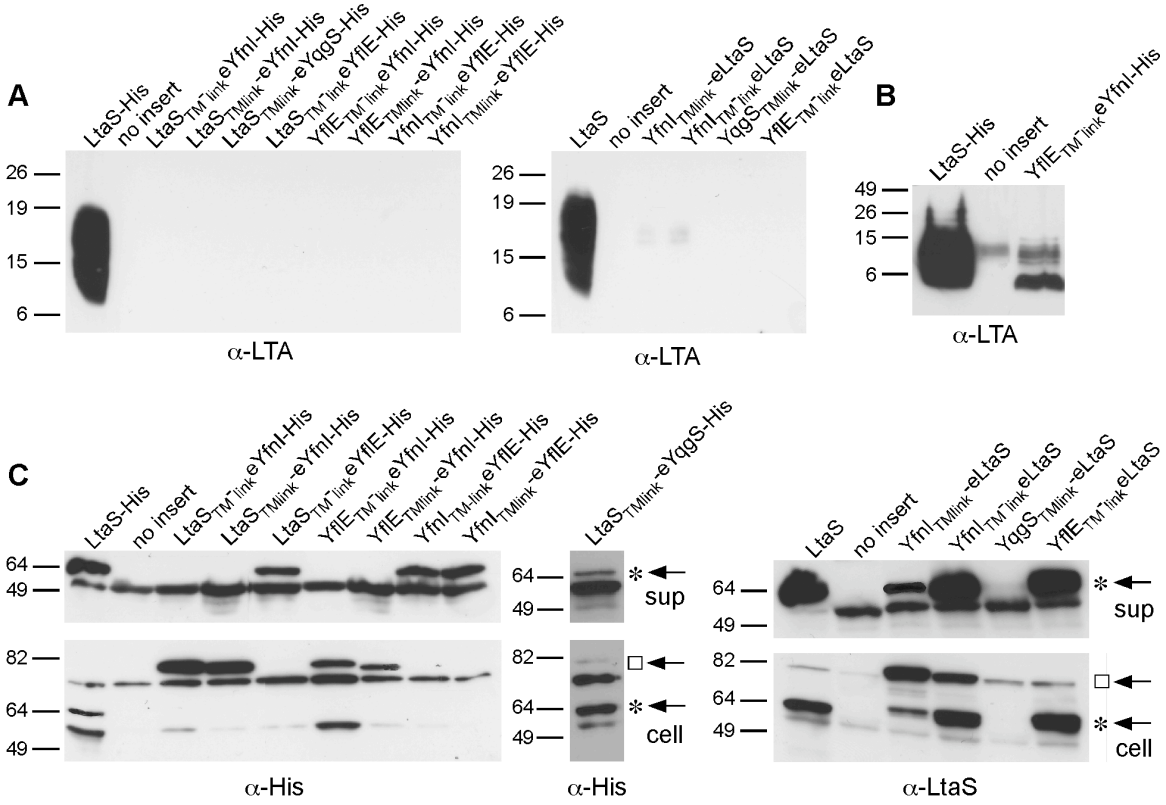

Figure 23: LTA and protein detection in *S. aureus* mutants expressing hybrid fusions between *S. aureus*/ *B. subtilis* LtaS-type enzymes. LTA detection by western blot using (A) Tris/glycine gels or (B) Trycine gels and (C) detection of hybrid fusion proteins by western blot. Samples from the same cultures analyzed for growth complementation in Fig. 22 and the LtaS-His expressing strain ANG587 were prepared and analyzed by western blot as described in the Materials and Methods chapter (section 2.5). Cell-associated LTA was detected using an LTA specific antibody, and the hybrid fusion proteins in the supernatant (sup) and the whole cell (cell) using an eLtaS-specific or a anti-His antibody. Sizes of protein standards separated alongside are given in kDa on the left of the panel. A square (□) indicates full-length protein and a star (∗) denotes the cleaved protein fragment.

Chapter 5
Discussion of chapters 3 and 4

S. aureus polyglycerolphosphate LTA is synthesized by LtaS, a membrane protein with five N-terminal transmembrane helices followed by a C-terminal extracellular enzymatic domain (eLtaS). The protein is cleaved during bacterial growth and the eLtaS domain released from the membrane (Ziebandt *et al*, 2001). In Chapter 3 and 4 evidence was provided that LtaS processing is most likely accomplished by the signal peptidase SpsB and serves as mechanism to irreversibly inactivate the enzyme so that it can no longer function in the LTA synthesis pathway.

In this study, it was shown that the *S. aureus* LtaS protein is efficiently cleaved and the eLtaS domain localizes to the supernatant and cell wall fraction. The main processing site in the LtaS protein was identified following residues ^{215}Ala-Leu-Ala^{217}, located within the linker region between the 5TM and eLtaS domains (Fig. 15D). Further experimental evidence is provided that the essential *S. aureus* type I signal peptidase SpsB is the protease responsible for this processing step, as depletion of SpsB leads to an accumulation of the full-length protein, whilst inactivation of any of the other currently known extracellular protease does not affect LtaS processing (sections 3.4 and 3.5). In addition, introduction of a proline residue at the +1 position with respect to the cleavage site, which is known to inhibit signal peptidase-dependent cleavage, prevents LtaS processing at this site (Fig. 15B). However, it should be noted that LtaS is a very atypical substrate for this type of protease. Usually signal peptidase substrates contain an N-terminal signal peptide that consists of a positively charged N-terminus, a central hydrophobic region and a polar extracellular C-terminal region, which contains the actual cleavage site, often ending with an Ala-X-Ala sequence at the -3 to -1 position of which the alanine at position -1 is especially important (van Roosmalen *et al*, 2004). Typically, the cleavage sites are placed 3-7 residues after the hydrophobic core, and this spacing is critical, as signal peptidases are integral membrane enzymes with an active site in close proximity to the bacterial membrane (van Roosmalen *et al*, 2004). LtaS is cleaved after an Ala-X-Ala motive, and this motif is quite conserved among LtaS-type enzymes, in particular the alanine at the -1 position, which is a typical feature for a signal peptidase substrate. However, the motif is not located after an N-terminal signal peptide but following multiple TM helices and furthermore, the processing site is more than 40 amino acids after the end of the last hydrophobic region. Therefore, we must assume that the binding of the eLtaS domain to its lipid substrate PG, or alternatively an interaction between the

eLtaS domain and the 5TM domain (discussed below) retains the cleavage site in close enough proximity to the membrane for signal peptidase to act upon. Usually it is thought that signal peptides are removed either during the translocation step or shortly afterwards (van Roosmalen *et al*, 2004). However, LtaS needs to persist intact long enough to perform its function in the LTA synthesis pathway, and therefore a mechanism might be in place that determines the exact timing of this processing step.

The *E. coli* MdoB protein is a Mn^{2+}-dependent metal enzyme that performs a reaction similar to that of LtaS (Goldberg *et al*, 1981; Jackson *et al*, 1984). MdoB catalyzes the transfer of GroP subunits from the membrane lipid PG onto periplasmic oligosaccharides under low-osmolarity conditions. Interestingly, similar to LtaS, MdoB consists of an N-terminal domain with multiple TM helices and a C-terminal extracellular enzymatic domain (Lequette *et al*, 2008). The enzymatic domain of MdoB is also cleaved during bacterial growth by a yet unknown protease also speculated to be signal peptidase and released from the membrane into the periplasmic space (Lequette *et al*, 2008). Recently, a model was proposed in which the full-length MdoB enzyme transfers GroP from the lipid PG onto nascent oligosaccharide molecules, whilst the cleaved protein is thought to swap GroP subunits from one oligosaccharide molecule to another (Lequette *et al*, 2008). Thus, it is thought that MdoB processing leads to a switch in substrate specificity, but that both the full-length and the cleaved forms are necessary for proper substitution of the membrane-derived oligosaccharides. It is not assumed that GroP subunits are transferred between different LTA chains in *S. aureus* or onto a different acceptor molecule. However, *S. aureus* LtaS is thought to perform two slightly different reactions; LtaS primes LTA synthesis by the addition of a GroP subunit to a hydroxyl group of the glycolipid anchor and subsequently polymerizes the LTA chain by the addition of GroP subunits to the hydroxyl group of the terminal GroP subunits, presumably using PG as substrate for both reaction. However, in contrast to MdoB, the data provided in this study suggest that the cleaved eLtaS fragment does not retain any activity relevant for the synthesis of LTA, as expression of the eLtaS domain alone neither results in polyglycerolphosphate chain formation nor in the production of the GroP-glycolipid intermediate (sections 4.2 and 4.3). It cannot formally be excluded that the eLtaS domain retains another *in vivo* activity, which was not observed because of the types of assays that were performed. It is possible that eLtaS

is still able to hydrolyze the membrane lipid PG without performing a transfer reaction. Alternatively, the eLtaS domain might indeed be involved in the transfer of GroP subunits between chains, from the LTA chain onto other molecules or the release and degradation of LTA chains, all of which is highly speculative. However, what seems to be clear is that in the absence of a functional full-length LtaS protein, the eLtaS domain alone is not sufficient to promote LTA synthesis and growth of *S. aureus*.

The data clearly indicate that the 5TM domain of LtaS plays an essential, yet unknown, role in LtaS enzyme function. It is possible that this domain recruits and "prepares" the PG lipid substrate for efficient hydrolysis by the active site located in the eLtaS domain. Interestingly, two enzymes, which were produced by fusing the 5TM and eLtaS domains of two functional LtaS-type enzymes, resulted in the formation of hybrid proteins that were unable to produce LTA (section 4.5). This indicates that very specific protein/protein interactions might occur between the 5TM and eLtaS domains and perhaps only through these interactions a fully functional active site will be formed. Moreover, it was found that expression of the N- and C-terminal LtaS domains as one protein is crucial for enzyme function, and the two domains cannot be expressed *in trans* without loss of function. Contrary to LtaS, the *S. aureus* MprF enzyme is composed of two distinct domains that can be physically separated, but the split protein remains functional. MprF catalyses the modification of PG with L-lysine resulting in the production of Lys-PG, which is thought to protect bacteria against antimicrobial peptides. Whilst the C-terminal domain of MprF is required for the synthesis of Lys-PG, the N-terminal domain is needed to flip Lys-PG from the inner to the outer leaflet of the bacterial membrane where the lysine-lipid is thought to function (Ernst *et al*, 2009).

In summary, the data presented in this work provide strong evidence that only the full-length LtaS enzyme is functional and active in the LTA synthesis pathway (Fig. 24). Furthermore, it is speculated that the LtaS processing step has a regulatory role and provides a mechanism for the cell to control LtaS activity. This might be of importance during the bacterial cell cycle and division process, or when bacteria enter the stationary phase and no longer divide. One can assume that under non-dividing conditions a halt in LTA synthesis is essential for bacteria to maintain a normal membrane composition and integrity.

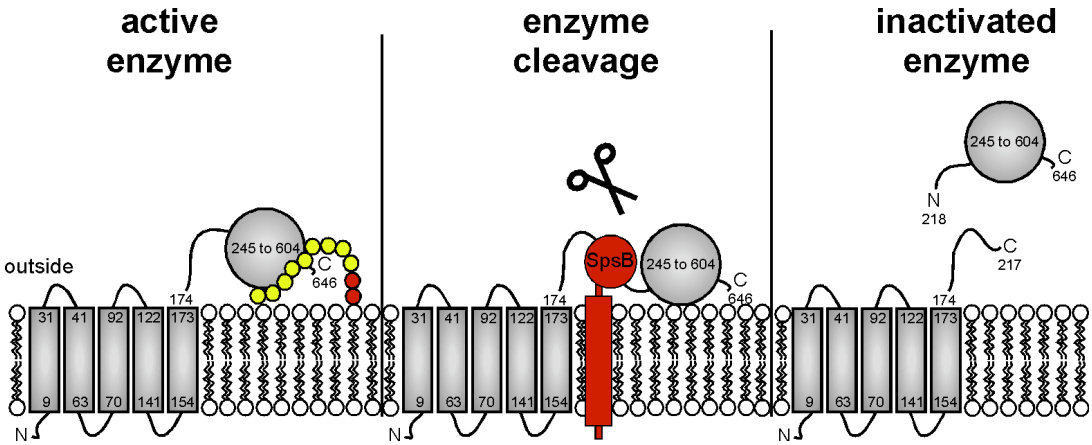

Figure 24: Model for LtaS enzyme function *in vivo*. The full-length LtaS protein is enzymatically active and synthesizes polyglycerolphosphate LTA. At some point the enzyme is proteolytically cleaved by the signal peptidase SpsB, and the eLtaS domain is released from the bacterial membrane. The cleaved LtaS protein is enzymatically inactive and no longer contributes to LTA synthesis.

Chapter 6

In vitro enzyme analysis of the *B. subtilis* LtaS orthologues

6.1 Objective of chapter 6

B. subtilis has four LtaS-like enzymes, namely YflE, YfnI, YqgS and YvgJ. All four enzymes show the same membrane topology consisting of five N-terminal transmembrane helices followed by a C-terminal extracellular enzymatic domain. In this chapter the enzymatic domains of all four *B. subtilis* LtaS-type enzymes were purified as N-terminal His-tag proteins from *E. coli* extracts and used for *in vitro* studies. A previously established *in vitro* assay for LtaS-type enzymes was used to determine enzyme kinetics of the purified proteins. The substrate specificity and ion dependency of all four *B. subtilis* LtaS-type enzymes was investigated.

6.2 All four *B. subtilis* LtaS orthologues are enzymatically active and hydrolyze fluorescently labeled PG

Enzymatic activities have previously only been detected for YflE and YfnI, two of the four *B. subtilis* LtaS orthologues (Gründling & Schneewind, 2007a). Recently, Karatsa-Dodgson *et al* developed an *in vitro* assay to measure *S. aureus* eLtaS enzyme activity (Karatsa-Dodgson *et al*, 2010). In this assay, purified enzyme was incubated with fluorescently labeled NBD-PG lipid, a labeled version of the proposed substrate for LtaS-type enzymes. It is assumed that LtaS hydrolyzes the glycerolphosphate head group of the lipid PG, and in the *in vitro* assay this reaction would result in the production of glycerolphosphate and fluorescently labeled diacylglycerol (NBD-DAG) (Fig. 25A). The input lipid NBD-PG, and the product lipid NBD-DAG can be separated on thin layer chromatography (TLC) and visualized with a fluorescence imager. Using this assay, it was determined that the purified enzymatic domain of *S. aureus* LtaS, eLtaS, but not the active site variant eLtaS-T300A, hydrolyzes fluorescently labeled NBD-PG (Karatsa-Dodgson *et al*, 2010). To determine if the *B. subtilis* LtaS orthologues can perform the same reaction, the enzymatic domains of all four *B. subtilis* proteins were cloned, expressed and purified as N-terminal His-tagged versions from *E. coli* extracts (Fig. 25B). Purified enzymes were mixed with NBD-PG lipid and incubated for 3 h in the presence of $MnCl_2$. Subsequently, lipids were extracted, separated by TLC and plates scanned using a fluorescence imager to visualize lipid bands. As a positive control, the commercially available *Bacillus cereus* phospholipase C (PLC) was used. This enzyme cleaves PG resulting in the production of DAG (Shinitzky *et al*, 1993). When the reactions were performed using each of the four *B. subtilis* proteins, two major fluorescent lipid bands were observed (Fig. 25C). The faster migrating band had the same mobility as the hydrolysis product produced by PLC, and presumably corresponds to NBD-DAG, and the slower migrating band had the mobility of the NBD-PG input lipid. No lipid corresponding to NBD-DAG was detected in reactions set up without enzyme. In summary, these data demonstrate that all four recombinant *B. subtilis* proteins are enzymatically active, and suggest that all proteins hydrolyze the phosphodiester bond of NBD-PG resulting in the production of NBD-DAG.

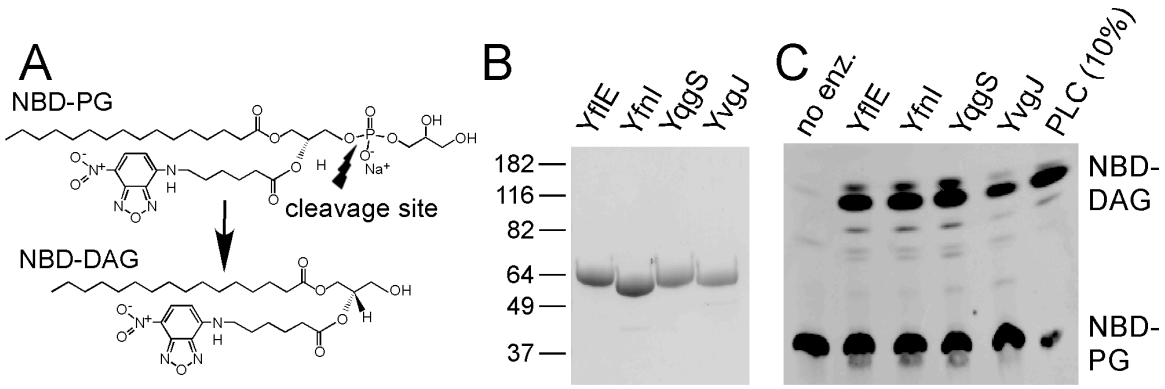

Figure 25: *In vitro* activity of *B. subtilis* LtaS-type enzymes. (A) Chemical structures of fluorescently labeled NBD-PG and NBD-DAG lipids with known *S. aureus* LtaS and *B. cereus* PLC cleavage site indicated by an arrow. (B) Coomassie stained gel of purified *B. subtilis* LtaS-like proteins. Extracellular enzymatic domains of *B. subtilis* YflE, YfnI, YqgS and YvgJ were purified as N-terminal His-tag fusion proteins, and ten µg purified protein separated on a 10 % (w/v) SDS-PAGE gel and visualized by staining with Coomassie brilliant blue. Sizes of protein standards in kDa are shown on the left. **(C) TLC analysis of *B. subtilis* YflE, YfnI, YvgJ and YqgS *in vitro* reaction products.** The NBD-PG lipid substrate was incubated with eYflE, eYfnI, eYvgJ or eYqgS enzyme. Subsequently, lipids were extracted and separated by TLC and fluorescent lipid bands visualized by scanning plates with a fluorescence imager. As negative and positive controls, reactions were set up without enzyme or with the *B. cereus* PLC enzyme, respectively. Note that only 10 % of the PLC reaction was run on the TLC plate. Positions of NBD-PG and presumed NBD-DAG reaction product are indicated on the left, and proteins added to each reaction are shown on the top of the panel.

To gain further insight into the relative activity of the four *B. subtilis* proteins, a time course experiment was performed. Reactions were set up as described above, samples removed at the indicated time points, and lipid reaction products analyzed (Fig. 26A). The amount of the NBD-DAG reaction product obtained was quantified using the AIDA software program, and % hydrolysis calculated based on the amount of NBD-DAG produced in the PLC control reaction, which proceeds to near completion (Fig 25C). Three independent experiments were performed, and the first three time points, during which the reaction speed appeared to be linear, were used to determine the maximal enzyme activity of the four *B. subtilis* protein (Fig. 26B). Enzyme activities ranging from 0.0067 (YfnI) to 0.0007 (YvgJ) ng lipid hydrolysis / [min × μM enzyme] were measured in this *in vitro* assay set up. These results indicate that while all four enzymes are active, YfnI, YflE and YqgS have > 4.6-fold higher activity as compared to YvgJ.

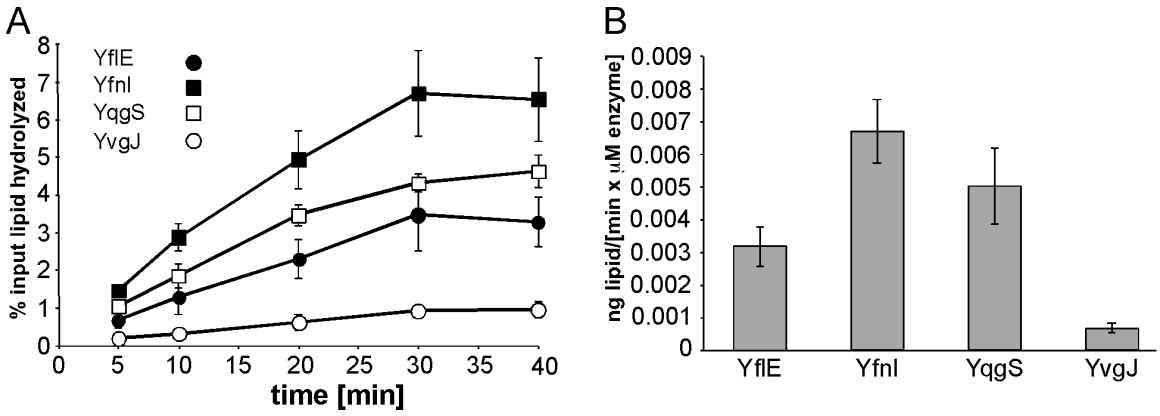

Figure 26: Kinetic measurements for recombinant YflE, YfnI, YqgS and YvgJ enzymes. (A) Time course experiment. Enzyme reactions were set up as described in the Materials and Methods chapter (section 2.9.2), aliquots removed at the indicated time points and reactions stopped by the addition of chloroform and methanol. Lipids were separated on TLC plates, and the NBD-DAG reaction product quantified. For each time point and enzyme the average value and standard deviation of three values is plotted. Three independent experiments were performed and a representative graph is shown. **(B) Maximal enzyme activity of *B. subtilis* YflE, YfnI, YqgS and YvgJ.** The slope of the linear fit through the first three data points of the curve shown in (A) was used to calculate the maximal enzyme activity for each *B. subtilis* LtaS orthologue. Three independent time course experiments were used to determine an average value and standard deviation for the maximal enzyme activity and these values are plotted.

6.3 All four *B. subtilis* LtaS orthologues are Mn^{2+}-dependent enzymes with substrate specificity for NBD-PG

S. aureus LtaS is a Mn^{2+}-dependent metal enzyme (Karatsa-Dodgson *et al*, 2010). In contrast, structural analysis of the soluble enzymatic domain of the *B. subtilis* YflE protein revealed the presence of a Mg^{2+} ion in the active center (Schirner *et al*, 2009). However, this ion was also present in the crystallization buffer and as such may not reflect the ion relevant for enzyme activity. To test which metal ion is required for the activity of the *B. subtilis* enzymes, *in vitro* assays were performed in the presence of different divalent metal ions, and the signal for the reaction product quantified. As presented in Fig. 27, all four proteins showed the highest activity in the presence of $MnCl_2$. Addition of $MgCl_2$ or $CaCl_2$ in place of $MnCl_2$ resulted only in weak enzyme activity, and no activity above background was seen in the presence of $ZnCl_2$.

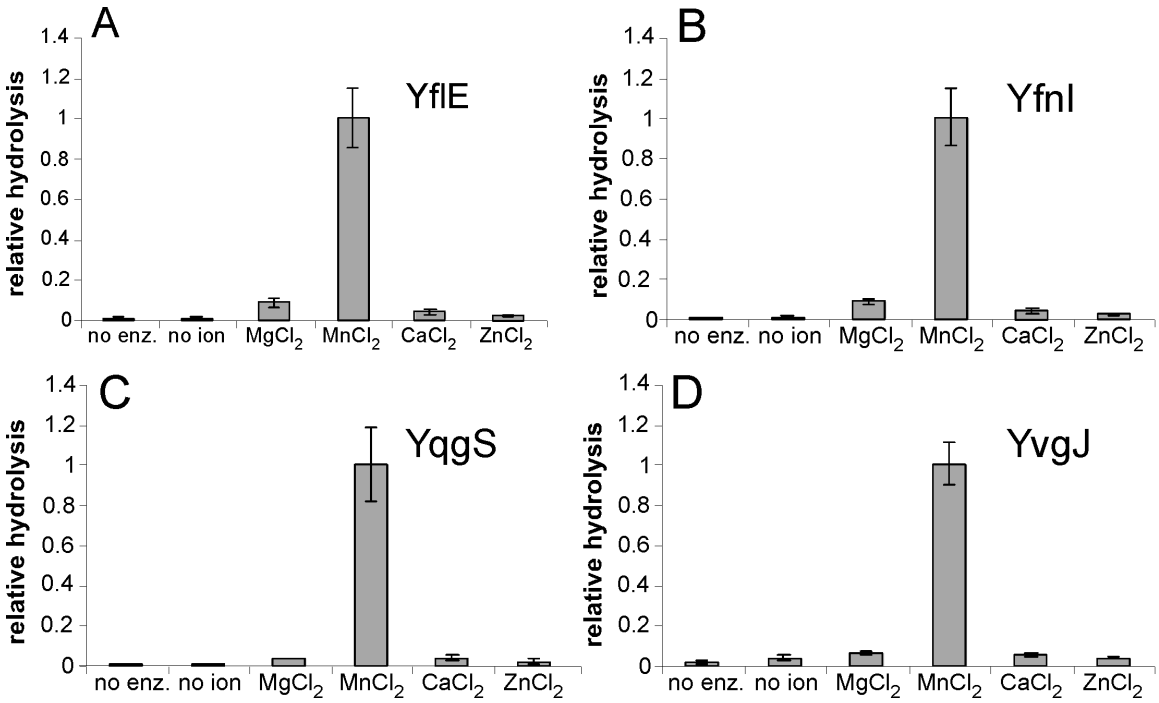

Figure 27: *B. subtilis* LtaS-type enzymes require Mn^{2+} for activity. *In vitro* enzyme assays were performed with NBD-PG lipid as the substrate in the presence of 10 mM $MgCl_2$, $MnCl_2$, $CaCl_2$ or $ZnCl_2$, and reactions initiated by the addition of eYflE (A), eYfnI (B), eYqgS (C) or eYvgJ (D). As controls, reactions were set up without enzyme, or without metal ion added. Samples were incubated for 3 h at 37°C, lipids extracted and separated by TLC. Plates were scanned and signals of the reaction product quantified. Reactions were performed in triplicate, and the average value and standard deviation plotted. The average fluorescence reading for the reactions set up with $MnCl_2$ was set to 1 and other values were adjusted accordingly.

S. aureus LtaS uses NBD-labeled PG lipid as substrate, but not NBD-PC, NBD-PS or NBD-PE (Karatsa-Dodgson *et al*, 2010). The substrate specificity of the four *B. subtilis* enzymes was examined, and it was found that these enzymes also only use NBD-PG as substrate, and not NBD-PC, NBD-PS or NBD-PE (Fig. 28). Taken together, these results strengthen the hypothesis that all members of the lipoteichoic acid synthase enzyme family are Mn^{2+}-dependent metal enzymes that only use lipids with a glycerolphosphate head group as substrate.

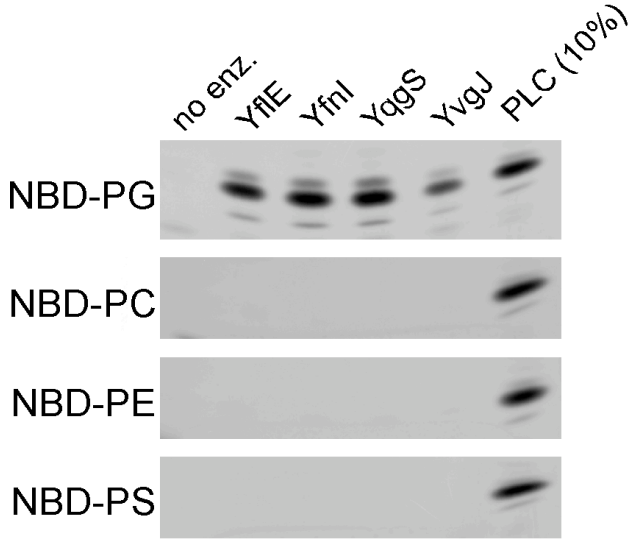

Figure 28: NBD-PG is the sole lipid substrate for *B. subtilis* YflE, YfnI, YqgS and YvgJ. Standard enzyme reactions were set up using NBD-PG, NBD-PS, NBD-PE or NBD-PC as substrate (indicated on the left of the panel) and reactions were initiated by the addition of the different *B. subtilis* enzymes. As negative control, lipid substrates were incubated without enzyme (no enzyme) and as a positive control, a PLC reaction using NBD-PG as substrate was run alongside on each TLC plate in order to determine the mobility of the reaction product. Note that only the upper part of the TLC plates is shown with the area of the reaction product.

Chapter 7

In vivo functions of the *B. subtilis* LtaS orthologues

7.1 Objective of chapter 7

In a previous study all four *B. subtilis* LtaS-type enzymes were expressed in an *ltaS* depleted *S. aureus* strain, and it was revealed that *yflE* and *yfnI* encode for LTA synthases (Gründling & Schneewind, 2007a). However, while YflE was able to complement staphylococcal growth, YfnI did not, and glycerolphosphate polymers synthesized by YfnI displayed an altered mobility on SDS-PAGE compared to WT LTA, indicative of structural alterations. No enzyme activity was observed for YqgS and YvgJ (Gründling & Schneewind, 2007a). In this chapter a different complementation assay was used to identify *in vivo* functions for YqgS and YvgJ. Moreover, the contribution of all four *B. subtilis* LtaS-type enzymes to LTA synthesis in their natural host was investigated in defined *B. subtilis* mutant strains. In addition, LTA was purified from *S. aureus* strains expressing either WT LtaS or *B. subtilis* YfnI, and the isolated glycerolphosphate polymers were analysed by NMR and standard biochemical assays.

7.2 *B. subtilis* YqgS is an LTA synthase, capable of producing polyglycerolphosphate

The finding that YqgS and YvgJ can cleave NBD-PG is in contrast to a previously performed complementation study that showed that YqgS and YvgJ could not promote LTA synthesis in *S. aureus* (Gründling & Schneewind, 2007a). One reason why no *in vivo* activity for YqgS and YvgJ was observed could be insufficient expression achieved from the single copy integration vector used in the previous study (Gründling & Schneewind, 2007a). To test whether expression of YqgS and YvgJ from a multi-copy plasmid would reveal an *in vivo* enzyme function for these proteins, all four *B. subtilis* genes coding for LtaS-type proteins, as well as the *S. aureus ltaS* gene, were cloned under Atet promoter control into the multi-copy plasmid vector pCN34 (Fig. 29A). In addition, the ribosome binding site (RBS) of *yqgS* was replaced with the RBS that precedes the *S. aureus ltaS* gene, in which a string of Gs is located 8 bases in front of the ATG start codon, indicative of a good RBS (Vellanoweth & Rabinowitz, 1992). For protein detection purposes, the four *B. subtilis ltaS* orthologues and the *S. aureus ltaS* gene were cloned as C-terminal *his*-tag fusions under Atet inducible promoter control into pCN34. Resulting plasmids and the empty pCN34 vector control were introduced into *S. aureus* strain ANG499, which carries the chromosomal copy of *ltaS* under IPTG inducible *spac* promoter control (Fig. 10). Functional complementation of *ltaS* was examined in the resulting strains after removal of IPTG by the addition of Atet to the growth medium for expression of the different *B. subtilis* LtaS orthologues. As described previously, YflE was able to complement both growth and LTA production in the *S. aureus ltaS* depletion strain, whereas YfnI could only promote polyglycerolphosphate synthesis but not the growth of *S. aureus* (Fig. 29B and C). Interestingly, expression of YqgS under these conditions could also restore bacterial growth, albeit to a lesser extent than YflE. Furthermore, upon increasing the exposure time of western blots, a YqgS-dependent signal for a faster migrating polyglycerolphosphate polymer was detected, next to other bands, which were also seen in the negative (no insert) control sample (Fig. 29C). It is assumed that these other bands, also present in the negative control sample, are LTA-specific (as they are detected with a monoclonal antibody) and either due to a slight leakiness of the inducible *spac* promoter system or due to small amounts of LTA remaining on the cells even four hours after the shut down of LtaS expression as

these bands are absent from samples isolated from a *S. aureus* strain with a complete *ltaS* deletion (R. Corrigan; unpublished results). In contrast, even under these conditions, YvgJ expression did not result in growth of *S. aureus* or LTA production. Expression of YflE, YfnI and YqgS, but not YvgJ was confirmed by western blot (Fig. 29D). Interestingly, in contrast to YflE, YfnI and YqgS were not processed in *S. aureus,* and only the full-length proteins were visible in whole cell samples. Taken together, these results demonstrate that YqgS functions as a lipoteichoic acid synthase, capable of promoting polyglycerolphosphate LTA backbone synthesis.

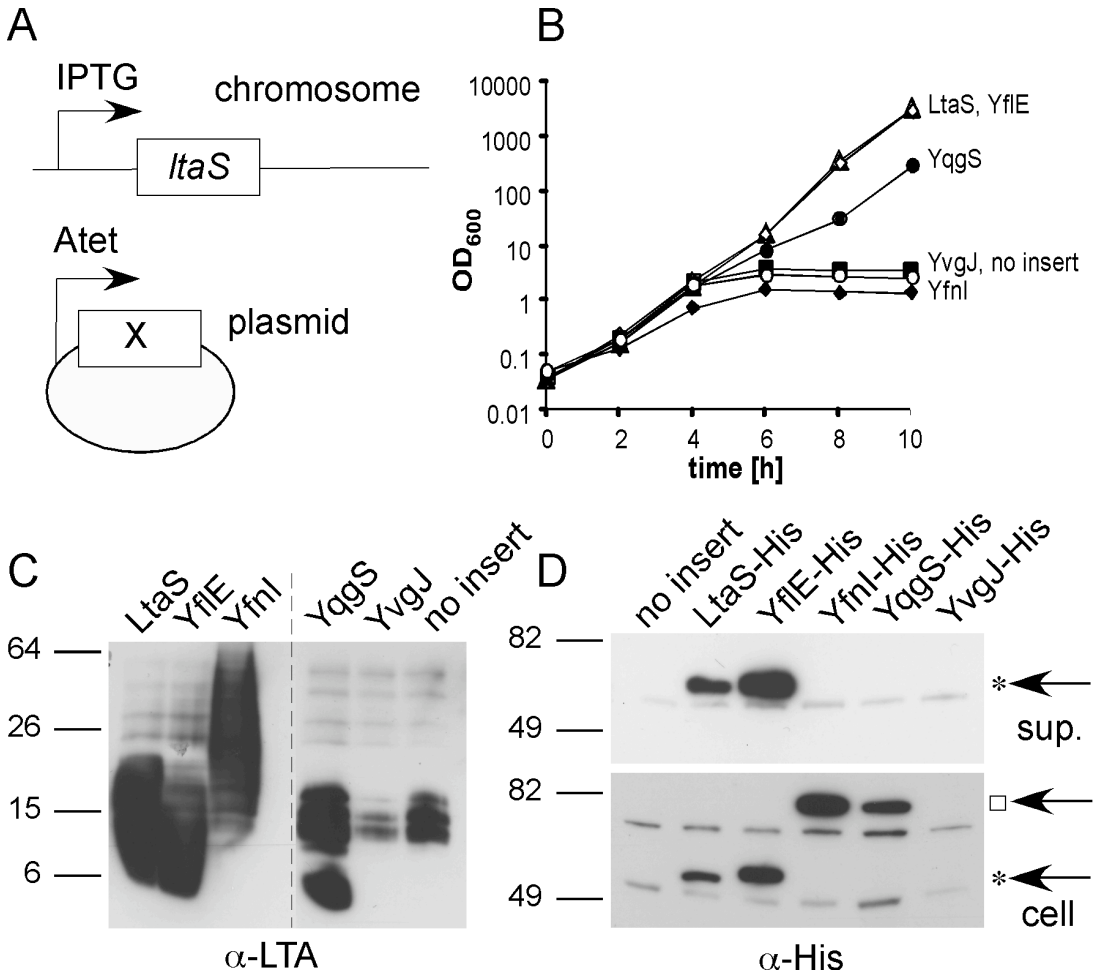

Figure 29: Functional complementation of an *S. aureus ltaS*-depletion strain with *B. subtilis yflE, yfnI, yqgS* or *yvgJ* expressed from a multi-copy plasmid. (A) Schematic representation of complementation strains. *S. aureus* strains used for complementation analysis contain the chromosomal copy of *ltaS* under IPTG inducible expression control and harbor a multi-copy plasmid (pCN34) for expression of LtaS orthologues from the Atet inducible promoter. **(B) Bacterial growth curves.** Washed overnight cultures of *S. aureus* strains expressing WT LtaS, *B. subtilis* YflE, YfnI, YqgS or YvgJ and a strain containing the empty pCN34 vector (no insert-negative control) were diluted 1:100 into fresh medium containing Atet and growth was monitored by determining OD_{600} readings at the indicated time points. All cultures were back-diluted 1:100 at the 4 h time point and cultures with strains expressing LtaS, YflE and YqgS were back diluted a second time at the 8 h time point, to maintain cultures in the logarithmic growth phase. *S. aureus* strains ANG1571, ANG1662, ANG1573, ANG1654, ANG1662 and ANG1130 were used for this experiment **(C) LTA and (D) protein detection by western blot.** The same *S. aureus* strains and growth conditions as described above were used for LTA analysis by western blot. For protein detection studies, *S. aureus* strains expressing WT LtaS, any of the four *B. subtilis* orthologues as C-terminal His-tag fusions, and a strain containing the empty pCN34 vector (no insert-negative control) were used (strains ANG1572, 1574, 1655, 1659, 1663 and 1130). Samples were prepared and analyzed by western blot as described in the Materials and Methods chapter (section 2.5). Cell associated LTA was detected using a LTA specific antibody and proteins in the supernatant (sup) and the whole cell (cell) using an anti-His antibody. Sizes of protein standards separated alongside are given in kDa on the left of the panel. A square (□) indicates full-length protein and a star (∗) denotes the cleaved protein fragment. Note that the LTA western blot with samples isolated from *S. aureus* strains expressing YqgS, YvgJ or containing the empty vector (no insert) was exposed 4 times longer, and the anti-His western blot with samples from the cell fraction was exposed 4.5 times longer than the blot with the supernatant samples.

7.3 *B. subtilis* YvgJ functions as an LTA primase

Expression of *yvgJ* from a strong promoter and a multi-copy plasmid did not restore growth or LTA production in the *S. aureus ltaS* depletion strain, and neither could the YvgJ protein fused to a C-terminal His-tag be detected by western blot (section 7.2). It was therefore assumed that either YvgJ does not function as an LTA synthase or that the protein is not expressed in *S. aureus*. In a previous study, it has been shown that the *L. monocytogenes* LtaS-type protein Lmo0644 encodes for an enzyme that can transfer one glycerolphosphate subunit onto the glycolipid anchor and hence this enzyme was termed LTA primase (Webb *et al*, 2009). In *S. aureus* and *B. subtilis* this reaction would lead to the production of the GroP-Glc_2-DAG. To test if YvgJ could function as an LTA primase, and to investigate if any of the other *B. subtilis* orthologues are involved in the production of glycolipid intermediates, membrane lipids were extracted and analyzed from *S. aureus* strains expressing *B. subtilis* YflE, YfnI, YqgS, YvgJ or *S. aureus* LtaS as a control. Lipids were extracted from log-phase cultures and 500 μg purified lipids were subsequently separated on TLC plates, and glycolipids visualized by staining with α-naphthol/H_2SO_4 (Fig. 30). The LTA glycolipid anchor Glc_2-DAG (Top band; see also mass spectrometry analysis below) could be detected in all samples. However, the intensity of this glycolipid band was reduced in samples isolated from YfnI and YvgJ expressing strains, and a concomitant accumulation of the lower glycolipid band was observed. This lipid species had the mobility as expected for a GroP-di-saccaride-DAG lipid (Webb *et al*, 2009), which would be consistent with the accumulation of the GroP-Glc_2-DAG intermediate. These experiments demonstrate that despite the fact that YvgJ could not by detected by western blot in *S. aureus*, the protein is expressed and involved in the synthesis of an LTA glycolipid intermediate.

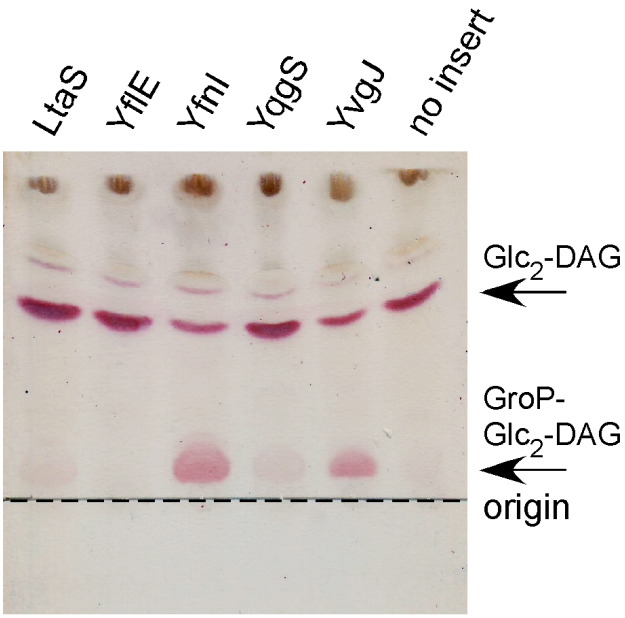

Figure 30: TLC analysis of glycolipids. *S. aureus* strains ANG1571 (LtaS-expressing), ANG1662 (YflE-expressing), ANG1573 (YfnI-expressing), ANG1654 (YqgS-expressing), ANG1658 (YvgJ-expressing) and ANG1130 (containing empty vector pCN34, no insert as negative control) were grown to mid-log phase and lipids extracted as described in the Materials and Methods chapter (section 2.10). Five hundred μg total membrane lipids were separated by TLC, and glycolipids visualized by staining with α-naphthol/sulphuric acid. The position of the origin is indicated by a dashed line, positions of presumed Glc_2-DAG (top band) and GroP-Glc_2-DAG (bottom band) lipids are marked with arrows on the right of the panel, and proteins expressed in the different strains are indicated above each lane.

To provide further experimental evidence for this notion, lipids from *S. aureus* strains expressing YflE (predominantly producing the top glycolipid band) and YvgJ (accumulating the bottom glycolipid band) were separated by TLC and lipids corresponding to α-naphthol/H_2SO_4 positive areas extracted and analyzed by MALDI TOF mass spectrometry, which was performed as described previously (Webb *et al*, 2009). Sodium adducts of the glycolipids Glc_2-DAG and GroP-Glc_2-DAG with C15 and C18 acyl-chains have an absolute calculated mass of 929.62 and 1083.72, respectively (Table 3). In agreement with these expected masses, m/z signals of 929.59 and 929.66 were observed for lipids isolated from the top bands of samples obtained from YflE and YvgJ expressing strains, respectively (Fig. 31A and C). In addition, a strong mass signal of 1083.73, as expected for GroP-Glc_2-DAG, was obtained for lipids isolated from the bottom band of the YvgJ-expressing strain (Fig. 31D). A corresponding signal was absent from samples prepared from the YflE expressing strains (Fig. 31B), which does not show an accumulation of this glycolipid. A complete list of predicted and observed masses for the glycolipids Glc_2-DAG and GroP-Glc_2-DAG with varying acyl-chain length is given in Table 3. Taken

together, these data suggest that YvgJ functions *in vivo* as an LTA primase capable of transferring the initial glycerolphosphate subunit onto the glycolipid anchor, producing GroP-Glc_2-DAG. Furthermore, despite the fact that YfnI acts as an LTA synthase, it also appears to be very efficient in synthesizing the GroP-Glc_2-DAG intermediate.

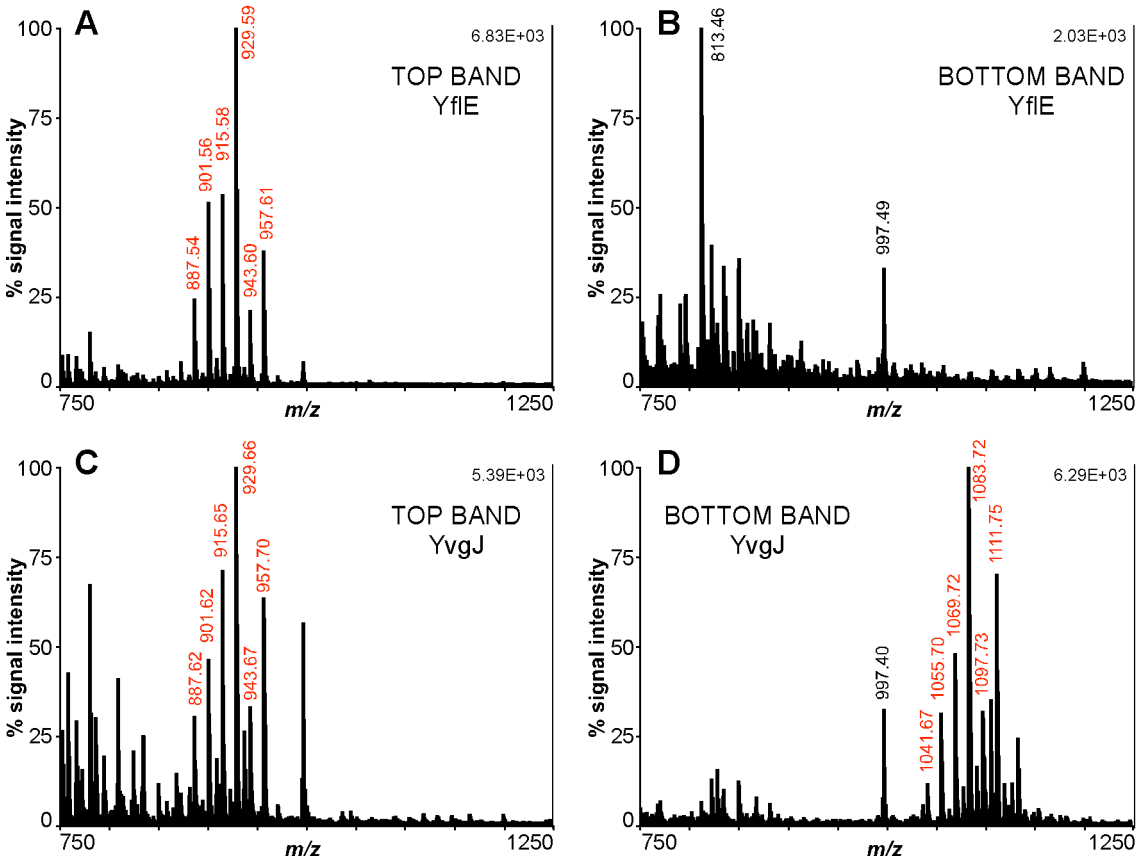

Figure 31: MALDI-TOF analysis of glycolipids produced by YflE and YvgJ-expressing *S. aureus* strains. A total of 2.5 mg lipids isolated from YflE or YvgJ-expressing *S. aureus* strains were separated by TLC, and lipids corresponding to top and bottom glycolipid bands extracted and analyzed by MALDI-TOF mass spectrometry. Spectra were recoded in the reflector positive ion mode and are shown for (A) YflE top band, (B) YflE bottom band, (C) YvgJ top band and (D) YvgJ bottom band. Maximal signal intensity is shown in the top right corner in each panel. Observed masses corresponding to calculated masses of glycolipids are shown in red. *S. aureus* strains ANG1662 (YflE-expressing) and ANG1573 (YfnI-expressing) were used for this experiment. Note that the MALDI-TOF analysis was performed by Dr. A. Gründling.

Table 3: Predicted and observed masses of glycolipids isolated from membranes of *S. aureus* strains expressing *B. subtilis* YflE or YvgJ.

Data were provided by Dr A. Gründling.

Top Band: Glc_2-DAG				
possible fatty acid chain length	**chemical formula**	**predicted mass**	**observed mass - YflE**	**observed mass – YvgJ**
C15/C15	$C_{45}H_{84}Na_1O_{15}$	887.57	887.54	887.62
C15/C16	$C_{46}H_{86}Na_1O_{15}$	901.59	901.56	901.62
C15/C17	$C_{47}H_{88}Na_1O_{15}$	915.60	915.58	915.65
C15/C18	$C_{48}H_{90}Na_1O_{15}$	929.62	929.59	929.66
C16/C18	$C_{49}H_{92}Na_1O_{15}$	943.63	943.60	943.67
C17/C18	$C_{50}H_{94}Na_1O_{15}$	957.65	957.61	957.70
Bottom Band: GroP-Glc_2-DAG				
possible fatty acid chain length	**chemical formula**	**predicted mass**	**observed mass - YflE**	**observed mass – YvgJ**
C15/C15	$C_{48}H_{91}Na_1O_{20}P_1$	1041.57	absent	1041.67
C15/C16	$C_{49}H_{93}Na_1O_{20}P_1$	1055.59	absent	1055.70
C15/C17	$C_{50}H_{95}Na_1O_{20}P_1$	1069.61	absent	1069.72
C15/C18	$C_{51}H_{97}Na_1O_{20}P_1$	1083.62	absent	1083.72
C16/C18	$C_{52}H_{99}Na_1O_{20}P_1$	1097.64	absent	1097.73
C17/C18	$C_{53}H_{101}Na_1O_{20}P_1$	1111.65	absent	1111.75

7.4 *B. subtilis* signal peptidase SipT and SipV do not promote YfnI cleavage in *S. aureus*

From protein detection analysis described in section 7.2, it became apparent that of the four *B. subtils* LtaS-type enzymes YflE, but not YfnI or YqgS, are processed when expressed in *S. aureus*. Interestingly, only YflE could fully complement growth, and LTA production in an *S. aureus ltaS* depleted mutant strain (Gründling & Schneewind, 2007a and Fig. 29B and C) In contrast, YfnI was able to promote LTA synthesis but not staphylococcal growth and polymers synthesized by YfnI migrated with a different mobility on SDS-PAGE compared to WT LTA. In sections 4.2-4.4 experimental evidence was provided that the full-length LtaS protein represents the active enzyme form, and once the protein is split into 5TM and eLtaS, the enzyme no longer functions in the LTA synthesis pathway. It was decided to test whether it would be possible to process YfnI in *S. aureus,* and whether enzyme cleavage would have an effect on the enzymatic activity of YfnI. In section 3.5, evidence was provided that LtaS cleavage is dependent on the signal peptidase SpsB. In contrast to *S. aureus*, which expresses a single functional signal peptidase enzyme, *B. subtilis* contains five chromosomal encoded signal peptidase (SipS, SipT, SipV, SipU, SipW). Proteomic studies on secreted proteins in *B. subtilis* identified processed forms of YflE and YfnI in the culture supernatant (Hirose 2000). Moreover, it was shown that YfnI cleavage was diminished in the combined absence of the two signal peptidases SipT and SipV, suggesting that either of these proteases recognizes YfnI as substrate (Antelmann *et al*, 2001). Based on this information, it was decided to construct a *S. aureus* strain that expresses both YfnI and SipT or SipV. *S. aureus* strain ANG1282 carries the native *ltaS* gene under IPTG inducible *spac* promoter control, and the YfnI protein fused to a C-terminal His-tag is expressed from the Atet inducible p*itet* promoter (Fig. 32A). A plasmid containing the *sipT* or *sipV* gene under the *ltaS* promoter control was introduced into this strain (Fig. 32A). For protein detection purposes the two genes coding for the signal peptidases SipT and SipV were additionally cloned as C-terminal His-tag fusions under *ltaS* promoter control, and the resulting plasmids (pCN34$_{PltaS}$-*sipT-his,* pCN34$_{PltaS}$-*sipV-his*) introduced into *S. aureus* strain ANG1282. The empty plasmid pCN34 was introduced into strain ANG587, which carries the WT *ltaS* gene under IPTG inducible promoter control and a second *ltaS* copy fused to a C-terminal *his*-tag under Atet inducible p*itet* promoter, and this

strain served as a positive control. In addition, the empty pCN34 plasmid was electroporated into strain ANG513, which harbors the WT *ltaS* gene under IPTG inducible promoter control and the empty p*itet* plasmid integrated into the chromosome. The resultant strain was used as a negative control in this experiment. Coexpression of YfnI and SipT or SipV in *S. aureus* did not result in YfnI processing, and polymers synthesized by YfnI in the presence of SipT or SipV displayed the same mobility shift on SDS-PAGE as observed for YfnI polymers produced in the absence of SipT and SipV (Fig. 32B and C). Western blot analysis of whole cell samples confirmed expression of SipT and SipV in *S. aureus* (Fig. 33A and B). Next, it was examined whether expression of multiple *B. subtilis* signal peptidases in *S. aureus* would promote YfnI cleavage. To investigate this the *B. subtilis sipS* gene or *sipS* fused to a C-terminal *his*-tag were cloned downstream of *sipT* or *sipV* into pCN34, and the resulting plasmids (pCN34$_{PltaS}$-*sipT/S*, pCN34$_{PltaS}$-*sipT/S-his*, pCN34$_{PltaS}$-*sipV/S,* pCN34$_{PltaS}$-*sipV/S-his*) were introduced into *S. aureus* strain ANG1282 (see strain description above). SipS was chosen for this experiment as the protein is classified as a major signal peptidase in *B. subtilis* and thought to be required for the secretion of many proteins (Tjalsma *et al*, 1998). Again, no processed forms of YfnI could be detected in culture supernatants upon its expression in combination with SipT/S or SipV/S (Fig. 32D and E). In addition, glycerolphosphate polymers synthesized by YfnI in these strains displayed the typical mobility shift on SDS-PAGE compared to WT LTA. Expression of SipS was verified by western blot analysis (Fig. 33C and D). These data are somewhat in contrast to the previous observation that YfnI processing in *B. subtilis* is SipT and SipV dependent. However, although we could confirm expression of all signal peptidases, it is possible that these enzymes are not functional in the heterologous host *S. aureus*. Another explanation for the above described observation could be that the YfnI enzyme does not assume a conformation in *S. aureus* that is accessible to SipT or SipV.

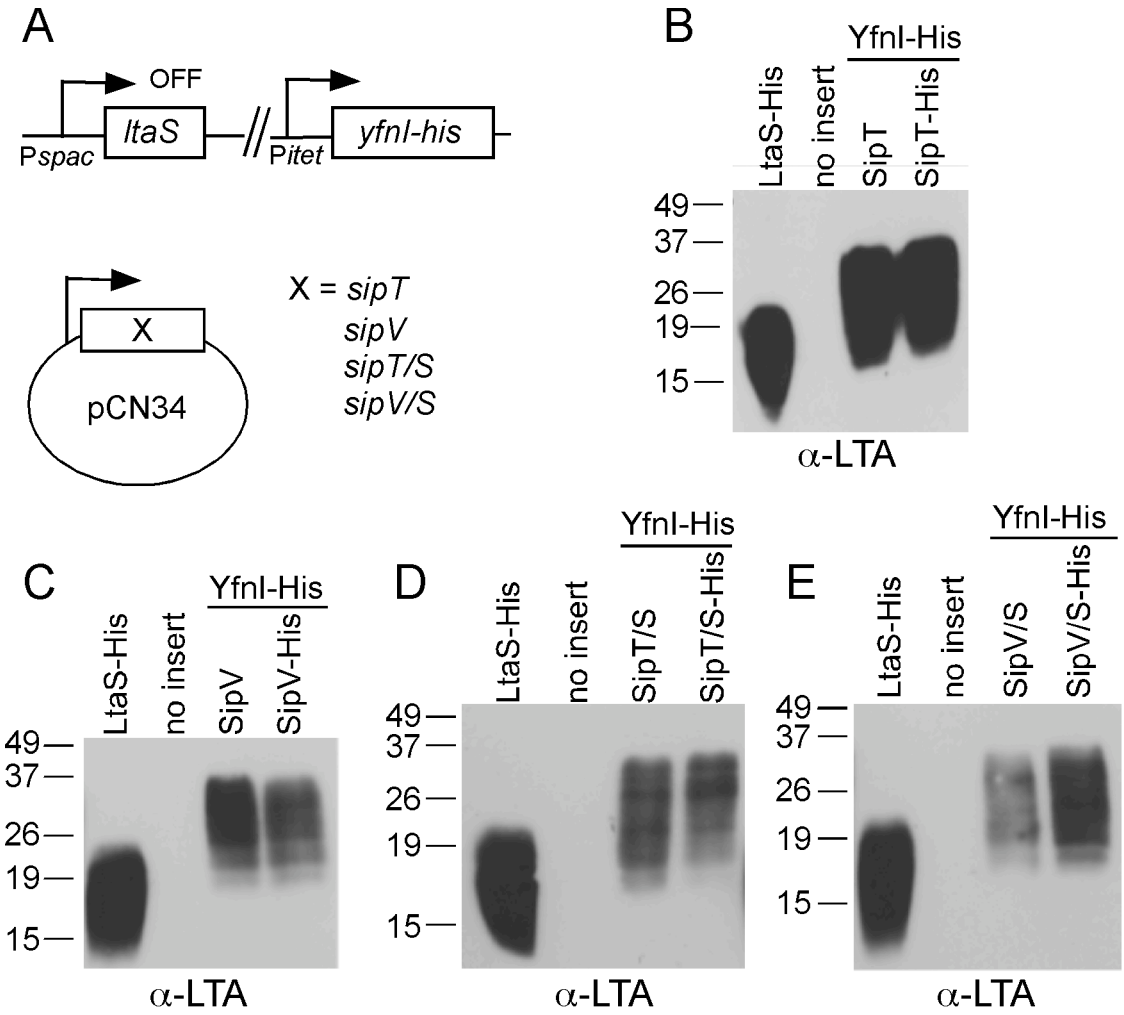

Figure 32: Functional complementation of LTA synthesis in an *ltaS* depleted *S. aureus* strain with *B. subtilis* YfnI and SipT, SipV and SipS. (A) Schematic representation of *S. aureus* strains used for the expression of YfnI and SipT, SipV and SipS. The *B. subtilis* YfnI protein was expressed as C-terminal His-tag fusion protein from a chromosomal integration vector by the addition of Atet, and the *B. subtilis* derived signal peptidases SipT, SipV and SipS were expressed from a multi-copy plasmid. **(B-E) LTA western blot analysis.** Washed overnight cultures of *S. aureus* strains expressing YfnI as C-terminal His tag fusion and SipT (A), SipV (B), SipT/S (C) or SipV/S (D) were grown for 4 h in the presence of Atet and absence of IPTG. A strain expressing LtaS fused to a C-terminal His-tag and containing the empty plasmid vector pCN34, and an *S. aureus* strain harboring the empty p*itet* and pCN34 vectors served as controls. Samples were prepared and analyzed by western blot using an LTA specific antibody. Sizes of protein standards separated alongside are given in kDa on the left of the panel. Proteins expressed are indicated above each lane and a square (□) indicates full-length protein and a star (∗) denotes the cleaved protein fragment. *S. aureus* strains ANG1359-ANG1362, ANG1524, ANG1525, ANG1528, ANG1529, ANG1598 and ANG1599 were used for this experiment.

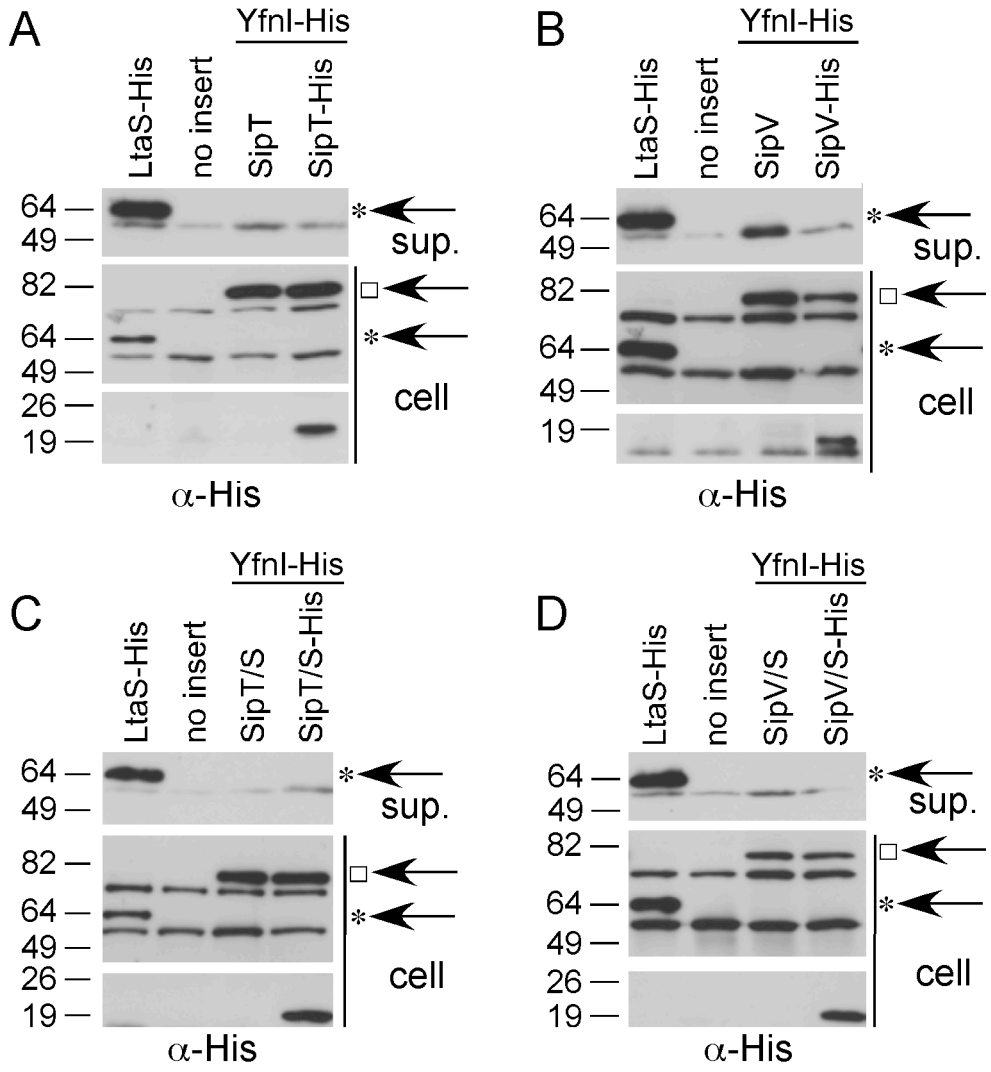

Figure 33: Protein detection by western blot. The same *S. aureus* strains and growth condition as described in Fig. 32 were used for protein detection studies. Samples were prepared and analyzed by western blot as described in Materials and Methods (section 2.5). Proteins in the whole cell (cell) and in the culture supernatant (sup) were visualized using an anti-His antibody. Sizes of protein standards separated alongside are given in kDa on the left of the panel, and proteins expressed are indicated above each lane. A square (□) indicates full-length protein and a star (∗) denotes the cleaved protein fragment.

7.5 Contribution of YflE, YfnI, YqgS and YvgJ to LTA synthesis in *B. subtilis*

A *B. subtilis* strain deleted of all four *ltaS*-like genes has been constructed previously and is viable (Schirner *et al*, 2009). Several phenotypes were associated with the deletion of these genes; a single *yflE* mutant formed chains, *yflE/yqgS* and *yflE/yvgJ* double mutants had sporulation defects, and cells lacking all four genes formed long chains and spiraled along their long axis (Schirner *et al*, 2009). To correlate deletions of *ltaS*-like genes with the cellular LTA content, *B. subtilis* 168 mutant strains lacking one, three or all four *ltaS*-like genes were analyzed. To this end, cell extracts were prepared from overnight cultures of WT and mutant *B. subtilis* strains, and the LTA content determined by western blot. Initially we attempted to use the mouse monoclonal LTA antibody, which was used for the previously described *S. aureus* experiments (chapters 3 and 4). However, when this antibody was used, the western blot signal was not strong enough to detect LTA from *B. subtilis*. It is possible that this is either be due to lower LTA amounts or to the additional sugar modifications present on the LTA backbone in *B. subtilis*. However, when a humanized monoclonal LTA-specific antibody was used, which is supplied at a higher concentration, an LTA specific signal was obtained for a sample isolated from the wild type *B. subtilis* 168 strain (WT) (Fig. 34). This signal was absent from samples isolated from a *B. subtilis* strain lacking all four *ltaS*-like genes (4×Δ) or a strain expressing YvgJ-only (Fig. 34). Of note, in several samples including the YvgJ-only and 4×Δ samples, an additional signal in the 30 kDa area was observed, which is assumed to be unrelated to LTA and could be cross-reactivity towards the wall teichoic acid polymer, which in *B. subtilis* 168 is also made up of glycerolphosphate subunits (Burger & Glaser, 1964). Indeed, this signal was less abundant in the *B. subtilis* 168 hybrid strain L5703 (Karamata *et al*, 1987) expressing ribitolphosphate WTA (ribitol-Pi WTA) in place of glycerolphosphate WTA (Fig. 34). Deletion of *yfnI, yqgS* or *yvgJ* alone did not significantly affect LTA production. Interestingly, deletion of *yflE* resulted in the production of LTA with an altered mobility on SDS-PAGE gels, indicative of structural changes (see below). The production of this altered LTA was attributed to the function of YfnI, as a *B. subtilis* strain expressing YfnI-only showed a similar altered LTA profile (Fig. 34). This also indicates that

YflE affects the activity of YfnI, revealing an unexpected enzymatic interdependence of the activity of two LTA-synthases in *B. subtilis*.

In the case of *L. monocytogenes,* which produces an LTA primase and one LTA synthase, a clear difference in LTA production was seen when the LTA primase was inactivated (Webb *et al*, 2009). In *B. subtilis* no obvious difference in LTA production was observed upon inactivation of the LTA primase YvgJ (Fig. 34; compare LTA profile of Δ*yvgJ* strain with wild type strain). To specifically examine if the *B. subtilis* YvgJ enzyme works together with one of the LTA synthases, LTA production in three *B. subtilis* double mutant strains in which YvgJ is expressed with one of the LTA synthase enzymes YflE, YfnI or YqgS, was compared to a strain which expresses the synthase alone. No difference in LTA production was observed for any of the LTA synthases in the absence of the LTA primase (Fig. 34; compare lanes YflE-only with express- YvgJ/YflE; YfnI-only with express-YvgJ/YfnI or YqgS-only with express-YvgJ/YqgS). This indicates that in contrast to *L. monocytogenes* all *B. subtilis* LTA synthases can efficiently initiate LTA production even in the absence of a dedicated LTA primase. However, as shown above and further analyzed below, in *B. subtilis* YflE affects the function of YfnI.

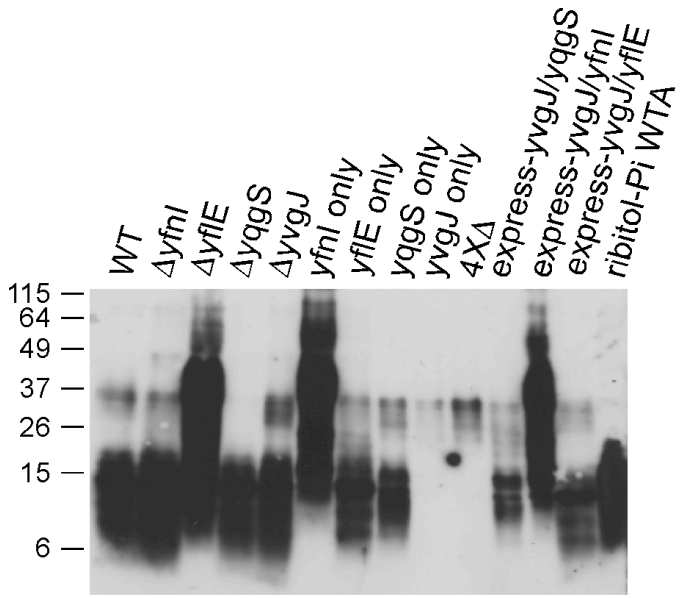

Figure 34: LTA production by WT and mutant *B. subtilis* strains. Samples for LTA analysis by western blot were prepared from overnight cultures of WT and mutant *B. subtilis* 168 strains, and from a *B. subtilis* 168 hybrid strain expressing ribitolphosphate wall teichoic acid. Samples were separated on a 15 % (w/v) SDS-PAGE gel, transferred to a PVDF membrane and LTA detected by western blot using the humanized monoclonal LTA-specific antibody (Biosynexus Incorporated), and the HRP-linked anti-human antibody (DakoCytomation) at 1:10,000 dilutions. Sizes of protein standards separated in parallel are indicated in kDa on the left of the panel, and strains used are indicated above each lane, with abbreviations given in strain Table 1.

7.6 YfnI synthesizes glycerolphosphate polymers of increased length

Polymers produced by YfnI in the absence of YflE migrate with a slower mobility on SDS-PAGE gels, both when synthesized in the natural host *B. subtilis* (Fig. 34) or in the heterologous host *S. aureus* (Gründling & Schneewind, 2007a and Fig. 29C). To gain insight into structural alterations of polymers synthesized by YfnI, the LTA from WT *B. subtilis* and the *B. subtilis* mutants expressing YflE or YfnI only was isolated. As can be seen in Fig. 35 purified LTA from the *B. subtilis* YfnI only expressing strain migrated slower on SDS-PAGE compared to WT and the YflE only expressing strain when analyzed by western blot. These data further strengthen the hypothesis that YfnI synthesises a polymer with structural alterations not only when expressed in *S. aureus* but also in its natural host *B. subtilis*.

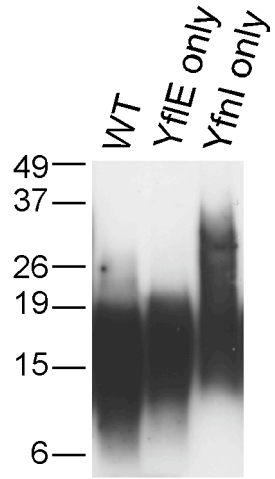

Figure 35: Detection of purified LTA from wild type and mutant *B. subtilis* strains. LTA was extracted from wild type and mutant *B. subtilis* 168 strains as described in the Materials and Methods chapter (section 2.6). Ten µg purified LTA was separated on a 15 % (w/v) SDS-PAGE gel and LTA detected by western blot using the humanized monoclonal LTA-specific antibody and the HRP-linked anti-human antibody. Sizes of protein standards separated in parallel are given in kDA on the left of the panel, and strains used are indicated above each lane, with abbreviations given in strain Table 1.

The LTA yield obtained from the YfnI only expressing *B. subtilis* strain was too low to allow any structural analysis on the polymer. Based on western blot analysis, it appeared that *S. aureus* produces larger amounts of LTA as compared to *B. subtilis*, and it was therefore decided to extract LTA from an *S. aureus* YfnI-expressing strain and compare its composition to polymers produced by LtaS. LTA was isolated from mid-log cultures of *S. aureus* strains ANG514 (LtaS-expressing) and ANG515 (YfnI-

expressing) using a 1-butanol extraction method and purified by hydrophobic interaction chromatography. LTA was purified from four independently grown cultures for each strain and analyzed by nuclear magnetic resonance (NMR) and standard biochemical assays (Fig. 36). Representative NMR spectra are shown in Fig. 36A and B. Based on the NMR analysis of all four independently isolated LTA samples, an average glycerolphosphate chain length of 35 ± 6 (LtaS) and 54 ± 6 (YfnI) and average D-Ala modification of 82 ± 5 % (LtaS) and 74 ± 6 % (YfnI) was calculated. The difference in chain length is considered to be statistically significant (p-value = 0.0048), while the difference in D-Ala modifications is not statistically significant (p-value = 0.083). In addition, standard biochemical assays were used to determine the phosphate, glucose and D-Ala content in the purified LTA samples (Grassl & Supp, 1995; Kunst *et al*, 1984; Schnitger *et al*, 1959). LTA in a wild type *S. aureus* strain is linked nearly exclusively to the glycolipid anchor Glc_2-DAG (Duckworth *et al*, 1975) and hence the ratio of the phosphate concentration per 2 glucose molecules can be used for the chain length determination, while the ratio of D-Ala to phosphate concentration gives a measure for % D-alanylation. Applying these calculations to LtaS- or YfnI-produced polymers revealed an average chain length of 47 ± 9 and 74 ± 14 (Fig. 36C) and % D-alanylation of 62 ± 4 and 68 ± 9 (Fig. 36D), respectively. This biochemical analysis gives a slightly longer chain length for LtaS and YfnI-produced LTA as compared to the NMR analysis. However, both methods indicate that YfnI-produced polymers are significantly longer; 1.5 × based on NMR or 1.6 × based on biochemical assays than LtaS-produced polymer, but remain linked to a glycolipid anchor. On the other hand there does not appear to be a statistically significant difference in the amount of D-Ala substitutions. While this analysis was performed in *S. aureus*, we speculate that the observed mobility shift of YfnI-produced polymers in the natural host *B. subtilis* is also due to an increase in chain length, suggesting that in the absence of LtaS, YfnI-becomes more efficient in LTA synthesis.

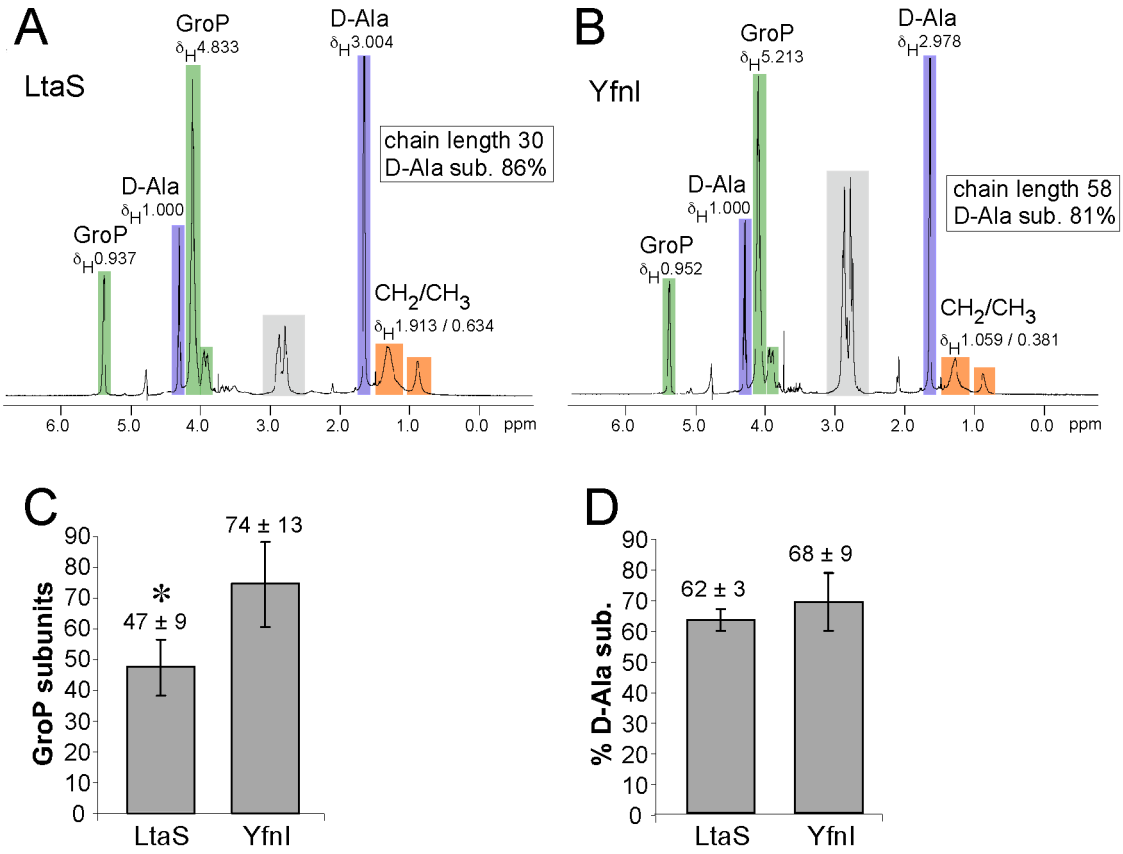

Figure 36: NMR and biochemical analysis of purified LTA. (A and B) NMR analysis. Large cultures of *S. aureus* strains (A) ANG514 (LtaS-expressing) and (B) ANG515 (YfnI-expressing) were grown and LTA purified as described in the Materials and Methods chapter (section 2.11.1). One mg purified LTA was suspended and lyophilized several times in D_2O to exchange ^1H for ^2H deuterons and ^1H NMR spectra were recorded at 600 MHz, 300 K. The signals derived from citrate, a buffer component used during LTA purification and retained in the samples are marked in grey. The different signals previously assigned to LTA components (Morath *et al*, 2002) are color coded [blue - D-Ala (4 protons per D-Ala group), green - GroP (5 protons per GroP group), orange - CH_2/CH_3 groups of fatty acids (59 protons per lipid anchor)]. The integration values are shown above each signal. Chain length was determined by calculating the ratio of integral values for GroP to CH_2/CH_3 groups in fatty acids and % D-Ala substitution by calculating the ratio of integral values for D-Ala to GroP × 100 and taking into account the number of protons for each signal. NMR analysis was performed on four independently isolated LTA samples for each strain and a representative result is shown. **(C and D) Biochemical analysis of LTA.** LTA extracted from strains ANG514 (LtaS) and ANG515 (YfnI) was subjected to a biochemical analysis. Phosphate, glucose and D-Ala contents were determined as described in the experimental procedures section. GroP, D-Ala and glucose solutions of known concentrations were used as standards. The chain length in GroP subunits (C) was determined by calculation of the ratio of phosphate / ½ glucose concentration and the % D-Ala substitution (D) by calculating the ratio of D-Ala / phosphate concentration × 100. Biochemical analysis was performed on four independently isolated LTA samples for each strain and the mean and standard deviation is shown. The difference in chain length is statistically significant and indicated with an asterisk (*) (two-tailed p-value of 0.017; unpaired T-test) while the difference in D-Ala modification is not (two-tailed p-value of 0.355, unpaired T-test).

Chapter 8
Discussion of chapters 6 and 7

Polyglycerolphosphate LTA is found in the cell wall envelope of many Gram-positive bacteria. In bacteria that belong to the Firmicutes phylum, the backbone of this polymer is synthesized by the lipoteichoic acid synthase enzyme LtaS (Gründling & Schneewind, 2007a; Rahman *et al*, 2009b). In contrast to *S. aureus*, which produces a single lipoteichoic acid synthase, *B. subtilis* encodes four LtaS-like proteins namely YflE, YfnI, YqgS and YvgJ. In chapters 6 and 7, the functions of these four proteins were investigated using both *in vivo* and *in vitro* enzyme assays. Enzymatic activities for all four *B. subtilis* LtaS orthologues were reported and experimental evidence provided that all proteins are either involved in the synthesis of an LTA glycolipid intermediate or directly in LTA backbone synthesis (sections 7.2 and 7.3).

Recently, Karatsa-Dodgson *et al* developed an *in vitro* enzyme system to quantify the activity of LtaS-type enzymes (Karatsa-Dodgson *et al*, 2010). Using this *in vitro* assay it was shown that the three recombinant LTA synthases (YflE, YfnI and YqgS) are > 4.5-fold more active compared to the enzymatic domain of the LTA primase YvgJ (Fig. 26). A similar observation was made with recombinant versions of the *L. monocytogenes* LTA synthase and LTA primase (Karatsa-Dodgson *et al*, 2010) indicating that there may be a correlation between the activity of these enzymes and their ability to produce actual glycerolphosphate polymers. Other general features revealed through the use of the *in vitro* assay system were that LTA synthases and primases require Mn^{2+} for *in vitro* enzyme activity and only seem to accept lipids with a glycerolphosphate head group as substrate but not lipids with other head groups such as PC, PE or PS (section 6.3).

For the *in vivo* protein expression studies and LTA analysis by western blot or glycolipid analysis by TLC we used both, *S. aureus* as heterologous host for the expression of individual *B. subtilis* LtaS-like proteins and defined *B. subtilis* mutants lacking individual *ltaS*-like genes or combinations of the four genes. It has been described previously that YflE and YfnI are LTA synthases capable of producing polyglycerolphosphate polymers (Gründling & Schneewind, 2007a). Here, it is shown that expression of YqgS in *S. aureus* from a multi-copy plasmid and an inducible promoter system leads to the production of a polyglycerolphosphate polymer (section 7.2), and hence is a bona-fide LTA synthase. Consistent with these expression studies in a heterologous host, polyglycerolphosphate polymers could also be detected in *B. subtilis* triple mutants expressing YflE, YfnI or YqgS as sole enzymes (Fig. 34). Only

when all three genes were deleted in combination, could the glycerolphosphate polymer no longer be detected (Fig. 34). Expression of the fourth protein, YvgJ, either as a sole LtaS-like protein in *B. subtilis,* or from a multi-copy plasmid and a strong promoter in *S. aureus,* did not lead to LTA production, suggesting that YvgJ does not function as an LTA synthase. Analysis of the lipid profile of an *S. aureus* YvgJ-expressing strain indicated that YvgJ acts as an LTA primase, capable of transferring the initial glycerolphosphate subunit onto the glycolipid anchor (section 7.3). The presence of an LTA primase enzyme has been described before in *L. monocytogenes,* which expresses two LtaS-like enzymes with distinct functions in LTA synthesis (Webb *et al*, 2009). $LtaP_{LM}$ (Lmo0644) is the LTA primase, which transfers the initial glycerolphosphate subunit onto the glycolipid anchor, whereas $LtaS_{LM}$ (Lmo0927) functions as an LTA synthase producing the polyglycerolphosphate backbone. However, deletion of the dedicated LTA primase YvgJ in *B. subtilis* does not lead to an obvious difference in LTA production, suggesting that all *B. subtilis* LTA synthases are able to efficiently initiate LTA synthesis independent of the activity of a dedicated LTA primase (Fig. 34). The role of YvgJ in LTA synthesis is not clear. It is possible that YvgJ only contributes to some extent and under certain growth conditions to the LTA synthesis process.

Expression of *B. subtilis* YflE, YfnI and YqgS, but not YvgJ in *S. aureus* could be confirmed by western blot. Interestingly, similar to LtaS, YflE is cleaved in *S. aureus*, but no processed forms of YfnI or YqgS could be detected in culture supernatant. The fact that only the full-length YfnI protein was visible in the heterologous host provided a tool to study which *B. subtilis* proteases might be involved in YfnI cleavage, and whether YfnI processing has an effect on the *in vivo* function of this enzyme. YfnI cleavage in *B. subtilis* is dependent on the two signal peptidases SipT and SipV (Antelmann *et al*, 2001). However, expression of YfnI and SipT or SipV, or multiple *B. subtilis* signal peptidases did not promote YfnI processing in *S. aureus*. We speculate that either the signal peptidases are not functional in the heterologous host, or that YfnI does not adopt a conformation in *S. aureus* that is accessible to SipT or SipV.

B. subtilis strains lacking individual *ltaS*-like genes or combinations of the four genes display several phenotypes. For instance, a single *yflE* mutant formed chains, an *yflE/yqgS* double mutant has a sporulation defect, and cells lacking all four genes

form long chains and spiraled along their long axis (Schirner *et al*, 2009). Here, it is shown that the mere presence or absence of polyglycerolphosphate polymers cannot account for the observed filamentation and sporulation defect, as a strain deleted for *yflE* or *yflE/yqgS* is still capable of producing a glycerolphosphate polymer (Fig. 34). Previously, both YflE and YqgS expressed as GFP-fusion proteins from an inducible promoter system were found to localize preferentially to the division site or sporulation septum (Schirner *et al*, 2009). Taken together with our finding on the LTA production in the different mutant strains (Fig. 34), this would indicate that in the absence of YflE, YqgS produces functional polyglycerolphosphate polymers at the sporulation septum, and that polymers synthesized by YfnI are either not produced at the sporulation septum or are not functional due to their structural alterations (see below).

In this work, it was shown that a *B. subtilis yflE* deletion strain, as well as a strain expressing YfnI as a sole LTA synthase, produces polymers that migrated slower on SDS-PAGE gels compared to wild type LTA (Fig. 34). This was also observed when *yfnI* was expressed in an *S. aureus ltaS* depletion strain (Gründling & Schneewind, 2007a and Fig. 29C) and, indicating that the altered mobility of LTA produced by YfnI in *S. aureus* is not an artifact, but reflects the natural property of this enzyme. NMR and biochemical analysis of LTA purified from *S. aureus* strains expressing LtaS or YfnI, revealed a 1.5 to 1.6-fold increase in chain length for YfnI-produced polymers (Fig. 36), and this presumably results in the slower mobility on SDS-PAGE gels. The presence of longer polymers in the absence of YflE is somewhat puzzling and suggests that either the activity of YfnI changes in the presence of YflE, or that YfnI and YflE compete for the PG lipid substrate and that YfnI can only synthesize long polymers in the absence of YflE due to an increased availability of PG. Alternatively, YflE could trim YfnI-produced polymers and hence these long polymers are only seen in the absence of YflE.

Currently it is not known if there are any natural conditions under which YfnI would be expressed in the absence of YflE and hence lead to the production of elongated LTA molecules. A previous study using transcriptional *lacZ* reporter gene fusions, showed low expression of *yqgS, yvgJ* and *yfnI* compared to *yflE* during growth of *B. subtilis* in PAB medium (Schirner *et al*, 2009), which together with all other evidence suggests that YflE is the "house-keeping" LTA synthase. In proteomic

studies, processed forms of both YflE and YfnI were detected in the culture supernatant of late-exponential phase *B. subtilis* cultures when grown in minimal medium (Hirose *et al*, 2000) showing that both of these LTA synthases are produced under these conditions. In addition, YfnI was found in culture supernatants of exponential as well as stationary phase *B. subtilis* cultures when grown in LB-broth (Antelmann *et al*, 2001). But most notably, it has also been described that *yfnI* expression is controlled by the alternative sigma factor sigma M (Eiamphungporn & Helmann, 2008; Jervis *et al*, 2007) and hence its expression is activated under specific stress conditions such as high salt, low pH, heat and presence of certain antibiotics (Eiamphungporn & Helmann, 2008; Jervis *et al*, 2007; Thackray & Moir, 2003). It could be that under these conditions LTA of slightly different structure is synthesized to better cope with specific stress conditions. However, it has been reported that a *yfnI* deletion strain is not more sensitive to salt stress as compared to a WT strain (Schirner *et al*, 2009). Additional studies are needed to determine if YfnI could indeed be a "stress LTA-synthase" (Fig. 37). During sporulation YqgS is essential in the absence of the "house-keeping" LTA synthase YflE (Schirner *et al*, 2009), and therefore could be termed sporulation LTA synthase (Fig. 37). The function of the LTA primase YvgJ during growth of *B. subtilis* is least clear, and only the somewhat reduced sporulation efficiency in the absence of both YflE and YvgJ would indicate that the GroP-Glc_2-DAG intermediate produced by YvgJ plays are role during the sporulation process (Schirner *et al*, 2009). It is interesting to note that accumulation of the GroP-Glc_2-DAG glycolipid intermediate upon YvgJ expression leads to a concomitant decrease in the amount of the glycolipid Glc_2-DAG (Fig. 30), suggesting that the total glycolipid pool is held constant in the cell, and that GroP-Glc_2-DAG is part of this glycolipid pool. This could indicate that GroP-Glc_2-DAG might still be able to traverse the membrane and reach the cytoplasm of the cell where it could cause a feedback inhibition on cytoplasmic glycolipid synthesizing enzymes (UgtP in *B. subtilis* or YpfP in *S. aureus*).

In conclusion the results presented in chapters 6 and 7 demonstrate that all four *B. subtilis* LtaS-type proteins are involved in the LTA synthesis process, they have distinct enzymatic activities within the cell, and there is a functional interdependency of their enzymatic activities.

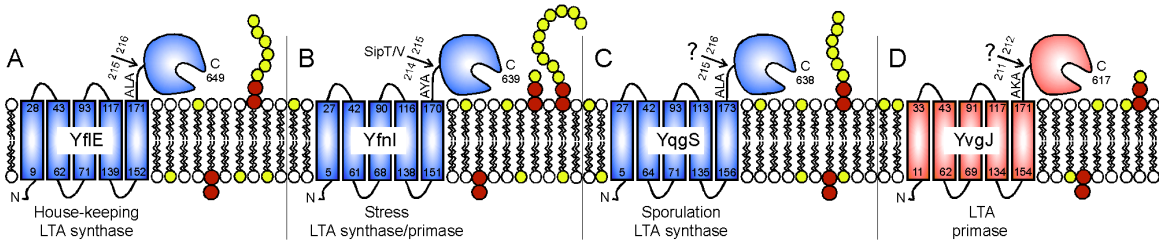

Figure 37: Schematic representation of *in vivo* activities of the four *B. subtilis* LtaS-type enzymes. (A) *B. subtilis* YflE is the "house-keeping" LTA synthase, which is active during vegetative growth. (B) *B. subtilis* YfnI is assumed to be the "stress" LTA synthase, as *yfnI* transcription is controlled by sigma M, which is important during cell envelope stress. YfnI is capable of promoting polyglycerolphosphate synthesis as well as of producing the GroP-Glc_2-DAG glycolipid intermediate. Here we show that YfnI activity is influenced by the presence/absence of YflE. Processed forms of both, YflE and YfnI have been detected in the culture supernatant, and processing of YfnI is reduced in the combined absence of the two signal peptidases SipT and SipV (Antelmann *et al*, 2001). (C) *B. subtilis* YqgS has LTA synthase activity and is important during the sporulation process. (D) YvgJ functions as an LTA primase synthesizing the glycolipid intermediate GroP-Glc_2-DAG. Although YqgS and YvgJ contain an AXA motif it is not clear if these enzymes are processed in *B. subtilis*. LTA synthases are depicted in blue and LTA primases in red. Numbers refer to amino acid positions and arrows indicate cleavage or potential cleavage sites.

Chapter 9

Final conclusions and perspectives

Polyglycerolphosphate LTA is a widespread polymer found in the cell wall envelope of many Gram-positive bacteria. In bacteria that belong to the phylum Firmicutes, the LTA backbone is synthesized by LtaS, the lipoteichoic acid synthase (Gründling & Schneewind, 2007a; Rahman *et al*, 2009b). *S. aureus* produces a single LtaS protein, which is essential for growth and LTA production under standard laboratory conditions (Gründling & Schneewind, 2007a). The LtaS protein contains five N-terminal transmembrane helices (5TM) and a large C-terminal extracellular enzymatic domain (eLtaS). The latter domain is cleaved during bacterial growth and released from the membrane. However, despite the fact that the enzyme is efficiently processed, only the full-length protein appears to function in the LTA synthesis pathway. My work provides evidence that both LtaS domains are required for enzyme function and that once the protein is cleaved into 5TM and eLtaS the enzyme no longer contributes to LTA synthesis (sections 4.2-4.4). Based on my data it can be speculated that LtaS cleavage provides a mechanism to regulate LtaS activity and that the LtaS processing step irreversibly inactivates the enzyme.

The observation that only the full-length LtaS protein is enzymatically active suggests that the LTA polymer remains in close proximity to the membrane at least during its synthesis. Recently, the existence of a periplasmic space in Gram-positive bacteria was reported (Matias & Beveridge, 2005; Matias & Beveridge, 2006). Based on cryotransmission electron microscopy images of unstained, ultrarapid frozen and hydrated sections of *B. subtilis* and *S. aureus* cells, two distinct cell wall zones could be identified. A low-density inner wall zone (IWZ) was observed immediately next to the bacterial membrane and this zone was denoted the periplasmic space in Gram-positive bacteria. Adjacent to the IWZ, a high-density outer wall zone (OWZ) was visible, which comprises the peptidoglycan. Whole cell labeling experiments with positively charged gold nanoparticles resulted in similar levels of these particles bound to the IWZ and OWZ, indicating the existence of large amounts of negatively charged components in the periplasm (Matias & Beveridge, 2008). After enzymatic hydrolysis of the OWZ, a surface diffuse layer extending from the bacterial membrane was observed. This layer was not significantly altered by protease treatment, but could be labeled with an LTA specific antibody conjugated to nanogold particles (Matias & Beveridge, 2008). These findings strongly suggest that LTA is a major component of

the Gram-positive periplasm and thus argue for a physiological function of the polymer in close proximity to the membrane (Matias & Beveridge, 2008).

Recent literature has highlighted the discovery of polyglycerolphosphate LTA in various bacterial species belonging to the phylum Actinomycetes (Rahman *et al*, 2009a; Rahman *et al*, 2009c). However, Actinomycetes appear to lack LtaS homologues and thus it was hypothesized that LTA synthesis occurs through an alternative pathway in these bacteria (Rahman *et al*, 2009c). Interestingly, Actinomycetes that produce polyglycerolphosphate LTA often also synthesize polyglycerolphosphate-type WTA rather than alternative secondary cell wall polysaccharides. Based on this observation it was hypothesized that the pathways of LTA and WTA synthesis in these bacterial species overlap and utilize a common precursor (Rahman *et al*, 2009b). In the future, it will be interesting to investigate how certain bacterial species, such as Actinomycetes, synthesize polyglycerolphosphate LTA.

In contrast to *S. aureus*, which has a single LtaS protein, *B. subtilis* encodes four LtaS-like proteins, namely YflE, YfnI, YqgS and YvgJ (Gründling & Schneewind, 2007a; Schirner *et al*, 2009). In this work, I show that all four *B. subtilis* LtaS-like proteins are enzymatically active and that YflE, YfnI and YqgS are bona-fide LTA synthases that can synthesize glycerolphosphate polymers (section 7.2). In contrast, YvgJ is an LTA primase, which uses the glycerolphosphate head group of the membrane lipid PG to form the glycolipid GroP-Glc2-DAG (section 7.3), which is assumed to be an LTA synthesis intermediate.

Two different models have been proposed for lipoteichoic acid biosynthesis that differ in the enzyme activity, which is required for the actual linkage of the glycerolphosphate polymer to the glycolipid anchor (recently reviewed in Rahman *et al*, 2009b). For one model, it was proposed that an "LTA transferase" moves fully synthesized polyglycerolphosphate polymers from a DAG lipid anchor onto a glycolipid anchor. This was based on the following observations: In *Streptococcus sanguis* a significant amount of polyglycerolphosphate "intermediates" linked to DAG are present in the membrane (Chiu *et al*, 1993). In the absence of glycolipids due to mutations in genes necessary for their synthesis (Button & Hemmings, 1976; Fedtke *et al*, 2007; Kiriukhin *et al*, 2001) or natural lack of these genes as found in some *Bacillus* sp. (Iwasaki *et al*, 1986) polyglycerolphosphate polymers are directly linked

to DAG. Hence, it was proposed that the DAG-linked polymers are natural LTA synthesis intermediates, which are subsequently moved by an LTA transferase enzyme onto the glycolipid anchor. In the second model an LTA primase adds the first glycerolphosphate subunit to the glycolipid anchor to form the GroP-glycolipid intermediate. Subsequently an LTA synthase adds additional glycerolphosphate subunits onto this GroP-glycolipid intermediate to produce the LTA backbone chain. The discovery of an LTA primase in *L. monocytogenes* (Webb *et al*, 2009) and, as described in this study, now also in *B. subtilis* favors the second model. However, it appears that the action of an LTA primase and the production of the GroP-glycolipid intermediate aid only in some cases and to some extent in the LTA synthesis process. In additional to this two-enzyme system, a slightly altered version of the latter model in which only a single enzyme is needed for LTA synthesis is proposed here. In this model, a single enzyme can directly start and extend the glycerolphosphate chain on the glycolipid anchor. It was shown that enzymes with LTA synthases and LTA primases activity belong to the same family of proteins (LtaS-type enzymes). Members of this protein family show a high degree of identity on the amino acid level and have the same predicted membrane topology and domain structure. Therefore, it appears that in the genome of *S. aureus* and several other Gram-positive bacteria, only one LtaS-type enzyme is encoded and hence it was suggested that this enzyme functions as both an LTA synthase and an LTA primase. In addition, the *B. subtilis* YfnI enzyme produces both polyglycerolphosphate polymers and the GroP-Glc_2-DAG intermediate (Gründling & Schneewind, 2007a and sections 7.2 and 7.3), providing further evidence that the same LtaS-type enzyme can be an LTA synthase and an LTA primase. Furthermore, deletion of the dedicated LTA primase YvgJ in *B. subtilis* does not lead to an obvious difference in LTA production suggesting that all *B. subtilis* LTA synthases are able to efficiently initiate LTA synthesis independent of the activity of a dedicated LTA primase (Fig. 34). Based on these observations, it can be suggested that while LtaS-type enzymes are very selective for their lipid substrate (they can only cleave the head group of PG), at least some of them have a relaxed specificity towards the acceptor lipid that can be used for the subsequent glycerolphosphate transfer reaction. For example, *S. aureus* LtaS can use DAG, Glc_2-DAG, GroP-Glc_2-DAG and the polyglycerolphosphate chain. However the efficiencies with which these different acceptor molecules can be used will vary

between each individual enzyme and dictate how efficient LTA can be synthesized in the absence of glycolipids or a dedicated primase and might also influence the final chain length of LTA molecules.

Using BLAST homology searches, it was investigated whether it is possible to distinguish between LTA synthases and dedicated LTA primases (such as the *B. subtilis* YvgJ and *L. monocytogenes* Lmo0644 proteins). However, no motif could be identified that would allow the prediction of which LtaS-type enzyme is an LTA synthase and which protein would only function as an LTA primase. Additional structural information on LTA synthases and LTA primases especially in their full-length membrane form, combined with additional *in vitro* assay studies investigating specifically the glycerolphosphate transfer reaction in the presence of different acceptor molecules, would help to shed light on this question.

Most *Bacillus* species produce LTA of the polyglycerolphosphate type (Iwasaki *et al*, 1986; Iwasaki *et al*, 1989). However, based on literature searches and sequence analysis at least *Bacillus circulans*, *Bacillus pseudofirmus* OF4 and *Bacillus halodurans* C125 lack the LTA polymer or LtaS-type enzymes. *B. circulans* falls into an ungrouped class of *Bacillaceae* species (Xu & Cote, 2003) and the latter two strains are alkaliphilic bacteria (Iwasaki *et al*, 1989; Takami *et al*, 2000). It has been shown that the alkaliphilic strain *B. halodurans* contains, in place of teichoic acids, teichuronopeptides as major cell wall components, which are co-polymers of polyglutamic acid and polyglucoronic acid (Takami *et al*, 2000). Several sequenced *Bacillus* species, namely *Bacillus selenitireducen*s MLS10, *Bacillus coagulans* 36D1 and *Bacillus coahuilensis* m4-4, apparently encode only a single LtaS homologue, which should be sufficient for polyglycerolphosphate LTA synthesis. However, the majority of *Bacillus* species encode multiple LtaS-type proteins. At present it is still not completely understood why bacteria such as *B. subtilis* produce multiple proteins. However as shown here, all four proteins are involved in the LTA synthesis process, they have distinct enzymatic activities within the cell and there is a functional interdependency of their enzymatic activities. Presumably the coordinate expression and activity of these proteins allows *B. subtilis* to fine-tune LTA synthesis under different growth and stress conditions and during the sporulation process. Based on this and previous studies, it is now becoming more and more apparent that LTA function is tied to its exact structure, spatial distribution and/or localized synthesis

(Schirner *et al*, 2009). To determine the exact function of LTA for bacterial growth and its alterations during different growth conditions warrants further analysis.

Bibliography

Akita M, Sasaki S, Matsuyama S, Mizushima S (1990) SecA interacts with secretory proteins by recognizing the positive charge at the amino terminus of the signal peptide in *Escherichia coli*. *J Biol Chem* **265:** 8164-8169

Antelmann H, Tjalsma H, Voigt B, Ohlmeier S, Bron S, van Dijl JM, Hecker M (2001) A proteomic view on genome-based signal peptide predictions. *Genome Res* **11:** 1484-1502

Arbeit RD, Karakawa WW, Vann WF, Robbins JB (1984) Predominance of two newly described capsular polysaccharide types among clinical isolates of *Staphylococcus aureus*. *Diagn Microbiol Infect Dis* **2:** 85-91

Atkins KL, Burman JD, Chamberlain ES, Cooper JE, Poutrel B, Bagby S, Jenkins AT, Feil EJ, van den Elsen JM (2008) *S. aureus* IgG-binding proteins SpA and Sbi: host specificity and mechanisms of immune complex formation. *Mol Immunol* **45:** 1600-1611

Atrih A, Bacher G, Allmaier G, Williamson MP, Foster SJ (1999) Analysis of peptidoglycan structure from vegetative cells of *Bacillus subtilis* 168 and role of PBP 5 in peptidoglycan maturation. *J Bacteriol* **181:** 3956-3966

Baba T, Bae T, Schneewind O, Takeuchi F, Hiramatsu K (2008) Genome sequence of *Staphylococcus aureus* strain Newman and comparative analysis of staphylococcal genomes: polymorphism and evolution of two major pathogenicity islands. *J Bacteriol* **190:** 300-310

Baddiley J, Buchanan JG, Hardy FE, Martin RO, Rajbhandary UL, Sanderson AR (1961) The structure of the ribitol teichoic acid of *Staphylococcus aureus* H. *Biochim Biophys Acta* **52:** 406-407

Banbula A, Potempa J, Travis J, Fernandez-Catalan C, Mann K, Huber R, Bode W, Medrano F (1998) Amino-acid sequence and three-dimensional structure of the *Staphylococcus aureus* metalloproteinase at 1.72 A resolution. *Structure* **6:** 1185-1193

Barkocy-Gallagher GA, Bassford PJ, Jr. (1992) Synthesis of precursor maltose-binding protein with proline in the +1 position of the cleavage site interferes with the activity of *Escherichia coli* signal peptidase I *in vivo*. *J Biol Chem* **267:** 1231-1238

Bateman BT, Donegan NP, Jarry TM, Palma M, Cheung AL (2001) Evaluation of a tetracycline-inducible promoter in *Staphylococcus aureus* in vitro and in vivo and its application in demonstrating the role of *sigB* in microcolony formation. *Infect Immun* **69:** 7851-7857

Batenburg AM, Demel RA, Verkleij AJ, de Kruijff B (1988) Penetration of the signal sequence of *Escherichia coli* PhoE protein into phospholipid model membranes leads

to lipid-specific changes in signal peptide structure and alterations of lipid organization. *Biochemistry* **27:** 5678-5685

Beaufort N, Wojciechowski P, Sommerhoff CP, Szmyd G, Dubin G, Eick S, Kellermann J, Schmitt M, Potempa J, Magdolen V (2008) The human fibrinolytic system is a target for the staphylococcal metalloprotease aureolysin. *Biochem J* **410:** 157-165

Beltzer JP, Wessels HP, Spiess M (1989) Signal peptidase can cleave inside a polytopic membrane protein. *FEBS Lett* **253:** 93-98

Bendtsen JD, Nielsen H, von Heijne G, Brunak S (2004) Improved prediction of signal peptides: SignalP 3.0. *J Mol Biol* **340:** 783-795

Bera A, Herbert S, Jakob A, Vollmer W, Götz F (2005) Why are pathogenic staphylococci so lysozyme resistant? The peptidoglycan O-acetyltransferase OatA is the major determinant for lysozyme resistance of *Staphylococcus aureus*. *Mol Microbiol* **55:** 778-787

Bhavsar AP, Erdman LK, Schertzer JW, Brown ED (2004) Teichoic acid is an essential polymer in *Bacillus subtilis* that is functionally distinct from teichuronic acid. *J Bacteriol* **186:** 7865-7873

Bjoorklind A, Jornvall H (1974) Substrate specificity of three different extracellular proteolytic enzymes from *Staphylococcus aureus*. *Biochim Biophys Acta* **370:** 524-529

Black MT (1993) Evidence that the catalytic activity of prokaryote leader peptidase depends upon the operation of a serine-lysine catalytic dyad. *J Bacteriol* **175:** 4957-4961

Boles BR, Thoendel M, Roth AJ, Horswill AR (2010) Identification of genes involved in polysaccharide-independent *Staphylococcus aureus* biofilm formation. *PLoS One* **5:** e10146

Boneca IG, Huang ZH, Gage DA, Tomasz A (2000) Characterization of *Staphylococcus aureus* cell wall glycan strands, evidence for a new beta-N-acetylglucosaminidase activity. *J Biol Chem* **275:** 9910-9918

Briggs MS, Cornell DG, Dluhy RA, Gierasch LM (1986) Conformations of signal peptides induced by lipids suggest initial steps in protein export. *Science* **233:** 206-208

Bruton G, Huxley A, O'Hanlon P, Orlek B, Eggleston D, Humphries J, Readshaw S, West A, Ashman S, Brown M, Moore K, Pope A, O'Dwyer K, Wang L (2003) Lipopeptide substrates for SpsB, the *Staphylococcus aureus* type I signal peptidase: design, conformation and conversion to alpha-ketoamide inhibitors. *Eur J Med Chem* **38:** 351-356

Bubeck Wardenburg J, Williams WA, Missiakas D (2006) Host defenses against *Staphylococcus aureus* infection require recognition of bacterial lipoproteins. *Proc Natl Acad Sci U S A* **103:** 13831-13836

Burger MM, Glaser L (1964) The synthesis of teichoic acids. I. Polyglycerophosphate. *J Biol Chem* **239:** 3168-3177

Burkholder PR, Giles NH (1947) Induced biochemical mutations in *Bacillus subtilis*. *Am J Bot* **33:** 345–348

Burman JD, Leung E, Atkins KL, O'Seaghdha MN, Lango L, Bernado P, Bagby S, Svergun DI, Foster TJ, Isenman DE, van den Elsen JM (2008) Interaction of human complement with Sbi, a staphylococcal immunoglobulin-binding protein: indications of a novel mechanism of complement evasion by *Staphylococcus aureus*. *J Biol Chem* **283:** 17579-17593

Button D, Hemmings NL (1976) Teichoic acids and lipids associated with the membrane of a *Bacillus licheniformis* mutant and the membrane lipids of the parental strain. *J Bacteriol* **128:** 149-156

Buzder-Lantos P, Bockstael K, Anne J, Herdewijn P (2009) Substrate based peptide aldehyde inhibits bacterial type I signal peptidase. *Bioorg Med Chem Lett* **19:** 2880-2883

Calander AM, Jonsson IM, Kanth A, Arvidsson S, Shaw L, Foster SJ, Tarkowski A (2004) Impact of staphylococcal protease expression on the outcome of infectious arthritis. *Microbes Infect* **6:** 202-206

Carballido-Lopez R, Errington J (2003) The bacterial cytoskeleton: in vivo dynamics of the actin-like protein Mbl of *Bacillus subtilis*. *Dev Cell* **4:** 19-28

Chan PF, Foster SJ (1998) Role of SarA in virulence determinant production and environmental signal transduction in *Staphylococcus aureus*. *J Bacteriol* **180:** 6232-6241

Charpentier E, Anton AI, Barry P, Alfonso B, Fang Y, Novick RP (2004) Novel cassette-based shuttle vector system for gram-positive bacteria. *Appl Environ Microbiol* **70:** 6076-6085

Chatterjee AN, Mirelman D, Singer HJ, Park JT (1969) Properties of a novel pleiotropic bacteriophage-resistant mutant of *Staphylococcus aureus* H. *J Bacteriol* **100:** 846-853

Chen L, Tai PC (1987) Effects of antibiotics and other inhibitors on ATP-dependent protein translocation into membrane vesicles. *J Bacteriol* **169:** 2373-2379

Chiu TH, Morimoto H, Baker JJ (1993) Biosynthesis and characterization of phosphatidylglycerophosphoglycerol, a possible intermediate in lipoteichoic acid biosynthesis in *Streptococcus sanguis*. *Biochim Biophys Acta* **1166:** 222-228

Claus D, Fritze D (1989) *Taxonomy of Bacillus, p. 5-26. In C.R. Harwood (ed.), Biotechnology Handbooks, vol. 2. Bacillus. Plenum Press, New York.*

Coulter SN, Schwan WR, Ng EY, Langhorne MH, Ritchie HD, Westbrock-Wadman S, Hufnagle WO, Folger KR, Bayer AS, Stover CK (1998) *Staphylococcus aureus* genetic loci impacting growth and survival in multiple infection environments. *Mol Microbiol* **30:** 393-404

Cregg KM, Wilding I, Black MT (1996) Molecular cloning and expression of the *spsB* gene encoding an essential type I signal peptidase from *Staphylococcus aureus*. *J Bacteriol* **178:** 5712-5718

D'Elia MA, Millar KE, Beveridge TJ, Brown ED (2006) Wall teichoic acid polymers are dispensable for cell viability in *Bacillus subtilis*. *J Bacteriol* **188:** 8313-8316

Daniel RA, Errington J (2003) Control of cell morphogenesis in bacteria: two distinct ways to make a rod-shaped cell. *Cell* **113:** 767-776

Dassy B, Hogan T, Foster TJ, Fournier JM (1993) Involvement of the accessory gene regulator (Agr) in expression of type 5 capsular polysaccharide by *Staphylococcus aureus*. *J Gen Microbiol* **139 Pt 6:** 1301-1306

Daum RS, Ito T, Hiramatsu K, Hussain F, Mongkolrattanothai K, Jamklang M, Boyle-Vavra S (2002) A novel methicillin-resistance cassette in community-acquired methicillin-resistant *Staphylococcus aureus* isolates of diverse genetic backgrounds. *J Infect Dis* **186:** 1344-1347

DeDent A, Bae T, Missiakas DM, Schneewind O (2008) Signal peptides direct surface proteins to two distinct envelope locations of *Staphylococcus aureus*. *Embo J* **27:** 2656-2668

Diekema DJ, Pfaller MA, Schmitz FJ, Smayevsky J, Bell J, Jones RN, Beach M (2001) Survey of infections due to *Staphylococcus* species: frequency of occurrence and antimicrobial susceptibility of isolates collected in the United States, Canada, Latin America, Europe, and the Western Pacific region for the SENTRY Antimicrobial Surveillance Program, 1997-1999. *Clin Infect Dis* **32 Suppl 2:** S114-132

Diep BA, Otto M (2008) The role of virulence determinants in community-associated MRSA pathogenesis. *Trends Microbiol* **16:** 361-369

Drapeau GR (1978) Role of metalloprotease in activation of the precursor of staphylococcal protease. *J Bacteriol* **136:** 607-613

Drapeau GR, Boily Y, Houmard J (1972) Purification and properties of an extracellular protease of *Staphylococcus aureus*. *J Biol Chem* **247:** 6720-6726

Dubin G (2003) Defense against own arms: staphylococcal cysteine proteases and their inhibitors. *Acta Biochim Pol* **50:** 715-724

Dubin G, Stec-Niemczyk J, Kisielewska M, Pustelny K, Popowicz GM, Bista M, Kantyka T, Boulware KT, Stennicke HR, Czarna A, Phopaisarn M, Daugherty PS, Thogersen IB, Enghild JJ, Thornberry N, Dubin A, Potempa J (2008) Enzymatic activity of the *Staphylococcus aureus* SplB serine protease is induced by substrates containing the sequence Trp-Glu-Leu-Gln. *J Mol Biol* **379:** 343-356

Dubnau D (1991) Genetic competence in *Bacillus subtilis*. *Microbiol Rev* **55:** 395-424

Duckworth M, Archibald AR, Baddiley J (1972) The location of N-acetylgalactosamine in the walls of *Bacillus subtilis* 168. *Biochem J* **130:** 691-696

Duckworth M, Archibald AR, Baddiley J (1975) Lipoteichoic acid and lipoteichoic acid carrier in *Staphylococcus aureus* H. *FEBS Lett* **53:** 176-179

Ehlert K, Schroder W, Labischinski H (1997) Specificities of FemA and FemB for different glycine residues: FemB cannot substitute for FemA in staphylococcal peptidoglycan pentaglycine side chain formation. *J Bacteriol* **179:** 7573-7576

Eiamphungporn W, Helmann JD (2008) The *Bacillus subtilis* sigma(M) regulon and its contribution to cell envelope stress responses. *Mol Microbiol* **67:** 830-848

Ellwood DC, Tempest DW (1972) Influence of culture pH on the content and composition of teichoic acids in the walls of *Bacillus subtilis*. *J Gen Microbiol* **73:** 395-402

Ernst CM, Staubitz P, Mishra NN, Yang SJ, Hornig G, Kalbacher H, Bayer AS, Kraus D, Peschel A (2009) The bacterial defensin resistance protein MprF consists of separable domains for lipid lysinylation and antimicrobial peptide repulsion. *PLoS Pathog* **5:** e1000660

Falconer SB, Brown ED (2009) New screens and targets in antibacterial drug discovery. *Curr Opin Microbiol*

Fedtke I, Mader D, Kohler T, Moll H, Nicholson G, Biswas R, Henseler K, Gotz F, Zahringer U, Peschel A (2007) A *Staphylococcus aureus ypfP* mutant with strongly reduced lipoteichoic acid (LTA) content: LTA governs bacterial surface properties and autolysin activity. *Mol Microbiol* **65:** 1078-1091

Fischer W (1988) Physiology of lipoteichoic acids in bacteria. *Adv Microb Physiol* **29:** 233-302

Fischer W (1994) Lipoteichoic acid and lipids in the membrane of *Staphylococcus aureus*. *Med Microbiol Immunol (Berl)* **183:** 61-76

Fischer W, Mannsfeld T, Hagen G (1990) On the basic structure of poly(glycerophosphate) lipoteichoic acids. *Biochem Cell Biol* **68:** 33-43

Fischer W, Rosel P (1980) The alanine ester substitution of lipoteichoic acid (LTA) in *Staphylococcus aureus*. *FEBS Lett* **119:** 224-226

Fischer W, Rosel P, Koch HU (1981) Effect of alanine ester substitution and other structural features of lipoteichoic acids on their inhibitory activity against autolysins of *Staphylococcus aureus*. *J Bacteriol* **146:** 467-475

Fischetti VA, Pancholi V, Schneewind O (1990) Conservation of a hexapeptide sequence in the anchor region of surface proteins from Gram-positive cocci. *Mol Microbiol* **4:** 1603-1605

Forsgren A, Nordstrom K (1974) Protein A from *Staphylococcus aureus*: the biological significance of its reaction with IgG. *Ann N Y Acad Sci* **236:** 252-266

Fournier JM, Hannon K, Moreau M, Karakawa WW, Vann WF (1987) Isolation of type 5 capsular polysaccharide from *Staphylococcus aureus*. *Ann Inst Pasteur Microbiol* **138:** 561-567

Fournier JM, Vann WF, Karakawa WW (1984) Purification and characterization of *Staphylococcus aureus* type 8 capsular polysaccharide. *Infect Immun* **45:** 87-93

Gally D, Archibald AR (1993) Cell wall assembly in *Staphylococcus aureus:* proposed absence of secondary crosslinking reactions. *J Gen Microbiol* **139:** 1907-1913

Gatlin CL, Pieper R, Huang ST, Mongodin E, Gebregeorgis E, Parmar PP, Clark DJ, Alami H, Papazisi L, Fleischmann RD, Gill SR, Peterson SN (2006) Proteomic profiling of cell envelope-associated proteins from *Staphylococcus aureus*. *Proteomics* **6:** 1530-1549

Gemmell C, Tree R, Patel A, O'Reilly M, Foster TJ (1991) Susceptibility to opsonophagocytosis of protein A, alpha-haemolysin and beta-toxin deficient mutants of *Staphylococcus aureus* isolated by allele-replacement. Zentralbl. Bacteriol. **21 (Suppl.)**, *273-277*.

Ghuysen JM, Strominger JL (1963) Structure of the cell wall of *Staphylococcus aureus*, Strain Copenhagen. Ii. Separation and structure of disaccharides. *Biochemistry* **2:** 1119-1125

Goldberg DE, Rumley MK, Kennedy EP (1981) Biosynthesis of membrane-derived oligosaccharides: a periplasmic phosphoglyceroltransferase. *Proc Natl Acad Sci U S A* **78:** 5513-5517

Gomez MI, Lee A, Reddy B, Muir A, Soong G, Pitt A, Cheung A, Prince A (2004) *Staphylococcus aureus* protein A induces airway epithelial inflammatory responses by activating TNFR1. *Nat Med* **10:** 842-848

Gomez MI, O'Seaghdha M, Magargee M, Foster TJ, Prince AS (2006) *Staphylococcus aureus* protein A activates TNFR1 signaling through conserved IgG binding domains. *J Biol Chem* **281:** 20190-20196

Grassl M, Supp M (1995) Methods of enzymatic analysis. In *Methods of Enzymatic Analysis*, Bergmeyer HU, Bergmeyer J, Grassl M (eds), Vol. VIII, pp 336-340. Weinheim: Verlag Chemie

Gross M, Cramton SE, Gotz F, Peschel A (2001) Key role of teichoic acid net charge in *Staphylococcus aureus* colonization of artificial surfaces. *Infect Immun* **69:** 3423-3426

Gründling A, Gonzalez MD, Higgins DE (2003) Requirement of the *Listeria monocytogenes* broad-range phospholipase PC-PLC during infection of human epithelial cells. *J Bacteriol* **185:** 6295-6307

Gründling A, Schneewind O (2007a) Synthesis of glycerol phosphate lipoteichoic acid in *Staphylococcus aureus*. *Proc Natl Acad Sci U S A* **104:** 8478-8483

Gründling A, Schneewind O (2007b) Genes required for glycolipid synthesis and lipoteichoic acid anchoring in *Staphylococcus aureus*. *J Bacteriol* **189:** 2521-2530

Hancock RE (2005) Mechanisms of action of newer antibiotics for Gram-positive pathogens. *Lancet Infect Dis* **5:** 209-218

Hartleib J, Kohler N, Dickinson RB, Chhatwal GS, Sixma JJ, Hartford OM, Foster TJ, Peters G, Kehrel BE, Herrmann M (2000) Protein A is the von Willebrand factor binding protein on *Staphylococcus aureus*. *Blood* **96:** 2149-2156

Hartman BJ, Tomasz A (1984) Low-affinity penicillin-binding protein associated with beta-lactam resistance in *Staphylococcus aureus*. *J Bacteriol* **158:** 513-516

Harwood CR (1992) *Bacillus subtilis* and its relatives: molecular biological and industrial workhorses. *Trends Biotechnol* **10:** 247-256

Hasegawa N, San Clemente CL (1978) Virulence and immunity of *Staphylococcus aureus* BB and certain deficient mutants. *Infect Immun* **22:** 473-479

Hashimoto M, Tawaratsumida K, Kariya H, Kiyohara A, Suda Y, Krikae F, Kirikae T, Gotz F (2006) Not lipoteichoic acid but lipoproteins appear to be the dominant immunobiologically active compounds in *Staphylococcus aureus*. *J Immunol* **177:** 3162-3169

Haupt K, Reuter M, van den Elsen J, Burman J, Halbich S, Richter J, Skerka C, Zipfel PF (2008) The *Staphylococcus aureus* protein Sbi acts as a complement inhibitor and forms a tripartite complex with host complement Factor H and C3b. *PLoS Pathog* **4:** e1000250

Hayhurst EJ, Kailas L, Hobbs JK, Foster SJ (2008) Cell wall peptidoglycan architecture in *Bacillus subtilis*. *Proc Natl Acad Sci U S A* **105:** 14603-14608

Heptinstall S, Archibald AR, Baddiley J (1970) Teichoic acids and membrane function in bacteria. *Nature* **225:** 519-521

Herbert S, Worlitzsch D, Dassy B, Boutonnier A, Fournier JM, Bellon G, Dalhoff A, Doring G (1997) Regulation of *Staphylococcus aureus* capsular polysaccharide type 5: CO2 inhibition in vitro and *in vivo*. *J Infect Dis* **176:** 431-438

Hermann C, Spreitzer I, Schroder NW, Morath S, Lehner MD, Fischer W, Schutt C, Schumann RR, Hartung T (2002) Cytokine induction by purified lipoteichoic acids from various bacterial species--role of LBP, sCD14, CD14 and failure to induce IL-12 and subsequent IFN-gamma release. *Eur J Immunol* **32:** 541-551

Hirose I, Sano K, Shioda I, Kumano M, Nakamura K, Yamane K (2000) Proteome analysis of *Bacillus subtilis* extracellular proteins: a two-dimensional protein electrophoretic study. *Microbiology* **146:** 65-75

Horton RM, Hunt HD, Ho SN, Pullen JK, Pease LR (1989) Engineering hybrid genes without the use of restriction enzymes: gene splicing by overlap extension. *Gene* **77:** 61-68

Houmard J, Drapeau GR (1972) Staphylococcal protease: a proteolytic enzyme specific for glutamoyl bonds. *Proc Natl Acad Sci U S A* **69:** 3506-3509

Hussain M, Ichihara S, Mizushima S (1982) Mechanism of signal peptide cleavage in the biosynthesis of the major lipoprotein of the *Escherichia coli* outer membrane. *J Biol Chem* **257:** 5177-5182

Hutchings MI, Palmer T, Harrington DJ, Sutcliffe IC (2009) Lipoprotein biogenesis in Gram-positive bacteria: knowing when to hold 'em, knowing when to fold 'em. *Trends Microbiol* **17:** 13-21

Inganas M (1981) Comparison of mechanisms of interaction between protein A from *Staphylococcus aureus* and human monoclonal IgG, IgA and IgM in relation to the classical FC gamma and the alternative F(ab')2 epsilon protein A interactions. *Scand J Immunol* **13:** 343-352

Inganas M, Johansson SG (1981) Influence of the alternative protein A interaction on the precipitation between human monoclonal immunoglobulins and protein A from *Staphylococcus aureus*. *Int Arch Allergy Appl Immunol* **65:** 91-101

Inouye M, Halegoua S (1980) Secretion and membrane localization of proteins in *Escherichia coli*. *CRC Crit Rev Biochem* **7:** 339-371

Inouye S, Wang S, Sekizawa J, Halegoua S, Inouye M (1977) Amino acid sequence for the peptide extension on the prolipoprotein of the *Escherichia coli* outer membrane. *Proc Natl Acad Sci U S A* **74:** 1004-1008

Ito T, Katayama Y, Asada K, Mori N, Tsutsumimoto K, Tiensasitorn C, Hiramatsu K (2001) Structural comparison of three types of staphylococcal cassette chromosome *mec* integrated in the chromosome in methicillin-resistant *Staphylococcus aureus*. *Antimicrob Agents Chemother* **45:** 1323-1336

Ito T, Ma XX, Takeuchi F, Okuma K, Yuzawa H, Hiramatsu K (2004) Novel type V staphylococcal cassette chromosome *mec* driven by a novel cassette chromosome recombinase, *ccrC*. *Antimicrob Agents Chemother* **48:** 2637-2651

Iwasaki H, Shimada A, Ito E (1986) Comparative studies of lipoteichoic acids from several *Bacillus* strains. *J Bacteriol* **167:** 508-516

Iwasaki H, Shimada A, Yokoyama K, Ito E (1989) Structure and glycosylation of lipoteichoic acids in *Bacillus* strains. *J Bacteriol* **171:** 424-429

Jackson BJ, Bohin JP, Kennedy EP (1984) Biosynthesis of membrane-derived oligosaccharides: characterization of *mdoB* mutants defective in phosphoglycerol transferase I activity. *J Bacteriol* **160:** 976-981

Jacobsson K, Frykberg L (1995) Cloning of ligand-binding domains of bacterial receptors by phage display. *BioTechniques* **18:** 878-885

Jain RG, Rusch SL, Kendall DA (1994) Signal peptide cleavage regions. Functional limits on length and topological implications. *J Biol Chem* **269:** 16305-16310

Jensen CL, Stephenson K, Jorgensen ST, Harwood C (2000) Cell-associated degradation affects the yield of secreted engineered and heterologous proteins in the *Bacillus subtilis* expression system. *Microbiology* **146:** 2583-2594

Jerga A, Lu YJ, Schujman GE, de Mendoza D, Rock CO (2007) Identification of a soluble diacylglycerol kinase required for lipoteichoic acid production in *Bacillus subtilis*. *J Biol Chem* **282:** 21738-21745

Jervis AJ, Thackray PD, Houston CW, Horsburgh MJ, Moir A (2007) SigM-responsive genes of *Bacillus subtilis* and their promoters. *J Bacteriol* **189:** 4534-4538

Jones LJ, Carballido-Lopez R, Errington J (2001) Control of cell shape in bacteria: helical, actin-like filaments in *Bacillus subtilis*. *Cell* **104:** 913-922

Jonquieres R, Bierne H, Fiedler F, Gounon P, Cossart P (1999) Interaction between the protein InlB of *Listeria monocytogenes* and lipoteichoic acid: a novel mechanism of protein association at the surface of gram-positive bacteria. *Mol Microbiol* **34:** 902-914

Jonsson IM, Mazmanian SK, Schneewind O, Bremell T, Tarkowski A (2003) The role of *Staphylococcus aureus* sortase A and sortase B in murine arthritis. *Microbes Infect* **5:** 775-780

Jonsson P, Lindberg M, Haraldsson I, Wadstrom T (1985) Virulence of *Staphylococcus aureus* in a mouse mastitis model: studies of alpha hemolysin, coagulase, and protein A as possible virulence determinants with protoplast fusion and gene cloning. *Infect Immun* **49:** 765-769

Jorasch P, Wolter FP, Zahringer U, Heinz E (1998) A UDP glucosyltransferase from *Bacillus subtilis* successively transfers up to four glucose residues to 1,2-

diacylglycerol: expression of *ypfP* in *Escherichia coli* and structural analysis of its reaction products. *Mol Microbiol* **29:** 419-430

Kanemasa Y, Yoshioka T, Hayashi H (1972) Alteration of the phospholipid composition of *Staphylococcus aureus* cultured in medium containing NaCl. *Biochim Biophys Acta* **280:** 444-450

Karamata D, Pooley HM, Monod M (1987) Expression of heterologous genes for wall teichoic acid in *Bacillus subtilis* 168. *Mol Gen Genet* **207:** 73-81

Karatsa-Dodgson M, Wormann ME, Gründling A (2010) *In vitro* analysis of the *Staphylococcus aureus* lipoteichoic acid synthase enzyme using fluorescently labeled lipids. *J Bacteriol* **192:** 5341-5349

Karlsson A, Saravia-Otten P, Tegmark K, Morfeldt E, Arvidson S (2001) Decreased amounts of cell wall-associated protein A and fibronectin-binding proteins in *Staphylococcus aureus sarA* mutants due to up-regulation of extracellular proteases. *Infect Immun* **69:** 4742-4748

Kates M (1972) Techniques of lipidology. In *Laboratory Techniques in Biochemistry and Molecular Biology*, Work TW, E (ed), pp 347-469. New York: American Elsevier

Kavanaugh JS, Thoendel M, Horswill AR (2007) A role for type I signal peptidase in *Staphylococcus aureus* quorum sensing. *Mol Microbiol* **65:** 780-798

Kiriukhin MY, Debabov DV, Shinabarger DL, Neuhaus FC (2001) Biosynthesis of the glycolipid anchor in lipoteichoic acid of *Staphylococcus aureus* RN4220: role of YpfP, the diglucosyldiacylglycerol synthase. *J Bacteriol* **183:** 3506-3514

Koch HU, Haas R, Fischer W (1984) The role of lipoteichoic acid biosynthesis in membrane lipid metabolism of growing *Staphylococcus aureus*. *Eur J Biochem* **138:** 357-363

Kreiswirth BN, Lofdahl S, Betley MJ, O'Reilly M, Schlievert PM, Bergdoll MS, Novick RP (1983) The toxic shock syndrome exotoxin structural gene is not detectably transmitted by a prophage. *Nature* **305:** 709-712

Krojer T, Garrido-Franco M, Huber R, Ehrmann M, Clausen T (2002) Crystal structure of DegP (HtrA) reveals a new protease-chaperone machine. *Nature* **416:** 455-459

Kubica M, Guzik K, Koziel J, Zarebski M, Richter W, Gajkowska B, Golda A, Maciag-Gudowska A, Brix K, Shaw L, Foster T, Potempa J (2008) A potential new pathway for *Staphylococcus aureus* dissemination: the silent survival of *S. aureus* phagocytosed by human monocyte-derived macrophages. *PLoS One* **3:** e1409

Kunst A, Draeger B, Ziegenhorn J (1984) *Methods of enzymatic analysis*, Vol. VI, 3rd edn. Weinheim: Verlag Chemie.

Kunst F, Ogasawara N, Moszer I, Albertini AM, Alloni G, Azevedo V, Bertero MG, Bessieres P, Bolotin A, Borchert S, Borriss R, Boursier L, Brans A, Braun M, Brignell SC, Bron S, Brouillet S, Bruschi CV, Caldwell B, Capuano V *et al* (1997) The complete genome sequence of the gram-positive bacterium *Bacillus subtilis*. *Nature* **390:** 249-256

Lambert PA, Hancock IC, Baddiley J (1977) Occurrence and function of membrane teichoic acids. *Biochim Biophys Acta* **472:** 1-12

Lapidot A, Irving CS (1979) Nitrogen-15 and carbon-13 dynamic nuclear magnetic resonance study of chain segmental motion of the peptidoglycan pentaglycine chain of ^{15}N-Gly- and $^{13}C_2$-Gly-labeled *Staphylococcus aureus* cells and isolated cell walls. *Biochemistry* **18:** 1788-1796

Lazarevic V, Soldo B, Medico N, Pooley H, Bron S, Karamata D (2005) *Bacillus subtilis* a-phosphoglucomutase is required for normal cell morphology and biofilm formation. *Appl Environ Microbiol* **71:** 39-45

Lee CY, Buranen SL, Ye ZH (1991) Construction of single-copy integration vectors for *Staphylococcus aureus*. *Gene* **103:** 101-105

Lee SM, Ender M, Adhikari R, Smith JM, Berger-Bachi B, Cook GM (2007) Fitness cost of staphylococcal cassette chromosome *mec* in methicillin-resistant *Staphylococcus aureus* by way of continuous culture. *Antimicrob Agents Chemother* **51:** 1497-1499

Lequette Y, Lanfroy E, Cogez V, Bohin JP, Lacroix JM (2008) Biosynthesis of osmoregulated periplasmic glucans in Escherichia coli: the membrane-bound and the soluble periplasmic phosphoglycerol transferases are encoded by the same gene. *Microbiology* **154:** 476-483

Liu GY, Essex A, Buchanan JT, Datta V, Hoffman HM, Bastian JF, Fierer J, Nizet V (2005) *Staphylococcus aureus* golden pigment impairs neutrophil killing and promotes virulence through its antioxidant activity. *J Exp Med* **202:** 209-215

Lowy FD (1998) *Staphylococcus aureus* infections. *New Engl J Med* **339:** 520-532

Lu D, Wörmann ME, Zhang X, Schneewind O, Gründling A, Freemont PS (2009) Structure-based mechanism of lipoteichoic acid synthesis by *Staphylococcus aureus* LtaS. *Proc Natl Acad Sci USA* **106:** 1584-1589

Lu M, Kleckner N (1994) Molecular cloning and characterization of the *pgm* gene encoding phosphoglucomutase of *Escherichia coli*. *J Bacteriol* **176:** 5847-5851

Luong T, Sau S, Gomez M, Lee JC, Lee CY (2002) Regulation of *Staphylococcus aureus* capsular polysaccharide expression by *agr* and *sarA*. *Infect Immun* **70:** 444-450

Ma XX, Ito T, Tiensasitorn C, Jamklang M, Chongtrakool P, Boyle-Vavra S, Daum RS, Hiramatsu K (2002) Novel type of staphylococcal cassette chromosome *mec*

identified in community-acquired methicillin-resistant *Staphylococcus aureus* strains. *Antimicrob Agents Chemother* **46:** 1147-1152

Marti M, Trotonda MP, Tormo-Mas MA, Vergara-Irigaray M, Cheung AL, Lasa I, Penades JR (2009) Extracellular proteases inhibit protein-dependent biofilm formation in *Staphylococcus aureus*. *Microbes Infect* **12:** 55-64

Massimi I, Park E, Rice K, Muller-Esterl W, Sauder D, McGavin MJ (2002) Identification of a novel maturation mechanism and restricted substrate specificity for the SspB cysteine protease of *Staphylococcus aureus*. *J Biol Chem* **277:** 41770-41777

Matias VR, Beveridge TJ (2005) Cryo-electron microscopy reveals native polymeric cell wall structure in *Bacillus subtilis* 168 and the existence of a periplasmic space. *Mol Microbiol* **56:** 240-251

Matias VR, Beveridge TJ (2006) Native cell wall organization shown by cryo-electron microscopy confirms the existence of a periplasmic space in *Staphylococcus aureus*. *J Bacteriol* **188:** 1011-1021

Matias VR, Beveridge TJ (2008) Lipoteichoic acid is a major component of the *Bacillus subtilis* periplasm. *J Bacteriol* **190:** 7414-7418

Mazmanian SK, Liu G, Ton-That H, Schneewind O (1999) *Staphylococcus aureus* sortase, an enzyme that anchors surface proteins to the cell wall. *Science* **285:** 760-763

Mazmanian SK, Ton-That H, Schneewind O (2001) Sortase-catalysed anchoring of surface proteins to the cell wall of *Staphylococcus aureus*. *Mol Microbiol* **40:** 1049-1057

Mazmanian SK, Ton-That H, Su K, Schneewind O (2002) An iron-regulated sortase anchors a class of surface protein during *Staphylococcus aureus* pathogenesis. *Proc Natl Acad Sci U S A* **99:** 2293-2298

McAleese FM, Walsh EJ, Sieprawska M, Potempa J, Foster TJ (2001) Loss of clumping factor B fibrinogen binding activity by *Staphylococcus aureus* involves cessation of transcription, shedding and cleavage by metalloprotease. *J Biol Chem* **276:** 29969-29978

McGavin MJ, Zahradka C, Rice K, Scott JE (1997) Modification of the *Staphylococcus aureus* fibronectin binding phenotype by V8 protease. *Infect Immun* **65:** 2621-2628

Mei JM, Nourbakhsh F, Ford CW, Holden DW (1997) Identification of *Staphylococcus aureus* virulence genes in a murine model of bacteraemia using signature-tagged mutagenesis. *Mol Microbiol* **26:** 399-407

Meijer WJ, de Jong A, Bea G, Wisman A, Tjalsma H, Venema G, Bron S, van Dijl JM (1995) The endogenous *Bacillus subtilis* (natto) plasmids pTA1015 and pTA1040

contain signal peptidase-encoding genes: identification of a new structural module on cryptic plasmids. *Mol Microbiol* **17:** 621-631

Mohammadi T, van Dam V, Sijbrandi R, Vernet T, Zapun A, Bouhss A, Diepeveen-de Bruin M, Nguyen-Disteche M, de Kruijff B, Breukink E (2011) Identification of FtsW as a transporter of lipid-linked cell wall precursors across the membrane. *EMBO J* **30:** 1425-1432

Moks T, Abrahmsen L, Nilsson B, Hellman U, Sjoquist J, Uhlen M (1986) Staphylococcal protein A consists of five IgG-binding domains. *Eur J Biochem* **156:** 637-643

Moran GJ, Krishnadasan A, Gorwitz RJ, Fosheim GE, McDougal LK, Carey RB, Talan DA (2006) Methicillin-resistant *S. aureus* infections among patients in the emergency department. *N Engl J of Med* **355:** 666-674

Morath S, Geyer A, Hartung T (2001) Structure-function relationship of cytokine induction by lipoteichoic acid from *Staphylococcus aureus*. *J Exp Med* **193:** 393-397

Morath S, Stadelmaier A, Geyer A, Schmidt RR, Hartung T (2002) Synthetic lipoteichoic acid from *Staphylococcus aureus* is a potent stimulus of cytokine release. *J Exp Med* **195:** 1635-1640

Moreau M, Richards JC, Fournier JM, Byrd RA, Karakawa WW, Vann WF (1990) Structure of the type 5 capsular polysaccharide of *Staphylococcus aureus*. *Carbohydr Res* **201:** 285-297

Navarre WW, Schneewind O (1999) Surface proteins of Gram-positive bacteria and mechanisms of their targeting to the cell wall envelope. *Microbiol Mol Biol Rev* **63:** 174-229

Nesbitt JA, 3rd, Lennarz WJ (1968) Participation of aminoacyl transfer ribonucleic acid in aminoacyl phosphatidylglycerol synthesis. I. Specificity of lysyl phosphatidylglycerol synthetase. *J Biol Chem* **243:** 3088-3095

Neuhaus FC, Baddiley J (2003) A continuum of anionic charge: structures and functions of D-alanyl-teichoic acids in gram-positive bacteria. *Microbiol Mol Biol Rev* **67:** 686-723

Nickerson NN, Joag V, McGavin MJ (2008) Rapid autocatalytic activation of the M4 metalloprotease aureolysin is controlled by a conserved N-terminal fungalysin-thermolysin-propeptide domain. *Mol Microbiol* **69:** 1530-1543

Nickerson NN, Prasad L, Jacob L, Delbaere LT, McGavin MJ (2007) Activation of the SspA serine protease zymogen of *Staphylococcus aureus* proceeds through unique variations of a trypsinogen-like mechanism and is dependent on both autocatalytic and metalloprotease-specific processing. *J Biol Chem* **282:** 34129-24138

Nielsen H, Engelbrecht J, Brunak S, von Heijne G (1997a) Identification of prokaryotic and eukaryotic signal peptides and prediction of their cleavage sites. *Protein Eng* **10:** 1-6

Nielsen H, Engelbrecht J, Brunak S, von Heijne G (1997b) A neural network method for identification of prokaryotic and eukaryotic signal peptides and prediction of their cleavage sites. *Int J Neural Syst* **8:** 581-599

O'Connell C, Pattee PA, Foster TJ (1993) Sequence and mapping of the *aroA* gene of *Staphylococcus aureus* 8325-4. *J Gen Microbiol* **139:** 1449-1460

O'Riordan K, Lee JC (2004) *Staphylococcus aureu*s capsular polysaccharides. *Clin Microbiol Rev* **17:** 218-234

O'Seaghdha M, van Schooten CJ, Kerrigan SW, Emsley J, Silverman GJ, Cox D, Lenting PJ, Foster TJ (2006) *Staphylococcus aureus* protein A binding to von Willebrand factor A1 domain is mediated by conserved IgG binding regions. *FEBS J* **273:** 4831-4841

Oku Y, Kurokawa K, Matsuo M, Yamada S, Lee BL, Sekimizu K (2009) Pleiotropic roles of polyglycerolphosphate synthase of lipoteichoic acid in growth of *Staphylococcus aureus* cells. *J Bacteriol* **191:** 141-151

Paetzel M, Karla A, Strynadka NC, Dalbey RE (2002) Signal peptidases. *Chem Rev* **102:** 4549-4580

Pallen MJ, Lam AC, Antonio M, Dunbar K (2001) An embarrassment of sortases - a richness of substrates? *Trends Microbiol* **9:** 97-102

Peacock SJ, de Silva I, Lowy FD (2001) What determines nasal carriage of *Staphylococcus aureus*? *Trends Microbiol* **9:** 605-610

Peng HL, Novick RP, Kreiswirth B, Kornblum J, Schlievert P (1988) Cloning, characterization, and sequencing of an accessory gene regulator (*agr*) in *Staphylococcus aureus*. *J Bacteriol* **170:** 4365-4372

Pereira PM, Filipe SR, Tomasz A, Pinho MG (2007) Fluorescence ratio imaging microscopy shows decreased access of vancomycin to cell wall synthetic sites in vancomycin-resistant *Staphylococcus aureus*. *Antimicrob Agents Chemother* **51:** 3627-3633

Perichon B, Courvalin P (2009) VanA-type vancomycin-resistant *Staphylococcus aureus*. *Antimicrob Agents Chemother* **53:** 4580-4587

Peschel A, Collins LV (2001) Staphylococcal resistance to antimicrobial peptides of mammalian and bacterial origin. *Peptides* **22:** 1651-1659

Peterson PK, Verhoef J, Sabath LD, Quie PG (1977) Effect of protein A on staphylococcal opsonization. *Infect Immun* **15:** 760-764

Peterson PK, Wilkinson BJ, Kim Y, Schmeling D, Quie PG (1978) Influence of encapsulation on staphylococcal opsonization and phagocytosis by human polymorphonuclear leukocytes. *Infect Immun* **19:** 943-949

Pinho MG, Errington J (2003) Dispersed mode of *Staphylococcus aureus* cell wall synthesis in the absence of the division machinery. *Mol Microbiol* **50:** 871-881

Pooley HM, Paschoud D, Karamata D (1987) The *gtaB* marker in *Bacillus subtilis* 168 is associated with a deficiency in UDP-glucose pyrophosphorylase. *J Gen Microbiol* **133:** 3481-3493

Potempa J, Dubin A, Korzus G, Travis J (1988) Degradation of elastin by a cysteine proteinase from *Staphylococcus aureus*. *J Biol Chem* **263:** 2664-2667

Potempa J, Watorek W, Travis J (1986) The inactivation of human plasma alpha 1-proteinase inhibitor by proteinases from *Staphylococcus aureus*. *J Biol Chem* **261:** 14330-14334

Powers ME, Smith PA, Roberts TC, Fowler BJ, King CC, Trauger SA, Siuzdak G, Romesberg FE (2011) Type I signal peptidase and protein secretion in *Staphylococcus epidermidis*. *J Bacteriol* **193:** 340-348

Priest FG (1989) Isolation and identification of aerobic endospore-forming bacteria. In C.R. Harwood (ed.), *Biotechnology Handbooks*, vol. 2. *Bacillus*. Plenum Press, New York.

Prokesova L, Potuznikova B, Potempa J, Zikan J, Radl J, Hachova L, Baran K, Porwit-Bobr Z, John C (1992) Cleavage of human immunoglobulins by serine proteinase from *Staphylococcus aureus*. *Immunol Lett* **31:** 259-265

Rahman O, Cummings SP, Sutcliffe IC (2009a) Phenotypic variation in *Streptomyces* sp. DSM 40537, a lipoteichoic acid producing actinomycete. *Lett Appl Microbiol* **48:** 226-229

Rahman O, Dover LG, Sutcliffe IC (2009b) Lipoteichoic acid biosynthesis: two steps forwards, one step sideways? *Trends Microbiol* **17:** 219-225

Rahman O, Pfitzenmaier M, Pester O, Morath S, Cummings SP, Hartung T, Sutcliffe IC (2009c) Macroamphiphilic components of thermophilic actinomycetes: identification of lipoteichoic acid in *Thermobifida fusca*. *J Bacteriol* **191:** 152-160

Rao S, Bockstael K, Nath S, Engelborghs Y, Anne J, Geukens N (2009) Enzymatic investigation of the *Staphylococcus aureus* type I signal peptidase SpsB - implications for the search for novel antibiotics. *FEBS J* **276:** 3222-3234

Reed SB, Wesson CA, Liou LE, Trumble WR, Schlievert PM, Bohach GA, Bayles KW (2001) Molecular characterization of a novel *Staphylococcus aureus* serine protease operon. *Infect Immun* **69:** 1521-1527

Reichmann NT, Gründling A (2011) Location, synthesis and function of glycolipids and polyglycerolphosphate lipoteichoic acid in Gram-positive bacteria of the phylum Firmicutes. *FEMS Microbiol Lett* **319:** 97-105

Rice K, Peralta R, Bast D, de Azavedo J, McGavin MJ (2001) Description of staphylococcus serine protease (*ssp*) operon in *Staphylococcus aureus* and nonpolar inactivation of *sspA*-encoded serine protease. *Infect Immun* **69:** 159-169

Rigoulay C, Entenza JM, Halpern D, Widmer E, Moreillon P, Poquet I, Gruss A (2005) Comparative analysis of the roles of HtrA-like surface proteases in two virulent *Staphylococcus aureus* strains. *Infect Immun* **73:** 563-572

Rigoulay C, Poquet I, Madsen SM, Gruss A (2004) Expression of the *Staphylococcus aureus* surface proteins HtrA1 and HtrA2 in *Lactococcus lactis*. *FEMS Microbiol Lett* **237:** 279-288

Rusch SL, Kendall DA (2007) Interactions that drive Sec-dependent bacterial protein transport. *Biochemistry* **46:** 9665-9673

Ruzin A, Severin A, Ritacco F, Tabei K, Singh G, Bradford PA, Siegel MM, Projan SJ, Shlaes DM (2002) Further evidence that a cell wall precursor [C(55)-MurNAc-(peptide)-GlcNAc] serves as an acceptor in a sorting reaction. *J Bacteriol* **184:** 2141-2147

Rzychon M, Sabat A, Kosowska K, Potempa J, Dubin A (2003) Staphostatins: an expanding new group of proteinase inhibitors with a unique specificity for the regulation of staphopains, *Staphylococcus* spp. cysteine proteinases. *Mol Microbiol* **49:** 1051-1066

Sabat A, Kosowska K, Poulsen K, Kasprowicz A, Sekowska A, van Den Burg B, Travis J, Potempa J (2000) Two allelic forms of the aureolysin gene (*aur*) within *Staphylococcus aureus*. *Infect Immun* **68:** 973-976

Sabath LD, Wallace SJ, Gerstein DA (1972) Suppression of intrinsic resistance to methicillin and other penicillins in *Staphylococcus aureus*. *Antimicrob Agents Chemother* **2:** 350-355

Sambrook J, Fritsch EF, Maniatis T (1989) Molecular cloning: a laboratory manual, Cold Spring Harbor, N. Y., Cold Spring Harbor Laboratory Press.

Sander P, Rezwan M, Walker B, Rampini SK, Kroppenstedt RM, Ehlers S, Keller C, Keeble JR, Hagemeier M, Colston MJ, Springer B, Bottger EC (2004) Lipoprotein processing is required for virulence of *Mycobacterium tuberculosis*. *Mol Microbiol* **52:** 1543-1552

Sankaran K, Wu HC (1994) Lipid modification of bacterial prolipoprotein. Transfer of diacylglyceryl moiety from phosphatidylglycerol. *J Biol Chem* **269:** 19701-19706

Sau S, Bhasin N, Wann ER, Lee JC, Foster TJ, Lee CY (1997) The *Staphylococcus aureus* allelic genetic loci for serotype 5 and 8 capsule expression contain the type-specific genes flanked by common genes. *Microbiology* **143:** 2395-2405

Sawai T, Tomono K, Yanagihara K, Yamamoto Y, Kaku M, Hirakata Y, Koga H, Tashiro T, Kohno S (1997) Role of coagulase in a murine model of hematogenous pulmonary infection induced by intravenous injection of *Staphylococcus aureus* enmeshed in agar beads. *Infect Immun* **65:** 466-471

Schagger H, von Jagow G (1987) Tricine-sodium dodecyl sulfate-polyacrylamide gel electrophoresis for the separation of proteins in the range from 1 to 100 kDa. *Anal Biochem* **166:** 368-379

Scheffers DJ, Pinho MG (2005) Bacterial cell wall synthesis: new insights from localization studies. *Microbiol Mol Biol Rev* **69:** 585-607

Schindler CA, Schuhardt VT (1964) Lysostaphin: A new bacteriolytic agent for the *Staphylococcus*. *Proc Natl Acad Sci U S A* **51:** 414-421

Schirner K, Marles-Wright J, Lewis RJ, Errington J (2009) Distinct and essential morphogenic functions for wall- and lipo-teichoic acids in *Bacillus subtilis*. *EMBO J* **28:** 830-842

Schleifer KH, Kroppenstedt RM (1990) Chemical and molecular classification of staphylococci. *Soc Appl Bacteriol Symp Ser* **19:** 9S-24S

Schmidt-Ioanas M, de Roux A, Lode H (2005) New antibiotics for the treatment of severe staphylococcal infection in the critically ill patient. *Curr Opin in Crit Care* **11:** 481-486

Schneewind O, Mihaylova-Petkov D, Model P (1993) Cell wall sorting signals in surface proteins of Gram-positive bacteria. *EMBO J* **12:** 4803-4811

Schneider T, Senn MM, Berger-Bächi B, Tossi A, Sahl HG, Wiedemann I (2004) In vitro assembly of a complete, pentaglycine interpeptide bridge containing cell wall precursor (lipid II-Gly5) of *Staphylococcus aureus*. *Mol Microbiol* **53:** 675-685

Schnitger H, Papenberg K, Ganse E, Czok R, Buecher T, Adam H (1959) Chromatography of phosphorus-containing metabolities in a human liver biopsy specimen. *Biochem Z* **332:** 167-185

Shaw L, Golonka E, Potempa J, Foster SJ (2004) The role and regulation of the extracellular proteases of *Staphylococcus aureus*. *Microbiology* **150:** 217-228

Shaw LN, Golonka E, Szmyd G, Foster SJ, Travis J, Potempa J (2005) Cytoplasmic control of premature activation of a secreted protease zymogen: deletion of staphostatin B (SspC) in *Staphylococcus aureus* 8325-4 yields a profound pleiotropic phenotype. *J Bacteriol* **187:** 1751-1762

Shibaev VN, Duckworth M, Archibald AR, Baddiley J (1973) The structure of a polymer containing galactosamine from walls of *Bacillus subtilis* 168. *Biochem J* **135:** 383-384

Shinitzky M, Friedman P, Haimovitz R (1993) Formation of 1,3-cyclic glycerophosphate by the action of phospholipase C on phosphatidylglycerol. *J Biol Chem* **268:** 14109-14115

Short SA, White DC (1971) Metabolism of phosphatidylglycerol, lysylphosphatidylglycerol, and cardiolipin of *Staphylococcus aureus*. *J Bacteriol* **108:** 219-226

Short SA, White DC (1972) Biosynthesis of cardiolipin from phosphatidylglycerol in *Staphylococcus aureus*. *J Bacteriol* **109:** 820-826

Sibbald MJ, Ziebandt AK, Engelmann S, Hecker M, de Jong A, Harmsen HJ, Raangs GC, Stokroos I, Arends JP, Dubois JY, van Dijl JM (2006) Mapping the pathways to staphylococcal pathogenesis by comparative secretomics. *Microbiol Mol Biol Rev* **70:** 755-788

Sieprawska-Lupa M, Mydel P, Krawczyk K, Wojcik K, Puklo M, Lupa B, Suder P, Silberring J, Reed M, Pohl J, Shafer W, McAleese F, Foster T, Travis J, Potempa J (2004) Degradation of human antimicrobial peptide LL-37 by *Staphylococcus aureus*-derived proteinases. *Antimicrob Agents Chemother* **48:** 4673-4679

Sompolinsky D, Samra Z, Karakawa WW, Vann WF, Schneerson R, Malik Z (1985) Encapsulation and capsular types in isolates of *Staphylococcus aureus* from different sources and relationship to phage types. *J Clin Microbiol* **22:** 828-834

Staubitz P, Neumann H, Schneider T, Wiedemann I, Peschel A (2004) MprF-mediated biosynthesis of lysylphosphatidylglycerol, an important determinant in staphylococcal defensin resistance. *FEMS Microbiol Lett* **231:** 67-71

Strauch KL, Johnson K, Beckwith J (1989) Characterization of *degP*, a gene required for proteolysis in the cell envelope and essential for growth of *Escherichia coli* at high temperature. *J Bacteriol* **171:** 2689-2696

Strominger JL, Izaki K, Matsuhashi M, Tipper DJ (1967) Peptidoglycan transpeptidase and D-alanine carboxypeptidase: penicillin-sensitive enzymatic reactions. *Fed Proc* **26:** 9-22

Suginaka H, Shimatani M, Ogawa M, Kotani S (1979) Prevention of penicillin-induced lysis of *Staphylococcus aureus* by cellular lipoteichoic acid. *J Antibiot (Tokyo)* **32:** 73-77

Takami H, Nakasone K, Takaki Y, Maeno G, Sasaki R, Masui N, Fuji F, Hirama C, Nakamura Y, Ogasawara N, Kuhara S, Horikoshi K (2000) Complete genome sequence of the alkaliphilic bacterium *Bacillus halodurans* and genomic sequence comparison with Bacillus subtilis. *Nucleic Acids Res* **28:** 4317-4331

Thackray PD, Moir A (2003) SigM, an extracytoplasmic function sigma factor of *Bacillus subtilis*, is activated in response to cell wall antibiotics, ethanol, heat, acid, and superoxide stress. *J Bacteriol* **185:** 3491-3498

Thakker M, Park JS, Carey V, Lee JC (1998) *Staphylococcus aureus* serotype 5 capsular polysaccharide is antiphagocytic and enhances bacterial virulence in a murine bacteremia model. *Infect Immun* **66:** 5183-5189

Tjalsma H, Antelmann H, Jongbloed JD, Braun PG, Darmon E, Dorenbos R, Dubois JY, Westers H, Zanen G, Quax WJ, Kuipers OP, Bron S, Hecker M, van Dijl JM (2004) Proteomics of protein secretion by *Bacillus subtilis:* separating the "secrets" of the secretome. *Microbiol Mol Biol Rev* **68:** 207-233

Tjalsma H, Bolhuis A, van Roosmalen ML, Wiegert T, Schumann W, Broekhuizen CP, Quax WJ, Venema G, Bron S, van Dijl JM (1998) Functional analysis of the secretory precursor processing machinery of *Bacillus subtilis*: identification of a eubacterial homolog of archaeal and eukaryotic signal peptidases. *Genes Dev* **12:** 2318-2331

Tjalsma H, Kontinen VP, Pragai Z, Wu H, Meima R, Venema G, Bron S, Sarvas M, van Dijl JM (1999a) The role of lipoprotein processing by signal peptidase II in the Gram-positive eubacterium *Bacillus subtilis*. Signal peptidase II is required for the efficient secretion of alpha-amylase, a non-lipoprotein. *J Biol Chem* **274:** 1698-1707

Tjalsma H, Noback MA, Bron S, Venema G, Yamane K, van Dijl JM (1997) *Bacillus subtilis* contains four closely related type I signal peptidases with overlapping substrate specificities. Constitutive and temporally controlled expression of different *sip* genes. *J Biol Chem* **272:** 25983-25992

Tjalsma H, van den Dolder J, Meijer WJ, Venema G, Bron S, van Dijl JM (1999b) The plasmid-encoded signal peptidase SipP can functionally replace the major signal peptidases SipS and SipT of *Bacillus subtilis*. *J Bacteriol* **181:** 2448-2454

Tjalsma H, Zanen G, Venema G, Bron S, van Dijl JM (1999c) The potential active site of the lipoprotein-specific (type II) signal peptidase of *Bacillus subtilis*. *J Biol Chem* **274:** 28191-28197

Ton-That H, Labischinski H, Berger-Bachi B, Schneewind O (1998) Anchor structure of staphylococcal surface proteins. III. Role of the FemA, FemB, and FemX factors in anchoring surface proteins to the bacterial cell wall. *J Biol Chem* **273:** 29143-29149

Uchikawa K, Sekikawa I, Azuma I (1986) Structural studies on teichoic acids in cell walls of several serotypes of *Listeria monocytogenes*. *J Biochem* **99:** 315-327

Uhlen M, Guss B, Nilsson B, Gatenbeck S, Philipson L, Lindberg M (1984) Complete sequence of the staphylococcal gene encoding protein A. A gene evolved through multiple duplications. *J Biol Chem* **259:** 1695-1702

van Heijenoort J (2001) Recent advances in the formation of the bacterial peptidoglycan monomer unit. *Nat Prod Rep* **18:** 503-519

van Roosmalen ML, Geukens N, Jongbloed JD, Tjalsma H, Dubois JY, Bron S, van Dijl JM, Anne J (2004) Type I signal peptidases of Gram-positive bacteria. *Biochim Biophys Acta* **1694:** 279-297

van Wamel W, Xiong YQ, Bayer AS, Yeaman MR, Nast CC, Cheung AL (2002) Regulation of *Staphylococcus aureus t*ype 5 capsular polysaccharides by *agr* and *sarA* in vitro and in an experimental endocarditis model. *Microb Pathog* **33:** 73-79

Vellanoweth RL, Rabinowitz JC (1992) The influence of ribosome-binding-site elements on translational efficiency in *Bacillus subtilis* and *Escherichia coli in vivo*. *Mol Microbiol* **6:** 1105-1114

Vijaranakul U, Nadakavukaren MJ, de Jonge BL, Wilkinson BJ, Jayaswal RK (1995) Increased cell size and shortened peptidoglycan interpeptide bridge of NaCl-stressed *Staphylococcus aureus* and their reversal by glycine betaine. *J Bacteriol* **177:** 5116-5121

von Heijne G (1989) The structure of signal peptides from bacterial lipoproteins. *Protein Eng* **2:** 531-534

von Heijne G (1990) The signal peptide. *J Membr Biol* **115:** 195-201

Ward JB (1973) The chain length of the glycans in bacterial cell walls. *Biochem J* **133:** 395-398

Waters CM, Hirt H, McCormick JK, Schlievert PM, Wells CL, Dunny GM (2004) An amino-terminal domain of *Enterococcus faecalis* aggregation substance is required for aggregation, bacterial internalization by epithelial cells and binding to lipoteichoic acid. *Mol Microbiol* **52:** 1159-1171

Weart RB, Lee AH, Chien AC, Haeusser DP, Hill NS, Levin PA (2007) A metabolic sensor governing cell size in bacteria. *Cell* **130:** 335-347

Webb AJ, Karatsa-Dodgson M, Gründling A (2009) Two-enzyme systems for glycolipid and polyglycerolphosphate lipoteichoic acid synthesis in *Listeria monocytogenes*. *Mol Microbiol* **74:** 299-314

Weidenmaier C, Kokai-Kun JF, Kristian SA, Chanturiya T, Kalbacher H, Gross M, Nicholson G, Neumeister B, Mond JJ, Peschel A (2004) Role of teichoic acids in *Staphylococcus aureus* nasal colonization, a major risk factor in nosocomial infections. *Nat Med* **10:** 243-245

Weidenmaier C, Peschel A (2008) Teichoic acids and related cell-wall glycopolymers in Gram-positive physiology and host interactions. *Nature reviews* **6:** 276-287

Weidenmaier C, Peschel A, Xiong YQ, Kristian SA, Dietz K, Yeaman MR, Bayer AS (2005) Lack of wall teichoic acids in *Staphylococcus aureus* leads to reduced interactions with endothelial cells and to attenuated virulence in a rabbit model of endocarditis. *J Infect Dis* **191:** 1771-1777

Weiss WJ, Lenoy E, Murphy T, Tardio L, Burgio P, Projan SJ, Schneewind O, Alksne L (2004) Effect of *srtA* and *srtB* gene expression on the virulence of *Staphylococcus aureus* in animal models of infection. *J Antimicrob Chemother* **53:** 480-486

Wilkinson BJ, Holmes KM (1979) *Staphylococcus aureus* cell surface: capsule as a barrier to bacteriophage adsorption. *Infect Immun* **23:** 549-552

Wilkinson BJ, Peterson PK, Quie PG (1979) Cryptic peptidoglycan and the antiphagocytic effect of the *Staphylococcus aureus* capsule: model for the antiphagocytic effect of bacterial cell surface polymers. *Infect Immun* **23:** 502-508

Wörmann ME, Corrigan RM, Simpson PJ, Matthews SJ, Gründling A (2011) Enzymatic activities and functional interdependencies of *Bacillus subtilis* lipoteichoic acid synthesis enzymes. *Mol Microbiol* **79:** 566-583

Xu D, Cote JC (2003) Phylogenetic relationships between *Bacillus* species and related genera inferred from comparison of 3' end 16S rDNA and 5' end 16S-23S ITS nucleotide sequences. *Int J Syst Evol Microbiol* **53:** 695-704

Yamagata H, Ippolito C, Inukai M, Inouye M (1982) Temperature-sensitive processing of outer membrane lipoprotein in an *Escherichia coli* mutant. *J Bacteriol* **152:** 1163-1168

Zhang L, Jacobsson K, Strom K, Lindberg M, Frykberg L (1999) *Staphylococcus aureus* expresses a cell surface protein that binds both IgG and beta2-glycoprotein I. *Microbiology* **145 (Pt 1):** 177-183

Zhang L, Jacobsson K, Vasi J, Lindberg M, Frykberg L (1998) A second IgG-binding protein in *Staphylococcus aureus*. *Microbiology* **144:** 985-991

Ziebandt AK, Weber H, Rudolph J, Schmid R, Hoper D, Engelmann S, Hecker M (2001) Extracellular proteins of *Staphylococcus aureus* and the role of SarA and sigma B. *Proteomics* **1:** 480-493